Inaugural dissertation

for obtaining the

doctoral degree of the

Combined Faculty of Mathematics, Engineering and Natural Sciences of the Ruprecht - Karls - University Heidelberg

Presented by

M.Sc. Eren Boğa

born in Izmir, Türkiye

Oral examination: 15.12.2023

Generation of a cellular library of CAR T cells for rapid screening and identification of antigen specific, functional CAR constructs

Referees: Prof. Dr. Ilse Hofmann
Prof. Dr. Hinrich Abken
Prof. Dr. Dirk Jäger

Eppur si muove

Abstract

Adoptive T cell therapy (ACT) with Chimeric Antigen Receptors (CARs) revolutionized the field of immunotherapy by achieving up to 90% complete responses in the treatment of hematological malignancies. Due to their success in clinical trials, there are currently 6 FDA approved CAR T cell products for treatment against B cell malignancies. Unlike TCR T cells, antigen recognition by CAR T cells is peptide-Major Histocompatibility Complex independent. Therefore, an isolated functional CAR construct can be used to treat a cohort of patients sharing a common antigen.

Unlike the success observed in the CAR T cells therapies against hematological malignancies, the treatment of solid tumors with CAR T cells showed a limited success so far. There are couple of reasons for impaired function of CAR T cells in the solid tumors. The highly immunosuppressive environment of the tumor stroma can hinder CAR T cell infiltration and activation in the tumor tissue. Moreover, there is limited number of identified CARs suitable for ACT against solid tumors. Therefore, more binders need to be screened to identify tumor specific CARs. Current golden standard for CAR identification is the use of single-chain phage display libraries. Screening of phage display libraries can yield in high affinity scFvs, but these constructs still need to be cloned into a functional CAR backbone for further characterization. It is known that not all isolated scFvs can give rise to functional CAR constructs. Moreover when cloned into a CAR context, scFvs may cause a tonic signaling effect that leads to early CAR T cell exhaustion, thus decreasing antitumor potential of T cells. Besides, one of the biggest disadvantage of phage display libraries is that a functional CAR identification can take up to several months. Thus, it is hardly possible to use phage display libraries for development of personalized CAR T cell therapies as during the CAR isolation and validation period, disease progression may render the generated CAR T cells unbeneficial to the patient.

In this study, an innovative platform was generated to accelerate identification of antigen-specific CAR constructs. To do so, a cellular CAR library screening approach was developed by engrafting a plasmid CAR library into a Jurkat reporter cell line. Generation and screening of such cellular CAR libraries for antigen-specific CAR identification has not been reported yet. For this purpose, an antigen-specific stimulation sensitive single-cell derived reporter Jurkat clone was cultivated. This clone was then transfected with a plasmid CAR library that was generated by cloning a randomly assembled naïve scFv repertoire into a functional CAR backbone. Since the CAR library was engrafted into the reporter cells directly, tonic signaling CARs were easily identified as they activated the cells in the absence of antigen-specific stimulation and excluded from further analysis. Consequently, remaining library cells that express functional CARs were screened for an antigen of interest on a single-cell level by using Bruker's Lightning™ device. Tumor antigen reactive cells were identified by induced reporter expression and exported from the Lightning™ device to have their CARs sequenced for subsequent functional validation. Above mentioned process, from generation of plasmid CAR libraries to *in vitro* validation, allows CAR-T cell discovery in as little as 6 weeks. Thus, cellular CAR libraries will enable the development of highly individualized CAR T cell therapies against patient derived tumor antigens in a timeframe that the patient can still benefit from.

Zusammenfassung

Die adoptive T-Zell-Therapie (ACT) mit chimären Antigenrezeptoren (CARs) hat den Bereich der Immuntherapie revolutioniert, indem sie bei der Behandlung von hämatologischen Malignomen bis zu 90 % vollständige Ansprechraten erzielt. Aufgrund ihres Erfolgs in klinischen Studien gibt es derzeit 6 von der FDA zugelassene CAR-T-Zell-Produkte für die Behandlung von B-Zell-Malignomen. Im Gegensatz zu TCR-T-Zellen ist die Antigenerkennung durch CAR-T-Zellen unabhängig vom Peptid-Major-Histokompatibilitätskomplex. Daher kann ein isoliertes funktionelles CAR-Konstrukt zur Behandlung einer Kohorte von Patienten mit einem gemeinsamen Antigen verwendet werden.

Im Gegensatz zu den Erfolgen, die bei den CAR-T-Zellen-Therapien gegen hämatologische Malignome beobachtet wurden, war die Behandlung von soliden Tumoren mit CAR-T-Zellen bisher nur begrenzt erfolgreich. Es gibt eine Reihe von Gründen für die eingeschränkte Funktion von CAR-T-Zellen in soliden Tumoren. Die stark immunsuppressive Umgebung des Tumorstromas kann die Infiltration und Aktivierung von CAR T-Zellen im Tumorgewebe behindern. Außerdem gibt es nur eine begrenzte Anzahl identifizierter CARs, die sich für ACT gegen solide Tumore eignen. Daher müssen mehr Bindemittel untersucht werden, um tumorspezifische CARs zu identifizieren. Der derzeitige goldene Standard für die Identifizierung von CARs ist die Verwendung von einkettigen Phagen-Display-Bibliotheken. Das Screening von Phage-Display-Bibliotheken kann zu hochaffinen scFvs führen, aber diese Konstrukte müssen zur weiteren Charakterisierung noch in ein funktionelles CAR-Backbone kloniert werden. Es ist bekannt, dass nicht alle isolierten scFvs zu funktionalen CAR-Konstrukten führen können. Außerdem können scFvs, wenn sie in einen CAR-Kontext geklont werden, einen tonischen Signaleffekt verursachen, der zu einer frühen Erschöpfung der CAR-T-Zellen führt und damit das Antitumorpotenzial der T-Zellen verringert. Einer der größten Nachteile von Phage-Display-Bibliotheken ist außerdem, dass die Identifizierung eines funktionalen CAR bis zu mehreren Monaten dauern kann. Daher ist es kaum möglich, Phage-Display-Bibliotheken für die Entwicklung personalisierter CAR-T-Zell-Therapien zu verwenden, da die generierten CAR-T-Zellen während der CAR-Isolierung und -Validierung durch das Fortschreiten der Krankheit für den Patienten unbrauchbar werden können.

In dieser Studie wurde eine innovative Plattform entwickelt, um die Identifizierung von antigenspezifischen CAR-Konstrukten zu beschleunigen. Zu diesem Zweck wurde ein zellulärer CAR-Bibliotheks-Screening-Ansatz entwickelt, bei dem eine Plasmid-CAR-Bibliothek in eine Jurkat-Reporterzelllinie transplantiert wird. Über die Generierung und das Screening solcher zellulären CAR-Bibliotheken zur Identifizierung antigenspezifischer CARs wurde bisher noch nicht berichtet. Zu diesem Zweck wurde ein antigenspezifischer, stimulationsempfindlicher einzelliger Reporter-Jurkat-Klon kultiviert. Dieser Klon wurde dann mit einer Plasmid-CAR-Bibliothek transfiziert, die durch Klonen eines zufällig zusammengestellten naiven scFv-Repertoires in ein funktionelles CAR-Backbone erzeugt wurde. Da die CAR-Bibliothek direkt in die Reporterzellen eingepflanzt wurde, konnten tonische, signalgebende CARs leicht identifiziert werden, da sie die Zellen ohne antigenspezifische Stimulation aktivierten und von der weiteren Analyse ausgeschlossen wurden. Folglich wurden die verbleibenden Bibliothekszellen, die funktionale CARs exprimieren, mit dem Lightning™-Gerät von Bruker auf ein Antigen von Interesse auf Einzelzellebene untersucht. Tumorantigen-reaktive Zellen wurden durch induzierte Reporterexpression identifiziert und aus dem LightningTM-Gerät exportiert, um ihre CARs für

die anschließende Funktionsvalidierung sequenzieren zu lassen. Der oben beschriebene Prozess, von der Erzeugung von Plasmid-CAR-Bibliotheken bis zur In-vitro-Validierung, ermöglicht die Entdeckung von CAR-T-Zellen in nur 6 Wochen. Somit ermöglichen zelluläre CAR-Bibliotheken die Entwicklung hoch individualisierter CAR-T-Zelltherapien gegen vom Patienten stammende Tumorantigene in einem Zeitrahmen, von dem der Patient noch profitieren kann.

Table of Content

Abstract 1

Zusammenfassung 2

1 **Introduction** 8

1.1 State-of-the-Art cancer immunotherapy 8

1.1.1 Active immunotherapies 8

1.1.2 Passive immunotherapies 9

1.2 Adoptive T cell therapy 10

1.2.1 CAR T cell therapy 11

1.2.2 CAR T cell activation 14

1.3 Tumor antigens 15

1.4 Problems associated with CAR T cell therapy 15

1.5 scFv phage display libraries for *de novo* CAR identification 16

1.6 nanoS/MARt vectors in development of ACT products 19

1.7 Microfluidics systems for antigen-specific TCR/BCR identification 20

1.8 Aim of the study 21

2 **Materials** 22

2.1 Equipments 22

2.2 Consumables 23

2.2.1 General Consumables 23

2.2.2 Bruker Consumables 24

2.2.3 MaxCyte Consumables 24

2.2.4 Oxford Nanopore Technologies Consumables 24

2.3 Standard Kits 24

2.4 Chemicals, media and additives 25

2.5 Antibodies and proteins 27

2.6 Enzymes 27

2.7 Bacteria Strains 28

2.8 Plasmids 28

2.8.1 Lentiviral plasmids 28

2.8.2 S/MAR plasmids 28

2.8.3 Other plasmids 29
2.9 Primers 29
2.9.1 Pansri et al. desalted primers 29
2.9.2 Self-designed desalted library amplification primers 31
2.9.3 PAGE purified library amplification primers 33
2.9.4 Working HPLC purified library amplification primers 33
2.9.6 qPCR primers 36
2.9.5 Library Sanger sequencing primers 36
2.9.6 Library cDNA amplification primers 36
2.9.7 Barcodes from Oxford Nanopore sequencing 36
2.10 Cell lines 37
3 **Methods** 38
3.1 Cell Culture 38
3.1.1 Maintenance and proliferation 38
3.1.2 Lentiviral particle production by HEK 293T co-transfection 38
3.1.3 Lentiviral transduction of Jurkat cells 39
3.1.4 PBMC isolation 39
3.1.5 Single-cell derived clone cultivation 39
3.1.6 Limiting Dilution 39
3.2 Molecular Biology 40
3.2.1 Agarose gel electrophoresis 40
3.2.2 Bacteria cultures 40
3.2.3 Transformation of *E. coli* strains 41
3.2.4 RNA isolation 42
3.2.5 Plasmid DNA isolation 42
3.2.6 Restriction enzyme digestion 43
3.2.7 Agarose gel purification 43
3.2.8 Plasmid CAR library cloning 43
3.2.9 CAR cDNA recovery from Lightning™ exports 46
3.2.10 Nucleic acid quality control 48
3.2.11 DNA preparation for Oxford Nanopore Sequencing 49

3.3 Jurkat electroporations 49
3.3.1 Electroporation with Neon™ device 49
3.3.2 Electroporation with GTx™ device 49
3.4 FACS/flow cytometry analysis 50
3.4.1 Flow cytometry staining and acquisition 50
3.4.2 FACS of stimulated Jurkat report cells 51
3.4.3 FACS J7i-Library cell pre-enrichment 51
3.5 *In vitro* experiments 51
3.5.1 Bulk unspecific PHA-L stimulation 51
3.5.2 Magnetic bead coupling and bulk antigen-specific stimulation 51
3.5.3 Bulk antigen-specific stimulation with antigen expressing cell lines 52
3.6 qPCR experiments 52
3.7 Single-cell stimulation experiments with Lightning™ device 53
3.7.1 Unspecific PHA-L stimulation 53
3.7.2 Antigen-specific stimulation 55
3.8 Oxford Nanopore sequencing analysis 57
4 **Results** 58
4.1 Generation of single-cell derived Jurkat reporter cell line 58
4.1.1 Establishment of Jurkat reporter cell line J7 58
4.1.2 Antigen-specific stimulation of J7 61
4.1.3 Refining the antigen-specific stimulation of J7i 64
4.1.4 CAR expression upon antigen-specific stimulation 67
4.1.5 Stimulation of electroporated cells at single-cell level 70
4.2 Generation of a plasmid CAR library 73
4.2.1 Crucial role of Leader sequence in CAR expression 73
4.2.2 Library cloning using an artificial leader sequence 76
4.2.3 Plasmid CAR library generation with reduced out of frame sequences 79
4.3 Generation of a cellular CAR Library 82
4.3.1 Setting up electroporation parameters 82
4.3.2 Effect of DNA quality on electroporation efficiency 84
4.3.3 Up scaling and optimization of library DNA electroporation 87

4.4 Screening of the cellular CAR library ... 90
4.4.1 Summary of the pipeline ... 90
4.4.2 The first proof-of-principle run of the pipeline ... 91
4.4.3 Sequencing analysis of the hits ... 93
4.4.4 *In vitro* analysis of the hits ... 97
5 **Discussion** ... 99
5.1 Development and characterization of a Jurkat reporter cell line ... 99
5.1.1 Cultivation and maintenance of highly responsive Jurkat reporter cells ... 99
5.1.2 Effect of antigen density on antigen-specific stimulation ... 100
5.1.3 Antigen-specific stimulation and CAR mRNA expression ... 102
5.1.4 Effect of electroporation on viability, CAR expression and activation ... 103
5.2 CAR library generation and possible improvements ... 106
5.3 CAR identification by cellular library screening ... 108
5.4 Outlook ... 111
6 **References** ... 112
7 **Appendix** ... 121
7.1 Supplementary data ... 121
7.1.1 Supplementary Figure 1: FACS/Flow Cytometry gating strategy ... 121
7.1.2 Supplementary Figure 2: Characteristics of reporter GFP+ LightningTM exports ... 122
7.1.3 Supplementary Figure 3: qPCR experiments ... 123
7.1.4 Supplementary Figure 4: Example amplicon sizes of recovered CARs from Lightning exports 124
7.1.5 Supplementary Figure 5: Sequencing quality, alignment and V gene annotations ... 125
7.1.6 Supplementary Table 1: Testing the effect of electroporated ligation product amount ... 130
7.1.7 Supplementary Table 2: The effect of primer purification on in frame sequences ... 130
7.2 Sequences and maps of the used plasmid DNA ... 131
7.3 List of figures ... 143
7.4 List of tables ... 144
7.5 Abbreviations ... 145
8 **Acknowledgements** ... 149

1 Introduction

1.1 State-of-the-Art cancer immunotherapy

Cancer ranks as a primary factor in worldwide mortality, causing nearly 10 million fatalities in 2020, which accounts for approximately one out of every six deaths [1]. In 2020, an estimated 18 million new cancer cases were reported [2]. It is a multidimensional disease that stems from modifications of the genome that result from the interaction between the individual's genetic makeup and their environment. Cells acquire several functional capabilities that enable them to form malignant tumors. Cancer cells grow independent from growth factors, and do not respond to signals that inhibit cell growth. Moreover, through loss of contact inhibition ability, they can proliferate in an uncontrolled manner while resisting cell death by circumventing apoptosis. Chronically activated angiogenesis results in formation of new blood vessels around the tumors to supply their metabolic demands. In addition, proliferating cancer cells also modify the metabolic composition of their surrounding extracellular environment. They create their microenvironment that is highly immunosuppressive [3, 4]. Until the emergence of immunotherapy, standard of care for cancer patients included surgery, radiotherapy and chemotherapy [5]. However, many patients were refractory to the treatment or had relapsed. Besides ineffectiveness, patients had to suffer from systemic side effects that affected their quality of life [6].

One of the main obstacles that malignant cells overcome is to escape from constant immune cell surveillance. The immune system is equipped with numerous receptors that can recognize and eliminate transforming cells. In fact, tumors are developed and get established by evading recognition by the immune system [7]. Therefore, invigorating the immune system for cancer therapy presents a promising approach. The first oncologic application of immunotherapy traces far back to 1891. William B. Colley, “Father of Immunotherapy”, was treating patients suffering from bone and soft-tissue sarcomas by injection of bacteria. This would successfully trigger the patients’ immune system and cause tumor shrinkage [8]. From 1891, cancer immunotherapy achieved incredible progress and became a monotherapy option for cancer patients. Currently, it is classified into 2 modalities: active and passive immunotherapy. In active immunotherapy, immune system of non-responsive patients are induced by application of e.g., cancer vaccines, immune checkpoint inhibitors or cytokines. These molecules then engage with the host immune system to stimulate antitumor activity. On the contrary, in passive immunization, patients receive agents that are equipped with intrinsic anti-tumor activity. Bispecific T cell engagers (BiTEs), bispecific antibodies (BsAbs), oncolytic viruses, tumor targeting monoclonal antibodies (mAbs) and cellular therapies fall into this category [9].

1.1.1 Active immunotherapies

Active immunotherapy agents activate the host existing immunity to trigger clearance of malignancies. The potency of this approach was revealed with immune checkpoint inhibitors (ICIs). These mAbs caused a major advancement in the field as their discovery and use in cancer immunotherapy was awarded with a Nobel Prize [10]. Immune checkpoint receptors, namely; programmed cell death protein 1 (PD1) and cytotoxic T-lymphocyte-associated protein 4 (CTLA4), are expressed by the activated T cells to terminate the immune reaction for prevention of possible over-reaction and autoimmunity [11]. In order to evade antitumor T cell activity, tumor cells induce expression of immunosuppressive cell surface

molecules such as programmed death-ligand 1 (PD-L1) [12]. In clinical trials, blocking PD-1/PD-L1 and CTLA-4 inhibitory axes with mAbs rescued the anti-tumor responses of T cells against solid tumors [13] [14]. As of 2023, there are 9 FDA approved mAbs targeting immune checkpoint proteins in treatment of variety of tumor entities [15]. However, accumulating data suggests that the effectiveness of the ICI therapy is restricted to the melanoma and non-small cell lung cancer (NSCLC) patients [16-18].

Besides immune checkpoint inhibitors, in 2010 Sipuleucel-T, a Dendritic cell (DC) vaccine, was approved by the Food Drug Administration (FDA) as a cell-based immunotherapy against prostate cancer [19]. In this therapy, autologous antigen presenting cells (APCs) are isolated from patient's peripheral blood. They are *ex vivo* matured and loaded with prostatic acid phosphatase (PAP), an antigen commonly expressed in prostate cancer. Consequently, activated APC prime patient's T cells for tumor eradication [20, 21].

In recent years, mRNA cancer vaccinations gained significant attention as they induced tumor specific CD4 and CD8 T cell responses [22-24] . In this treatment, mRNAs encoding patient derived tumor antigen are encapsulated within lipid nanoparticles. Upon injection, these particles are taken up by the DCs and tumor antigens are translated. They are processed by the native antigen presentation mechanism of the cells and presented by the major histocompatibility complex (MHC) class I and II to stimulate antigen specific CD8 and CD4 T cell populations, respectively [25]. Besides mRNA vaccines, short or long peptide vaccinations are used to invoke CD4 and CD8 T cell responses by targeting APCs [26]. Both CD4 and CD8 T cell responses have to be induced by the vaccination for optimal effector functions [27].

1.1.2 Passive immunotherapies

As mentioned earlier, passive immunotherapies do not depend on an active response against the tumor by the patient's immune system. In this modality, patients are infused with agents that are already designed to recognize and destroy tumor cells. Therefore, the result of this therapy can be observed immediately upon infusion.

As a passive therapy option, mAbs have become a standard of care treatment for both solid tumors and hematologic malignancies. Their specificity is determined by the fragment antigen-binding (Fab) region that targets tumor antigens with potentially nanomolar affinity. The choice of constant domain (Fc) in these antibodies defines the effector function that they carry out [28]. For example, certain Fc gamma receptors (FcγR) target the tumor cells to Fc receptors of macrophages or Natural Killer (NK) cells, leading to antibody-dependent cellular cytotoxicity (ADCC) [29, 30]. Moreover, with the same principle, mAbs can recruit complement system proteins to the target tumor cell and mediate their lysis by complement-dependent cytotoxicity (CDC) [31]. mAbs are also used in combination with cytotoxic drugs to formulate antibody-drug conjugates (ADCs) that can specifically target and kill tumor cells. ADCs Ibritumomab tiuxetan and tositumomab-Iodine-131 were approved by FDA for treatment of non-Hodgkin's lymphoma as early as 2002 and 2003, respectively [32, 33]. Even though these drugs were ruled out, currently there are 11 FDA approved ADC targeting both solid and hematological malignancies [34].

Unlike mAbs, bsAbs express two Fab regions with two different specificities. They are used as "IgG-like" molecules and carry out all the functions mentioned above for mAbs through their Fc domains [35]. However, "non-IgG-like" bsAbs do not contain an Fc domain. As they have 2 single-chain variable fragment (scFv) regions, they are used to bring two different cell types in proximity. BiTEs falls into this

category. While one arm of the BiTE binds to CD3 expressed on T cells, the other arm recognizes an antigen expressed by the tumor cells. Therefore, bystander T cells are recruited to the proximity of the tumor cells. BiTEs cause CD3 clustering on the recruited T cells' surface, leading to the activation of the T cells in the absence of costimulation and TCR-pMHC engagement. Consequently, activated T cell perform lysis of the tumor cells. [36, 37]. Blinatumomab, a BiTE therapy targeting CD19, was granted approval by the FDA in 2014 for treatment of relapsed or refractory (r/r) B-cell precursor acute lymphoblastic leukemia (B-ALL) [38, 39].

1.2 Adoptive T cell therapy

In the recent decade, adoptive T cell therapy (ACT) has emerged to treat patients with late-stage malignancies. It is a highly personalized immunotherapy in which the patient receives tumor specific autologous lymphocytes [40]. Encouraging results have been observed in clinical trials where patients received *ex vivo* expanded tumor-infiltrating lymphocytes (TILs) that were isolated from their resected tumor [41, 42]. Besides TILs, T cells found in the peripheral blood mononuclear cells (PBMCs) isolated from cancer patients and engineered to express chimeric antigen receptors (CARs) or T cell receptors (TCRs) recognizing a tumor antigen (Figure 1.2.1) [43]. Due to their incredible success in treating hematological malignancies, CD19 targeting CAR T cells received FDA approval [44]. As of 2019, ACT became the second to ICIs in terms of the number active of clinical trials for cancer immunotherapy [45].

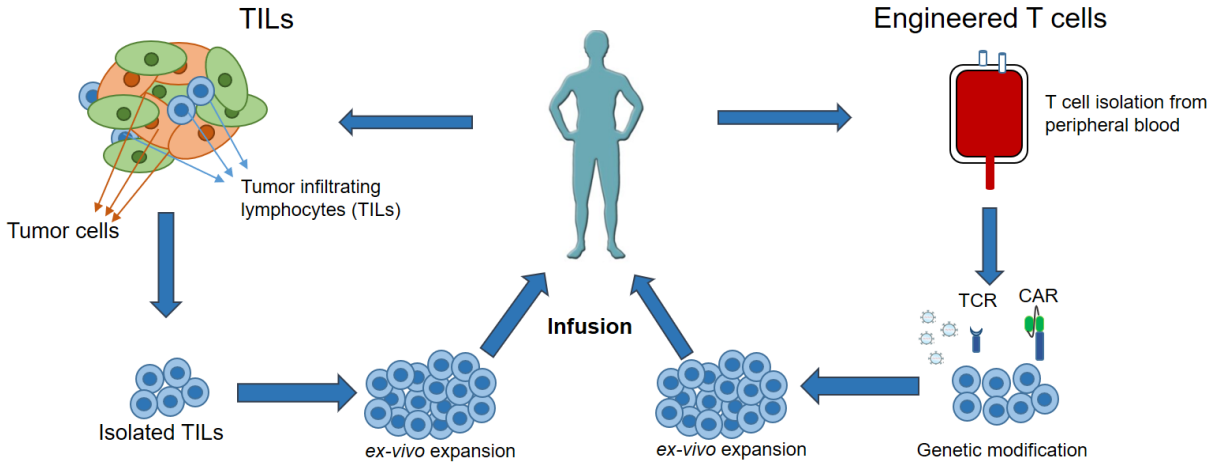

Figure 1.1.2.1: Current landscape in adoptive T cell therapy. The first ACT trials were done by isolation and expansion of TILs from resected tumors. As these T cells are isolated directly from the tumors, they are expected to contain tumor-reactive T cell clones that would lead to tumor eradication upon infusion. On the other hand, in TCR T and CAR T cell therapies, T cells are isolated from peripheral blood of the patients. They are genetically modified to express a transgenic CAR or TCR that is specific for the antigens presented on the patients' tumor. T cells modified with a tumor antigen-specific receptor are then ex vivo expanded to be infused back into the patient.

The first ACT reported in medical history came from Steven Rosenberg's group in 1994 where they isolated TILs from metastatic melanoma patients. These TILs were then *ex vivo* expanded and infused back into the patient [46]. In the following years, promising objective tumor responses were observed in several phase I/II clinical trials with TILs isolated from metastatic melanoma patients [41, 42, 47]. Besides melanoma, TILs with varying reactivity were successfully produced in different tumor entities like breast cancer [48], renal cell cancer [49] and cervical cancer [50]. Despite its clinical success, TIL therapy proved to be a challenging task. As high as 70% drop out rate was reported during TIL production. Moreover,

due to lengthy expansion protocols, the products were deemed unbeneficial as rapid progression of the patients' tumors [51].

On the other hand, in TCR transgenic T cell therapy, T cells of the patient are isolated from the peripheral blood and these autologous cells are *ex vivo* expanded to be genetically engineered with a tumor antigen specific α/β TCR. Engineered cells are infused back into the patient for tumor regression [52]. Since cells are transduced with a TCR, their epitope recognition is restricted to MHC presentation. Due to wide variety in HLA types in the human population, broad application of an isolated TCR is still challenging [53]. However, MHC restriction provides a window of opportunity for TCR T cells. Since MHC Class I proteins can present peptides derived from any synthesized intracellular protein, there is almost no antigen restriction. The first ever application of TCR T cells dates back to 2004. T cells from 17 metastatic melanoma patients were transduced with a TCR recognizing melanoma-melanocyte differentiation antigen 1 (MART-1) antigen as 80-95% of melanoma cases express this antigen [54, 55]. Although there is no FDA approved TCR T cell therapy available, remarkable outcomes have been observed in clinical trials. For example, to prolong relapse-free survival of acute myeloid leukemia (AML) patients after allogeneic hematopoietic cell transplantation (HCT), patient's T cells were transduced with a high affinity TCR against Wilms' Tumor Antigen 1 (WT1). All patients achieved relapse free survival for median 44 months, while concurrent comparative group had 54% relapse free survival [56]. However, when a high affinity TCR against MART-1 was used in a trial, severe off-tumor, on-target toxicity was observed in the ears, eyes and skin of the patients due to destruction healthy melanocytes [57]. Moreover, treatment related deaths occurred when TCR T cells recognized another related epitope present in the grey matter of the brain besides their target. The epitope presented in the brain was different from the therapeutic target but both epitopes were derived from the same protein family [58]. Thus, epitope selection and affinity have to be fine-tuned to be able to eliminate the cancer cells while sparing the healthy tissue.

1.2.1 CAR T cell therapy

Similar to TCR T cells, CAR T cells are generated by engrafting CARs into patient's autologous T cells. CARs combine B cell like antigen recognition with T cell proficiency in cytotoxicity [59]. They consist of an scFv derived from a B cell receptor (BCR) for antigen recognition, a transmembrane (TM) domain and intracellular signaling domains responsible for T cell activation [60]. Unlike TCRs, antigen recognition by CARs do not require peptide presentation by MHC molecules. This restricts potential CAR targets to cell surface proteins. However, the same CAR construct can be used for treating a cohort of patients expressing the same antigen, independent from their HLA haplotypes. Impressive clinical outcomes were obtained in treatment of B cell malignancies by using anti-CD19 CAR T cells. In two separate trials, r/r ALL patients achieved 70% and 90% complete remissions upon infusion with CD19 CAR T cells [44, 61]. In another study with CD19 CAR T cells, overall response rate in chronic lymphocytic leukemia (CLL) patients was 57% [62]. As mentioned before, the efficacy of CD19 CAR T cells led to their approval by FDA for treatment of several B cell malignancies. Currently there are 4 CD19 targeting and 2 B- cell maturation antigen (BCMA) targeting CAR T cell therapies approved by FDA [63]. Several side effects have been observed when patients were treated with CAR T cell products. Cytokine release syndrome (CRS) happens onset of infusion of the cell products and the severity of the syndrome is correlated with

the tumor burden [64]. CRS is characterized by the induction of IL-1, IL-6 and IFNγ secretion caused by the activation of infused products [65]. However, severe cases of CRS found to be manageable by blocking IL-6 signaling pathway [66]. More severe side effect observed in CD19 CAR T cell therapy is the neurotoxicity. Symptoms of neurotoxicity includes confusion, encephalopathy, seizures and in rare cases results in death [67].

The first ever generated CAR T cells established in the 1990s, termed as first generation CAR T cells, consisted of an scFv fragment, a hinge and TM domain connecting antigen recognition with CD3 ζ chain intracellular signaling domain to mediate T cell activation [68]. The 4 iterative generations that CARs undergone during their development is depicted in Figure 1.2.1.1. The efficacy of first generation CARs were underwhelming due to lack of *in vivo* persistence of the infused cell [69, 70]. In early 2000s, it was revealed that inclusion of CD28 costimulatory domain in CAR design induces IL-2 secretion and enhances proliferation and persistence of CAR T cells [71, 72]. Engineering the first generation CAR construct by placing a costimulatory domain membrane proximal to CD3 ζ chain resulted in the second generation of CAR T cells. Most prominent costimulatory domains used in second generation CARs were CD28 [61] and 4-1BB [44]. Both versions of second generation CARs achieved outstanding remission rates for the treatment of B cell malignancies and as mentioned before the CAR T cell therapy has become the first transgenic T cell products to be approved by the FDA. Impressively, patients infused with a second generation 4-1BB CAR targeting CD19 sustained functional CAR T cells and remained in remission nearly a decade after the treatment [73].

Considerable differences were observed between CD19 CAR T cells used in the trials with respect to the costimulatory domain. CD28 costimulation found to be causing a robust expansion upon antigen contact followed by a rapid contraction phase. This is reflected in the long term survival of the CAR T cells as most of the patients had B cell recovery around 60 days post infusion, suggesting that persistence was limited to 2 months [61] [74]. CAR T cells were found to be mostly driven to effector memory phenotype [75]. On the other hand, CD19 CAR T cells with 4-1BB costimulation found to have a slower expansion kinetic. Furthermore, larger cell population differentiated into central memory like T cells upon 4-1BB costimulation [75]. These consequently boosted the persistence of CD19 CAR T cells as median duration of B cell aplasia after infusion found to be 11 months [76]. Besides CD28 and 4-1BB; CD27 [77], ICOS [78] and OX40 [79] costimulatory domains were also investigated in preclinical settings. The anti-tumor responses observed in CARs expressing CD27, ICOS and OX40 were found be mirroring the slower reaction kinetics of 4-1BB CARs, but CAR T cells expressing these molecules achieved higher degree of anti-tumor function with enhanced proliferation and persistence.

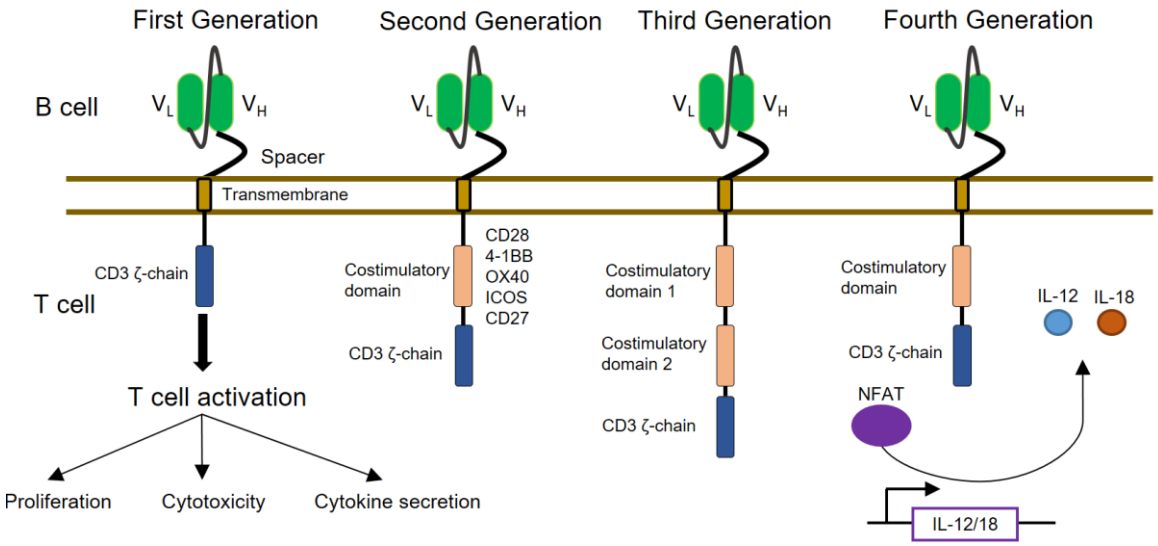

Figure 1.2.1.1: Generations of CAR constructs. The first generation of CAR constructs consist of a scFv domain, a spacer, a TM domain and a CD3 ζ chain. The antigen recognition is done by a scFv that is derived from a BCR. The scFv is linked to the cell membrane by a spacer and a TM domain, that bridge the antigen recognizing B cell part with the signal transduction domain CD3 ζ chain that is derived from a T cell. When the scFv of a CAR engages with a target antigen, CD3 ζ chain starts several signaling cascades that provide CAR T cells with proliferation, cytotoxicity and cytokine secretion. In the second and third generations of CAR constructs, one or two costimulatory domains were added membrane proximal to the CD3 ζ chain to enhance the activity and persistence of CAR T cells. Most commonly used costimulatoty domains are CD28, 4-1BB, OX40, ICOS and CD27. In 4th generation CAR T cells, also known as TRUCKs, are additionally engineered with an NFAT mediated transgene expression cassette to become living factories for cytokine secretion in the tumor proximity.

In order to increase the potential anti-tumor activity and persistence of CAR T cells, third generation CAR constructs were generated by addition of a secondary costimulatory domain. In preclinical models, third generation CARs with CD28 and 4-1BB costimulatory domains outperformed their second-generation counterparts with improved tumor lysis, proliferation and persistence [80, 81]. In a concluded phase I clinical trial, consistent with preclinical data, third-generation CD19 CAR T cells with CD28 and 4-1BB co-stimulatory domains were found to be superior to their second-generation CD28 counterpart with enhanced T cell expansion and persistence [82]. Currently there are two clinical trials running with third-generation CD19 CAR T cells to further evaluate their clinical relevance [83, 84]. In a preclinical study, OX40 costimulation rescued the CD28 derived apoptotic tendency observed in anti-CEA CAR T cells [85]. In another study, 2 third-generation anti-CD30 CARs incorporating either CD28+OX40 or CD28+4-1BB costimulatory domains were compared in preclinical settings. It was found that anti-CD30 CD28+OX40 CAR T cells showed superior anti-tumor activity with prolonged persistence. Only the mice treated with CD28+OX40 CAR T cells were able reject the tumors upon a rechallange [86].

In fourth-generation of CAR T cells, activated T cells were engineered to express a transgene of interest by introducing synthetic nuclear factor of activated T-cells (NFAT) response elements followed by a minimal IL-2 promoter. This concept turns functional CAR T cells into factories for secretion of pro-inflammatory cytokines to facilitate better infiltration and activation of immune cells in a locally restricted manner in the tumor vicinity. Therefore, this generation is also called as T cells redirected for antigen-unrestricted cytokine-initiated killing (TRUCKs) [87]. As CD3ζ-mediated NFAT signaling pathway is

shared between both CAR T cells and TCR T cells, TRUCKs are generated with T cells expressing a transgenic TCR [88]. In preclinical models, TRUCKs engineered to express IL-12 or IL-18 upon antigen engagement lead to complete eradication of tumors by providing better infiltration of CAR T cells into tumor lesions and recruiting innate immunity elements like macrophages [89, 90].

1.2.2 CAR T cell activation

To understand the activation of CAR T cells, it is crucial to understand how a T cell is activated upon antigen-specific stimulation as the activation of CAR T cells is driven by mimicking the signaling through the same pathways. The α/β TCR-CD3 complex which consist of α/β TCR heterodimer, one CD3γ, one CD3δ, two CD3ε, and 2 CD3ζ chains. Besides CD3ζ chain that contains 3 immunoreceptor tyrosine-based activation motifs (ITAMs), the rest of the CD3 chains comprise one ITAM per molecule. Thus, in total a TCR complex include 10 ITAMs. The signal transduction in T cells start with the initiation of TCR peptide-MHC interaction stabilized by TCR co-receptors CD4/CD8. This interaction causes activation of lymphocyte-specific protein tyrosine kinase (Lck) and in turn, Lck phosphorylates the tyrosine residues in the ITAMs. Phosphorylated ITAMs serve as docking sites for ZAP70, another kinase crucial for signal transduction. Docked ZAP70 is phosphorylated by Lck and ZAP70 initiates the phosphorylation of further downstream targets like linker of activation in T cells (LAT) and phospholipase Cγ (PLC-γ) that leads to gene expression changes facilitating T cell activation [91-93].

Phosphorylated PLC-γ catalyzes phosphatidylinositol bisphosphate (PIP_2) into inositol trisphosphate (IP_3) and diacylglycerol (DAG). IP_3 causes release of Ca^{2+} from endoplasmic reticulum (ER) to cytosol. Increasing Ca^{2+} concentration in the cytosol activates a calcium dependent phosphatase calcineurin which in turn dephosphorylates NFAT. This causes influx of NFAT to the nucleus where it acts as transcription factor (TF) for genes responsible for T cell activation and proliferation. DAG and increased Ca^{2+} concentration activates protein kinase C (PKC) which later activates nuclear factor 'kappa-light-chain-enhancer' of activated B-cells (NF-κB) that translocates into nucleus and act as a TF like NFAT. Lastly, ZAP70 induces a phosphorylation cascade, activated mitogen-activated protein (MAP) kinase facilitates the formation of Activator protein 1 (AP-1) TF, another pillar for expression of T cell specific genes. Thus, TFs NFAT, NF-κB and AP-1 cause expression of new set of genes responsible for activation, differentiation and effector function of T cells upon antigen-specific stimulation [94].

Besides TCR-pMHC interaction initiated signaling, co-stimulatory receptors found in T cells greatly amplifies the magnitude of TCR driven signaling together with facilitating the expression of completely new set of genes. CD28, one of the most studied co-stimulatory receptor, is constitutively expressed in naïve T cells to assure proper T cell activation. CD28 interacts with B7 family molecules B7-1 (CD80) and B7-2 (CD86) that are expressed by activated APC. This interaction initiates 3 different signal transduction cascades from 3 independent motifs found in its cytoplasmic domain [95]. These cascades share a great deal of downstream signaling pathways initiated by TCR-pMHC interaction, thus converging on activation of NFAT, NF-κB and AP-1 TFs [96]. OX40 is another co-stimulatory molecule that is expressed upon antigen-specific stimulation. The signal transduction from OX40 is initiated by interaction with OX40 ligand (OX40L) expressed by activated APCs. OX40 signaling results in expression of non-apoptotic proteins that mediate T cell clonal expansion and memory formation [97]. It has been shown that OX40 signaling also activates NFAT [98], and NF-κB [99] pathways.

By signaling via the CD3ζ chain, all CAR generations are able to use the same pathways for T cell activation as it happens in TCR mediated signaling. In 2nd and 3rd generation CAR constructs, inclusion of signaling domains of co-stimulatory molecules on top of CD3ζ chain can compensate for the lack of 7 ITAMs to some extent. The success observed in third-generation CAR T cells can be attributed to cumulative effect of CD3ζ, CD28 and OX40 signaling to drive T cell activation, differentiation and effector function [85, 86].

1.3 Tumor antigens

Cancer eradication with transgenic T cell therapies relies on the recognition of tumor antigens by the infusion products. Tumor antigens have been classified into two categories: tumor-associated antigens (TAAs) and tumor-specific antigens (TSAs). TAAs are self, non-mutated epitopes that show abnormal expression in tumor cells. Generally, they were found to be weakly immunogenic due to central T cell tolerance [100]. Some TAAs are expressed linage specific manner and their expression are limited to a duration in fetal development. As mentioned before, targeting an oncofetal antigen, WT1, achieved unpresented success in treatment against AML [56]. Cancer testis antigens (CTAs) are another category of TAAs and they are expressed by human germ line, but not by healthy tissues. Their frequent re-expression in tumor cells have made them ideal target for ACT [101]. Currently, there are several TCR T therapies in development against CTAs [102]. Overexpressed antigens like CEA, hTERT, and HER2, can also be targeted as they occur in certain epithelial cancers. However, targeting these antigens resulted in mild to severe side effects. In a clinical trial with a TCR T cells recognizing a CEA epitope, besides tumor regression, severe transient colitis was observed [103]. Similarly, targeting HER2 caused a range of adverse effects in the lungs, gastrointestinal tract and liver of the patients [104]. On the other hand, two phase I clinical trials performed with CAR T cells targeting HER2 [105] and CEA [106] demonstrated safety and feasibility.

In contrast to TAA, TSAs are neoantigens derived from tumor-specific genomic alterations. They are not expressed by the healthy tissue and T cells are not negatively selected against these antigen during their thymic development. Therefore, TSAs are highly immunogenic and targeting these epitopes possess little no adverse toxicity as they are absent in the healthy tissue [107]. TSAs occur due to single-nucleotide variants (SNVs), base insertions and deletions (in/dels), gene fusions, aberrant splicing events, post-translational modifications and oncogenic viruses [100]. The ICI and TIL therapies try to reinvigorate CD8 T cell responses against these antigens. In recent years, next-generation sequencing allowed detection of tumor-specific neoantigens in a cost efficient manner and subsequently enabled development of highly individualized cancer vaccines and ACT products [108].

1.4 Problems associated with CAR T cell therapy

Although durable responses observed in r/r ALL patients treated with CD19 CAR T cells, high rate of recurrence has been observed due to a common tumor escape mechanism, which is antigen loss [109]. The same resistance mechanism has occurred in multiple myeloma (MM) patients treated with anti-BCMA CAR T cells [110]. To solve this problem, dual tumor antigen targeting CAR constructs have been developed [111]. According to preliminary data from several clinical studies, dual antigen targeting resulted in improved anti-tumor responses [112, 113].

Unlike B cell malignancies, CAR T cells targeting solid tumors face a series of problems that severely limits their clinical use. After administration, CAR T cells are insufficiently trafficked to the tumor site due to altered chemokine signature of the tumor cells. Matching chemokine receptors in CAR T cells with chemokines secreted by the tumor showed enhanced recruitment of the CAR T cells to the tumor sites [114]. After migrating to the tumor site, tumor stroma acts as a physical barrier preventing CAR T cells from proper infiltration. Cells have to pass through a dense extracellular matrix composed of heparin sulfate proteoglycan (HSPG). To solve this problem and improve the infiltration and anti-tumor activity of CAR T cells, T cells are genetically modified to express heparanase, an enzyme that catalyzes HSPG, to thin the extracellular matrix [115].

Upon proper infiltration, CAR T cells are exposed to highly immunosuppressive tumor microenvironment (TME). Tumor cells upregulate the expression of PD-L1 that abolishes the ability of T cells to expand and persist in TME. Moreover, regulatory T cells (Tregs), tumor-associated macrophages (TAMs) and myeloid-derived suppressor cells (MDSCs) can promote further inhibition of the CAR T cell activity by secretion of immunosuppressive cytokines [116]. Combining CAR T cell therapy with ICIs offers improved performance of CAR T cells [117]. In a phase I trial, PD1 blockade with CAR T cell infusion demonstrated safety, feasibility and enhanced T cell activity and persistence [118]. The immunosuppressive environment of TME when combined with chronic antigen stimulation drives CAR T cells towards an “exhausted” phenotype. Exhausted T cells are no longer able to perform their effector function, thus resulting in the failure of the ACT. Expression of PD-L1 in an acidic and hypoxic TME further inhibits T cell activation and accelerates their exhaustion [119]. Besides chronic antigen dependent signaling, CAR T cells have proven to get exhausted by tonic signaling. Tonic signaling is caused by antigen-independent multimerization of CARs on the cell surface [120]. This multimerization results in constitutive signaling through NFAT, NF-κB and kinases activated during CAR mediated signal transduction. This drives CAR T cells to get activated in the absence of any antigen stimulation and induce secretion of cytokines, proliferation and progression of differentiation to more effector phenotypes, subsequently resulting in diminished *in vivo* functionality [121]. Recently, evidence suggests that the positively charged patches (PCPs) found in scFvs facilitates the antigen independent multimerization of the CARs, leading to tonic signaling. Mutating positively charged amino acids into uncharged amino acids reduced the level of tonic signaling [122].

On the other hand, the number of CAR molecules used in clinical trials is rather limited with respect to their antigen specificity. Overwhelming majority of the CAR T cell trials are done with CARs targeting several B cell antigens. With regards to solid tumors, a handful of TAAs like Mesothelin, Mucin 1, HER2, CEA are targeted by CAR T cell therapies [123]. Limited number of identified CARs to be used in ACT arsenal is underwhelming considering the heterogeneity and possible targets in diverse tumor entities. Therefore, new CAR constructs that are specific against the diverse tumor antigens need to be identified to make CAR T cell therapy applicable to broader range of patients.

1.5 scFv phage display libraries for *de novo* CAR identification

Currently, the golden standard for CAR identification is construction and screening of scFv phage display libraries. In early 1990s, John McCafferty and Gregory Winter established the first scFv phage display libraries by cloning scFv sequences into ORF of filamentous phage coat protein III (pIII). This resulted

in capsid formation with human scFv-phage pIII phusion that displayed the scFv on the phage surface [124]. Generated phage library was then bound to an antigen-immobilized surface and bound phages were isolated to have their antigen-reactive scFv sequences analyzed. Before the use of immunoglobulin (IG) loci humanized transgenic mouse models in generation of hybridoma cells [125, 126], only scFv phage display libraries offered isolation of human mAbs for therapeutic use that does not evoke any immune reaction in the host that they were applied. The groundbreaking mAb isolation platforms received 2 Nobel prizes in the last decades. As Georges Köhler and César Milstein who were awarded with Nobel prize in 1984 for inventing the hybridoma technology, while George Smith and Gregory Winter received Nobel prize in 2018 for developing phage display libraries of peptides and scFvs [124] [127, 128].

As illustrated in Figure 1.5.1, establishment of scFv phage display libraries starts with amplification of human variable heavy (V_H) and light chain (V_L) sequences. Amplified V_H and V_L sequences are linked together with a flexible Glycine-Serine linker [129]. Assembled scFv sequences are then cloned into a phagemid vector into the ORF of pIII capsid protein. Electrocompetent bacteria are electroporated with the scFv library ligated phagemid plasmid vectors. With the use of helper phages, bacteriophages displaying scFv are isolated to be layered onto an antigen-coated surface in a process called “panning”. Panning ensures binding of phages expressing an antigen-specific scFv to the surface. The unbound phages are washed and bound phages are eluted from the surface to be reamplified in bacteria. The panning and reamplification process is repeated for 2 to 6 times to increase the specificity of the scFvs. After the last panning process, selected phages’ genomes are sequenced to identify the antigen-specific scFvs. Isolated scFv sequences are then cloned into a CAR vector for CAR T cell [130, 131].

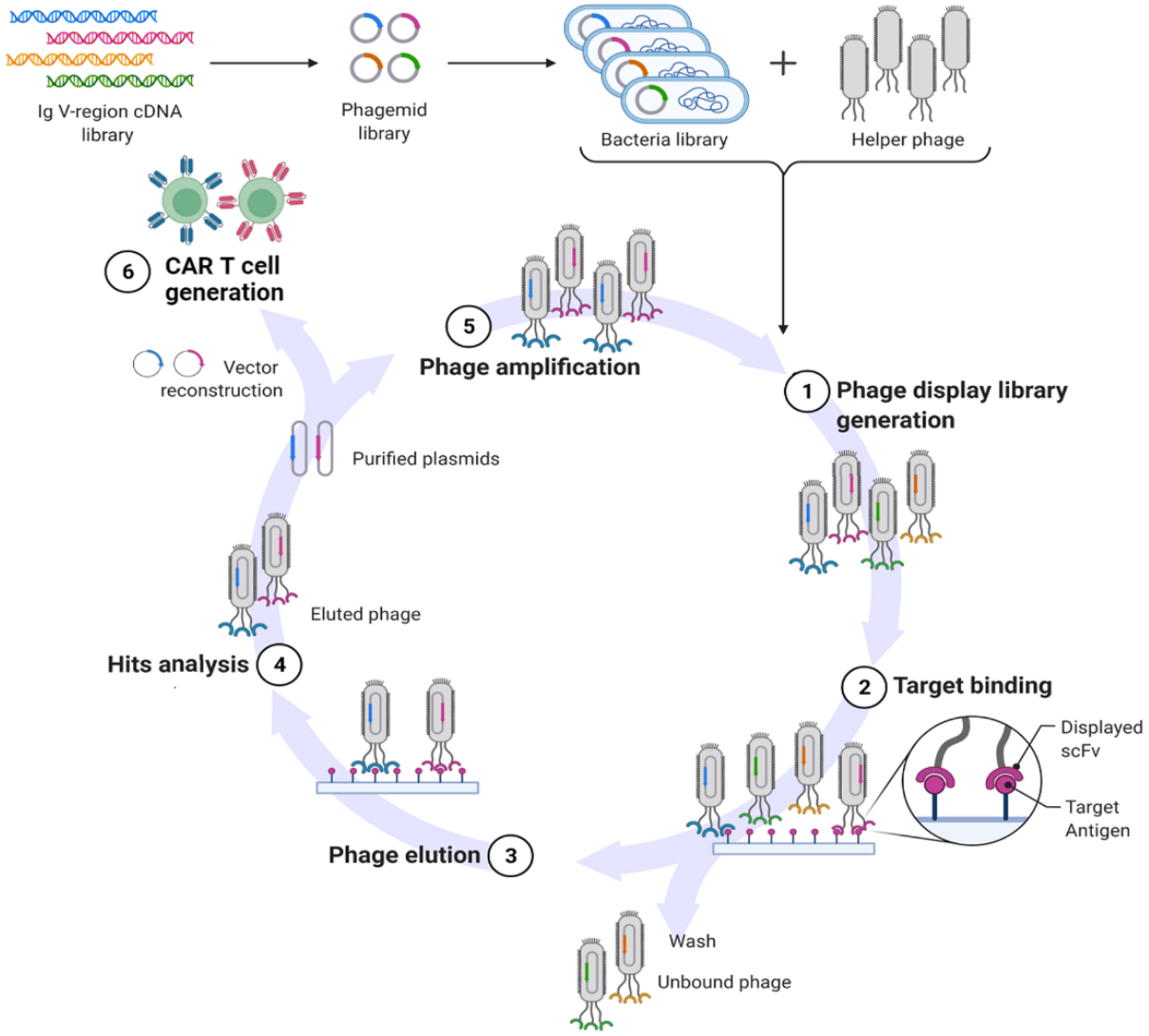

Figure 1.5.1: scFv phage display screening platform. Human variable IG sequences are amplified from a cDNA library. Amplified variable heavy and light chains are randomly assembled and cloned into phagemid plasmids. Bacteria is electroporated with the ligation products and phagemid library is rescued by the addition of helper phages. The generated phage library presents the scFv fragments in their capsid formation. The library is then panned onto an antigen coated surface. Phages that present antigen-reactive scFvs get anchored to the surface and unbound phages are washed. Bound phages are eluted to be reamplified in bacteria. This panning process is repeated 2-6 times depending on the intended affinity. The more panning process is performed, the higher the affinity of scFvs against the cognate antigen gets. Isolated hits are sequenced to obtain antigen-specific scFv sequences. Finally, scFvs are cloned into a functional CAR construct for generation of CAR T cells.

In late 2010s, Eric Smith and Renier Brentjens have successfully identified 2 scFvs against MM antigens, BCMA [132] and GPRC5D [133] by using scFv phage display libraries. Their lead scFvs gave rise to functional CAR constructs and demonstrated *in vivo* tumor eradication and memory formation in CAR T cells tested by tumor rechallange. Currently, both developed CAR constructs are tested in phase I clinical trials [134, 135]. Despite their success in development of functional CAR constructs, authors performed several rounds of validations of the isolated clones after panning. Validated clones still had to be cloned into a CAR backbone individually to check if they give rise to a functional CAR construct.

In these studies, they observed high tonic signaling in several of their lead CAR candidates. Consequently, isolation of these 2 CAR constructs would have taken the researchers around half a year. Although scFv phage display library screening gives rise to highly specific and functional CAR constructs, it is a challenging task to use it for generating personalized CAR T cells therapies due to the associated time and effort intensive CAR isolation procedure. For this purpose, alternative, high-throughput screening platforms have to be developed to accelerate identification of functional CARs.

1.6 nanoS/MARt vectors in development of ACT products

So far, the majority of TCR T or CAR T cell used in clinical trials were generated by engrafting the autologous T cells with lentiviral [134] or gamma-retroviral transduction [118]. During production of transgenic T cells for ACT, every material used must be produced according to good manufacturing practice (GMP) guidelines. This strict compliance to GMP guidelines significantly increases the associated cost of generation of ACT agents. It is estimated that only the cost of GMP grade viral particle production constitutes to 66% of the whole expense [136]. Thus, alternatively, GMP compliant genetic engineering systems are needed to lower the production cost. The use of Sleeping Beauty (SB) transposon/transposase system for engraftment of CAR sequences offers a solution to the problem [137]. On the other hand, despite resulting stable engraftment of the cells with the transgene, both viral transductions and transposon systems possess random integration associated risks. So far, no genotoxicity was observed in the clinical trials with virally transduced T cells. However, in a recent phase I trial with a transposon/transposase system *piggyBac*, 2 out of 10 patients developed CD19 CAR T cell lymphoma. This was the first trial that used a transposase system, and development of lymphoma immediately raised safety concerns about T cell engineering with *piggyBac* [138]. Transfection of T cells with mRNA encoding for the CAR or TCR overcomes both the cost and random integration associated problems. However, mRNA transfection results in transient expression of the transgene. In order for total tumor eradication, patients may need to receive several subsequent doses of transfected T cells that may not be possible to manufacture [139].

Use of plasmid with scaffold/matrix attachment region (S/MAR) motifs provides episomal maintenance of these vectors in mitotically active cells. As these plasmids bind to nuclear matrix proteins, they do not possess any random integration capability. Moreover, they replicate during cell division, thus providing persistent expression of the transgene in daughter cells [140]. Large quantities of GMP grade plasmids can be produced in a cost-efficient manner. Therefore, plasmids containing S/MAR sequences show potential to solve the problems associated with current ACT agent production. For this purpose, Bozza and colleagues developed pS/MARt vectors by removal of 1.5kb from 3kb bacterial backbone present in Plasmid Episomal (pEPI) [141]. The pEPI vectors were developed in 1999 as the first non-viral plasmid vector system that possessed an S/MAR sequence and retained in low copy number in mammalian cells [142]. pS/MARt vectors were further developed into next generation nanoS/MARt DNA vectors by removal of CpG islands and majority of bacterial sequences like origin of replication and antibiotics resistance. It has been shown that nanoS/MARt vectors provide efficient transfection of activated primary T cells with minimum toxicity. These vectors consist of only clinically approved sequences and do not pose any immunogenicity [141]. They possess an antibiotics free RNA-OUT selection system that is used in combination with a special DH5α strain. The genome of this DH5α strain has been engineered to

express the levansucrase enzyme. Levansucrase metabolizes sucrose into a toxic compound that leads to cell death. A small interference RNA is encoded by the minimal bacterial backbone in nanoS/MARt vectors that binds and inhibits the translation of levansucrase mRNA. Therefore, successfully transformed cells survive in a selection media containing sucrose and start to proliferate [143]. In preclinical xenograft mouse models, CAR T cells generated with nanoS/MARt vectors outperformed their counterparts generated with lentiviral transduction in terms of anti-tumor activity [141].

1.7 Microfluidics systems for antigen-specific TCR/BCR identification

During the last decade, development of microfluidics systems accelerated the identification of antigen-specific TCR and BCR sequences from single cells. In this innovative technologies, individual cells are separated into oil drops as small as pico to nanoliter range. These cells are then subjected to single-cell RT-PCR followed by immunoreceptor gene amplification [144]. In recent studies, single B cells or T cells were encapsulated within microdroplets and cells were either stimulated with target cells or stained against an epitope of interest within these compartments. The droplets containing antigen-reactive cells were separated from the rest of the population. Subsequently, immunoreceptor sequences from single cells were amplified and sequenced with varying recovery rates [145-147].

One such technology developed specifically for single-cell level immunological applications is Bruker's Lightning™ device (Figure 1.7.1 A, left). In this technology, immune cells are imported into an OptoSelect™ chip that has 1535 cavities called "pens" with 40µm x 40µm x 370µm dimensions for width, depth and length, respectively (Figure 1.7.1 A, right). Single cells imported to the channels of the chip are enclosed in an electric field gradient generated by using light. These light cages apply enough force to move objects like cells or beads to desired pens (Figure 1.7.1 B). This unique manipulation of cell movement is termed as optoelectro-positioning (OEP™). As this technology utilizes light assisted microfluidics to move the cells, it is also called an optofluidics system. The chip is supplied with growth media throughout the experiment. Thus, single cells in pens proliferate for a desired period to give rise to single-cell derived colonies (Figure 1.7.1 C) [148].

Besides proliferation, on-chip real-time functional assays can be performed and visualized by using 5 fluorescent filter cubes. Figure 1.7.1 D illustrates an example assay that Lightning™ device is capable of conducting. CAR T cells that are engineered with an NFAT responsive reporter construct to express a fluorescent protein (FP) are incubated together with antigen coupled beads. Cells expressing a functional CAR construct that is specific for the antigen presented by the beads get activated and start expressing the reporter FP. According to the excitation and emission spectrum of the FP expressed by the cells, the chip is then imaged with the respective fluorescent filter cube in defined interval. After overnight incubation, reactive cells are identified by the analysis of the whole chip for reporter FP expression. Subsequently, reactive cells can be proliferated inside the pens or directly be exported for further off-chip applications like further proliferation or sequencing. The most significant advantage of this technology over fluorescence-activated cell sorting (FACS) is that, single cells can be screened in real-time for their functionality and desired cells could be gently recovered from the device by causing minimum stress to the cells. During the COVID-19 pandemic, broadly neutralizing antibodies against the spike protein of COVID-19 were identified in an unprecedented pace by using the optofluidics technology [149, 150].

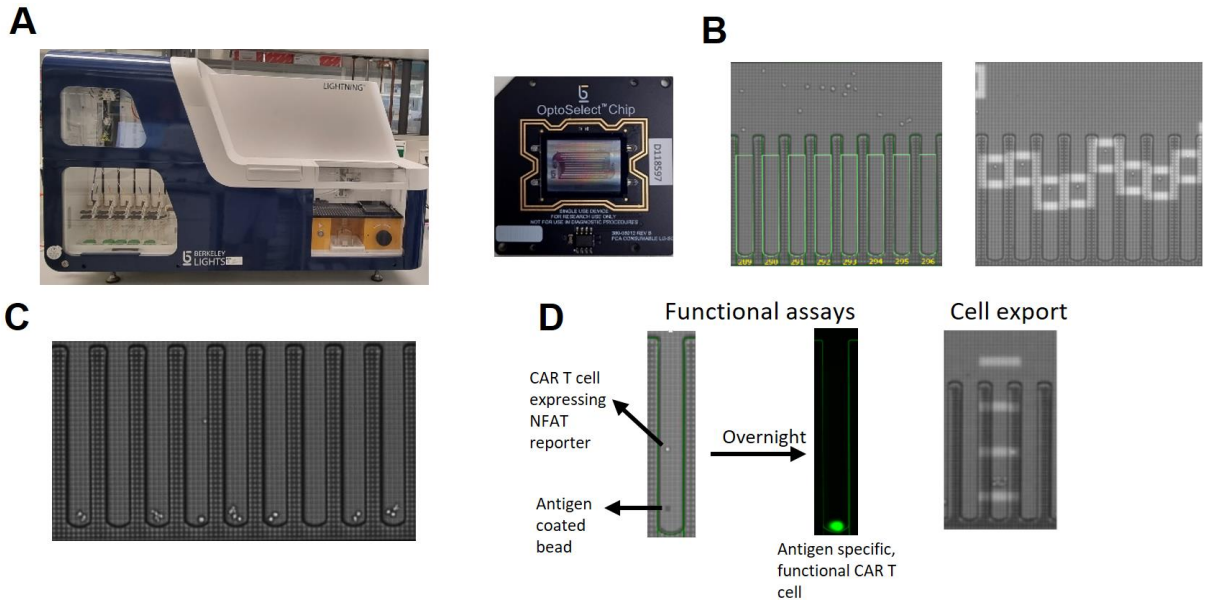

Figure 1.7.1: Single-cell assays by using Bruker's Lightning™ device. A: (Left) An image of the Lightning™ device located in DKFZ main building is shown. (Right) An illustration of OptoSelect™ chip that contains 1535 nanometric scale pens. **B:** (Left) The cells imported into the channel areas of an OptoSelect™ chip are shown. (Right) Penning of single cells is depicted. Single cells are encapsulated into a light cage by using the OEP™ technology. Due to the generated electrical field gradient, cells are moved individually to respective pens. **C:** A representative image of cells cultured inside the OptoSelect™ chip. **D:** An example functional assay that is performed by using the Lightning™ device. CAR T cells with an NFAT responsive reporter element is co-incubated with antigen coupled beads. After overnight incubation, cells expression an antigen-specific functional CAR construct get activated by the presented antigen and upregulate the expression of reporter FP. The chip is imaged in the respective fluorescent filter that allows the detection of FP expressed by activated cells. Identified antigen-specific CAR T cells can be exported from the Lightning™ device for further off-chip applications.

1.8 Aim of the study

As mentioned earlier, state-of-the-art for identification of CAR constructs is scFv phage display libraries. However, with this platform reaching the final product, that is an antigen-specific functional CAR, takes considerable amount of time. Therefore, this platform fails to yield personalized CAR T cell products in a time frame that a cancer patient can still benefit from the applied therapy. Thus, with this project, an innovative screening platform was developed by combining cellular CAR libraries with single-cell microfluidic analysis. This platform aims to shorten the time required for CAR identification from months to weeks, so that patients may receive individualized CAR T cell therapies as a standard of care. To achieve this goal, cellular CAR libraries are generated by engrafting a nanoS/MARt plasmid CAR library into Jurkat cells expressing an NFAT mediated FP reporter. This cellular CAR library is then pre-enriched for an antigen of interest. Enriched cells are stimulated in single-cell resolution with antigen coupled beads by using the Lightning™ device. Identified Jurkat cells expressing an antigen-specific CAR are exported from the Lightning™ device to have their CARs sequenced. Finally, obtained CAR sequences are subjected to functional validation.

2 Materials

2.1 Equipments

Equipment	Manufacturer
Biophotometer plus	Eppendorf
Bunsen burner	Campingaz
CKX31 Microscope	Olympus
CKX41 Microscope	Olympus
Compact Fluorescent Microscope	Keyence
EG Präzisionswaage	Kern
FACS Canto™ II	BD Biosciences
FACS Symphony A3	BD Biosciences
Fragment Analyzer	Agilent
GridION	Oxford Nanopore Technologies
HERAcell 240i	ThermoFisher Scientific
HERAEUS Multifuge X1R	ThermoFisher Scientific
HULA mixer	ThermoFisher Scientific
Innova® 44 Incubator Shaker	New Brunswick
L8-70M Ultracentrifuge	Beckmann
LightCycler 480 II	Roche
Lightning™	Bruker
MagDTR 96-Well Magnetic Separator	Edge Biosystems
Magnetic Stand -96	Invitrogen
MicroPulser™ Electroporation Apparatus	Bio-Rad
ExPERT GTx®	MaxCyte
Mini Vortex Mixer	ThermoFisher Scientific
NanoDrop ONE	ThermoFisher Scientific
Neon Transfection System	ThermoFisher Scientific
Power Pac 300	Bio-Rad
PowerPac HC	Bio-Rad
ROTINA 420 R	Hettich
Quantum-ST4	Peqlab Biotechnologie GmbH
Qubit™ 3.0 Fluorometer	ThermoFisher Scientific
Sub Cell ® GT	Bio-Rad
T3000 Thermocycler	Biometra

2.2 Consumables

2.2.1 General Consumables

Product	Catalog Number	Manufacturer
14 ml PP Tube	187261	Greiner Bio-One
15 ml Conical Polypropylene Tube	188271	Greiner Bio-One
175 ml graduated Conical tube	352076	Falcon
5 ml PS round bottom with Cell Strainer cap	352235	Falcon
50 ml Conical Polypropylene Tube	227261	Greiner Bio-One
50 ml Plastipak Syringe	300866	BD
Amicon Ultra-15, Centrifugal Filter, 50kDa	UFC905024	Merck
Cell Culture dishes (15 cm)	353025	Falcon
Cell Culture Flask (T175)	660175	Greiner Bio-One
Cell Culture Flask (T25)	690175	Greiner Bio-One
Cell Culture Flask (T75)	658175	Greiner Bio-One
Cell Culture Microplate (96 well, Flat-bottom)	655180	Greiner Bio-One
Cell Culture Microplate (96 well, U-bottom)	650185	Greiner Bio-One
Cell Culture Microplate (96 well, V-bottom)	651160	Greiner Bio-One
Cell Culture Multiwell Plate (24 well)	662102	Greiner Bio-One
Cell Culture Multiwell Plate (48 well)	677180	Greiner Bio-One
Cell Culture Multiwell Plate (6 well)	657160	Greiner Bio-One
Cell Stack culture chamber	3313	Corning
Centricon® Plus-70	UFC703008	Merck Millipore
CryoTube TM Vials	377267	ThermoFisher Scientific
Disposable Cell Counting Plate	177-112C	Watson Biolab
GenePulser™ Cuvettes	165-2089	Bio-Rad
Multiply™ µStrip Pro 8-stripe	71.991.02	SARSTEDT
Nalgene™ 250 mL conical PPCO tube	3143-0175	ThermoFisher Scientific
Needle (20G x 0,90X40mm)	CH20112	Medoject
Neon™ tips	MTK10096T	Invitrogen
Sealing Mats	AB0674	ThermoFisher Scientific
Syringe 50 mL	309628	BD
Twin.tec PCR Plates 96 Lobind Semi-skirted	0030129504	Eppendorf

2.2.2 Bruker Consumables

Product	Catalog Number
Cleaning Solution	520-08000
Flush Chip	500-00045
OptoSelect™ 1500 Chip	500-13001
Wetting Additive	520-08016
Wetting Solution	520-00009

2.2.3 MaxCyte Consumables

Product	Catalog Number
CL-2™ GMP	GCL-2
Electroporation Buffer, Large	EPB-5
OC-100x™	SOC-1x2
OC-25x3™	SOC-25x3
R-1000™	ER001M1-10
R-50x8™	ER050U8-03

2.2.4 Oxford Nanopore Technologies Consumables

Product	Catalog Number
Flow Cell (R10.4.1)	FLO-MIN114
Flow Cell (R9.4.1)	FLO-MIN106D
Flow Cell Priming Kit	EXP-FLP004
Flow Cell Wash Kit	EXP-WSH004
Native Barcoding Kit 96 V14	SQK-NBD114.96

2.3 Standard Kits

Kit name	Catalog Number	Manufacturer
EndoFree Plasmid Maxi Kit (10)	12362	QIAGEN
HS NGS Fragment Kit	DNF-474-0500	Agilent
HS RNA Kit (15NT)	DNF-472-0500	Agilent
Maxima H Minus First Strand cDNA Synthesis kit	K1652	ThermoFisher Scientific
Monarch DNA Gel Extraction Kit	T1020	New England Biolabs
Monarch Plasmid Miniprep Kit	T1010	New England Biolabs
NucleoBond Xtra Maxi Plus EF Kit	740426.50	Machery-Nagel
NucleoBond Xtra Midi Kit	740410	Machery-Nagel

PureLink™ RNA Mini Kit	12183018A	Invitrogen
Platinum™ II Hot-Start Green PCR Master Mix (2X)	14001013	Invitrogen
Platinum™ SuperFi™ II Green PCR Master Mix (2X)	12369010	Invitrogen
ReliaPrep™ RNA Miniprep Systems	Z6011	Promega
QIAquick PCR Purification Kit	28104	QIAGEN
qPCRBIO SyGreen Mix Hi-ROX	PB20.12	PCR Biosystems
Qubit™ dsDNA HS Assay Kit	Q32851	Invitrogen

2.4 Chemicals, media and additives

Product	**Catalog number**	**Manufacturer**
10X T4 DNA Ligase	B0202S	New England Biolabs
20% arabinose	-	Kindly provided by AG Harbottle
50 % sucrose	-	Kindly provided by AG Harbottle
Adhesive PCR Plate Seals	AB0558	ThermoFisher Scientific
Agar-Agar	1347.2	Carl Roth
Agarose	16500500	ThermoFisher Scientific
Albumin Fraktion V (BSA)	T844.4	Carl Roth
Ambion™ Nuclease-Free Water	AM9932	Invitrogen
AMPure XP beads	A63880	Beackman Coulter
ATP Solution 25mM	SS000408-D1	Biosearch Technologies
B27™ Plus	A3582801	ThermoFisher Scientific
Bacto™ Agar	-	BD Biosciences
Buffer TCL 2x	1070498	QIAGEN
Carbenicillin disodium salt	6344.2	Carl Roth
CutSmart Buffer	B7204	New England Biolabs
Dimethyl Sulfoxide (DMSO)	20385	Serva
DMEM + GlutaMAX™-I	61965-026	ThermoFisher Scientific
DMEM, high glucose, no glutamine, no phenol red	31053028	ThermoFisher Scientific

DNA Ladder, 100 bp	N3231	New England Biolabs
DNA Ladder, 1kb	N3232	New England Biolabs
DNA AWAY™ Surface Decontaminant	7010	ThermoFisher Scientific
DPBS (1X)	14190-094	ThermoFisher Scientific
Dynabeads™ M-270 Streptavidin	65305	Invitrogen
Ethanol 99%	32221	Sigma-Aldrich
Ethidium Bromide	2218.1	Carl Roth
Ethylenediaminetetraacetic acid (EDTA)	E5134	Sigma-Aldrich
FCS	P40-47500	PAN-Biotech
Ficoll	17-1440-03	ThermoFisher Scientific
Gel Loading Dye, Purple (6X)	B7024	New England Biolabs
Glycerol 87% BioChemica	A0970	AppliChem
Hydrogen chloride (HCl)	4625	Carl Roth
Isopropanol	33539	Sigma-Aldrich
Kanamycin	T832.1	Carl Roth
Minreal oil	M5904	Sigma-Aldrich
NEBNext Ultra II End Prep Reaction Buffer	E7647AVIAL	New England Biolabs
NEBNext® Quick Ligation Reaction Buffer	B6058	New England Biolabs
Opti-MEM™ I no phenol red	11058021	ThermoFisher Scientific
Pen/ Strep (Penicillin Streptomycin)	15070-063	ThermoFisher Scientific
Phytohemagglutinin-L (PHA-L)	11249738001	Roche
Plasmid-Safe™ 10X Reaction Buffer	SS000272-D8	Lucigen
PureProteaome™ Streptavidin Magnetic Beads	LSKMAGT02	MerckMillipore
Recovery Media	46-0706	ThermoFisher Scientific
RNAClean XP Beads	A63987	Beckmann Coulter
RNase AWAY™ Surface Decontaminant	7002PK	ThermoFisher Scientific
RPMI 1640 no phenol red	11835030	ThermoFisher Scientific
RPMI 1640 + GlutaMAX™-I	61870-010	ThermoFisher Scientific
SOC medium	636763	Takara Bio

Sodium Acetate	S2889-250G	Sigma-Aldrich
Sodium azide (NaN3)	S2002	Sigma-Aldrich
Sodium chloride (NaCl)	3957	Carl Roth
T4 DNA Ligase Reaction Buffer	B0202	New England Biolabs
Terrific-Broth vegetal	8952.1	Carl Roth
Tris	4855	Carl Roth
Trypan blue	T8154	Sigma-Aldrich
TrypLE™ Express Enzyme (1X)	12605010	ThermoFisher Scientific
Trypsin-EDTA	25300-054	ThermoFisher Scientific
Tryptone	8952.1	Carl Roth
Yeast extract	2363.3	Carl Roth

2.5 Antibodies and proteins

Antibody	**Clone**	**Host**	**Catalog number**	**Manufacturer**
anti-human CD2 APC conjugated	RPA-2.10	mouse	300214	BioLegend
anti-human CD66 PE conjugated	-	mouse	551480	BD
AffiniPure F(ab')2 Fragment anti-hIgG, Fcγ Fragment specific, APC conjugated	polyclonal	goat	109-136-098	Jackson Immuno Research
AffiniPure F(ab')2 Fragment anti-hIgG, Fcγ Fragment specific, AF647 conjugated	polyclonal	goat	109-606-098	Jackson Immuno Research
Biotinylated Human CEACAM-5 / CD66e Protein, His,Avitag™	-	HEK293	CE5-H82E0	ACRO Biosystems
THE™ His Tag Antibody iFluor 647 conjugated	6G2A9	mouse	A01802	GenScript

2.6 Enzymes

Enzyme	**Catalog number**	**Manufacturer**
DNaseI from bovine pancreas	D4263	Merck
NEB Blunt/TA Ligase Master Mix	M0367	New England Biolabs
NEBNext Ultra II End repair/dA-tailing Module	E7546	New England Biolabs
NEBNext Quick Ligation Module	E6056	New England Biolabs
NheI HF	R3131S	New England BioLabs
NotI HF	R3189S	New England BioLabs
Plasmid-Safe™ ATP-Dependent DNase	E0054-10D1	Biosearch Technologies
T4 DNA Ligase	M0202	New England BioLabs

2.7 Bacteria Strains

Strain	Catalogue number	Description	Supplier
E. coli DH10B	C640003	High efficiency electrocompetent bacteria	ThermoFisher Scientific
E. coli DH5α	-	IP of Nature technologies that hosts nanoS/MAR plasmids	Nature Technologies
E. coli XL-1	-	Lab-grown chemo-competent bacteria	-

2.8 Plasmids

2.8.1 Lentiviral plasmids

Plasmid Name	Description
pCMV-VSV-G	Lentiviral helper plasmid that encodes for envelope protein VSV-G
pCMV-dR874	Lentiviral helper plasmid that encodes for HIV-gag and HIB-pol proteins
pRRL-cPPT-hEF1a-scFv06-hFc-hCD28tm-h4-1BB-hCD3z-WPRE	Lentiviral transfer vector that encodes for scFv isolated from barcode 6 in the CAR format scFv06-hFc-hCD28tm-h4-1BB-hCD3z
pRRL-cPPT-hEF1a-scFv11-hFc-hCD28tm-h4-1BB-hCD3z-WPRE	Lentiviral transfer vector that encodes for scFv isolated from barcode 11 in the CAR format scFv11-hFc-hCD28tm-h4-1BB-hCD3z
#53: pRRL-cPPT-hPGK-Lk-flag-SCA431scFv-hFc-hCD28tm-hCD3z-hOX40-WPRE	Lentiviral transfer vector that encodes for model mouse derived anti-CEA SCA431 scFv in the CAR format hPGK-Lk-flag-SCA431scFv-hFc-hCD28tm-hCD3z-hOX40

2.8.2 S/MAR plasmids

Plasmid Name	Description
#272: p/SMARt-Lk-flag-SCA431scFv-hFc-hCD28-hCD3z-hOX40-apolipoB SMAR	pS/MARt plasmid backbone that encodes for model mouse derived anti-CEA SCA431 scFv in the CAR format SCA431scFv-hFc-hCD28-hCD3z-hOX40-apolipoB MAR
#320: nanoS/MARt-Lk-flag-CEAscFv-hFc-hCD28-hCD3z-hOX40-COREapolipoB SMAR	nanoS/MARt plasmid backbone that encodes for model mouse derived anti-CEA SCA431 scFv in the CAR format SCA431scFv-hFc-hCD28-hCD3z-hOX40- COREapolipoB SMAR

#1468: nanoS/MARt-Lk-flag-CEAscFv-hFc-hCD28-hCD3z-hOX40-ApoI CMAR	nanoS/MARt plasmid backbone that encodes for model mouse derived anti-CEA SCA431 scFv in the CAR format SCA431scFv-hFc-hCD28-hCD3z-hOX40- ApoI CMAR
#1475: p/SMARt-Lk-flag-scFv06-hFc-hCD28-hCD3z-hOX40-apolipoB SMAR	pS/MARt plasmid backbone that encodes for scFv isolated from barcode 6 in the CAR format SCA431scFv-hFc-hCD28-hCD3z-hOX40-apolipoB SMAR
#1477: p/SMARt-Lk-flag-scFv11-hFc-hCD28-hCD3z-hOX40-apolipoB SMAR	pS/MARt plasmid backbone that encodes for scFv isolated from barcode 11 in the CAR format SCA431scFv-hFc-hCD28-hCD3z-hOX40-apolipoB SMAR

2.8.3 Other plasmids

Plasmid Name	**Description**
pcDNA3.1(-)	Mammalian expression vector that contains CMV promoter. CMV promoter is followed by an MCS in the reverse (-) orientation
pUC19	Plasmid provided with MegaX DH10B T1R Electrocomp™ Cells for positive control during electroporation

2.9 Primers

2.9.1 Pansri et al. desalted primers

Primer	**Sequnce 5' to 3'**
V_H5'-NheI	
VH5'-NheI 1	CCTTTCTATGCGCTAGCATGGCCCAGGTGCAGCTGGTGCAGTCTGG
VH5'-NheI 2	CCTTTCTATGCGCTAGCATGGCCGAGGTACAGCTGCAGCAGTCAGG
VH5'-NheI 3	CCTTTCTATGCGCTAGCATGGCCCAGGTCAACTTAAGGGAGTCTGG
VH5'-NheI 4	CCTTTCTATGCGCTAGCATGGCCGAGGTGCAGCTGGTGGAGTCTGG
VH5'-NheI 5	CCTTTCTATGCGCTAGCATGGCCCAGGTGCAGCTGCAGGAGTCGGG
VH5'-NheI 6	CCTTTCTATGCGCTAGCATGGCCGAGGTGCAGCTGTTGCAGTCTGC
V_H3'linker	
VH3'link 1	ACCAGAGCCGCCGCCGCCGCTACCACCACCACCTGAGGAGACGGT GACCAGGGTGCC
VH3'link 2	ACCAGAGCCGCCGCCGCCGCTACCACCACCACCTGAGGAGACGGT GACCGTGGTCCC
VH3'link 3	ACCAGAGCCGCCGCCGCCGCTACCACCACCACCTGAAGAGACGGT GACCATTGTCCC
VH3'link 4	ACCAGAGCCGCCGCCGCCGCTACCACCACCACCTGAGGAGACGGT GACCAGGGTTCC

V_L5'link-κ	
VL5'link-κ 1	AGCGGCGGCGGCGGCTCTGGTGGTGGTGGATCCGACATCCAGATG ACCCAGTCTCC
VL5'link-κ 2	AGCGGCGGCGGCGGCTCTGGTGGTGGTGGATCCGAAATTGTGCTG ACTCAGTCTCC
VL5'link-κ 3	AGCGGCGGCGGCGGCTCTGGTGGTGGTGGATCCGATGTTGTGAT GACTCAGTCTCC
VL5'link-κ 4	AGCGGCGGCGGCGGCTCTGGTGGTGGTGGATCCGAAATTGTGTTG ACGCAGTCTCC
VL5'link-κ 5	AGCGGCGGCGGCGGCTCTGGTGGTGGTGGATCCGACATCGTGATG ACCCAGTCTCC
VL5'link-κ 6	AGCGGCGGCGGCGGCTCTGGTGGTGGTGGATCCGAAACGACACTC ACGCAGTCTCC
V_L5'link-λ	
VL5'link-λ 1	AGCGGCGGCGGCGGCTCTGGTGGTGGTGGATCCAATTTTATGCTGA CTCAGCCCCA
VL5'link-λ 2	AGCGGCGGCGGCGGCTCTGGTGGTGGTGGATCCCAGTCTGTGTTGA CGCAGCCGCC
VL5'link-λ 3	AGCGGCGGCGGCGGCTCTGGTGGTGGTGGATCCCAGTCTGCCCTGA CTCAGCCTGC
VL5'link-λ 4	AGCGGCGGCGGCGGCTCTGGTGGTGGTGGATCCTCCTATGTGCTGA CTCAGCCACC
VL5'link-λ 5	AGCGGCGGCGGCGGCTCTGGTGGTGGTGGATCCTCTTCTGAGCTGA CTCAGGACCC
VL5'link-λ 6	AGCGGCGGCGGCGGCTCTGGTGGTGGTGGATCCCACGTTATACTGA CTCAACCGCC
VL5'link-λ 7	AGCGGCGGCGGCGGCTCTGGTGGTGGTGGATCCCAGGCTGTGCTCA CTCAGCCGTC
V_L3'NotI-κ	
VL3'NotI-κ 1	CAGTCATTCTCGACTTGCGGCCGCACGTTTGATTTCCAGCTTGGTCCC
VL3'NotI-κ 2	CAGTCATTCTCGACTTGCGGCCGCACGTTTAATCTCCAGTCGTGTCCC
VL3'NotI-κ 3	CAGTCATTCTCGACTTGCGGCCGCACGTTTGATCTCCAGCTTGGTCCC
VL3'NotI-κ 4	CTCGACTTGCGGCCGCACGTTTGATATCCACTTTGGTCCC
VL3'NotI-κ 5	CTCGACTTGCGGCCGCACGTTTGATCTCCACCTTGGTCCC
V_L3'NotI-λ	
VL3'NotI-λ 1	CAGTCATTCTCGACTTGCGGCCGCACCTAAAACGGTGAGCTGGGTCCC
VL3'NotI-λ 2	CTCGACTTGCGGCCGCACCTAGGACGGTGACCTTGGTCCC
VL3'NotI-λ 3	CTCGACTTGCGGCCGCACCTAGGACGGTCAGCTTGGTCCC
PT-PCR	

PT forward	CCTTTCTATGCGCTAGCATGGCC
PT reverse	CAGTCATTCTCGACTTGCGGCCGCACG

2.9.2 Self-designed desalted library amplification primers

Primer	**Sequence 5' to 3'**
Leader Sequence	
Leader Reverse	GGAGTGTACACCTCTAGACATT
hPGK forward	GTTGACCGAATCACCGACCTC
V_H5'-Leader	
MHVH1/7	AATGTCTAGAGGTGTACACTCCCAGGTGCAGCTGGTGCAGTCTGG
MHVH2	AATGTCTAGAGGTGTACACTCCCAGGTCACCTTGAAGGAGTCTGG
MHVH3 1	AATGTCTAGAGGTGTACACTCCGAGGTGCAGCTGGTGGAGTCTGG
MHVH3 2	AATGTCTAGAGGTGTACACTCCGAGGTGCAGCTGGTGGAGTCCGG
MHVH4 1	AATGTCTAGAGGTGTACACTCCCAGGTGCAGCTGCAGGAGTC
MHVH4 2	AATGTCTAGAGGTGTACACTCCCAGGTGCAGCTACAGCAGTGGGG
MHVH5	AATGTCTAGAGGTGTACACTCCGAAGTGCAGCTGGTGCAGTCCGG
MHVH6	AATGTCTAGAGGTGTACACTCCCAGGTACAGCTGCAGCAGTCAGG
V_H3'linker	
HuJH1-2	ACCAGAGCCGCCGCCGCCGCTACCACCACCACC TGAGGAGACGGTGACCAGGGTGCC
HuJH3	ACCAGAGCCGCCGCCGCCGCTACCACCACCACC TGAAGAGACGGTGACCATTGTCCC
HuJH4-5	ACCAGAGCCGCCGCCGCCGCTACCACCACCACC TGAGGAGACGGTGACCAGGGTTCC
HuJH6	ACCAGAGCCGCCGCCGCCGCTACCACCACCACC TGAGGAGACGGTGACCGTGGTCCC
V_L5'link-λ	
MHVL1	AGCGGCGGCGGCGGCTCTGGTGGTGGTGGATCC CAGTCTG TGTTGACGCAGCCGCC
MHVL1 2	AGCGGCGGCGGCGGCTCTGGTGGTGGTGGATCC CAGTCTG TGCTGACTCAGCCACC
MHVL2	AGCGGCGGCGGCGGCTCTGGTGGTGGTGGATCC CAGTCTGC CCTGACTCAGCCT
MHVL3 1	AGCGGCGGCGGCGGCTCTGGTGGTGGTGGATCC TCCTATGAG CTGACTCAGCCA
MHVL3 2	AGCGGCGGCGGCGGCTCTGGTGGTGGTGGATCC TCCTATGAG CTGACACAGCTAC

MHVL3 3	AGCGGCGGCGGCGGCTCTGGTGGTGGTGGATCC TCTTCTGAG CTGACTCAGGACCC
MHVL3 4	AGCGGCGGCGGCGGCTCTGGTGGTGGTGGATCC TCCTCTGGG CCAACTCAGGTGCC
MHVL4 1	AGCGGCGGCGGCGGCTCTGGTGGTGGTGGATCC CTGCCTGTG CTGACTCAGCCCCC
MHVL4 2	AGCGGCGGCGGCGGCTCTGGTGGTGGTGGATCC CAGCCTGTG CTGACTCAATC
MHVL5-9	AGCGGCGGCGGCGGCTCTGGTGGTGGTGGATCC CAGCCTGTG CTGACTCAGCCA
MHVL5 2	AGCGGCGGCGGCGGCTCTGGTGGTGGTGGATCC CAGGCTGTG CTGACTCAGCCGTC
MHVL6	AGCGGCGGCGGCGGCTCTGGTGGTGGTGGATCC AATTTTATGC TGACTCAGCCCCA
MHVL7-8	AGCGGCGGCGGCGGCTCTGGTGGTGGTGGATCC CAGACTGTG GTGACTCAGGAGCC
MHVL10	AGCGGCGGCGGCGGCTCTGGTGGTGGTGGATCC CAGGCAGG GCTGACTCAGCCACC
MHVL11**	AGCGGCGGCGGCGGCTCTGGTGGTGGTGGATCC CGGCCCGT GCTGACTCAGCCGCC
V_L3'NotI-λ	
HuJl1	CTCGACTTGCGGCCGC ACCTAGGACGGTGACCTTGGTCCC
Hu Jl2-3	CTCGACTTGCGGCCGC ACCTAGGACGGTCAGCTTGGTCCC
HuJl4	CTCGACTTGCGGCCGC ACCTAAAATGATCAGCTGGGTTCC
HuJl5	CTCGACTTGCGGCCGC ACCTAGGACGGTCAGCTCGGTCCC
HuJl6	CTCGACTTGCGGCCGC ACCGAGGACGGTCACCTTGGTGCC
HuJl7	CTCGACTTGCGGCCGC ACCGAGGACGGTCAGCTGGGTGCC
V_L5'link-κ	
MHVK1 1	AGCGGCGGCGGCGGCTCTGGTGGTGGTGGATCC GACATCCAGATGACCCAGTCTCC
MHVK1 2	AGCGGCGGCGGCGGCTCTGGTGGTGGTGGATCC GCCATCCGGATGACCCAGTCTCC
MHVK2 1	AGCGGCGGCGGCGGCTCTGGTGGTGGTGGATCC GATGTTGTGATGACTCAGTCTCC
MHVK2 2	AGCGGCGGCGGCGGCTCTGGTGGTGGTGGATCC GATATTGTGATGACCCAGACTCC
MHVK3 1	AGCGGCGGCGGCGGCTCTGGTGGTGGTGGATCC GAAATTGTGTTGACGCAGTCTCC

MHVK3 2	AGCGGCGGCGGCGGCTCTGGTGGTGGTGGATCC GAAATTGTGATGACGCAGTCTCC
MHVK4	AGCGGCGGCGGCGGCTCTGGTGGTGGTGGATCC GACATCGTGATGACCCAGTCTCC
MHVK5	AGCGGCGGCGGCGGCTCTGGTGGTGGTGGATCC GAAACGACACTCACGCAGTCTCC
MHVK6	AGCGGCGGCGGCGGCTCTGGTGGTGGTGGATCC GAAATTGTGCTGACTCAGTCTCC
V_L3'NotI-κ	
HuJk1	CTCGACTTGCGGCCGC ACGTTTGATTTCCACCTTGGTCCC
HuJk2	CTCGACTTGCGGCCGC ACGTTTGATCTCCAGCTTGGTCCC
HuJk3	CTCGACTTGCGGCCGC ACGTTTGATATCCACTTTGGTCCC
HuJk4	CTCGACTTGCGGCCGC ACGTTTGATCTCCACCTTGGTCCC
HuJk5	CTCGACTTGCGGCCGC ACGTTTAATCTCCAGTCGTGTCCC
PT-PCR	
PT forward	CCTTTCTATGCGCTAGCATGGCC
PT reverse	CAGTCATTCTCGACTTGCGGCCGCACG

2.9.3 PAGE purified library amplification primers

Primer	**Sequence 5' to 3'**
HUJH1-2	ACCAGAGCCGCCGCCGCCGCTACCACCACCACCTGAGGAGACGGTGAC CAGGGTGCC
HUJK1	CTCGACTTGCGGCCGCACGTTTGATTTCCACCTTGGTCCC
MHVK1 1	AGCGGCGGCGGCGGCTCTGGTGGTGGTGGATCCGACATCCAGATGACC CAGTCTCC
MHVH1/7	AATGTCTAGAGGTGTACACTCCCAGGTGCAGCTGGTGCAGTCTGG

2.9.4 Working HPLC purified library amplification primers

Primer	**Sequences 5' to 3'**
Leader Sequence	
Leader Reverse	GGAGTGTACACCTCTAGACATT
hPGK forward	GTTGACCGAATCACCGACCTC
V_H5'-Leader	
MHVH1/7	AATGTCTAGAGGTGTACACTCCCAGGTGCAGCTGGTGCAGTCTGG
MHVH2	AATGTCTAGAGGTGTACACTCCCAGGTCACCTTGAAGGAGTCTGG
MHVH3 1	AATGTCTAGAGGTGTACACTCCGAGGTGCAGCTGGTGGAGTCTGG

MHVH3 2	AATGTCTAGAGGTGTACACTCCGAGGTGCAGCTGGTGGAGTCCGG
MHVH4 1	AATGTCTAGAGGTGTACACTCCCAGGTGCAGCTGCAGGAGTC
MHVH4 2	AATGTCTAGAGGTGTACACTCCCAGGTGCAGCTACAGCAGTGGGG
MHVH5	AATGTCTAGAGGTGTACACTCCGAAGTGCAGCTGGTGCAGTCCGG
MHVH6	AATGTCTAGAGGTGTACACTCCCAGGTACAGCTGCAGCAGTCAGG
V_H3'linker	
HuJH1-2	ACCAGAGCCGCCGCCGCCGCTACCACCACCACCTGAGGAGACGGT GACCAGGGTGCC
HuJH3	ACCAGAGCCGCCGCCGCCGCTACCACCACCACCTGAAGAGACGGTG ACCATTGTCCC
HuJH4-5	ACCAGAGCCGCCGCCGCCGCTACCACCACCACC TGAGGAGACGGTGACCAGGGTTCC
HuJH6	ACCAGAGCCGCCGCCGCCGCTACCACCACCACC TGAGGAGACGGTGACCGTGGTCCC
V_L5'link-λ	
MHVL1	AGCGGCGGCGGCGGCTCTGGTGGTGGTGGATCC CAGTCTGTGTTGA CGCAGCCGCC
MHVL1 2	AGCGGCGGCGGCGGCTCTGGTGGTGGTGGATCC CAGTCTGTGCTGA CTCAGCCACC
MHVL2	AGCGGCGGCGGCGGCTCTGGTGGTGGTGGATCC CAGTCTGCCCTGA CTCAGCCT
MHVL3 1	AGCGGCGGCGGCGGCTCTGGTGGTGGTGGATCC TCCTATGAGCTGA CTCAGCCA
MHVL3 2	AGCGGCGGCGGCGGCTCTGGTGGTGGTGGATCC TCCTATGAGCTGA CACAGCTAC
MHVL3 3	AGCGGCGGCGGCGGCTCTGGTGGTGGTGGATCC TCTTCTGAGCTGA CTCAGGACCC
MHVL4 1	AGCGGCGGCGGCGGCTCTGGTGGTGGTGGATCC CTGCCTGTGCTGA CTCAGCCCCC
MHVL4 2	AGCGGCGGCGGCGGCTCTGGTGGTGGTGGATCC CAGCCTGTGCTGA CTCAATC
MHVL5-9	AGCGGCGGCGGCGGCTCTGGTGGTGGTGGATCC CAGCCTGTGCTGA CTCAGCCA
MHVL5 2	AGCGGCGGCGGCGGCTCTGGTGGTGGTGGATCC CAGGCTGTGCTGA CTCAGCCGTC
MHVL6	AGCGGCGGCGGCGGCTCTGGTGGTGGTGGATCC AATTTTATGCTGAC TCAGCCCCA
MHVL7-8	AGCGGCGGCGGCGGCTCTGGTGGTGGTGGATCC CAGACTGTGGTGA CTCAGGAGCC

MHVL10	AGCGGCGGCGGCGGCTCTGGTGGTGGTGGATCC CAGGCAGGGCTGA CTCAGCCACC
V_L3'NotI-λ	
HuJl1	CTCGACTTGCGGCCGC ACCTAGGACGGTGACCTTGGTCCC
Hu Jl2-3	CTCGACTTGCGGCCGC ACCTAGGACGGTCAGCTTGGTCCC
HuJl5	CTCGACTTGCGGCCGC ACCTAGGACGGTCAGCTCGGTCCC
HuJl6	CTCGACTTGCGGCCGC ACCGAGGACGGTCACCTTGGTGCC
HuJl7	CTCGACTTGCGGCCGC ACCGAGGACGGTCAGCTGGGTGCC
V_L5'link-κ	
MHVK1 1	AGCGGCGGCGGCGGCTCTGGTGGTGGTGGATCCGACATCCAGATGAC CCAGTCTCC
MHVK1 2	AGCGGCGGCGGCGGCTCTGGTGGTGGTGGATCCGCCATCCGGATGAC CCAGTCTCC
MHVK2 1	AGCGGCGGCGGCGGCTCTGGTGGTGGTGGATCCGATGTTGTGATGAC TCAGTCTCC
MHVK2 2	AGCGGCGGCGGCGGCTCTGGTGGTGGTGGATCCGATATTGTGATGAC CCAGACTCC
MHVK3 1	AGCGGCGGCGGCGGCTCTGGTGGTGGTGGATCCGAAATTGTGTTGAC GCAGTCTCC
MHVK3 2	AGCGGCGGCGGCGGCTCTGGTGGTGGTGGATCCGAAATTGTGATGAC GCAGTCTCC
MHVK4	AGCGGCGGCGGCGGCTCTGGTGGTGGTGGATCCGACATCGTGATGAC CCAGTCTCC
MHVK5	AGCGGCGGCGGCGGCTCTGGTGGTGGTGGATCCGAAACGACACTCAC GCAGTCTCC
MHVK6	AGCGGCGGCGGCGGCTCTGGTGGTGGTGGATCCGAAATTGTGCTGAC TCAGTCTCC
V_L3'NotI-κ	
HuJk1	CTCGACTTGCGGCCGCACGTTTGATTTCCACCTTGGTCCC
HuJk2	CTCGACTTGCGGCCGCACGTTTGATCTCCAGCTTGGTCCC
HuJk3(848)	CTCGACTTGCGGCCGCACGTTTGATATCCACTTTGGTCCC
HuJk4(849)	CTCGACTTGCGGCCGCACGTTTGATCTCCACCTTGGTCCC
HuJk5	CTCGACTTGCGGCCGCACGTTTAATCTCCAGTCGTGTCCC
PT-PCR	
PT Reverse	CAGTCATTCTCGACTTGCGGCCGCAC
PT Forward new	CCGAAGCCGCTAGCATGGATT

2.9.6 qPCR primers

Primer [10μM]	Sequence 5' to 3'
β-actin forward	CACCATTGGCAATGAGCGGTTC
β-actin reverse	AGGTCTTTGCGGATGTCCACGT
Venus forward	ACGTAAACGGCCACAAGTTC
Venus reverse	AAGTCGTGCTGCTTCATGTG
Anti-CEA CAR forward	GACTACAAAGACGAGCAGGTCCAACTG
Anti-CEA CAR reverse	CCCGCCACCGCCCGATCCACCTCC

2.9.5 Library Sanger sequencing primers

Primer	Sequence 5' to 3'
hPGK forward	GTTGACCGAATCACCGACCTC
Hinge reverse	CGGTGGGCATGTGTGAGTTTTGTCAGGAGATTTG
Linker forward	GGAGGTGGTGGATCGGGCGGT

2.9.6 Library cDNA amplification primers

Primer	Sequence 5' to 3'
Leader forward	ATGGATTTTCAGGTGCAGATTTT
OX40 reverse	TCTCGAGCTAGATTTTAGCCAGG

2.9.7 Barcodes from Oxford Nanopore sequencing

Component	Forward sequence	Reverse sequence
NB01	CACAAAGACACCGACAACTTTCTT	AAGAAAGTTGTCGGTGTCTTTGTG
NB02	ACAGACGACTACAAACGGAATCGA	TCGATTCCGTTTGTAGTCGTCTGT
NB03	CCTGGTAACTGGGACACAAGACTC	GAGTCTTGTGTCCCAGTTACCAGG
NB04	TAGGGAAACACGATAGAATCCGAA	TTCGGATTCTATCGTGTTTCCCTA
NB05	AAGGTTACACAAACCCTGGACAAG	CTTGTCCAGGGTTTGTGTAACCTT
NB06	GACTACTTTCTGCCTTTGCGAGAA	TTCTCGCAAAGGCAGAAAGTAGTC
NB07	AAGGATTCATTCCCACGGTAACAC	GTGTTACCGTGGGAATGAATCCTT
NB08	ACGTAACTTGGTTTGTTCCCTGAA	TTCAGGGAACAAACCAAGTTACGT
NB09	AACCAAGACTCGCTGTGCCTAGTT	AACTAGGCACAGCGAGTCTTGGTT
NB10	GAGAGGACAAAGGTTTCAACGCTT	AAGCGTTGAAACCTTTGTCCTCTC
NB11	TCCATTCCCTCCGATAGATGAAAC	GTTTCATCTATCGGAGGGAATGGA
NB12	TCCGATTCTGCTTCTTTCTACCTG	CAGGTAGAAAGAAGCAGAATCGGA
NB13	AGAACGACTTCCATACTCGTGTGA	TCACACGAGTATGGAAGTCGTTCT

2.10 Cell lines

Cell line	DSMZ No.	Medium
HEK293T	ACC 635	DMEM + 10% FCS + 1% Pen/Strep
Jurkat	ACC 282	RPMI + 10% FCS + 1% Pen/Strep
J7	ACC 282	RPMI + 10% FCS + 1% Pen/Strep
J7-53	ACC 282	RPMI + 10% FCS + 1% Pen/Strep
J7i	ACC 282	RPMI + 10% FCS + 1% Pen/Strep
J7i-320	ACC 282	RPMI + 10% FCS + 1% Pen/Strep
J7i-53	ACC 282	RPMI + 10% FCS + 1% Pen/Strep
J7i-1475	ACC 282	RPMI + 10% FCS + 1% Pen/Strep
J7i-Library	ACC 282	RPMI + 10% FCS + 1% Pen/Strep
MCF-7	ACC 115	RPMI + 10% FCS + 1% Pen/Strep

3 Methods

3.1 Cell Culture

3.1.1 Maintenance and proliferation

Jurkat and its derivative cell lines, and HEK293T cells were cultured at 37°C and 5% CO^2 in humidified incubators. Jurkat derived cell lines were split 1:6 every 2-3 day with RPMI 1640 + GlutaMAX™-I supplemented with 10% FCS and 1% Pen/Strep. J7i cells were grown in Cell Stack culture chamber (Corning) for large-scale electroporation experiments. After removal of the culture media, 80-90% confluent MCF7 cells were treated with trypsin-EDTA solution (0.05%) for cell detachment. Detached cells were washed with DPBS, and seeded according to experimental need in complete RPMI media. HEK 293T cells were treated in the same way as MCF7 cells, however they were cultured in complete DMEM media. All cells were frozen in FCS containing 10% Dimethylsulfoxide (DMSO). After 1 day in -80 °C, cells were replaced to liquid nitrogen tank's vapor phase to be stored long term at -150 °C. The cell were thawed rapidly by a brief incubation at 37 °C. After thawing majority of the frozen aliquot, remaining frozen material was resuspended by pipetting and cells were immediately put into 9 mL of warmed cell culture media. Cells are washed with warm media once more to get rid of residual DMSO, before being placed into cell culture flasks.

3.1.2 Lentiviral particle production by HEK 293T co-transfection

HEK 293T cells were co-transfected with two helper plasmids; pCMV-VSV-G that endoces for envelope protein VSV-G and pCMV-dR874 that encodes for HIV-gag and HIB-pol proteins, together with respective lentiviral transfer vectors. 2 days before transfection, 6E+6 HEK 293T cells were seeded into 15 cm cell culture dishes in 22.5 mL complete DMEM media. Depending on the size of the production, appropriate amount of helper plasmids and lentiviral transfer plasmid were mixed in OptiMEM and the plasmid mixture was encapsulated in polyethyleneimine (PEI). Solution was vortexed for 10 seconds and incubated in room temperature for 10 minutes. Transfection of HEK 293T cells was done by addition of the prepated mixture in dropwise manner on top of the attached HEK 293T cells. 24 hours post transfection, the culture media was removed and replaced with 14 ml DMEM without phenol red. 48 hours post transfection, media was collected and centrifuged at 300g to pellet detached HEK 293T cells. Supernatant was pass through a 0.45 µm filter and poured into Centricon® centrifugal filters to be centrifuged at 3500 g for 30 minutes. The Centricon® centrifugal filters were inverted and centrifuged at 1000 g for 2 minutes for virus titer concentration. Centricon® centrifugation was done until the whole supernatant was processed. The concentrated viral particles are then aliquoted and stored at -80 °C. To determine the virus titer, 1E+05 Jurkat cells were seeded in 1 ml complete RPMI and transduced with a titration series of viral particles. 48 hours post transduction, the cells are analyzed with flow cytometry for titer determination.

Table 3.1.2.1 Preparation of the transfection medium

Component	For 1x 15 cm cell culture dish	For 10x 15 cm cell culture dishes
pCMV-VSV-G plasmid	7.9	79
pCMV-dR874 plasmid	14.6	146
Lentiviral transfer vector	22.5	225
OptiMEM (ml)	2.5	25
PEI 1mg/ml (µl)	180	1800
Total:	2725	27250

All plasmid concentrations are 1µg/µL Add 2.7ml drop by drop per 15 cm cell culture dishes.

3.1.3 Lentiviral transduction of Jurkat cells

The Jurkat cells were transduced with pre-determined lentiviral particle titers in MOI of 5 in the presence of 8µg/ml Polybrene. Cells were cultured in S2 incubator for 48 hours in complete RPMI media. 48 hours later, cells are analyzed with flow cytometry for transgene expression.

3.1.4 PBMC isolation

Peripheral Blood Mononuclear Cells (PBMCs) were isolated from blood of healthy donors with Ficoll density gradient centrifugation. 15 mL Ficoll was put the bottom of 50 mL falcons. 35 ml of blood that is diluted with Dulbecco's phosphate-buffered saline (DPBS) was carefully layered on top of Ficoll. Layers were centrifuged with 2200 RPM for 20 minutes at room temperature with deceleration set to 0. Formed PBMC ring was transferred into a fresh 50 mL falcon for washing. 2 times wash with PBS was performed to get rid of any residual Ficoll carryover. Cells were counted and prepared for total RNA isolation.

3.1.5 Single-cell derived clone cultivation

Penning and stimulation of the "GFP+" cells (see section 4.1.1) inside an OptoSelect™ chip is explained in section 3.7.1. During the PHA-L treatment of the cells, the fluorescent images of the chip was taken every hour for 24 hours. 1 week after the start of single-cell stimulation experiment, 36 PHA reactive single-cell derived clones were exported from the Lightning™ device into a U-bottom 96 well plate. Exported cells were cultivated and grown off-chip for further characterization with PHA-L. Depending on their growth, single-cell derived clones were gradually moved into well plates with larger surface areas. Eventually, when all clones were grown enough to be placed into T25 cell culture flasks, several aliquots of cells were frozen.

3.1.6 Limiting Dilution

Limiting Dilution with dilution factor of 0.5 cells per well was prepared. To do so, a serial dilution was performed and to have 1000 cells in 1 mL of conditioned media prepared as explained in section 3.1.5. From this dilution, 50µl of media was taken out and put into 10 mL conditioned media. In theory, 5

cells/mL concentration was achieved. Therefore, upon seeding 100 µL from this suspension into 96 well plates, there is a 50% chance that each well receives a single cell, decreasing the possibility of pipetting 2 cells in one well. Cells were grown and gradually moved to well plates with larger diameters. When they moved into T25 cell culture flasks, aliquots of the cells were frozen as described at section 3.1.1.

3.2 Molecular Biology

3.2.1 Agarose gel electrophoresis

Agarose gel electrophoresis was performed to separate DNA samples according to their size. Before loading, DNA samples were mixed with respective µls of 6X Gel Loading Dye. Depending on the sample number 50ml or 150ml 1% agarose gels prepared in Tris-acetate EDTA (TAE) buffer (w/v) were casted. Electrophoresis was done in TAE buffer with 90 or 110 Volts for 50ml and 150ml agarose gels, respectively.

Table 3.2.1.1 Preparation of TAE buffer

Component	Concentration (mM)
Tris	40
EDTA	1
Acetic acid	20
H_2O	

3.2.2 Bacteria cultures

3.2.2.1 XL-1 strain cultures

Home made XL-1 bacteria cultures were grown in lysogeny broth (LB) medium containing Kanamycin (50 µg/mL) or Carbenicillin (100 µg/mL) at 37 °C with moderate shaking (140 RPM). Bacteria suspension was spread or streaked depending on the application onto agar plates containing 15 g/L agar-agar in LB medium to obtain single colonies. Single colonies were inoculated into 3 ml, 100 ml or 300ml antibiotics containing LB media for small-scale (Miniprep), medium-scale (Midiprep) or large-scale (Maxiprep) DNA isolation, respectively. Bacteria was frozen at -80 °C by preparing bacteria suspension with 20% final glycerol concentration.

Table 3.2.2.1 Preparation of Lysogeny broth (LB) medium

Component	Concentration (g/L)
Yeast extract	5
Tryptone	10
Sodium chloride	10
H_2O	Up to 1L

3.2.2.2 DH5α strain cultures

DH5α strain that hosts the nanoS/MAR vectors were grown in Terrific Broth (TB) according to the optimized protocol from Nature Technology Corporation (NTC). The following protocol is for cloning a certain sequence into nanoS/MAR vectors. For preparation of CAR libraries in nanoS/MAR vectors, a different protocol was applied (3.2.8). The growth conditions are IP of NTC. Bacteria suspension was spread onto agar plates with 15 g/L agar-agar in Selection Medium containing sucrose and arabinose to obtain single colonies. Emerging single colonies were inoculated into 6 ml Selection Medium containing sucrose and arabinose and grown overnight. Frozen aliquots were prepared with bacteria grown in Selection Medium with 20% final glycerol concentration and stored at -80 °C. For Maxiprep isolation, cells grown in Selection Medium were inoculated into 300ml sucrose and arabinose containing TB media for DNA isolation.

Table 3.2.2.2: Preparation of Selection medium

Component	Concentration (g/L)
Yeast extract	5
Tryptone	10
H_2O	Up to 1L

Table 3.2.2.3: Preparation of Terrific broth (LB) medium

Component	Amount
Terrific-Broth vegetal	50.8 gram
Glycerol	10 ml
H_2O	Up to 1L

3.2.3 Transformation of *E. coli* strains

3.2.3.1 XL-1 strain transformation

Chemo-competent, lab grown XL-1 strain were thawed on ice and 25µl bacteria suspension was mixed with 5µl ligated pDNA or 50ng isolated pDNA for retransformation. pDNA and bacteria suspension is incubated on ice for 20 minutes. Heat shock was performed for 45 seconds at 42 °C. Cells were briefly cooled down on ice and supplemented with 250µL antibiotics free LB media to be shaken at 37 °C for an hour. Cells were spread over antibiotics containing LB agar plates and grown at 37 °C overnight to obtain single colonies. Emerging single colonies were inoculated into 3 ml LB media for Miniprep DNA isolation.

3.2.3.2 MegaX DH10B T1R Electrocomp™ strain transformation

MegaX DH10B™ T1R Electrocomp™ Cells were thawed on ice and 25µl bacteria suspensions were mixed ligation products containing 0.1 µg, 0.5 µg or 1 µg vector DNA. Bacteria and ligation products were mixed by gentle tapping. Suspension was pipetted into a pre-chilled 0.1-cm cuvette and electroporated with “ec1” program of MicroPulser™. Immediately after electroporation, cells were

resuspended in 1 mL Recovery Medium (Thermo Fisher Scientific) pre-warmed to 37°C. Cells are incubated at 37 °C for 1 hour. 10^{-4} and 10^{-5} dilutions were spread onto LB agar plates containing 100µg/mL Carbenicillin. Emerging single colonies were counted to calculate the total number colony forming units present in the 1 mL bacteria suspension.

3.2.3.3 DH5α strain transformation

The transformation protocol for DH5α strain that hosts nanoS/MAR vectors are confidential.

3.2.4 RNA isolation

Before performing RNA isolation, the bench area, pipettes and materials that used for the process are treated with RNase AWAY™ to sterilize the environment from RNases. For plasmid CAR library generation, isolated PBMCs were lysed and lysates are homogenized with a rotor-stator according to instructions of PureLink RNA mini kit (Invitrogen). The RNA bound columns were digested with PureLink® DNase to remove any genomic DNA contamination. Purified total RNA was eluted with 30µl Nuclease-Free (NF) water and kept on ice till being frozen at -80 °C. The quality of isolated RNAs were evaluated with Fragment Analyzer (Agilent). For qPCR experiments, half of the co-incubation samples were taken from the cultures. They were cleared from the magnetic beads by application of a magnetic field. The RNA from the remaining cells were isolated with ReliaPrep™ RNA Miniprep kit according to manufacturer's instructions with on-column DNase treatment. Total RNA was eluted with 17 NF water.

3.2.5 Plasmid DNA isolation

3.2.5.1 Plasmid DNA isolation from XL-1 strain

Single colonies grown in 3 mL LB were processed with Monarch® Plasmid Miniprep Kit (New England BioLabs) according to the manufacturer's instructions for plasmid isolation. Isolated plasmids were confirmed by control restriction digestion analysis and/or with Sanger sequencing (GENEWIZ, Azenta). Colonies with correct inserts or cells from frozen glycerol stocks were inoculated into antibiotics containing 100 mL or 300mL LB media for Midiprep and Maxiprep DNA isolation, respectively. Inoculated cultures were grown overnight at 37 °C. Later, cells were harvested by centrifugation at 4500 x g for 15 minutes. The supernatants were discarded and bacteria pellets were either immediately processed with NucleoBond Xtra Midi/Maxi Endotoxin-Free (EF) kit (MACHEREY-NAGEL) according manufacturer's instructions, or frozen at -20 °C to be processed later. DNA pellets were resuspended in EF H_2O. Concentration and purity of the isolated DNA was determined by NanoDrop ONE (Thermo Fisher Scientific).

3.2.5.2 Plasmid DNA isolation from DH5α strain

Single colonies grown in 6 mL Selection Media were processed with Monarch® Plasmid Miniprep Kit (New England BioLabs) according to the manufacturer's instructions for plasmid isolation. Isolated plasmids were confirmed by control restriction digestion analysis and/or with Sanger sequencing (GENEWIZ, Azenta). Colonies with correct inserts were inoculated into 300mL sucrose and arabinose containing TB media for Maxiprep DNA isolation. For CAR library DNA production, 166µl from glycerol

stocks of κ and λ libraries were inoculated into 300 mL TB. Inoculated cultures were grown according to optimized protocol from NTC. Cells were harvested by centrifugation at 4500 x g for 15 minutes. The supernatants were discarded and bacteria pellets were either immediately processed with MN NucleoBond Xtra Maxi EF kit or EndoFree Plasmid Maxi Kit (Qiagen) according instructions obtained from NTC, or frozen at -20 °C to be processed later. DNA pellets were resuspended in EF H_2O. Concentration and purity of the isolated DNA was determined by NanoDrop ONE (Thermo Fisher Scientific).

3.2.6 Restriction enzyme digestion

To confirm the ligation outcomes or to check the genomic DNA contamination of the isolated plasmid CAR DNA, control digestions have been performed. For both tests, 2µg pDNA were digested with 1µl of respective restriction enzymes resuspended in a total of 20 µL reaction containing 2 µL 10X CutSmart™ buffer for 2 hours at 37 °C (New England Biolabs). 4 µL 6X gel loading dye was added to restriction digestion reactions prior to agarose gel electrophoresis loading.
Restriction digestions performed for plasmid CAR library cloning is explained in section 3.2.8.

Table 3.2.6.1: An example restriction digestion reaction

Component	Volume (µL)
DNA	x
Restriction Enzyme 1	1
Restriction Enzyme 2	1
CutSmart Buffer (10x)	2
H_2O	Fill up to 20µl

3.2.7 Agarose gel purification

Restriction enzyme digested inserts or vectors were loaded into an agarose gel for separation according to their molecular weight. The products were observed under UV light and fragments of interest were cut out from the agarose gel. DNA was isolated from the cut fragments by using Monarch® DNA Gel Extraction Kit (NEB) according to manufacturer's instructions.

3.2.8 Plasmid CAR library cloning

For library construction Platinum™ II Hot-Start Green PCR Master Mix (2X) (Invitrogen) was used for amplification requiring a Taq polymerase. Similarly, Platinum™ SuperFi™ II Green PCR Master Mix (Invitrogen) was used for PCRs requiring a high fidelity DNA polymerase. These enzyme mixes provided a universal primer annealing temperature of 60 °C. Both enzyme mixes contained optimized concentrations of salts, magnesium, and dNTPs for optimal function of DNA polymerases. Both mixtures were also supplied with density reagent and two tracking dyes, one blue one yellow, for direct agarose gel analysis of the amplified products. To generate a plasmid CAR library, firstly heavy-κ and heavy-λ scFv libraries were constructed. The following protocol was used to generate the plasmid CAR library

with HPLC purified primers (Section 4.2.3). Generation of small-scale libraries for testing the surface expression and scFvs with correct ORF (Sections 4.2.1 - 4.2.2) will be explained later in this section. To generate heavy-κ and heavy-λ scFv libraries, RNA isolations from 11 healthy donors were thawed and first strand cDNA synthesis was performed with Maxima H Minus First Strand cDNA Synthesis kit by reverse transcribing 3 µg RNA in 20 µL total reaction by using random hexamers (Invitrogen). 20 µL aliquots of generated cDNAs from each donor were pooled to have 220 µL total cDNA. Only primers that give rise to a PCR product were used. 32, 45, and 65 PCRs were performed for amplification of V_H, V_L κ and λ chains, respectively. In these PCRs, forward and reverse primers were not pooled. Each single forward primer was used in combination with a single reverse primer to increase the diversity. PCRs were done in 20 µL Platinum™ II Hot-Start Green PCR Master Mix with 1.5µl pooled cDNA template according to the manufacturer's instructions. Table 3.2.8.1 illustrates the PCR cycles used during the first amplification step. 2µl from each amplification were analyzed in the agarose gel to confirm the success of PCRs. From each successful amplification, several µls were pooled into separate V_H, V_L κ and λ pools. These pools were then loaded into an agarose gel for size separation. Products around 400 bp were cut from the gel and purified. In the meantime, one additional PCR was performed to amplify the artificial V_L κ leader sequence and 328 bp long product was purified from agarose gel. To assemble leader-V_H-V_L κ and leader-V_H-V_L λ scFv libraries, Overlap Extension PCRs (OE-PCRs) were performed. In this step, no primers were used. Equal molar mixture of gel purified leader, V_H V_L (κ or λ) sequences (~200 fmol) were subjected to OE-PCR by using Platinum™ SuperFi™ II Green PCR Master Mix according to manufacturer's instructions in 2 50 µl reactions. Due to 21 bp overlapping sequences, the 3 DNA pieces were assembled into full length scFv fragments. PCR conditions for OE-PCR is illustrated in Table 3.2.8.2 . 2 µL from leader-V_H-V_L κ and leader-V_H-V_L λ OE-PCRs were used as template for Pull Through (PT-PCR) PCRs that were performed with Platinum™ II Hot-Start Green PCR Master Mix with PT primers in 50 µL reactions. Table 3.2.8.3 depicts the PCR conditions used. PT primers facilitated the amplification of only fully assembled scFv fragments. The amplification products were purified with PCR purification kit according to manufacturer's instructions (Qiagen).

To generate plasmid CAR libraries, 5 µg nanoS/MARt plasmid #1468, and 5µg V_H-κ and V_H-λ PT PCR products were digested with NheI-HF and NotI-HF enzymes overnight at 37 °C in 35 µL final volume. Restriction digested vector #1468 was purified from agarose gel. As the cut out fragments were 10 bp long for PT PCR products, digested inserts were purified with PCR purification columns. 1 µg vector was ligated with V_H-κ and V_H-λ scFv libraries in 3:1 insert to vector ratio overnight at 16 °C in 100 µl reaction by using T4 DNA Ligase (NEB). Ligation reactions were heat inactivated at 65 °C for 10 minutes. Products were precipitated with 1/10^{th} of the ligation volume 3 M sodium acetate pH 5.2 in final 70% ethanol concentration overnight at -20 °C. The next day samples were centrifuged at 4 °C, 16000g for 30 minutes. Pellets were washed with 500 µL 70% ethanol and left for air drying. Dried pellets were resuspended with 5 µL NF water. 2.5 µL from each ligation reaction (containing 0.5 µg vector DNA) were mixed with 25 µL NTC's DH5α strain and transfected according to NTC protocols. Transformed bacteria were left overnight at RT with lid slightly open. The next day, 10^{-5} dilutions were plated for κ and λ plasmid CAR libraries to have estimate about the size of the generated libraries. The rest of the transformed bacteria was spread over 25cm x 25cm selection agar plates containing sucrose and

arabinose. After overnight incubation, bacteria grown in 25cm x 25cm agar plates were scraped off and resuspended in Selection Media. ODs were measured and a fraction of the bacteria was inoculated into sucrose and arabinose containing 300 ml TB according to NTC protocols. These cultures were grown as NTC suggests and bacteria was processed for Maxiprep DNA isolation. Both cultures had around 12.5 OD after scraping. Assuming 1 OD in 1 liter equals 1E+12 bacteria, thus 1E+09 bacteria/ml multiplied with ~12.5 OD equals 1.25E+10 bacteria/ml. Freezing 800 µL bacteria with 200 µL 99% glycerol would result in final bacteria count of 1E+10 bacteria per aliquot. For further pDNA isolations, an aliquot from κ and λ libraries are thawed and 166µl inoculated into 300 mL sucrose and arabinose suppled TB.

Besides large-scale plasmid CAR library production, small-scale libraries were generated to check the percentage of scFv in correct ORF and whether these scFvs are expressed on the cell surface. To do so, 50 ng NheI/NotI disgested plasmid #272 was ligated with NheI/NotI disgested κ and λ scFv libraries in 3:1 insert to vector ratio in 20 µL reaction for 1 hour at RT. The ligation reaction was inactivated by incubating the solution at 65 °C for 10 minutes. 5 - 10 µL of the ligation products was mixed with thawed XL-1 for transformation. Single colonies were obtained by following 3.2.3.1. Miniprep, Midiprep or Maxipreps for DNA isolation were performed as explained in 3.2.5.1.

Table 3.2.8.1: PCR conditions for amplification of heavy and light chain variable regions

Step	Cycles	Temperature °C	Time
Initial Denaturation	1	94	2’
Denaturing	35	94	15’’
Annealing		60	15’’
Extension		68	20’’
Final extension	1	68	10’

Table 3.2.8.2: PCR conditions for OE-PCR

Step	Cycles	Temperature °C	Time
Initial Denaturation	1	94	2’
Denaturing	5	94	30’’
Annealing		60	45’’
Extension		72	50’’
Final extension	1	72	5’

Table 3.2.8.3: PCR conditions for PT-PCR

Step	Cycles	Temperature °C	Time
Initial Denaturation	1	94	2’
Denaturing	30	94	15’’
Annealing		60	15’’
Extension		72	25’’
Final extension	1	72	10’

3.2.9 CAR cDNA recovery from Lightning™ exports

Bruker has established protocols for recovery and sequencing of T cell receptors from single T cells exported from Lightning™ device. However, for amplification and sequencing of CAR construct, new protocols had to be developed and optimized. Following protocol was developed to recover and identify CAR sequences from the hits obtained during single-cell stimulation experiment using Lightning™ device.

Before starting the experiment, the working space and pipettes were cleaned with DNA AWAY and RNase AWAY soaked wipes. Single cells were exported into individual wells of a twin.tec 96-Well LoBind PCR Plates (Eppendorf). In the wells, a drop of mineral oil was layer on top of 10 µL 2x TCL buffer. Cells were exported in 10 µL 0.2% Sodium Azide dPBS solution into TCL buffer carefully according to manufacturer’s instructions. RNAClean XP Beads (Beckmann Coulter) were acclimatized to RT and resuspended by vigorous shaking. 20 µL of magnetic beads were added to each export sample containing well. Plate was sealed and incubated for 10 minutes at RT for RNA capture. Plate was placed onto the magnet and supernatant was discarded from the wells. Wells were washed with 50 µL 80% ethanol two times. Throughout the experiment, beads were air dried after the second wash. Dried beads were resuspended in 4 µL of RT Mix 1 (Table 3.2.9.1). Plate was resealed to be incubated in a thermocycler that is preheated to 72 °C for 3 minutes to resolve 2ndary structures followed by a gradual cooling to 4 °C. Plate was put on to ice and 3µl of RT Mix 2 was added to each well (Table 3.2.9.2).

Table 3.2.9.1: RT Mix 1

Reagents	Amount for 1 well
OligodT	1.0 µL
dNTP Mix	1.0 µL
NF water	2 µL

Table 3.2.9.2: RT Mix 2

Reagents	Amount for 1 well
RT Buffer	1.4 µL
Maxima H minus enzyme	0.1 µL
NF water	1.5 µL

Resealed plate was placed into a thermocycler that is preheated to 42 °C for first-strand cDNA synthesis with Maxima H minus kit (Invitrogen) (Table 3.2.9.3). After RT-PCR, add 43 µL of RT Mix 3 (Table 3.2.9.4) to have 50 µL total volume in each well to perform second strand cDNA amplification (Table 3.2.9.5). After second strand cDNA synthesis, fresh 20 µL of magnetic beads was added on top of already existing beads. After 10 minutes of RT incubation, beads were pelleted with a magnet and washed 2 times with 50 µL 80% ethanol. Dried pellets were incubated with 20 µL NF water for 5 minutes to elute the ds cDNA. Eluates were then transferred into a new well plate.

Table 3.2.9.3: First strand cDNA synthesis

Step	Cycles	Temperature °C	Time
Hold	1	42	50’
Cycle	10	50	2’
		42	2’
Hold	1	85	5’

Table 3.2.9.4: RT Mix 3

Reagents	Amount for 1 well
First strand cDNA	7 µL
Platinum™ II HS Green MM	25 µL
Leader forward primer [10µM]	1 µL
NF water	17 µL

Table 3.2.9.5: Second strand cDNA synthesis

Step	Cycles	Temperature °C	Time
Initial Denaturation	1	94	3’
Denaturing	25	94	20’’
Annealing		60	30’’
Extension		68	1’
Final extension	1	68	10’

5 µL of the eluates were used as a template for first CAR amplification in 20 µL final reaction volume with primers targeting the 5’ end of the leader and the 3’ end of OX40 sequences, see section 2.9.6, (Table 3.2.9.6) with PCR conditions indicated in Table 3.2.9.7. Amplified CAR sequences were captured by adding 20 µL of magnetic beads. Samples were washed 2 times and eluted in 10 µL as mentioned before. 1 µL eluate from all samples were submitted to Fragment Analyzer (Agilent) for confirming amplicon sizes.

Table 3.2.9.6: First CAR cDNA PCR mix

Reagents	Amount for 1 well
Purified cDNA	5 µL
Platinum™ II HS Green MM	10 µL
Leader forward primer [10µM]	0.4 µL
OX40 reverse primer [10µM]	0.4 µL
NF water	4.2 µL

Table 3.2.9.7: First CAR cDNA PCR conditions

Initial Denaturation	1	94	3’
Denaturing	28	94	20’’
Annealing		60	30’’
Extension		68	1’
Final extension	1	68	10’

4.5 µL from the first PCRs were used as templates for a second round of amplification (Table 3.2.9.8) with PCR cycles written in Table 3.2.9.9). Amplified CAR sequences were captured with fresh 20 µL of magnetic beads. As before, samples were washed twice and eluted with 10 µL NF water. The DNA concentrations of the eluates were quantified with Qubit™ measurement (Invitrogen).

Table 3.2.9.8: Second CAR cDNA PCR mix

Reagents	Amount for 1 well
Template from 1st CAR PCR	4.5 µL
Platinum™ II SuperFi Green MM	10 µL
Leader forward primer [10µM]	1 µL
OX40 reverse primer [10µM]	1 µL
NF water	3.5 µL

Table 3.2.9.9: Second CAR cDNA PCR conditions

Initial Denaturation	1	98	3’
Denaturing	20	98	30’’
Annealing		60	30’’
Extension		72	1’
Final extension	1	72	5’

3.2.10 Nucleic acid quality control

RNA (HS RNA Kit, Agilent) and DNA (HS NGS Kit, Agilent) samples were processed according to manufacturer’s instructions. For RNA isolations, only the samples with RQN value greater than 9.5 were

considered for cDNA synthesis. DNA measurements were performed to evaluate the size of the amplification products during CAR sequence recovery from single cell Lightning™ exports.

3.2.11 DNA preparation for Oxford Nanopore Sequencing

As Oxford Nanopore Technologies offers optimized protocols for sequencing PCR amplicons, their suggested protocol “Ligation sequencing amplicons - Native Barcoding Kit 96 V14 (SQK-NBD114.96)” was followed to prepare single-cell derived CAR libraries.

3.3 Jurkat electroporations

Regardless of the device or scale used during electroporation experiments, Jurkat cells were split a day prior to ensure that they were in a proliferative state. The cells were counted with trypan blue staining and the electroporation was carried out only when the samples had viability greater than 90%. All the materials used during electroporation experiments were tested for endotoxins.

3.3.1 Electroporation with Neon™ device

Neon™ device is able to electroporate 5E10+6 cells with one shock. Therefore, it was used for small-scale electroporation experiments. Required amount of cells were centrifuged at 300g for 5 minutes. Cells were washed with DPBS to remove any residual antibiotics that is present in the culture media. 3 mL E2 electroporation buffer was put to the electroporation reservoir. 5E10+6 cells were resuspended in 100 µL T Buffer supplied with Neon™ electroporation kit. For each EP, 10 µg plasmid DNA was used. Cell-plasmid mixture in 100µl T Buffer was suspended into the Neon pipette tip. 3 electric pulses with 1400 Volts and 10 ms width were applied to the cells. Cells were immediately resuspended in 5 mL prewarmed RPMI basal media without phenol red, FCS and Pen/Strep. 24 hours post EP, the cells were centrifuged, washed with DPBS and resuspended in 5 mL complete RPMI medium.

3.3.2 Electroporation with GTx™ device

3.3.2.1 Single cassette electroporations

The single cassette electroporation with GTx™ described here encompasses electroporation experiments performed with process assemblies; OC-25x3, OC-100x2, R-50x8 and R-1000, allowing electroporation of 5E10+6 cells to 2E10+8 cells. The required cell amount was harvested and centrifuged with 100g for 10 minutes. Cells were washed DBPS twice. The supernatant was discarded and cells were resuspended with Maxcyte Electroporation (MEB) buffer or OPTI-MEM (OM), depending on the experiment. The cells were resuspended in 1.0E+08 or 2.0E+08 cells/ml concentration and plasmid DNA was added in pre-defined µg/mL plasmid concentration varying from 100µg/mL to 250 µg/mL. Cell, plasmid DNA mixture was pipetted into the cavities of the cassettes and cassettes were plugged into electroporation chamber of GTx™ electroporator. In the user interface of the GTx™ device, the right cassette type and electroporation program for Jurkat cells was selected and electroporation was performed. Cells were taken out from the cavities and placed into appropriate cell culture dishes to be rested for 20 minutes at 37 °C. At this step, the DNaseI (Sigma-Aldrich) treatment was introduced to

the workflow later on. The DNaseI was resuspended in NF water in 2 Kunitz per µL concentration and for each shock 1/20th of the electroporation volume of DNaseI was added to shocked cells. 20 minutes later, cells were resuspended in 2.0E+6 cells/mL concentration in prewarmed RPMI basal media without phenol red, FCS and Pen/Strep. 10% FCS was added to the cell cultures 6 hours after electroporation and cells were incubated at 37 ^{o}C overnight. The next day, cells were washed with DPBS once and resuspended in complete RPMI media in 1.0E+6 cells/mL concentration.

To test the effect of the MEB and OM mixture on electroporation efficiency and viability, cells were resuspended in OM during the second wash. After centrifugation, the excess OM was discarded and cells were resuspended in 50% OM, 50% MEB mixture in the volume needed for EP.

3.3.2.2 Automated flow electroporations

In large-scale electroporation experiments, the cells were washed with DPBS and OM in two consecutive washes, respectively. For flow electroporation, 1.6E10+9 cells were resuspended in 1.0E+08 cells/ml concentration again in 50% MEB and 50% OM mixture with 150µg/mL CAR library plasmid DNA concentration. Cell loading, flow electroporation processing assembly and electroporation was carried out according to manufacturer's instruction. After automated EP, 800 µL DNaseI was inserted into the sterile bag where the cells were collected after EP. Cells were discarded from the collection bag into a T125 flask and rested in 37 ^{o}C for 20 minutes. Cells were placed into a Cell Stack culture flask with the addition of 720 mL RPMI basal without any additives in 2.0E+6 cell concentration. 6 hours later 80mL FCS was added to the Cell Stack and cells were incubated 37 ^{o}C overnight. The next day, 400 mL of culture was transferred into another Cell Stack and 550 mL complete RPMI with antibiotics was added to each stack. Cells were grown in Cell Stacks in total for 3 days and their activation, CAR expression and viability were analyzed before commencing with cellular CAR library screening.

3.4 FACS/flow cytometry analysis

3.4.1 Flow cytometry staining and acquisition

As stimulated cells upregulate reporter gene Venus expression, no antibody staining is required to analyze activation of J7 or J7i cells. The Venus is quantified by measuring fluorescent intensity of the cells in FITC channel of BD FACS CantoII or BD FACS Symphony A3 devices. Antibody staining were done with antibody concentrations recommended by the manufacturer of the antibody. Before staining, cells were washed with DPBS supplemented with 2% FCS, also known as FACS buffer. After washing, cells were resuspended in 100µl antibody solution prepared in FACS buffer and incubated at 4 ^{o}C for 25 minutes. Before flow cytometry acquisition cells are washed twice, resuspended in appropriate amount of FACS buffer containing 0.1µg/ml DAPI. Cells are run through the FACS tubes with Cell Strainer caps to remove cell duplets or dead cell clumps. For FACS/flow cytometry data analysis FlowJo^{TM} (BD) was used. During data analysis, unstained cells or stained mock cells were used to identify the staining positive cell population.

3.4.2 FACS of stimulated Jurkat report cells

Overnight PHA stimulated cells were washed two times with appropriate amount of FACS buffer. As the activated cells express the reporter gene Venus, no antibody staining was needed. After second wash, cells were resuspended in 1.0E+7 cells per mL concentration in the presence of 0.1µg/mL DAPI and pass through a Cell Strainer cap into a FACS tube. Cells with desired level of reporter expression were sorted into 15 mL falcons that contained 5 mL culture media. After the sort, cells were acquired for a brief period to check the purity of the sort.

3.4.3 FACS J7i-Library cell pre-enrichment

3 days post electroporation of J7i cells in CL-2 process assembly, 3.0E+8 J7i-Library cells were harvested and washed once with FACS buffer. Cells were incubated in 3 mL FACS buffer with 2µg/mL rCEACAM5 protein at 4 ^{o}C for 30 minutes. Excess amount of rCEACAM5 protein was washed away and the cells were stained with 3mL FACS buffer containing 2µg/mL THE™ iFluor 647 conjugated anti-His Tag secondary antibody for another 30 minutes at ^{o}C. Cells were washed 2 times with FACS buffer and pass through Cell Strainer caps into FACS tubes in 1.0E+7 cells/mL concentration. Before the sort, cells were supplied with 0.1µg/mL DAPI for dead cell identification. As a negative control, mock electroporated cells were incubated with CEACAM-5 and stained with secondary anti-His Tag antibody in parallel to J7i-Library cells. Activated cells that were identified through increased fluorescent intensity in FITC channel were excluded from further analysis, as they were suspected to be expressing tonic signaling CARs. FACS gate for the cells with AF647 staining was arranged according to the background staining observed in the mock electroporated cell staining. 120.000 cells were sorted and rested overnight at 37 ^{o}C for loading into an OptoSelect™ chip the following day.

3.5 *In vitro* experiments

3.5.1 Bulk unspecific PHA-L stimulation

For unspecific, antigen-independent stimulation, 0.5x10^{6} Jurkat repoter cells were seeded in 1 mL complete cell culture media into 1 well of 24 well plates. PHA-L stimulation experiments were done in duplicates or triplicates. The cells were stimulated with 5µg/mL PHA-L overnight. The cells were analyzed in flow cytometry the next day by acquisition in FITC channel. Unstimulated cells were used to quantify percentage of activated cells and FITC mean fluorescent intensity (MFI) fold change (FC). The percentage of activated cells was calculated by gating on the activated cells with respect to FITC FACS plot of unstimulated negative control cells. For calculation of FITC MFI FC, the FITC MFI of the stimulated cells was divided to FITC MFI of unstimulated cells.

3.5.2 Magnetic bead coupling and bulk antigen-specific stimulation

Bulk antigen-specific stimulation of reporter Jurkat cells were done with M-270 Streptavidin Dynabeads (Thermo Fisher Scientific) or PureProteome™ (PP) Magnetic Beads (Merck). The coupling reaction was performed in V-bottom 96 well plates with Magnetic Stand-96 (Invitrogen). Wells that were used for bead

coupling were coated with FCS for 20 minutes at 37 °C. The magnetic beads were coupled with Biotinylated Human CEACAM-5 / CD66e Protein, His, Avitag™ (Acro Biosystems) according to manufacturer's instructions. Protein concentration present during the coupling reaction was titrated by taking the manufacturer's recommended protein concentration as the baseline. Coupling of the beads was evaluated with a flow cytometry experiment. Magnetic beads were stained with PE conjugated anti-human CD66 antibody for 25 minutes at 4 °C. Beads were washed two times by application of magnetic field and acquired via flow cytometry. Uncoupled, antibody-stained beads served as negative control. After confirming the coupling, J7 or J7i cells expressing anti-CEA CAR were incubated overnight with 1:10 and 1:1 cell to bead ratio when Dynabeads or PP beads used for antigen-specific stimulation, respectively. The next day, cells were stained with APC conjugated AffiniPure F(ab')2 Fragment anti-hIgG antibody and analyzed in flow cytometry for CAR expression and activation. CAR staining was performed to quantify the level of CAR downmodulation upon antigen-specific stimulation. To evaluate activation of the cells, percentage of activated cells and FITC MFI FC were calculated by using the CAR expressing cells incubated with uncoupled beads as negative control, as mentioned in 3.5.1.

3.5.3 Bulk antigen-specific stimulation with antigen expressing cell lines

The J7i-53 cells were co-incubated with a CEACAM5 expressing cell line MCF-7 for antigen- specific stimulation. To do so, 650.000 MCF-7 cells were seeded into 6 well plates. The next day, the confluency of the seeded cells was confirmed. 500.000 J7i-53 cells were co-incubated with confluent MCF-7 cells overnight. The next day, the cells were resuspended and analyzed via flow cytometry. The J7i-53 cells were distinguished from MCF-7 cells by their basal Venus expression. J7i-53 cells that were incubated with antigen irrelevant HEK293 T cell line were used as negative control. The percentage of activated cells and FITC MFI FC was calculated as explained in 3.5.1.

3.6 qPCR experiments

qPCR experiments were performed by incubating CEACAM5 coupled PP beads with single-cell derived clones of J7i-53 or J7i cells electroporated with plasmid #320 to express the anti-CEA CAR. 50.000 anti-CEA CAR expressing cells were stimulated with antigen-coupled PP beads in 1:1 bead to cell ratio. Firstly, the relative changes in CAR mRNA expression and Venus mRNA expression were quantified 24 hours after the beginning of antigen-specific stimulation. Then, CEA CAR expressing J7i cells were stimulated with beads to be analyzed 2, 4, 8, 12 and 24 hours post antigen-specific stimulation. For each time point, 50.000 cells were stimulated in 1:1 cell to bead ratio in different wells. CAR expressing J7i cells incubated with uncoupled beads were used to calculate the relative FC in mRNA expression levels according to a reference gene.

After co-incubation with antigen-coupled or uncoupled beads for respective amount of time, the cells were separated from magnetic beads by application of a magnetic field. Total RNA was isolated from the cells by following the instructions of Promega's ReliaPrep RNA kit. 100ng RNA from each condition was reverse transcribed into cDNA in 20µl reaction using Maxima H minus First Strand Synthesis kit (Invitrogen) according to manufacturer's instruction. In total, 3 qPCRs were performed for each condition

to quantify Ct values of CAR mRNAa and Venus mRNA as experimental conditions, and β-actin as the reference gene to calculate ΔCt values. All experiments were performed in duplicates and PCR efficiency was assumed to be 100% for all primer pairs. For each sample, 2.5x reactions were prepared according to Table 3.6 to ensure enough material for duplicates. qPCRs were performed in 10 µL samples. Each sample contained 10ng cDNA. Prepared 25 µL master mixes were mixed thoroughly and pipetted into qPCR plates. In total, 35 cycles were performed and melting curves for each amplification were generated. Samples showed uniform melting curves for all the 3 genes that were amplified. To quantify the relative mRNA expression levels $2^{-\Delta\Delta Ct}$ method was used. Briefly, duplicates with Ct values greater than 0.5 standard deviation were filtered out. The remaining duplicates' Ct values were averaged. ΔCt values of each sample was calculated by subtracting Ct value of β-actin from the Ct values of experimentally tested genes. This subtraction normalizes the expression of gene of interest to a house-keeping gene whose expression should not be affected by the experiment. Then, ΔΔCt values were calculated by subtracting ΔCt values of unstimulated cells from the stimulated cells. The formula $2^{-\Delta\Delta Ct}$ was then used to calculate fold change in the gene expression between the stimulated cells and unstimulated cells. 2 separate analysis were done to quantify the changes in gene expression of CAR and Venus mRNA expression relative to β-actin mRNA expression.

Table 3.6: Preparation of qPCR samples for duplicates

Reagent	For 1x reaction (µL)	For 2.5x reactions (µL)
2x SYBR Green Mix	5	12.5
Forward Primer (10µM)	0.2	0.5
Reverse Primer (10µM)	0.2	0.5
Template cDNA (10ng/rxn)	2	5
NF water	2.6	6.5

3.7 Single-cell stimulation experiments with Lightning™ device

3.7.1 Unspecific PHA-L stimulation

In order to obtain a stimulation sensitivity single-cell derived clone from $(NFAT)_{12}$-hIL2p-Venus reporter expression cassette transduced Jurkat cells, single "GFP+" cells (Section 4.1.1) were penned into an OptoSelect™ chip inside the Lightning™ device. To do so, "GFP+" cells were counted and 500 mL cell suspension with 2.5E+06 cells/mL concentration was prepared. Cells were resuspended in conditioned media that was produced by mixing the media that the cells were cultured in with fresh complete RPMI in 1:1 ratio. 5X B27™ Plus supplement (Thermo Fisher Scientific) was provided to the resuspension media to protect the cells from reactive oxygen species (ROS) that is created during OptoElectro Positining™ (OEP™). Before the experiment, "Full clean" workflow was performed according to prompts provided by the Lightning™ Cell Analysis Suite (CAS) software for sterilization of the lines. Afterwards, an OptoSelect™ chip was wet by following the "Wetting" workflow by using Wetting Solution and Wetting Additive provided by Bruker. Before importing the cells to the channels of the chip, the chip and the lines were primed with condition media containing 5X B27™ Plus. 25 µL cell suspension was imported to the

chip via import/export needle. Single “GFP+” cells were penned into 12 Field of Views (FOVs), each FOV consisting around 150 pens. The device is able to handle one FOV at a time. Therefore, cell penning is performed 12 times for 12 different FOVs. Penned cells were cultivated inside the OptoSelect™ chip for 3 days with “Pulse Culture” workflow that pumps 4 µL fresh conditioned media every 2 minutes. At day 4, 5 µg/mL PHA-L was added to the conditioned media that was used supply the chip. Cells were stimulated with PHA-L for 24 hours with “Spectral Imaging with Culture“ workflow that imaged the chip with brightfield and FITC filter cube (Exposure: 1000ms) every hour for 24 hours. 24 hours later, PHA-L stimulation was stopped by supplying the chip with the condition media without PHA-L. Cells were grown for inside OptoSelect™ 2 days more before exporting the PHA-L responsive single-cell derived cells. PHA-L reactive cells were identified in “Image Analyzer” software of Bruker. In total 36 single-cell derived clones were exported from the Lightning device by the import/export needle into condition media pre-filled U-bottom 96 well plates. Table 3.7.1.1 and Table 3.7.1.2 illustrates the parameters used during cell import and export workflows, respectively.

Table 3.7.1.1: Parameters used during import of “GFP+” cells into the channels of the OptoSelect™ chip

Parameter	Value
Import Location	Manual
Import Type	Import
Import Volume (µL)	25
QC Check	Manual QC
Penning Operation	Pen Chip
Penning Algorithm	Pen Singles
Cage Speed (µm/s)	4
Waveform Voltage (V)	4.7

Table 3.7.1.2: Parameters used during export of “GFP+” cells into a U-bottom 96 well plate

Parameter	Value
Operation	Unload
Pre-export Treatment	Extended Flush with TrypLe
Pruning	Yes
# of Exports	36
Minimum Yield Threshold (cells)	2
Max # of Unpen Cycles	4
# of Split Cycles	2
Cage Speed (µm/s)	4
Waveform Voltage (V)	4.7
Frequency (MHz)	1.3

3.7.2 Antigen-specific stimulation

For antigen-specific stimulation of J7 or J7i cells expressing anti-CEA CAR, CEACAM5 coupled magnetic beads were prepared the day of the single-cell stimulation experiment. The coupling of the beads were confirmed via flow cytometry (3.5.2). The Lightning™ device was sterilized with "Full clean" workflow before the experiment began. An OptoSelect™ chip was wet as described in 3.7.1. Magnetic beads in 1.0E+7 beads/mL concentration were imported into the chip first (Table 3.7.2.1). The beads were penned by "Bulk Penning" workflow that pushes the content found in the channels into the pens. As the beads does not get affected by the Voltage and frequency of the applied voltage, maximum Voltage and frequency was applied while bulk penning of the beads. Later, bulk penning of the beads was replaced with another workflow, "Gravity Penning" as it does not require processing of 12 FOVs consecutively. As the name suggests, the beads imported into the channels were penned by using gravitational force. To do so, after import of the beads, the OptoSelect™ chip was displaced from its nest and placed into a sterile Petri dish. The Petri dish was then placed into a 37 ^{o}C incubator in an upright position that allows beads to migrate to the bottom of the pens due to gravity. 5 minutes incubation in the mentioned position was found to be sufficient to cause bead penning. The bottleneck of the bead penning was the uneven distribution of the beads in the channels after their import. During repeated bead penning trials, this problem was solved by increasing the speed of the bead import from import vessel to the channels from 0.5 µL/second to 2 µL/second. After successful penning of the beads, J7 or J7i cells expressing the anti-CEA CAR were resuspended in 5X B27™ Plus containing media in 2.5E+6 cells/mL and single cells were penned into antigen coupled bead containing pens.

When PP beads were used to stimulate the J7i-53 and antigen pre-enriched J7i-Library cells, the Lightning™ device was unable to distinguish the cells from the beads as they had similar brightness and size, around 10 µm. PP beads were found to have no autofluorescence in any of the filter cubes that the Lightning™ device operates. Upon performing a cell counting workflow in brightfield filter cube, device recognized the penned beads as cells. As beads were registered as cells in each pen, the "Pen Singles" algorithm could not be used. To solve this problem, Jurkat cells were stained with an APC conjugated anti-hCD2 antibody that is recognized by the CY5 filter cube. Before importing stained Jurkat cells, pen counts were cleared and another count was performed with CY5 filter cube with 4000 ms exposure time by implementation of a Target Pen Selection (TPS) script. Upon introduction of a cut off for CY5 median brightness during counting, the device was enabled to distinguish APC stained cells from the PP beads and only processed Jurkat cells. Therefore, the cell penning was performed with CY5 filter cube with a median brightness cut off 3000. Similarly, cells were counted in CY5 filter cube with the mentioned cut off instead of being counted in brightfield filter. Number of cells counted in each pen with CY5 imaging was confirmed by manual inspection of the count results. Table 3.7.2.2 shows the parameters used to pen J7i-53 or J7i-Library cells. Upon penning single Jurkat cells, "TPS Imaging with Culture" was performed in "Pulse Culture" culture setting to image and quantify the FITC MFI of each single cell by taking images every hour in brightfield and FITC filter cube (1000 ms exposure). When J7i-53 were tested in single-cell stimulation experiments, all 12 FOVs were penned with J7i-53 cells. During the cellular CAR library screening, 1 FOV was penned with J7i-1468 cells that are expressing the model anti-CEA CAR as the positive control. Remaining 11 FOVs were penned with pre-

enriched J7i-Library cells. Activated cells were identified by using Image Analyzer software as before. For J7i-Library cells, cells from 14 pens were exported in 10 µL 0.2% Sodium Azide dPBS the parameters indicated in Table 3.7.2.3 into 2X TCL buffer.

Table 3.7.2.1: Parameters used during import of magnetic beads

Parameter	Value
Operation	Small Volume Import
Leading Volume (µL)	0
Package Volume (µL)	10
Lagging Volume (µL)	15
Import Location	Manual
Flow Rate (Package Volume) (µL/s)	2
Flow Rate (Lagging Volume) (µL/s)	2

Table 3.7.2.2: Parameters used during import of J7i-53 and J7i-Library cells

Parameter	Value
Import Location	Manual
Import Type	Import (J7i-53) – Small Volume Import (J7i-Library)
Import Volume (µL)	25 (J7i-53) – 10 (J7i-Library)
QC Check	Manual QC
Penning Operation	Pen Chip
Penning Algorithm	TPS script
Cage Speed (µm/s)	10
Waveform Voltage (V)	4.7
Cell Counting	TPS script

Table 3.7.2.3: Parameters used during export of J7i-Library hits

Parameter	Value
Operation	Unload
Pre-export Treatment	-
Pruning	No
# of Exports	30
Minimum Yield Threshold (cells)	1
Max # of Unpen Cycles	10
# of Split Cycles	4
Cage Speed (µm/s)	4
Waveform Voltage (V)	8
Frequency (MHz)	2.3

3.8 Oxford Nanopore sequencing analysis

CAR cDNAs from exported cells were recovered as explained in section 3.2.9. During the recovery process, 1 out 14 hits did not result in a product with correct length which is 2.1 kb. The recovered PCR amplicons were processed according to “Ligation sequencing amplicons - Native Barcoding Kit 96 V14 (SQK-NBD114.96)” manual provided by Oxford Nanopore Technologies. Briefly, recovered CAR cDNAs from each hit was subjected to end repairing and dA tailing. Barcodes 1 to 13 were ligated to the end repaired products and barcoded libraries were pooled into one sample. Adapter proteins that guide the DNA molecules into the Nanopores were ligated. Final library was diluted to the 20 fmol for loading into a MinION Flow Cell according to the manufacturer’s instructions. Library was sequenced for 24 hours till only 5% of the pores were left available for sequencing.

To analyze sequencing result, the cryptic read with less than 2kb were filtered out for all the barcodes. The remaining sequences were submitted into IMGT’s V-QUEST software. Each filtered barcode was individually submitted to the website. As output format, “Excel file” was selected and option 12 that is for scFv analysis was activated. In the “Advanced parameter”, all settings were left as default except for “Search for insertion and deletions in V-REGION” that was enabled. Lastly, “Analysis of single chain Fragment variable (scFv)” was enabled. Each barcode was submitted with these settings for annotation. Barcode 13, that is the positive control expressing uniformly model anti-CEA CAR with mouse derived SCA431 scFv was analyzed against *Mus musculus* genome. Barcode 13 was also run against human database to set the V-region similarity cut off for the annotated alleles of the barcodes that contain human sequences. Reads in each barcode were filtered for the 90% similarity cut off set to the annotated V_H and V_L genes. Remaining reads were filtered for their functionality and only the reads with a recognized heavy and light chain CDR3 sequences were taken into consideration. Each barcode’s raw excel file was filtered against the heavy chain CDR3 sequence of SCA431 scFv to find out whether there is plasmid #1468 spill over. The number of unique productive scFvs in a barcode was calculated by subtracting the scFvs comprising of the same V_H and V_L alleles from the total number of productive reads. By using Prism 8.0, pie charts were generated for each unique human allele and the size of the slices were distributed according to the number of reads these unique alleles were annotated. The next set of pie charts were generated with the inclusion of the annotated *Mus musculus* sequences in the barcodes with plasmid #1468 spill over and the overrepresented sequences were sliced out. For each barcode, heavy and light chain CDR3 regions were constructed by using SnapGene. To do so, CDR3 sequences obtained from V-QUEST were uploaded to SnapGene’s “Align Multiple Protein Sequences” tool and the alignments were generated by using MUSCLE algorithm.

4 Results

4.1 Generation of single-cell derived Jurkat reporter cell line

To generate a cellular CAR library, my first task was to cultivate a reporter Jurkat cell line. This cell line had to be sensitive enough to respond to antigen-specific stimulation via an engrafted CAR. To generate this cell line, I cultivated several single-cell derived clones and challenged them with various antigen independent and antigen dependent stimulation experiments that were performed either in bulk population or on single-cell level. The cell line obtained after several optimization experiments was then ready to be used in the production of cellular CAR libraries.

4.1.1 Establishment of Jurkat reporter cell line J7

To generate a cellular CAR library, the first step was to obtain a reporter Jurkat clone that is sensitive to antigen-specific stimulation. In order to generate a Jurkat reporter cell line, wild type Jurkat cells were transduced with lentivirus that encodes for 12 times NFAT response element (RE) followed by a minimal human IL2 promoter that drives the expression of Venus ($(NFAT)_{12}$-hIL2-Venus), an eGFP variant (Figure 4.1.1.1 A). I tested the responsiveness of the transduced cells by treating them with 5µg/ml phytohemagglutinin (PHA) for 24 hours (3.5.1). Cells were acquired by flow cytometry and FITC filter was selected for analysis of Venus expression. Supplementary Figure 1 displays the gating strategy of all the FACS plots analyzed. Cells are pre-gated on single, live population. As shown in Figure 4.1.1.1 B top, the stimulation of transduced cells was very heterogeneous. The experiment was repeated 3 times with 3 technical replicates and I found around 13% of the cells responsive to PHA treatment. The cells were stimulated in an antigen-specific stimulation experiment (3.5.2) to test if they show better reactivity. CAR-Jurkat cells were incubated with antigen-coated beads and further analyzed by FACS (Figure 4.1.1.1 C). To challenge Jurkat reporter cells in antigen-specific stimulation context, I either lentivirally transduced the cells with the lentiviral vector #53 (3.1.3) or electroporated them with plasmid #272 that has a pS/MARt expression cassette (3.3.1). Both vectors drive the expression of a model anti-CEA-CAR. 2 days after electroporation, a FACS staining was performed to analyze the CAR expression level (Figure 4.1.1.1 D top) (3.4.1). 99.3% of the lentivirally transduced cells and 84.5% of the electroporated cells expressed the CAR. After confirming CAR expression, I coupled Dynabeads (Thermo Fisher, MA USA) with biotinylated CEACAM5 antigen and started the co-incubations in 1:1 bead to cell ratio (3.5.2). Reporter cells that do not express any CAR were used as negative control. After overnight incubation, I determined the reporter expression of the cells via flow cytometry. I observed that Jurkat reporter cells in bulk population did not react to antigen-specific stimulation (Figure 4.1.1.1 D bottom). Therefore, I stimulated the cells with PHA and sorted out responsive top 10% of the cells via FACS (Figure 4.1.1.1 B). The sorted cells were labelled as “GFP+”.

My hypothesis to obtain a sensitive, homogenously reactive cell line was to generate single-cell derived clones out of the sorted GFP+ subpopulation. In order to achieve this goal, I used the Phenomex Lightning™ device and performed a single-cell stimulation assay. To do so, single cells from the sorted GFP+ population were penned inside an OptoSelect™ chip by using single cell penning algorithm (3.7.1). Empty pens together with pens with multiple cells inside were excluded from further analysis as they would not give rise to a single-cell derived colony. After penning the cells, proliferation of the cells

inside the chip was quantified. As Figure 4.1.1.1 E depicts, the mean number of cells in each pen increased steadily over 6 days of incubation. After assuring cell growth inside the chip, on day 3, the chip was treated with PHA overnight. The chip was imaged with brightfield and FITC fluorescent filter cube every hour starting from the PHA stimulation. Figure 4.1.1.1 F shows the activation of a single cell after as little as 4 hours of PHA stimulation. I grew the cells inside the chip for 6 days and exported 36 single-cell derived clones off the chip. Some of the exported clones' brightfield and FITC fluorescent images are shown in Figure 4.1.1.1 G. 8 out of these 36 clones further proliferated off-chip. Emerging clones were characterized after overnight PHA treatment with flow cytometry analysis. I determined the percentage of activated cells and FITC mean fluorescent intensity (MFI) fold change (FC). The FITC MFI FC was calculated by dividing FITC MFI of the stimulated cells by the unstimulated cells. Clone derived from pen number 215 resulted in the highest percentage of activated cells and FITC MFI FC compared to other exported clones (Supplementary Figure 1A). 75% of the cells derived from pen 215 responded to overnight PHA incubation and had FITC MFI FC of 8. When PHA treatment was stopped at day 1, cells returned to their basal reporter expression levels at day 10 (Figure 4.1.1.1 H, top). However, as depicted in Figure 4.1.1.1 H, the stimulation of the clone 215 was not uniform. Even though the initial pictures taken during the penning process showed it derived from a single cell, it was contaminated with cells escaped from the surrounding pens during its export (Supplementary Figure 1B). In order to remove the contaminating cells, I generated single-cell derived clones out of 215 by performing a limiting dilution experiment (3.1.6). From emerging single-cell derived clones of 215, clone 7 showed the most potent activation with 63 times FITC MFI FC upon PHA treatment (Figure 4.1.1.1 I). I named this clone "J7" and tested its turn-on, turn-off capability as a reporter cell line. To do so, I stimulated the clone with PHA overnight and acquired the cells by flow cytometry. Compared to their parent clone 215, J7 achieved homogeneous upregulation of the reporter and activated cells gave rise to a single peak shift in the FACS plot. After the flow cytometry analysis, PHA stimulation was stopped. On day 10, cells returned to basal reporter expression level and were indistinguishable from their unstimulated counterparts (Figure 4.1.1.1 H bottom).

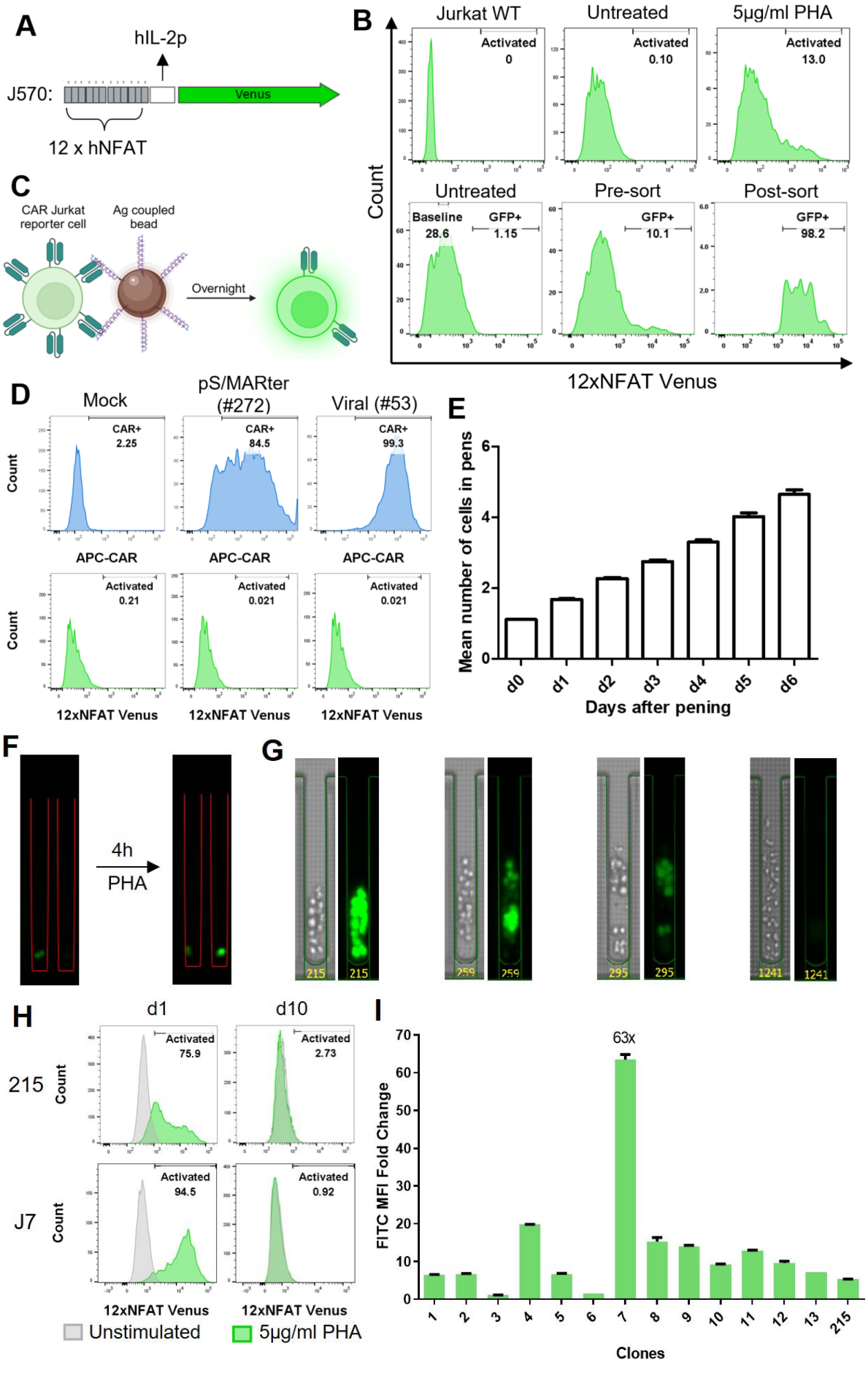
A
hIL-2p
J570:
Venus
12 x hNFAT
B
Jurkat WT
Untreated
5µg/ml PHA
Activated
0
Activated
0.10
Activated
13.0
Count
Untreated
Pre-sort
Post-sort
Baseline
GFP+
28.6
GFP+
1.15
GFP+
10.1
GFP+
98.2
12xNFAT Venus
C
CAR Jurkat reporter cell
Ag coupled bead
Overnight
D
Mock
pS/MARter (#272)
Viral (#53)
CAR+
2.25
CAR+
84.5
CAR+
99.3
Count
APC-CAR
APC-CAR
APC-CAR
Activated
0.21
Activated
0.021
Activated
0.021
Count
12xNFAT Venus
12xNFAT Venus
12xNFAT Venus
E
Mean number of cells in pens
0
2
4
6
d0
d1
d2
d3
d4
d5
d6
Days after pening
F
4h
PHA
G
215
215
259
259
295
295
1241
1241
H
d1
d10
215
J7
Count
Activated
75.9
Activated
2.73
Activated
94.5
Activated
0.92
12xNFAT Venus
12xNFAT Venus
Unstimulated
5µg/ml PHA
I
FITC MFI Fold Change
63x
0
10
20
30
40
50
60
70
1
2
3
4
5
6
7
8
9
10
11
12
13
215
Clones

Figure 4.1.1.1: Establishment of Jurkat reporter cell line J7 by single cell cloning. A: Lentiviral particles were used to transduce wild type Jurkat cells (ACC282) with depicted $(NFAT)_{12}$-hIL2-Venus. **B:** (Top) Transduced Jurkats, cells were stimulated with 5µg/ml PHA for 24 hours. From left to right, FACS plots depict the induced expression of Venus upon PHA treatment of untransduced cells, transduced but unstimulated cells and transduced and stimulated cells, respectively. Cells were pre-gated as explained in Supplementary Figure 1. Data is representative of 3 independent experiments each performed with 3 technical replicates. (Bottom) Reporter cells were stimulated with 5µg/ml PHA overnight, and top 10% responsive cells were sorted from the bulk population. The left plot shows the reporter expression of unstimulated cells. The middle plot depicts the reporter expression of bulk Jurkat reporter cells that were stimulated with 5µg/ml PHA overnight pre-sort. The purity post-sort was evaluated as shown in the right plot. **C:** Representative image of how antigen-specific stimulation is carried out. CAR expressing Jurkat reporter cells were incubated with target antigen coated beads overnight to be analyzed via FACS the next day. **D:** J570 cells were engrafted with an anti-CEA-CAR construct either by a pS/MARt plasmid (#272) or by viral transduction (#53). The CAR expression levels of mock, plasmid engrafted and virally transduced cells were shown on the top panel, respectively. 2 days post engraftment, cells were co-incubated with CEACAM5 coupled Dynabeads in 1:1 cell to bead ratio for 24 hours for antigen-specific stimulation. Cells were analyzed by flow cytometry. Bottom panel shows the activation status of the samples matched with CAR expression profiles shown in the top panel. Data is representative of 3 technical replicates. **E:** Single GFP+ J570 cells were penned into the Optoselect™ chip. Cell count in pens were followed up to 6 days. Data is shown as mean ± standard error of the mean. **F:** A representative image of an early responding J570 clone showing reporter expression induction before and after 4-hour PHA treatment. **G:** Representative brightfield and fluorescent images of single-cell derived clones that were exported from Lightning™ to be grown off-chip. **H:** (Top) Clone exported from pen number 215 was stimulated with 5µg/ml PHA overnight. After overnight incubation, cells were washed and allowed to cool down. Left plot depicts the stimulation of clone 215 after overnight incubation. 10 days post stimulation, cells were acquired with FACS and compared to unstimulated cells. Data is representative of 3 independent experiments each performed with 3 technical replicates. (Bottom) Clone number 7 was stimulated with 5µg/ml PHA overnight. Left plot depicts the stimulation of clone 215-7 (J7) after overnight incubation. 10 days post stimulation, cells returned to their basal state as shown in the right plot. Data is representative of 3 independent experiments each performed with 3 technical replicates. **I:** A limiting dilution experiment was performed with Lightning export clone 215. Emerging clones were screened for their stimulation capacity with 5µg/ml PHA overnight. FITC MFI fold change (FC) of stimulated clones are depicted in bar plot. Data are shown as mean ± standard deviation of 3 technical replicates.

4.1.2 Antigen-specific stimulation of J7

The reporter cells J7 were able to get activated when stimulated with PHA. However, their response to antigen-specific stimulation also had to be analyzed. Therefore, I performed a proof of principle experiment in which I tested the generated clone J7 in the context of antigen-specific stimulation. To do so, I transduced J7 cells with a lentiviral vector #53 in order to stably express the anti-CEA-CAR and generated J7-53 cells. In this nomenclature, characters before dash represent the cell line and it is followed by the plasmid identifier that is used to transfect/transduce the cell line. After confirming the CAR expression, I coupled Dynabeads with biotinylated CEACEM5 protein according to manufacturer's instructions. Successful coupling of the protein was determined by staining the beads with the PE conjugated anti-CEACAM5 antibody. Figure 4.1.2.1 A depicts the flow cytometry analysis of a representative antigen coupling experiment. Beads that were successfully coupled with CEACAM5 are shown in purple (3.5.2). I coupled the Dynabeads in the presence of 1x and 2.5x more than recommended amount of CEACAM-5 protein to test if higher protein concentration results in better

coupling, thus a higher degree stimulation of the J7-53 cells. After overnight co-incubation of J7-53 with uncoupled beads, and with the beads coupled in the presence of 1x or 2.5x times recommended protein, the cells were analyzed via flow cytometry to quantify their activation and CAR expression. Dynabeads coupled with 1x and 2.5x times recommended concentration of CEACAM5 activated 24.9% and 49% of the J7-53 cells, respectively (Fig. 4.1.2.1 B). Upon incubation with their target antigen, J7-53 cells downmodulated their CAR expression both in day 1 and day 2 (Fig. 4.1.2.1 C). Condition with 2.5x excess protein, caused a higher degree of CAR downmodulation compared to 1x. Moreover, beads conjugated with higher protein concentration resulted in higher activation level of J7-53 cells with 3.9 FITC MFI FC compared to 3 FITC MFI FC achieved by beads coupled as recommended.

As increased protein concentration during bead coupling caused a higher degree of stimulation of the J7-53 cells, I performed further antigen-specific stimulation experiments with the beads that were conjugated in the presence of higher concentrations of CEACAM5. In this experiment, protein concentrations from 1x to 5x times the recommendation were used for bead coupling. As observed before, increasing protein concentration during bead coupling resulted in serially increasing CAR downmodulation. The percentage of activated cells also increased with higher protein concentrations used during coupling. However, the percentage of activated cells plateaued around 55% as beads coupled with 3x or more than recommended protein resulted in similar activation levels. Moreover, the level of reporter expression also was not to affected by the increasing protein concentration. Except for 1x condition, all other conditions resulted in FITC MFI FC around 6 (Figure 4.1.2.1 D).

As J7 cells were responsive against antigen-specific stimulation in bulk population, I stimulated J7-53 cells at single-cell resolution by using the Lightning^{TM} device (3.7.2). To do so, CEACAM5 coupled Dynabeads were loaded first to the pens (Fig. 4.1.2.1 E, left). After penning of single J7-53 cells, cells were imaged in brightfield and FITC filter cube for 24 hours (Fig. 4.1.2.1 E, middle). Taken brightfield and FITC images were overlaid. In the next 24 hours, cells settled to the bottom of the pens due to 1% angle of the chip nest. J7-53 single cells were activated after 24 hours of antigen-specific stimulation. Stimulated cells were displayed in green due to activation induced reporter expression (Fig. 4.1.2.1 E, right).

To quantify the stimulation of single cells, I set filter criteria to eliminate the pens that had one of the following conditions:

1. Pens with insufficient amount of beads were filtered out. Pens that had bead surface area equal to or greater than the decided cut off were analyzed further.
2. Pens with several cells inside.
3. Pens that did not receive any cells.
4. Pens that had already activated cells in the beginning of the overnight incubation.
5. Pens that do not have paired measurements at the beginning and 24 hours after the start of the incubation. These two measurements had to be taken to be able to calculate FITC MFI FC in single cell level.

In total, 477 pens remained after filtering with the listed criteria. The FITC MFI FC of each of these 477 cells was calculated and depicted in a heat map as shown in Figure 4.1.2.1 F. 16% of the cells achieved

at least 4 FITC MFI FC after 24 hours of bead stimulation, in total 57% of the cells showed some degree of reporter expression induction.

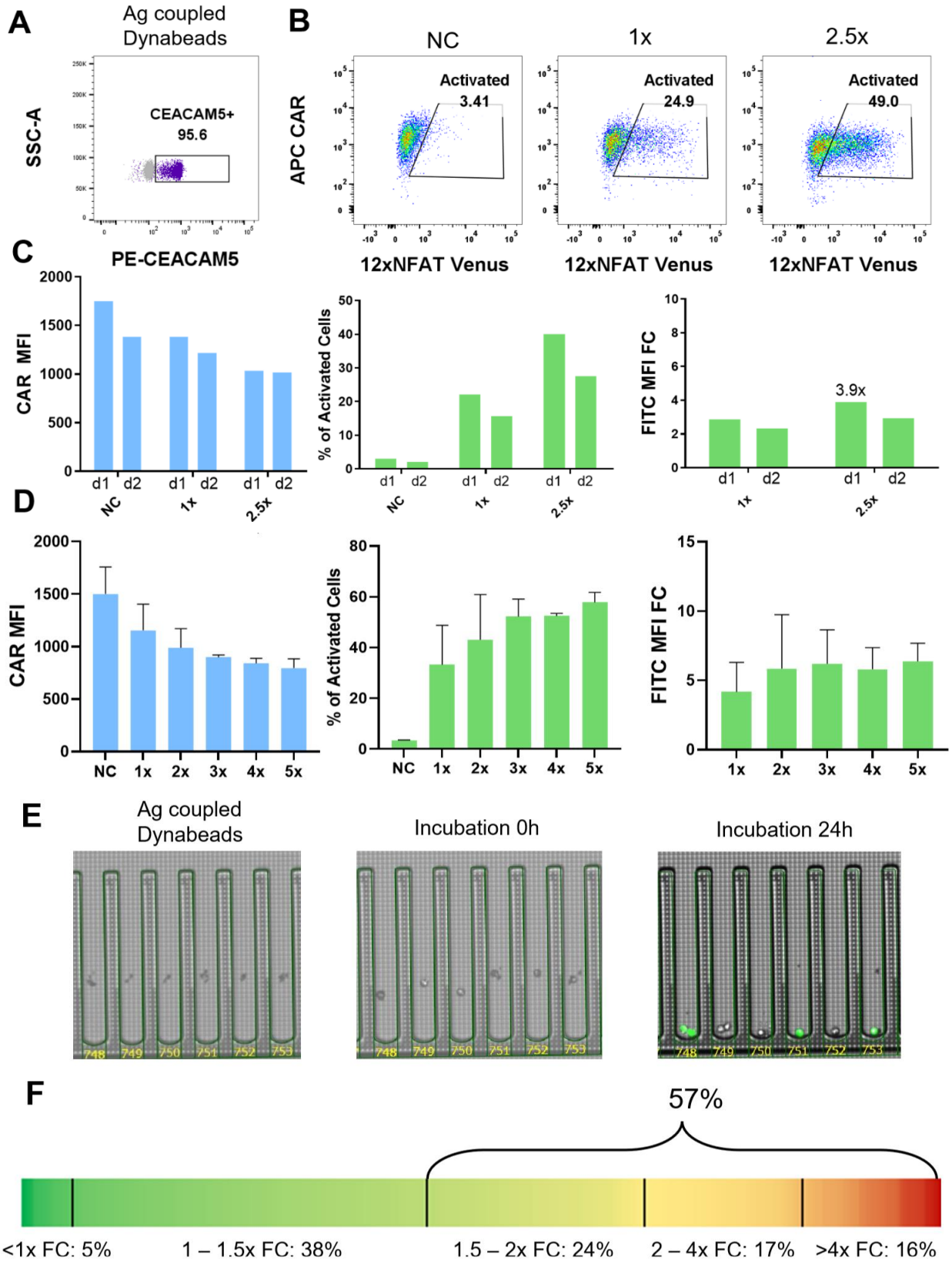

Figure 4.1.2.1: Testing antigen-specific stimulation capacity of J7. A: CEACAM5 coupled Dynabeads were stained with anti-CEACAM5 PE antibody and acquired in flow cytometry. Dynabeads that were successfully coupled with the antigen are depicted in purple. **B:** Dynabeads that were coupled with 1x CEACAM-5 concentration and 2.5x CEACAM-5 concentration recommended by the manufacturer's instructions from left to right, respectively. J7-53 cells were incubated overnight with coupled or uncoupled Dynabeads in 1:10 cell to beads ratio. 1:10 cell to beads ratio was kept constant for antigen-specific stimulation experiments with Dynabeads. Plots depict stimulation of cells and CAR expression for each condition in x and y-axes, respectively. **C:** CAR expression, percentage of activated cells and FITC MFI FC of the cells depicted in B are quantified and depicted in bar plots. (Left) CAR expression of J7-53 cells that were incubated with respective Dynabeads are depicted for two days of incubation. (Middle) Percentage of activated cells was determined according to the gating strategy depicted in B. (Right) Parallel with percentage of activated cells, FITC MFI FC was calculated during 2 days of Dynabead incubation. **D:** Similar to C, from left to right; CAR expression, percentage of activated cells and FITC MFI FC of the cells that were stimulated for 24 hours with Dynabeads coupled with respective times of antigen recommended are depicted. Experiment was performed in two biological replicates. Error bars depict the standard variation **E:** J7-53 cells were tested in a single cell antigen-specific stimulation experiment. A representative image of the pens from 748 to 753 is shown. (Left) CEACAM-5 coupled Dynabeads were penned with Bulk Penning algorithm and imaged in brightfield. (Middle) Single J7-53 cells were penned into each pen. Image is an overlay of the brightfield and fluorescent imaging in FITC filter cube. (Right) The stimulation of the cells depicted in the middle image recorded for 96 hours. Image is an overlay of the brightfield and fluorescent imaging in FITC filter cube. It depicts the induction of reporter expression after 24 hours of antigen-specific stimulation. **F:** All the pens that received a single cell and had sufficient mass of Dynabeads were analyzed for their reporter expression. Only the cells that have a paired measurement in the beginning of the experiment and after 24 hours of stimulation were considered for analysis. 477 pens satisfied the two criteria. For each these 477 pens that has a paired measurement, FITC MFI FC was calculated by dividing the FITC MFI after 24 hours of stimulation to the FITC MFI in the beginning of the incubation.

4.1.3 Refining the antigen-specific stimulation of J7i

During the establishment of the antigen-specific stimulation of J7 cells in single-cell level or in bulk population, the responsiveness of the J7 and J7-53 to the PHA treatment was decreasing over time. The percentage of PHA responsive cells was decreased from 94.5% (Figure 4.1.1.1 H, bottom) to 90.7 and 83.5% in J7 and J7-53 cells, respectively (Figure 4.1.3.1 A, top). Moreover, compared to Figure 4.1.1.1 H bottom, the activation was no longer a single peak shift observed during characterization of J7, meaning their response was becoming heterogeneous. To solve this problem, I stimulated J7 and J7-53 cells with PHA overnight and I sorted the cells with top 40% FITC MFI the next day (3.4.2). The newly sorted populations were then named J7i and J7i-53. To see the effect of the sort, J7i and J7i-53 populations were stimulated with PHA and unlike their parent clones, they achieved a single peak shift in FITC MFI. The percentage of activated cells also increased to 96.6% and 93.1% for J7 and J7-53 (Fig. 4.1.3.1 A, bottom). Moreover, I calculated the FITC MFI FC of the cells shown in Figure 4.1.3.1 A and found out that the FITC MFI FC of J7i increased from 30 to 40, and similarly for J7i-53 from 20 to 30 (Fig. 4.1.3.1 B).

After restoring sensitivity of the cells, they were again tested by an antigen-specific stimulation experiment. To increase the antigen density on the surface of the beads, PureProteome (PP) beads with a larger diameter were used (Merck, Darmstadt). PP beads had 10 µm nominal diameter and they are about 4 times larger than Dynabeads in diameter. This translates into 16 times higher surface area

for antigen presentation. Due to their increased size, they were able coat more CEACAM5 protein. Figure 4.1.3.1 C shows the FACS result of a representative CEACAM-5 coupling experiment. 97.4% of the beads were successfully coupled and depicted in purple. I compared the real time images of antigen-specific stimulation of anti-CEA-CAR expressing reporter cells with either Dynabeads or PP beads. First images show respective penned beads. Second images depict the interaction of the beads with the cells (Fig. 4.1.3.1 D).

To test the efficiency of PP beads in stimulating J7i-53 cells, I co-incubated J7i-53 cells in 1:1 to ratio with CEACAM-5 coated PP beads that were prepared according to manufacturer's instructions. After 24 hours of co-incubation, PP beads coated with target antigen were able to activate 88.1% of the J7i-53 cells with a higher degree of reporter expression compared to Dynabeads (Fig. 4.1.3.1 E). As the stimulation of the cells with PP beads was comparable to a PHA treatment, I titrated the amount of protein that I used during coupling of the beads and kept cell to bead ratio at 1:1. I used 0.25x, 0.5x or 1x amount of protein that is recommended by the manufacturer during coupling reaction. J7i-53 cells were stimulated overnight with the beads prepared under mentioned conditions and were analyzed for their CAR expression, percentage of activated cells and FITC MFI FC. Compared to Dynabead antigen-specific stimulation experiments (Figure 4.1.2.1 C & D, left), PP beads caused a higher degree of CAR downmodulation in J7i-53 cells. In every condition, CAR downmodulation occurred in a similar level. Activated cell percentage was around 85% and FITC MFI FC ranged between 30 to 35 (Figure 4.1.3.1 F). Protein concentrations under 0.25x less than manufacturer's recommendation resulted in partial bead coupling and lower degree of cell activation (data now shown). Therefore, for PP bead coupling, the condition with 0.25x less protein was used in the following experiments.

After successful stimulation of the cells in bulk population, they were challenged at single-cell resolution by using the Lightning^{TM} device. Like Dynabeads, CEACAM5 coated PP beads were placed into each pen by bulk penning algorithm (Figure 4.1.3.1 G, left). Single J7i-53 cells were penned together with PP beads. A gravity penning was done to have beads and the cells settle down to the bottom of the pens (MM). Subsequently, cells were followed by capturing images in FITC and brightfield filter cubes every hour. The brightfield and FITC images are overlaid. Cells got activated in the representative part of the chip after 24 hours of co-incubation with antigen-coupled beads (Figure 4.1.3.1 G middle, right).

I analyzed the activation of single cells after 24 hours of bead stimulation and only considered the pens passing the following filter criteria:

1. Pens that did not receive any cells.
2. Pens that did not receive any beads.
3. Pens that received multiple cells
4. Pens that did not have a paired FITC MFI measurement at the beginning and 24 hours after bead incubation.

782 pens satisfied all the criteria and their FITC MFI FC was calculated like done for Dynabead experiment. PP beads achieved to stimulate 32% of the cells over 16x according to measured FITC MFI (Figure 4.1.3.1 H). 45% of the cells had a FITC MFI FC of greater than 4 compared to 16% achieved with Dynabeads. 62% of the cells reacted against the antigen-specific stimulation and upregulated the reporter expression to a certain degree.

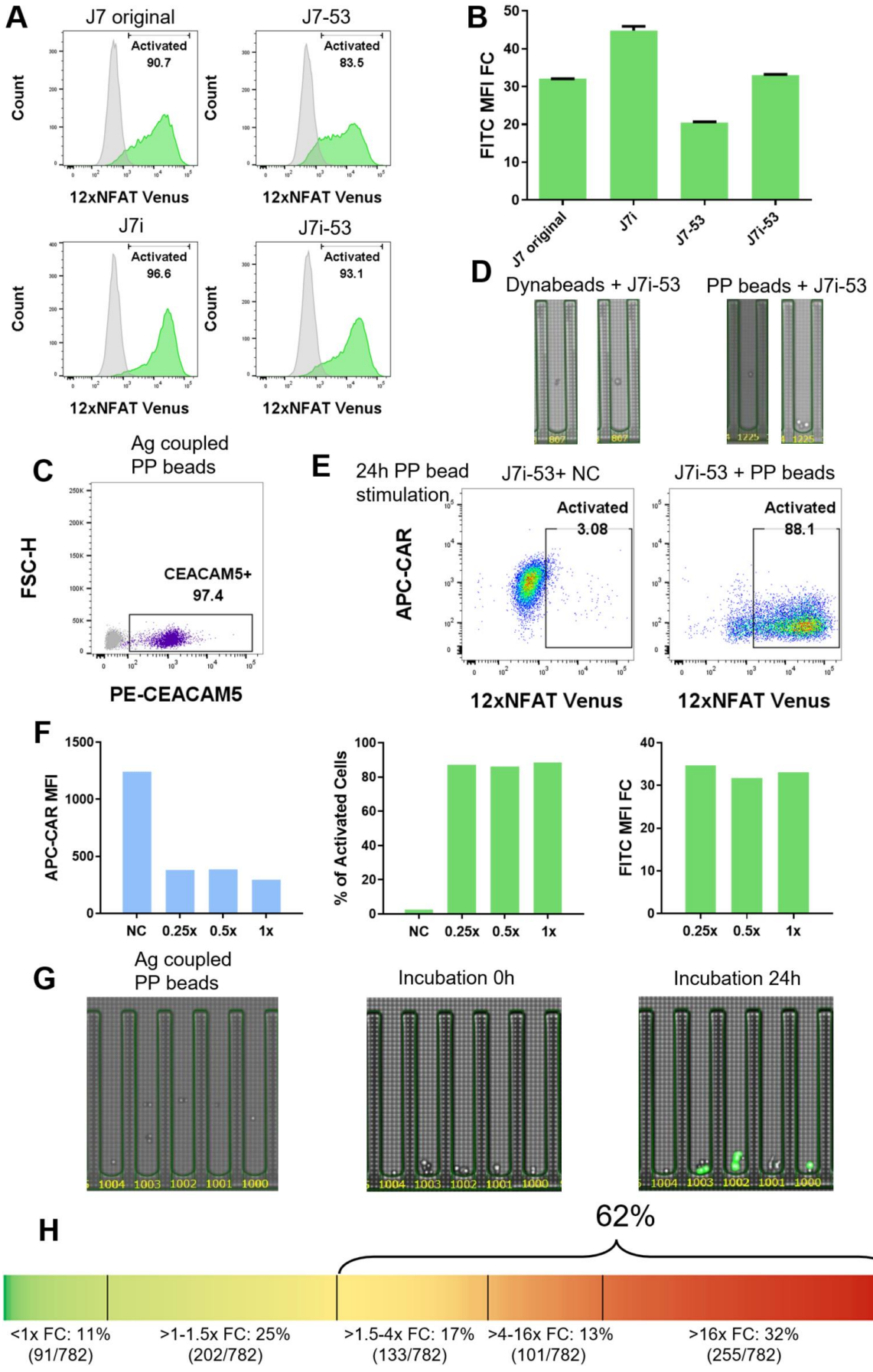
A
J7 original
Activated
90.7
Count
12xNFAT Venus
J7-53
Activated
83.5
Count
12xNFAT Venus
J7i
Activated
96.6
Count
12xNFAT Venus
J7i-53
Activated
93.1
Count
12xNFAT Venus
B
FITC MFI FC
50
40
30
20
10
0
J7 original
J7i
J7-53
J7i-53
D
Dynabeads + J7i-53
PP beads + J7i-53
C
Ag coupled
PP beads
FSC-H
CEACAM5+
97.4
PE-CEACAM5
E
24h PP bead
stimulation
J7i-53+ NC
J7i-53 + PP beads
APC-CAR
Activated
3.08
Activated
88.1
12xNFAT Venus
12xNFAT Venus
F
APC-CAR MFI
1500
1000
500
0
NC
0.25x
0.5x
1x
% of Activated Cells
100
80
60
40
20
0
NC
0.25x
0.5x
1x
FITC MFI FC
40
30
20
10
0
0.25x
0.5x
1x
G
Ag coupled
PP beads
Incubation 0h
Incubation 24h
1004 1003 1002 1001 1000
1004 1003 1002 1001 1000
1004 1003 1002 1001 1000
H
62%
<1x FC: 11%
(91/782)
>1-1.5x FC: 25%
(202/782)
>1.5-4x FC: 17%
(133/782)
>4-16x FC: 13%
(101/782)
>16x FC: 32%
(255/782)

Figure 4.1.3.1: Improving antigen-specific stimulation of J7i. A: Top 40% of the most responsive cells to PHA stimulation from J7 and J7-53 were sorted via FACS. Columns show the overlaid reporter expression of overnight 5µg/ml PHA stimulated and unstimulated cells before and after FACS. On top left, stimulation of unsorted cells (J7), on the bottom left stimulation of sorted cells (J7i) are depicted. The right column depicts the result of the same experiment performed with J7-53 and sorted J7i-53. Data is representative of 3 independent experiments. **B:** FITC MFI FC is calculated for sorted and unsorted populations of J7 and J7-53 as described before. Data is representative of 3 technical replicates. Data are shown as mean ± standard deviation. **C:** CEACAM5 coupled PP beads were stained with anti-CEACAM5 PE antibody and acquired by flow cytometry. PP beads that were successfully coupled with the antigen are depicted in purple. **D:** (Left) An example image of bulk penned CEACAM5 coupled Dynabeads is shown in the left image. Second image depicts the interaction of Dynabeads with J7-53 cells. (Right) Example image of a CEACAM5 coupled PureProteome bead is shown in the first image. The interaction of 2 J7i-53 with a PP bead is depicted. **E:** J7i-53 cells were incubated overnight in 1:1 cell to bead ratio with uncoupled PureProteome (left), or PP coupled with 1x CEACAM-5 concentration recommended by the manufacturer's instructions (right). Plots depict stimulation of the cells and CAR expression in x and y axes, respectively. **F:** PP beads were coupled to CEACAM5 with 1x, 0.5x and 0.25x protein concentration recommended by the manufacturer. CAR expression, percentage of activated cells and FITC MFI FC of the cells 24 hours after incubation with the beads are depicted. (Left) CAR expression of J7i-53 cells that were incubated with respective beads are shown. (Middle) Percentage of activated cells are displayed according to the gating strategy in E after overnight stimulation. (Right) FITC MFI FC is calculated as mentioned before and illustrated for cells stimulated by the PP beads with respective coupling reactions. **G:** Single J7i-53 cells were stimulated with CEACAM5 coupled PP beads at single-cell level inside an OptoSelect™ chip. Representative images of the pens from 1000 to 1004 is depicted in chronological order of the experiment described as Figure 4.1.2.1 E. (Left) CEACAM5 coupled PureProteome beads were penned into the chip by bulk penning algorithm. (Middle) Single J7i-53 were moved into each pen and incubated with CEACAM5 coupled beads for 96 hours. Image is an overlay of the brightfield and fluorescent imaging in FITC filter cube. (Right) Activation of the cells after overnight incubation is illustrated as overlays with brightfield images. **H:** All the pens that have at least 1 CEACAM5 coupled bead together with a single J7i-53 were analyzed for their reporter expression. For 782 pens that have a paired measurement, FITC MFI FC for paired measurements were calculated and shown in a heat map as explained in Figure 4.1.2.1 E.

4.1.4 CAR expression upon antigen-specific stimulation

To see the effect of antigen-specific stimulation on the expression level of CAR mRNA, I used several single-cell derived clones that I obtained from previous single cell experiment when I stimulated J7i-53 cells with CEACAM5 coupled PP beads (Section 4.1.3). These single-cell derived clones were named after their position in the 96 well plate that they were grown after being exported from the Lightning™ device. From the clones that were able to grow off-chip, I randomly picked 6representative ones for testing and included wild type Jurkat cells and another J7i line expressing an irrelevant TCR as my negative controls (NCs). These 8 different clones were incubated with either antigen coupled beads or uncoupled beads for 24 hours. During the first experiment, only expression of CAR mRNA was quantified. mRNA from the clones was isolated 24 hours after bead incubation. I used β-actin as the reference gene in qPCRs to calculate ΔCt values. CAR expression fold changes were calculated by using $2^{-\Delta\Delta Ct}$ method (3.6). Upon antigen-specific stimulation, change in the expression of the CAR mRNA varied from 2-fold upregulation to 4-fold downregulation (Supplementary Figure 2 A). As expected, no CAR amplification was detected in the NCs. These 2 cell lines were kept constant as NC throughout all qPCR experiments.

As there was not a clear trend in the regulation of CAR expression, the experiment was repeated. However, this time I also analyzed the expression of Venus mRNA as positive control. The cells were again stimulated with either uncoupled or antigen coupled beads as before and fluorescent microscopy images of the clones were taken before and after 24 hours of bead incubation (Figure 4.1.4.1 A). Venus mRNA expression FC was analyzed first to confirm that qPCR experiment was carried out correctly (Figure 4.1.4.1 B, left). After 24 hours of stimulation, I observed a heterogeneous response amongst the clones. B2 was the most responsive clone with FC of ~17, and C7 was the least responsive clone with ~4 FC, more than 4-fold less reporter expression induction than B2. Nevertheless, comparison of the qPCR results with fluorescent images revealed a direct correlation between the two results. When clones were ranked visually according to their reporter expression in the images after 24 hours of stimulation, it overlapped with ranking according to Venus mRNA expression FC. Results of the qPCR done for Venus expression was assuring that the generated qPCR data was reliable. In parallel with the first qPCR experiment that was performed, there was no clear trend in terms of CAR expression profiles of the cells after 24 hours of stimulation. According to Figure 4.1.4.1 B, they either kept the CAR expression constant, or downregulated to varying degrees.

In the next experiment, I looked at the earlier time points of stimulation rather than 24 hours later assuming that the CAR expression kinetics might be faster than what I previously tested for. In this experimental design, only 2 clones, B2 and C3 were stimulated. I took samples from the cells after 2, 4, 8, 12 and 24 hours of incubation with coupled or uncoupled beads. qPCRs for β-actin, Venus and CAR expression were performed as before. For both clones, I was able to see the upregulation of Venus expression to varying degrees, however the CAR expression did not show a clear trend. B2 and C7 downregulated their CAR expression by 50%. On the other hand, the rest of the clones upregulated the CAR expression by at most 2 fold (Supp. Fig. 2 B).

So far, only the virally transduced J7i-53 clones were used in qPCR experiments. However, in the antigen-specific CAR screening pipeline, cells are engrafted with the CARs not by viral transduction but by electroporation. Therefore, I decided to test the J7i cells that were electroporated with plasmid #320. Plasmid #320 has a nanoS/MART backbone and it encodes for the same CAR construct as the lentiviral vector #53. J7i-320 cells were analyzed together with the clones B2 and C3 in earlier time points to compare both engraftment methods in terms of CAR expression upon antigen-specific stimulation. Consistent with the previous data, Venus expression increased in varying degrees in every condition (Figure 4.1.4.1 C, top). For virally transduced cells, CAR expression either stayed the same or was downregulated by around 50%. For electroporated cells, on the other hand, CAR expression FC was around 0.3 consistently in each time point. Meaning that starting as early as 2 hours after incubation with antigen coupled beads, CAR expression level in J7i-320 cells equaled 33% of the unstimulated cells (Figure 4.1.4.1 C, bottom). To confirm these results, I repeated the qPCRs for J7i-320 cells investigating same genes. As expected, various degrees of Venus upregulation were detected for every time point. However, consistent with previous experiment, CAR expression in stimulated J7i-320 cells was downregulated, reaching its lowest FC of 0.3 FC after 24 hours bead incubation (Supplementary Figure 2C).

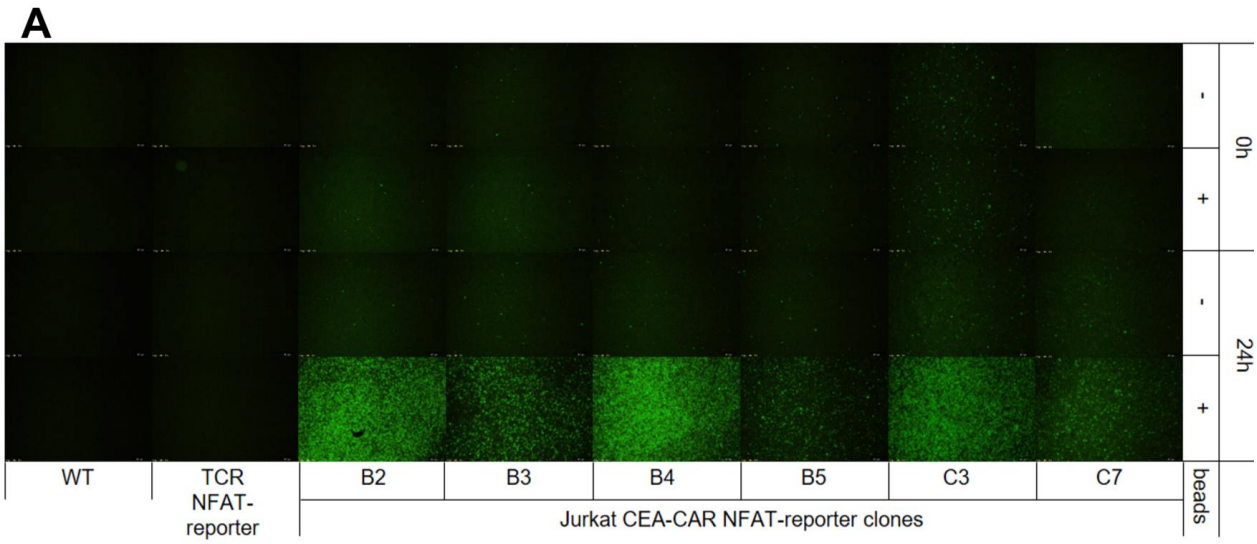
A
0h
24h
-
+
-
+
WT
TCR NFAT-reporter
B2
B3
B4
B5
C3
C7
beads
Jurkat CEA-CAR NFAT-reporter clones

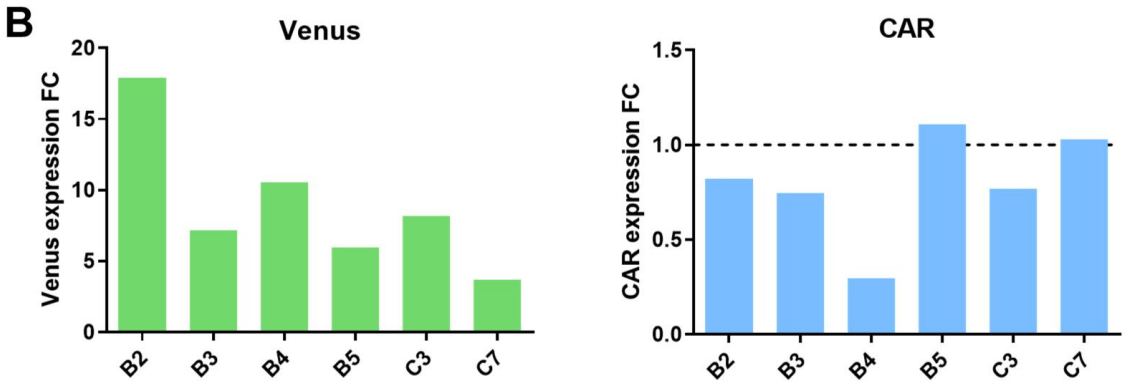
B
Venus
Venus expression FC
20
15
10
5
0
B2
B3
B4
B5
C3
C7
CAR
CAR expression FC
1.5
1.0
0.5
0.0

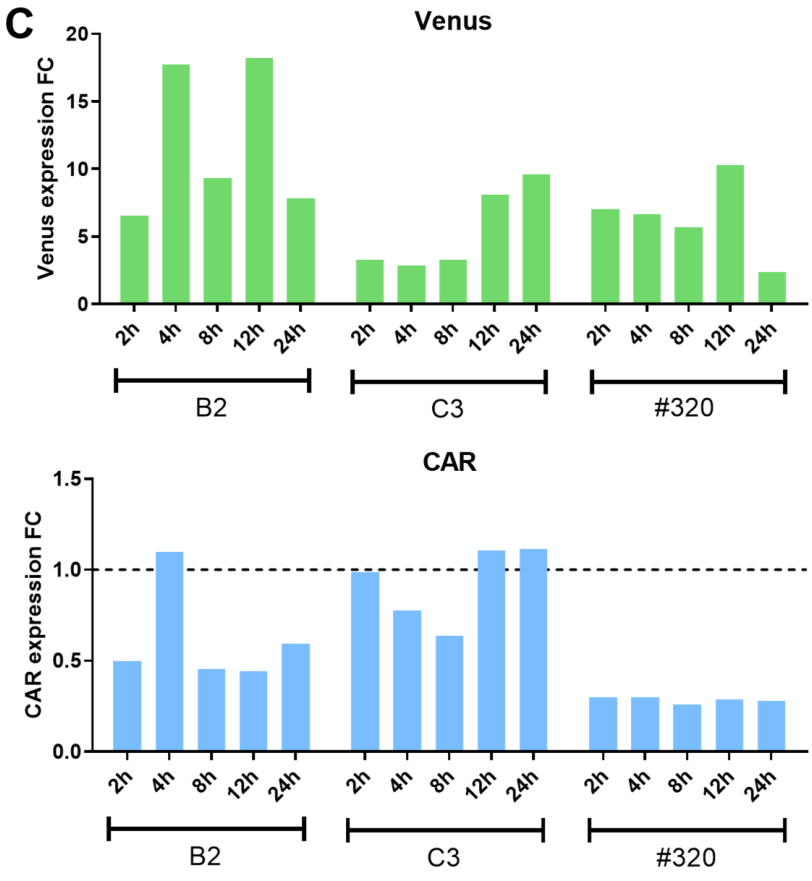
C
Venus
Venus expression FC
20
15
10
5
0
2h
4h
8h
12h
24h
B2
C3
#320
CAR
CAR expression FC
1.5
1.0
0.5
0.0

Figure 4.1.4.1: Protein and mRNA CAR expression upon antigen-specific stimulation. A: Single-cell derived clones exported from the single cell experiment, that was performed with CEACAM5 coupled PPbead to stimulate J7i-53 cells, are grown off the chip. Each exported clone was incubated in bulk population with CEACAM5 coupled, depicted on “beads” tab as (+), or uncoupled, depicted on “beads” tab as (-), PP beads. WT Jurkat cells and Jurkat reporter cells expressing an irrelevant receptor were used as negative controls. Cells were incubated with antigen-coupled or uncoupled beads for 24 hours and FITC fluorescent images were taken at the beginning (0h) and end of the incubation (24h). **B:** qPCR experiment was done with the cells shown in A after 24 hours of incubation PP beads. Per qPCR reaction, 30ng RNA was reverse transcribed. qPCRs were done in duplicates. β-actin was used for reference gene expression to normalize for cDNA input and calculate ΔCt values for Venus and CAR expression. Gene expression fold changes were calculated by using ΔΔCt method. ΔΔCt values were calculated by subtracting ΔCt values of unstimulated cells from stimulated cells for Venus and CAR expression separately. Relative fold change of gene expression level was calculated by $2^{-\Delta\Delta Ct}$ formula. Left graph depicts the FC in Venus expression, and right graph depicts the FC in CAR expression after 24 hours of antigen-specific stimulation. **C:** J7i cells were electroporated with a nanoS/MARt vector (#320) that encodes for the anti-CEA-CAR by using Neon™ Transfection System (Thermo Fisher). 2 days after electroporation, these cells were incubated with beads for 24 hours, together with B2 and C3. Samples were taken after 2, 4, 8, 12 and 24 hours of bead incubation. For each cell type, qPCRs for β-actin, Venus and CAR were performed for each respective time point in duplicates. Top graph shows the Venus expression FC, and bottom graph shows the CAR expression in respective time points.

4.1.5 Stimulation of electroporated cells at single-cell level

As mentioned before, during the screening pipeline J7i cells were electroporated with a plasmid CAR library. Thus, the antigen-specific stimulation ability of electroporated J7i cells had to be tested first in bulk population. To do so, I electroporated J7i with plasmid #320 and two days after electroporation, I confirmed the CAR expression and set up the following experiment. Virally transduced J7i-53 cells and electroporated J7i-320 cells were incubated in 1:1 effector to target (E:T) ratio with either CEACAM5-coupled beads or MCF-7 cell line which expresses CEACAM5. “Unstimulated” means that J7i-53 and J7i-320 cells were incubated with uncoupled beads or with an antigen irrelevant cell line HEK293T. J7i-53 stimulated with PHA was used as positive control. Antigen-specific stimulation of J7i-53 cells in both scenarios was comparable to the PHA treated positive control. 88.7% of the J7i-53 cells were activated in positive control, while 81% of the J7i-53 cells were activated upon both antigen specific stimulation settings. J7i-320 cells got slightly activated and started expressing Venus upon electroporation in the absence of any stimulation. This “shoulder effect” is observed when unstimulated J7i-53 and J7i-320 cells depicted in grey are compared to each other. Nevertheless, 87% of J7i-320 cells incubated with MCF7 cells got stimulated and gave rise to a single peak shift. Cells incubated with antigen-coupled beads also managed to get activated tough to a lower degree, possibly due to insufficient antigen coupling to the beads (Fig. 4.1.5.1 A). FITC MFI FC were calculated for the conditions shown in Figure 4.1.5.1 A. J7i-53 cells that were stimulated via beads or MCF7 cells achieved approximately 32 FITC MFI FC, comparable to positive control with 35.8 FC. However, due to the shoulder effect, the FITC MFI FC was lower for J7i-320 cells. 8.5 and 17.5 FITC MFI FC were observed for cells stimulated with beads and MCF7 cells, respectively. (Fig. 4.1.5.1 B). In both J7i-320 incubations, activated cells showed a distinct peak due to antigen-specific stimulation, surpassing the activation caused by the electroporation (EP).

After confirming reactivity of J7i-320 cells in bulk antigen-specific stimulation experiment, they were challenged for their antigen-specific stimulation capacity on single-cell level to see the effect of EP on the cells (3.7.2). As before, J7i cells were electroporated with plasmid #320 using Neon™ transfection system and their CAR expression was confirmed 2 days post EP. At day 2, single-cell stimulation experiment was started by using the Lightning™ device. I bulk penned antigen-coupled PP beads as before together with single J7i-320 cells. Right before J7i-320 cells were penned, they were stained with anti-hIgG PE antibody that targets the Fc domain of the anti CEA-CAR. In the beginning of the experiment, cells were imaged with PE filter cube and the CAR expression levels of individual cells were quantified by the obtained PE MFIs. The stimulation of the cells was followed by imaging via FITC filter cube every hour for 30 hours. The following pens were excluded from further analysis:

1. pens without any cells,
2. pens with multiple cells,
3. pens without any beads,
4. pens that had more than 1 missing FITC MFI measurements over 30 hours of imaging.

The remaining 1170 cells were clustered according to their Venus expression for 30 hours and a heat map was generated (Fig. 4.1.5.1 C, left). It was observed that different clusters of cells reacted against antigen-specific stimulation in varying times to various degrees. For example, cells depicted in green box are the ones reacting to stimulation early after several hours, compared to cells in yellow box that did rather late after 24 hours of stimulation. Moreover, there have been cells with already activated state shown in red boxes and over 30 hours antigen-specific stimulation, they did not react to antigen. Their reporter expression got less over time. Finally, a population of cells, shown in blue box, was observed responding to the antigen, but over the course of 30 hours of imaging, committed apoptosis possibly due to activation induced cell death (AICD). Additionally, the initial CAR expression of each single cell was analyzed. Cells were divided into 5 categories according to their relative CAR expression. After clustering according to these arbitrary categories, it was revealed that cells with a high or very high CAR expression did not respond to antigen stimulation. Rather, they burned out over time, especially cells with very high CAR expression. According to these clusters, the best responses were observed in cells with medium CAR expression level followed by the low CAR expressers (Fig. 4.1.5.1 C, right). CAR expression levels were able to explain some degree of the heterogeneity observed upon antigen-specific stimulation.

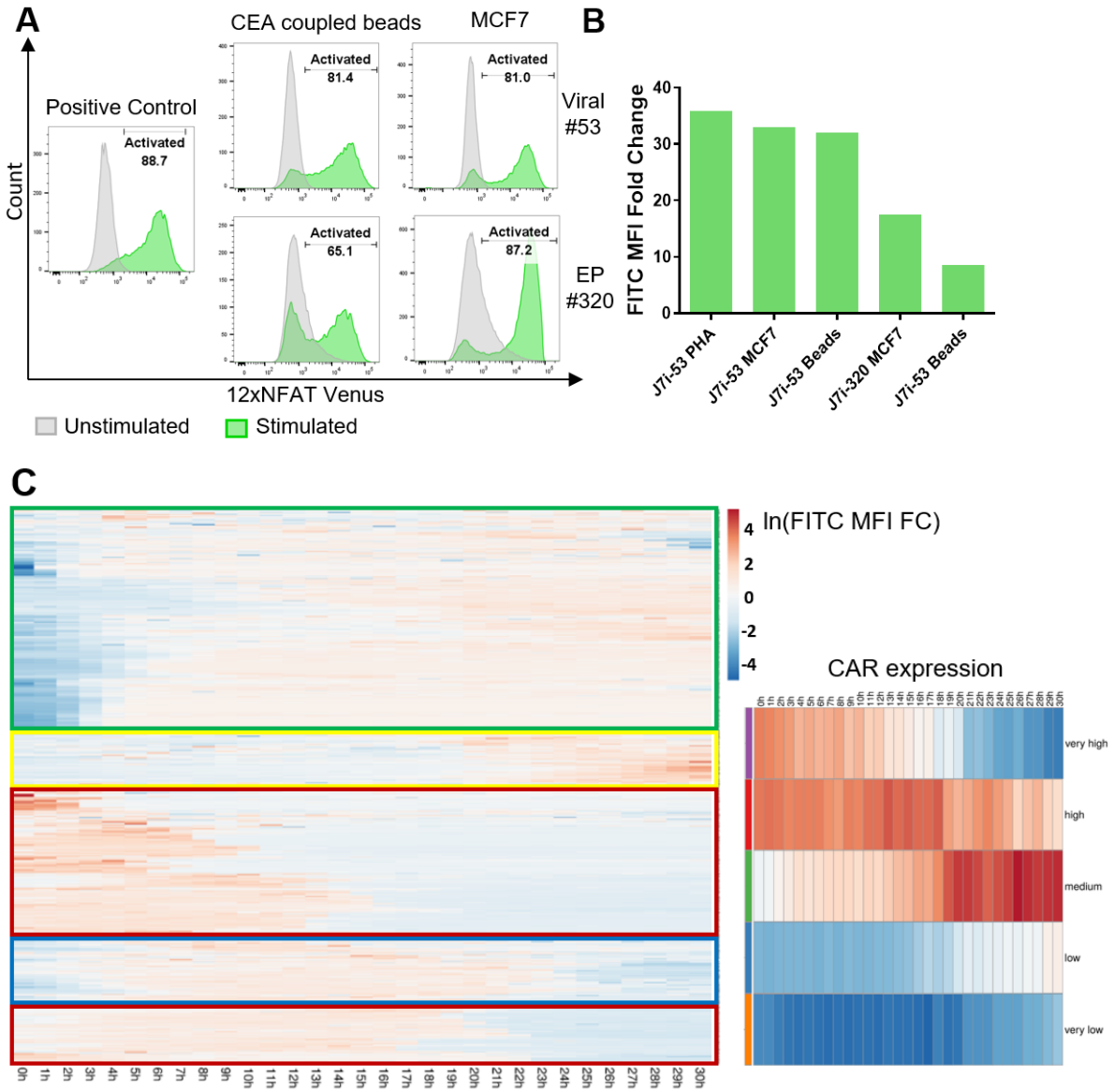

Figure 4.1.5.1: Challenging J7i in bulk and single-cell level stimulation A: J7i cells have been electroporated (#320) or virally transduced (#53) with the same CAR construct targeting CEACAM5 with either nanoS/MARt plasmids or lentiviruses, respectively. Cells were incubated overnight with either MCF7 cells or PP beads coated with CEACAM5 with 1:1 effector to target ratio. Unstimulated cells were incubated with either uncoupled beads or HEK293T cells as negative control Virally transduced cells were stimulated with PHA as positive control. Venus expression of stimulated cells (in green) are overlaid with unstimulated cells (in grey). **B:** FITC MFI FC was calculated for each condition depicted in section A by dividing the FITC MFI of stimulated cells to unstimulated cells. **C:** J7i cells were electroporated with vector #320 that encodes for the anti-CEA-CAR. 2 days after electroporation, cells were stained for their CAR expression with anti hIgG-PE antibody. Single cells were penned into an Optoselect™ chip and incubated with bulk penned CEACAM5 coupled PP beads. Chip was imaged for 96 hours by taking bright field and fluorescent FITC images every hour. (Left) A heat map was generated by plotting the ln(x) transformed FITC MFI measurement of each cell during the first 30 hours of incubation (Clustvis). Clusters with different activation patterns during the first 30 hours of antigen-specific stimulation are highlighted with colored boxes. (Right) In the beginning of the experiment, a PE imaging was done to characterize the CAR expression level of each cell that has been penned. Cells were clustered according to their CAR expression level from very high to very low. The median FITC MFI that represents the activation statues of all the cluster for each time point is visualized in a heat map for the first 30 hours of incubation.

4.2 Generation of a plasmid CAR library

In order to generate a cellular CAR library, I had to generate its components first: a reporter cell line and a plasmid CAR library. So far, I showed that I successfully cultivated a reporter cell line, J7i that achieved potent activation in bulk and on single-cell level upon antigen-specific stimulation. After characterization of the J7i cell line, I focused on generating a plasmid CAR library. My strategy to achieve this goal was to first assemble random scFv libraries from PBMCs of healthy donors and clone these scFv libraries directly into an expression vector, in a functional CAR backbone open reading frame (ORF). Therefore, this so-called plasmid CAR library is ready to be engrafted into cells for the purpose of cellular CAR library generation. Generated cellular CAR library can then be immediately screened for antigen of interest or stored in liquid nitrogen to be screened for various other antigens upon request.

4.2.1 Crucial role of Leader sequence in CAR expression

As mentioned before, to generate a CAR library, it was necessary to assemble scFv libraries. Figure 4.2.1.1 A illustrates the cloning strategy that I used for generating scFv libraries. The process started with isolation of PBMCs from 11 healthy donors (3.1.4). Total RNA extractions were performed for each donor separately (3.2.4). All the extracted RNAs were reverse transcribed into cDNA and kept separately. In order to capture the highest diversity of variable regions of B cell receptor (BCR) heavy and light chains, cDNA pools were prepared from these 11 donors. To assemble scFv libraries, I adapted the methodology developed by Pansri et al. [151] During the first attempts to generate scFv libraries, I used already established primer pairs that they modified from previously published work (2.9.1). In total, for heavy chain amplification, I used 6 forward (V_H5') primers and 4 reverse (V_H3') primers (2.9.1). In order to increase the diversity of assembled scFv library, I performed 24 separate PCRs by pairing each single V_H5' primer with a single V_H3' primer (3.2.8). To be able to clone assembled scFvs into a functional CAR backbone, V_H5' primers included NheI restriction site recognition sequence extensions right before the start of V genes, shown in red in Figure 4.2.1.1 A. Additional random 6 base pairs were added to the beginning of the primers to allow NheI restriction enzyme with enough anchor site to perform its function. V_H3' primers, on the other hand, had 33 base pairs extensions that were encoding for a Glycine-Serine flexible linker $(G_4S)_3$ that is commonly used in scFv assemblies, as depicted in grey in Figure 4.2.1.1 A [129].

To amplify variable regions of light chains, 2 different sets of primers were used for kappa (κ) and lambda (λ) subfamilies. Like heavy chain variable region amplification, forward primers were abbreviated as V_L5' and reverse primers as V_L3'. 6 V_L5' primers and 5 V_L3' primers were used for κ light chain amplification. On the other hand, 7 V_L5' primers and 3 V_L3' primers were used for λ light chain amplification. Like amplification of heavy chain, each V_L5' primer was used with a single V_L3' primer, resulting in 51 (30 for κ + 21 for λ) PCRs for amplification of light chain variable regions. Together with amplifications performed for heavy chain sequences, a total of 75 PCRs were conducted. Like V_H5' primers, V_L3' primers harbored NotI restriction enzyme recognition sequence extension for cloning scFvs into a functional CAR backbone shown in dark blue in Figure 4.2.1.1 A, together with 6 extra bp at the end for proper enzyme anchor and function. V_L5' primers also had 33 bp extensions that encodes for the rest of the $(G_4S)_3$ flexible linker (2.9.1). V_H3'linker primers and V_L5'linker primers has 21bp complementary sequence that is depicted in light grey in Figure 4.2.1.1 A. Due to this complementarity, when amplified

V_H and V_L sequences were put into a PCR reaction with a proof-reading DNA polymerase in the absence of any primer, they were randomly assembled into scFvs. This PCR is called sewing PCR or Overlap Extension PCR (OE PCR). The products of OE PCR were then put into a Pull-through PCR (PT PCR) where only the correctly assembled scFvs were amplified by the PT primers. The generated scFv library was ready to be cloned into an expression plasmid for generation of cellular CAR library.

After performing initial 75 PCRs to amplify V_H and V_L regions, PCR products were run in an agarose gel. All the V_H and κ V_L chain PCRs gave rise to a product around 400bp. However, as Figure 4.2.1.1 B depicts, agarose gel image of λ V_L chain PCRs revealed certain primer pairs did not result in any amplification. Nevertheless, to avoid any unspecific amplification, products around 400bp were cut from the rest of the gel and purified with agarose gel purification kit (NEB, USA). Purified V_H, κ and λ V_L regions were pooled separately. 2 scFv libraries, V_H-V_L κ and V_H-V_L λ, were assembled with OE PCR by putting equal molar mixture of pooled V_H and V_L gene repertoires. Finally, the correctly assembled scFvs were amplified in PT-PCR. Figure 4.2.1.1 C shows the PT-PCR results of V_H-V_L κ and V_H-V_L λ OE PCRs, respectively. The products were around 800bp range that is generally the length of a scFv [152].

Products of PT-PCR and plasmid #272 were cut with NheI and NotI. These two enzymes cut out the SCA431 scFv [153] in the vector DNA #272 and upon ligation, it allows to clone scFv libraries directly into the CAR backbone (Figure 4.2.1.1 D). Before starting with large-scale bacteria electroporation experiments to generate the κ and λ plasmid CAR libraries, I performed a small-scale V_H-V_L κ and V_H-V_L λ CAR plasmid library production to determine the CAR expression in Jurkat cells (3.2.8). I picked couple of emerging colonies on the LB agar plates and submitted the isolated plasmids to Sanger sequencing. From the sequenced colonies, 9 out of 10 colonies CARs' were out of frame. Only one colony had the whole CAR sequence in the correct ORF. I electroporated J7i cells with plasmid #272 as positive control and with plasmid obtained from library generation that had the CAR sequence in correct ORF. FACS analysis 1 day post electroporation showed that plasmid #272 had its CAR expressed on the cell surface as expected but CAR derived from the library was not expressed (Figure 4.2.1.1 E).

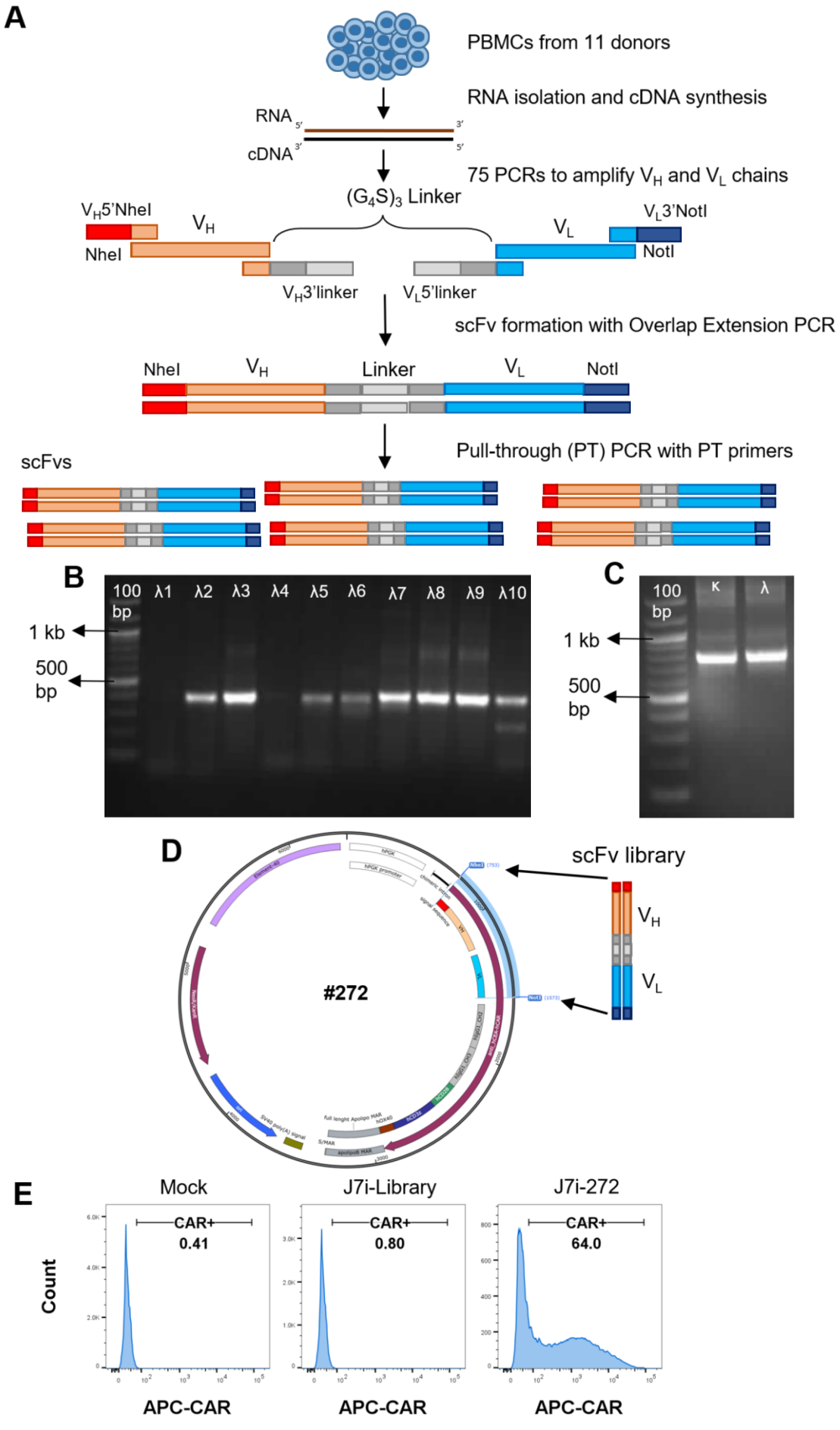
A
PBMCs from 11 donors
RNA isolation and cDNA synthesis
RNA
cDNA
75 PCRs to amplify V_H and V_L chains
$(G_4S)_3$ Linker
V_H5'NheI
NheI
V_H
V_L
V_L3'NotI
NotI
V_H3'linker
V_L5'linker
scFv formation with Overlap Extension PCR
NheI
V_H
Linker
V_L
NotI
scFvs
Pull-through (PT) PCR with PT primers
B
100 bp
λ1
λ2
λ3
λ4
λ5
λ6
λ7
λ8
λ9
λ10
1 kb
500 bp
C
100 bp
κ
λ
1 kb
500 bp
D
scFv library
V_H
V_L
#272
E
Mock
J7i-Library
J7i-272
CAR+
0.41
CAR+
0.80
CAR+
64.0
Count
APC-CAR
APC-CAR
APC-CAR

Figure 4.2.1.1: First attempt to generate the plasmid CAR library. A: Initial cloning strategy for generating a scFv library is depicted. PBMCs were isolated from 11 healthy donors via Ficoll gradient centrifugation and total RNA extraction was performed. Isolated RNAs were reverse transcribed into cDNA and cDNA pools were prepared. PCRs were performed by using the primers adopted from Pansri et. al. In total, 75 PCRs were done to amplify the human variable BCR genes. All VH forward primers included NheI restriction site extensions and all VH reverse primers had an extension that encodes for a flexible $(Gly_4S)_3$ linker. Similarly, all VL reverse primers were extended with NotI restriction site and all VL forward primers were extended with 33 bps that encode for a flexible $(Gly_4S)_3$ linker. Due to complementarity between the Linker sequence extensions, separately amplified VH and VL sequences were randomly sewed together with an Overlap Extension PCR (OE PCR). Correctly assembled scFvs were then amplified with Pull-through PCR. **B:** Figure depicts the example amplification of primers used for VL λ sequences. Expected products of the reaction is around 400bp. 100bp DNA ladder is labelled. **C:** After OE PCR, correctly assembled scFv libraries of heavy-kappa and heavy-lambda were amplified in PT-PCR. Resulting products from the PT-PCR were run in an agarose gel. Expected products of the reaction is around 800bp. 100bp DNA ladder is labelled. **D:** Figure depicts the schematic illustration of cloning scFv library into a functional CAR backbone by replacing the scFv SCA431 in plasmid #272. **E:** A clone with correct ORF was inoculated into a maxi prep and isolated DNA was electroporated into J7i cells to confirm expression of the CAR. CAR expression is depicted for mock electroporation as NC, electroporation with CAR library derived plasmid DNA and #272 as PC (pS/MARter anti-CEA-CAR) from left to right respectively.

4.2.2 Library cloning using an artificial leader sequence

In order to have a CAR library expressed on the cell membrane, the CAR sequences had to be provided with an artificial leader sequence after NheI recognition site and before the start of V_H sequence. I chose V_L κ leader sequence for this purpose as it is present in the lentiviral vector #53, plasmids #272 and #320. To clone the leader sequence, I revised the overall strategy. I decided to piece an additional DNA sequence containing the leader sequence to the beginning of each scFv during the assembling OE PCR. Subsequently, primers used during PT PCR would amplify the sequences that have successfully assembled 3 DNA pieces together (Figure 4.2.2.1 A). 2 of the 3 pieces were the V_H and V_L sequences that were amplified from cDNA pools as described before. The last piece was a PCR product amplified from #272 with forward primer targeting the human phosphoglycerate kinase (hPGK) promoter and reverse primer targeting the last 21 bp of the V_L κ leader sequence. Reaction resulted in 237 bp product encompassing a fraction of hPGK promoter, followed by NheI recognition site and the complete leader sequence as highlighted with a "*" in Figure 4.2.2.1 A. To be able to assemble V_H with the amplified leader sequence during OE PCR, I designed new V_H primers that had 21 bp extensions complementary to the 3' end of leader sequence. The rest of the scFv cloning strategy remained the same.

The results obtained with the primers that were adopted from Pansri et al. were rather unsatisfactory, especially for λ V_L sequences. To check the quality of these primer designs, I obtained all the reported V_H and V_L sequences from The International Immunogenetics Information System (IMGT) database [154]. When I analyzed how specific the primers were against the V_H and V_L sequences, I decided that they had to be revised. Therefore, new primer pairs for V gene amplification were designed. With the new set of primers, I was able to amplify all the existing functional V_H and V_L sequences that were present in the IMGT database. I performed *in silico* PCRs with each primer pair and verified the PCR products by using SnapGene (GSL Biotech, USA) software. All ordered primers were purified by desalting. 8 V_H5' and 4 V_H3' primers were used for V_H amplification, totaling 32 PCRs. During V_L amplifications, 15 V_L5'

and 6 V_L3' primers were used for λ subfamily (90 PCRs). Similarly, 9 V_L5' and 5 V_L3' primers were used for κ subfamily amplification (45 PCRs). In total, 177 PCRs were done to maximize the diversity of the libraries. All the primer pairs that were used to amplify heavy and κ chains gave a product around the expected 400 bp band (data not shown). However, 2 V_L5' (HVL3 4, HVL11) and 1 V_L3' (HJL4) primers used to amplify λ subfamily failed to give any product in all reactions that they were used. Figure 4.2.2.1 B shows the unproductive PCRs for samples λ3 and λ9 that were amplified with unproductive HJL4. Nevertheless, 142 PCRs gave products in correct size.

In the next step, PCR products from 142 reactions had to be gel purified. However, to avoid performing 142 separate gel purifications, I decided to pool aliquots from each heavy and light chain amplifications into 3 large pools for heavy, κ and λ amplifications. Instead of performing gel electrophoresis with 142 sample, PCR products were put into 9 pockets in the gel and subsequently gel purified (Figure 4.2.2.1 C). One additional gel purification was performed to purify the PCR product that contained the leader sequence and NheI recognition site. After purification of the amplification products, I performed the OE PCR with V_H, V_L and leader sequence DNA fragments mixed in equal moles to assemble the leader-heavy-κ and leader-heavy-λ scFv libraries. As before, the products of OE PCR were used to amplify correctly assembled scFv fragments in PT PCR. Amplified products and vector #272 were cut with NheI and NotI. scFv libraries were cloned into the linearized #272 backbone. A small-scale plasmid library production was performed with the ligated products as explained in section 3.2.8. From this library, I selected several clones whose CARs were in correct ORF and electroporated these CARs into the J7i cells together with plasmid #272 as positive control. Addition of leader sequence to the generated scFv libraries resulted in expression of the CARs on the cell surface in J7i-Library cells (Figure 4.2.2.1 D).

All the small-scale CAR libraries were generated so far with lab grown chemo competent XL-1 bacteria. However, to generate highly diverse scFv libraries, it is recommended to use electrocompetent bacteria due to their higher transformation efficiency compared to chemo competent bacteria. I performed several optimization experiments where I tested the transformation efficiency of an electrocompetent DH10B strain (Thermo Fisher, USA). In these experiments, I electroporated the bacteria with different amount of ligation products solubilized in ddH_2O. I ligated 100 ng, 500 ng and 1 µg cut vector DNA with κ and λ libraries in 3:1 insert to vector ratio separately. The same amount of bacteria was electroporated with the mentioned ligation products to find out which condition would result in the highest number of colonies in the agar plates (Supplementary Table 1). After electroporation of the bacteria, several dilution factors of the reactions were plated onto agar plate. Number of emerging colonies were counted and multiplied with dilution factor to find out theoretically how many colonies were present in the generated libraries. For both κ and λ libraries, electroporation of with 100ng vector did not give rise to any colony. Ligation with 500ng vector resulted in 1.62x10E8 colonies in combined κ and λ libraries. On the other hand, electroporation of ligation product with 1 µg vector generated 7.7x10E7 colonies in combined κ and λ colonies libraries. Electroporation with 500ng vector ligation achieved more than 2 times more colony formation than condition with 1 µg vector.

Plasmids were isolated from 27 emerging colonies of the vector DNA amount optimization experiment and were sequenced by Sanger sequencing. In 27 colonies that were sequenced, every scFv consisted of a unique sequence with a unique V_H-V_L allele composition. However, I realized that more than 50%

of the scFvs were out of frame. I found 40.7% of the colonies had their scFvs in the correct ORF (Figure 4.2.2.1 E). Further analysis of the data showed that scFvs were out of frame mostly due to mutations happening in primer binding sites or in the linker sequence. When a single nucleotide is omitted in one of the mentioned regions, the whole frame after this nucleotide shifts and plasmid fails to give rise to a functional CAR construct. 7.4% of the scFvs were out of frame, even though no mutation was observed in primer binding sites or in the linker sequence. Therefore, I named these sequences out of frame due to other reasons as depicted in yellow in Figure 4.2.2.1 E. Occurrence of mutations exclusively in the primer binding sites indicated that problem might be caused by faulty primer synthesis. Therefore, I called 51.9% of the scFvs in this category as out of frame due to primer related reasons, depicted in red in Figure 4.2.2.1 E.

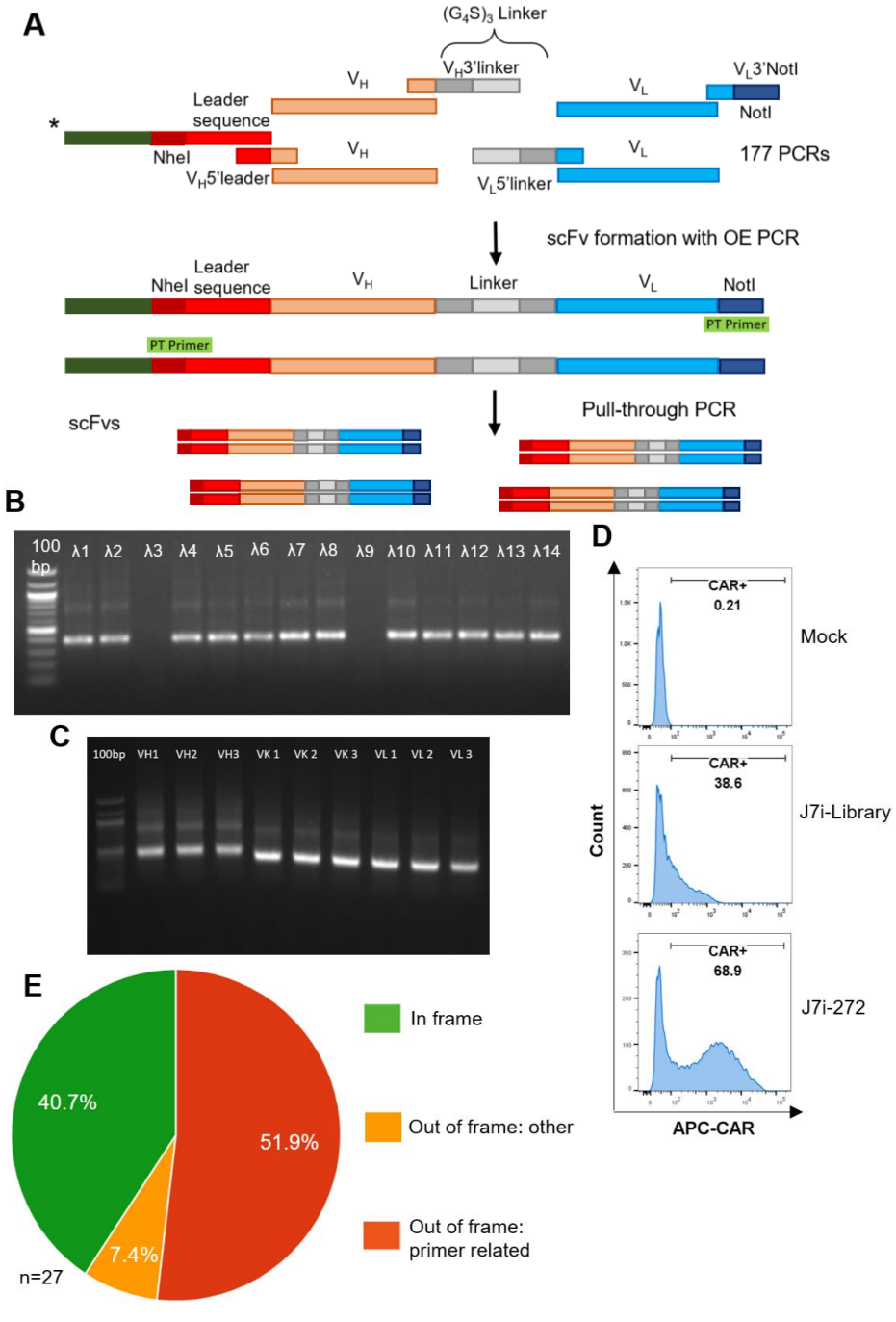

Figure 4.2.2.1: Cloning scFv library with revised primers. A: V_H forward primer extension was switched from NheI recognition sequence to a sequence that has 21bp complementary to Leader sequence used in the vectors #272 and #320. The rest of the extensions present in V_H reverse and V_L primers were kept the same. 177 PCRs were done to amplify all possible human VH and VL genes. One additional PCR is done to amplify Leader sequence and subsequent NheI restriction site with extra bases in the 5'. Unlike previously, 3 DNA pieces were assembled with the OE PCR. First assembly occurs between sequences encoding for the Linker, generating the single chains. Generated scFv fragments further assemble with Leader sequence due to 21bp complementary sequence between the 5' extension of V_H to the 3' end of the Leader sequence. Then, a PT-PCR with revised PT primer pair amplifies scFv fragments that were assembled correctly from Leader sequence to end of V_L chain. **B:** Figure depicts the example amplification with primers used for VL λ sequences. Expected products of the reaction is around 400bp. 100bp DNA ladder is labelled. **C:** A total of 100µl from each heavy, κ and λ amplifications were pooled and each pool was run in 3 pockets of an agarose gel. Products around 400 bp were gel purified to be used in OE PCR. **D:** One of the emerging clones that has a correctly assembled in-frame scFv was electroporated into J7i cells to test expression of the CAR. CAR expression is depicted for mock electroporation as NC, electroporation with CAR library derived plasmid DNA as J7i-Library and J7i-272 as PC from top to bottom, respectively. **E:** Generated heavy-kappa and heavy-lambda scFv libraries were cloned into #272 vector backbone as described in Figure 4.2.1.1 D. From two different small-scale plasmid CAR library generation experiments, plasmids from 27 emerging clones were sequenced with Sanger sequencing. The pie chart shows the percentage of scFv fragments in the correct ORF in green or out of frame scFv fragments due to amplified V genes in yellow and out of frame scFv fragments due to faulty primer in red.

4.2.3 Plasmid CAR library generation with reduced out of frame sequences

As mentioned before, mutations occurring exclusively in the primer binding sites or in the linker sequence extensions pointed towards the abortive synthesis of primers. So far, all the primers ordered for scFv library generations were purified by desalting. Before generating the final plasmid CAR libraries, a representative sample from each V_H5', V_H3', V_L5' and V_L3'primers that were purified with advanced methods than desalting were ordered. Therefore, to investigate the effect of primer purification quality on percentage of in frame scFvs in a library, ordered primer samples were used to generate small-scale CAR libraries. I chose to order primers purified with high pressure liquid chromatography (HPLC), and denaturing polyacrylamide gel electrophoresis (PAGE). During V gene PCRs, heavy and light chains were amplified with either Taq polymerase or High Fidelity polymerase by using primer pairs that were purified with desalting, HPLC and PAGE. As before, High Fidelity polymerase was used to assemble the scFvs and PT PCR was done with the Taq polymerase (Supplementary Table 2). Generated scFv libraries were cut with NheI/NotI to be cloned into the linearized plasmid #272 as before. Ligation of the cut vector and inserts generated 6 small scale CAR libraries that were transformed into chemo competent XL1 bacteria. 5 colonies were picked from each library generation and isolated plasmids were sequenced by Sanger sequencing. Desalted, HPLC purified and PAGE purified oligos achieved 60%, 70% and 80% in frame scFv fragments, respectively (Supplementary Table 2). All working primers were ordered as HPLC purified.

142 PCRs were performed with HPLC purified primers that previously resulted in amplification of V genes. Due to high number of PCRs, I again pooled heavy, κ and λ amplifications into 3 separate pools to have less samples for agarose gel purification (Fig. 4.2.3.1 A). scFv libraries for heavy- κ and heavy-λ libraries were prepared with the strategy depicted in Figure 4.2.2.1 A. Figure 4.2.3.1 B illustrates the

results of PT PCRs done with heavy-κ and heavy-λ libraries. Products of the 2 PT PCRs were cloned into plasmid #1468 by replacing the SCA431 scFv. Plasmid #1468 is another vector with nanoS/MAR backbone. It has the same sequence with plasmid #320 differing only with a 300bp shorter S/MAR sequence variant. As established before, 500ng of #1468 was linearized with NheI/NotI restriction digestion for ligation of κ and λ scFv libraries to generate plasmid CAR libraries (Fig. 4.2.3.1 C). Generated plasmid CAR libraries were precipitated and resuspended in ddH_2O. Only a special DH5α strain could be used for transformation when nanoS/MARt vectors are cloned. As mentioned before, an antisense RNA (RNA-OUT) is synthesized by the transformed nanoS/MAR vectors. RNA-OUT later binds to levansucrase enzyme that is expressed by the host's genome. This inhibits the toxic activity of levansucrase catalyzed in the presence of sucrose [143]. Thus, in a selection media containing sucrose, only the transformed cells can survive and proliferate. The aliquots of the DH5α strain for electroporation of ligation products were kindly provided by Dr. Richard Harbottle. Electroporated cells were grown overnight on agar plates to be scraped off the following day. Separate κ and λ library glycerol stocks were generated from the scraped off bacteria solutions. Counting emerging colonies on petri dishes where 10^{-4} dilutions of both κ and λ libraries were plated onto offered an estimation about the possible size of the libraries. According to the colony count, there were around 7.0E+06 and 1.0E+07 colony forming units for κ and λ libraries, respectively. In total, both libraries gave rise to a theoretical diversity of 1.7E+07 different CAR molecules. As before, I isolated plasmids of 12 colonies from both κ and λ libraries submitted to Sanger sequencing. I analyzed the sequences to determine the ratio of CARs in correct ORF. Figure 4.2.3.1 D illustrates the results of the Sanger sequencing. The percentage of in frame CARs was increased from 40.7% to 43.5%. 43.5% of the CARs were out of frame due to faulty primers. In the rest 13%, primers were bound correctly, however they were out of frame due to amplified heavy or light chains. With this experiment, the CAR library cloning part of the project was concluded. When more library plasmid DNA was needed, the thawed aliquots from the frozen libraries were inoculated into maxi preps. After growing cultures according to their optimal growth protocol established by Dr. Harbottle's group, plasmid DNA were isolated and stored in Endotoxin-Free H_2O, ready for electroporation.

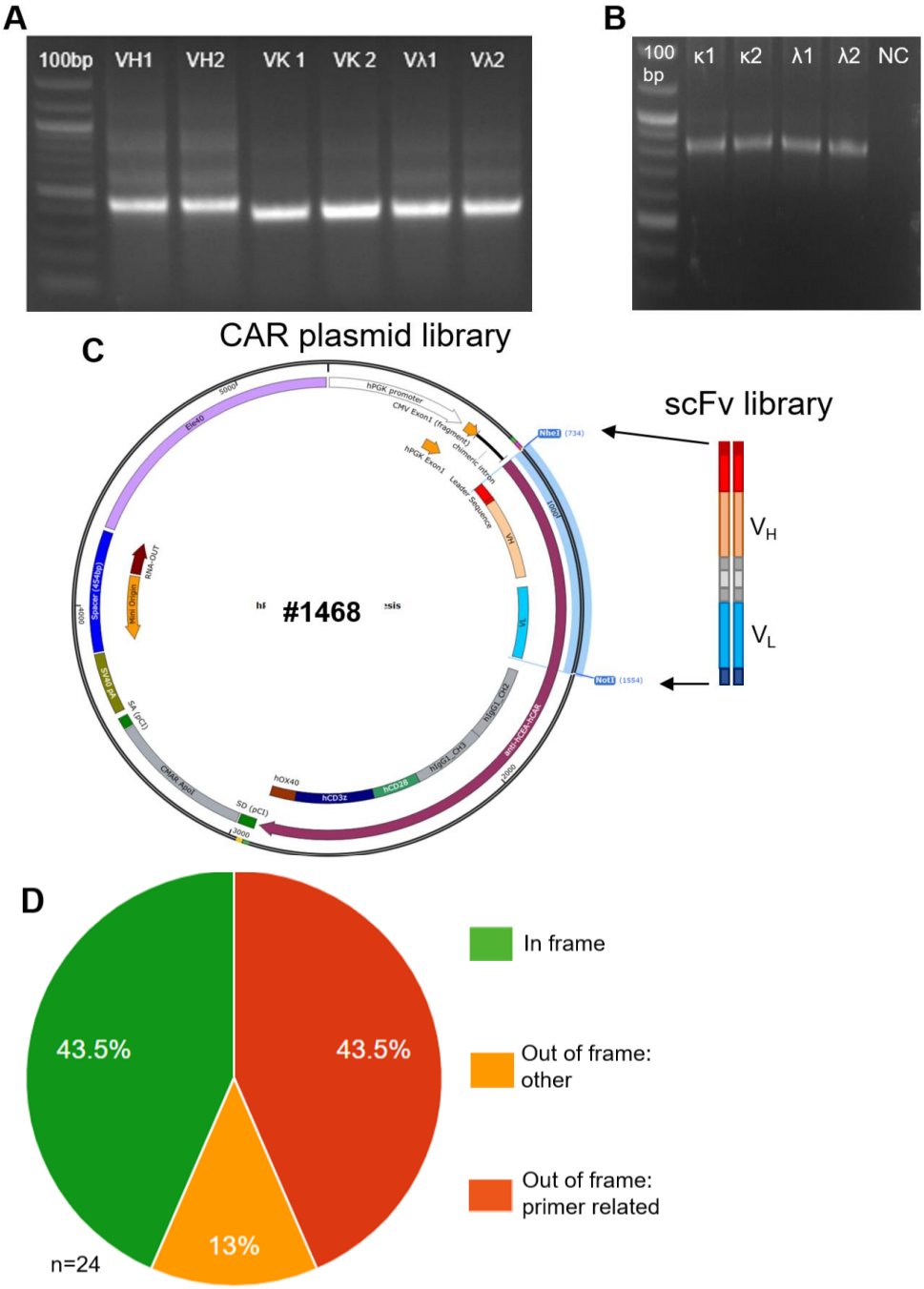

Figure 4.2.3.1: Generation of the plasmid CAR libraries with HPLC purified primers. A: To generate the scFv library, a total of 142 PCRs were done amplifications that failed to generate a product. After variable gene amplification, aliquots from each VH, VL κ and VL λ reactions were pooled and run in an agarose gel. Bands with correct size were gel purified (NEB) and OE-PCRs were performed as described in 4.2.2.1 A to generate heavy-kappa and heavy-lambda scFv libraries. **B:** After OE PCR, assembled scFv libraries of heavy-kappa and heavy-lambda were used as template for amplification in PT-PCR. Samples from resulting PT-PCR products were run in an agarose gel. Expected products of the reaction was around 800bp. 100bp DNA ladder is labelled. **C:** Figure is depicting the schematic illustration of cloning a scFv library into a functional CAR backbone by replacing the scFv SCA431 in a new nS/MARt backbone (#1468) that is kindly by Prof. Harbottle DNA Vector Lab (F160). Vector, heavy-kappa and heavy-lambda scFv libraries were digested with NheI/NotI. Ligatation products were electroporated into nanobacteria. **D:** 12 clones from κ and λ libraries each were picked from 10^{-4} dilution plates and sent for Sanger sequencing. Pie chart depicts the sequencing results of the clones similar to 4.2.2.1 C.

4.3 Generation of a cellular CAR Library

In the first chapter of the results, I explained the establishment and characterization of the Jurkat reporter cell line J7i. Generated cell line was challenged in various settings as bulk population and in single-cell level. After confirming robustness of the generated J7i cell line, I started with the second chapter of my thesis that I generated plasmid CAR libraries. Consequently, I successfully generated the necessary components for production of cellular CAR libraries. In the third chapter, I described how I managed to optimize electroporation of my reporter cells with generated plasmid CAR libraries. Once the correct electroporation parameters for optimal CAR expression were established, large-scale electroporation experiments to generate cellular CAR libraries could be started.

4.3.1 Setting up electroporation parameters

Previously, all the electroporation experiments that I performed were done by using Neon™ electroporator. However, it can only shock up to 5E+06 cells per shot. It is not upscalable to process billions of cells in a single experiment that was planned to be shocked to generate cellular CAR library. Therefore, I switched to MaxCyte GTx™ electroporator due to its capacity of electroporating a wide range of cell numbers starting from 5E+06 to 2E+11 [155].

In order to set up electroporation settings of GTx™ device, I electoporated different plasmid DNA concentrations into the cells that were resuspended in either Opti-MEM (OM) or in MaxCyte Electroporation Buffer (MEB). 1.0E+07 cells in 2.0E+08 cells/ml concentration were electroportated during parameter establishment. Vector #1468 was used in optimization experiments. I compared 100, 200 and 300 µg/ml plasmid concentrations shocked into J7i cells resuspended in either OM or MEB. Neon™ EP was done as before for comparison of the results with samples shocked using GTx™. 1 day post EP, cell viability of each condition was calculated by gating on the DAPI negative cells during flow cytometry analysis. Relative viability, including mock electroporated cells, were calculated by dividing the viability of experimental conditions to untreated J7i cells. Mock electroporation in all 3 different settings resulted in viability similar to untreated cells (Fig. 4.3.1.1 A). For both OM and MEB, viability of the cells decreased with increasing concentration of plasmid DNA used. Toxicity of 100 µg/ml plasmid DNA seemed negligible. However, 200 µg/ml and 300 µg/ml DNA concentrations resulted in 90% and 80% cell viability, respectively. Nevertheless, cell suspensions electroporated with GTx™ showed higher viability in every condition compared to 65% viability of the cells shocked with Neon™ electroporator.

I followed the cells for CAR expression and percentage of activated cells for 4 days. Therefore, I stained the cells against anti-CEA-CAR 1, 2 and 4 days post EP and determined their CAR expression levels via flow cytometry. In the samples shocked with GTx™, the level of CAR expression was directly proportional to the concentration of plasmid DNA used (Fig. 4.3.1.1 B). Moreover, OM and MEB conditions expressed similar amount of CAR in all 3 time points when samples shocked with the same plasmid concentrations compared to each other. The only exception was the d2 measurement of the cells shocked in MEB with 300 µg/ml DNA. They had elevated levels of CAR expression, but this phenomenon was not observed on day 4. Cells shocked with Neon™ electroporator, on the other hand, achieved the highest CAR expression on day 1. On day 2, CAR expression was decreased to the level of cells shocked with lowest DNA concentration 100 µg/ml in OM or MEB. Interestingly, they showed the same level of CAR expression at day 4 equivalent the cells shocked with highest DNA concentration

300 µg/ml. Nevertheless, as Figure 4.3.1.1 A and B illustrates, GTx™ shocks resulted in comparable CAR expression levels in J7i cells with Neon but with less cytotoxicity.

As the last parameter, I analyzed the percentage of activated cells up to 4 days post EP. In both OP and MEB shocks, activated cell percentage peaked on day 2 and decreased on day 4. The same pattern was observed in Neon EP with 53%, 62% and 57% of cells getting activated at day 1, 2 and 4 post EP, respectively. 1 day post EP, 63% and 50% of the cells were activated after electroporation with 300 µg/ml in OM and MEB, respectively. 2 days post EP, percentages were increased to 70.8 and 60.8 and decreased to 53.3% and 39.8% at day 4 for the same OM and MEB conditions, respectively. In all 3 time points, cells electroporated with MEB had a fewer percentage of activated cells consistently than their OP counterparts. Also compared to Neon™ EP, all conditions shocked in MEB had less activated cells, especially at day 4. Therefore, electroporation in MEB was the most promising condition by having the least amount of activated cells. When I analyzed all the data generated, I decided to use MEB with 200 µg/ml DNA concentration for the following shocks. This condition had 90% viability at day 1 and Neon comparable CAR expression with the least cell activation at day 4.

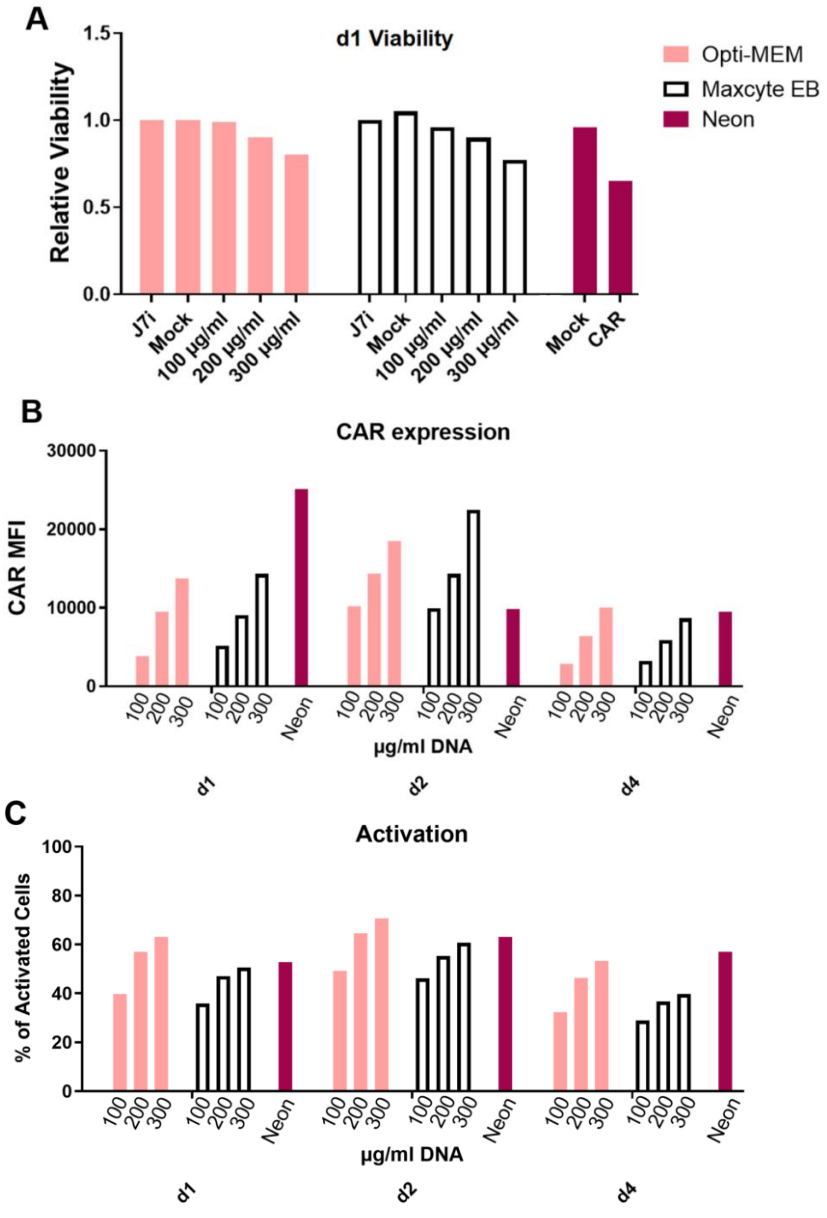

Figure 4.3.1.1: Initial setup of the electroporation parameters. 1.0E+07 J7i cells were electroporated in 50µl with 100, 200 and 300 µg/ml plasmid #1468 in either Opti-MEM (OM) or Maxcyte Electroporation Buffer (EB). 5.0E+06 cells were also electroporated with Neon for comparison. Viability, CAR expression and percentage of activated cells were followed throughout 4 days post electroporation. **A:** Plot depicts the relative viability of electroporated cells at day 1 according to flow cytometry analysis with DAPI staining. Untreated cells were used to calculate relative viability. **B:** CAR expression of J7i-1468 cells were followed for 4 days post electroporation. Data is shown for 1 day, 2 days and 4 days post EP for respective conditions. **C:** Similar to B, percentage of activated cells 1 day, 2 days and 4 days post EP are depicted.

4.3.2 Effect of DNA quality on electroporation efficiency

To assess the robustness of GTx™, I planned to electroporate 2.0E+08 cells as an intermediate scale with the conditions that I set up in section 4.3.1. To produce more #1468 plasmid, new maxi preps from were inoculated and plasmids were isolated by using Macherey-Nagel (MN) EF maxi prep kit. 2 µg plasmid aliquot was restriction digested and loaded into an agarose gel together with 2 µg uncut plasmid. The agarose gel image in Figure 4.3.2.1 A shows the uncut and cut samples. The red rectangular box indicates the contaminating high molecular weight genomic DNA. The 1kb DNA ladder was used for comparison, as successful plasmid isolations should have the same level of purity. Despite the presence of genomic DNA contamination, I shocked 2.0E+08 cells with the established settings as planned and analyzed their viability and CAR expression levels (Fig. 4.3.2.1 A middle, right). DAPI staining of the cells day 2 post EP revealed that 92.6% of the cells were alive. FACS plot on the right displays the CAR expression level of mock in grey and cells electroporated with plasmid #1468 in blue. To see the effect of genomic DNA contamination on electroporated cells, I compared Figure 4.3.2.1 A and B with each other. Figure 4.3.2.1 B depicts from left to right; the purity of the plasmid batch used during shock parameter set up experiment (section 4.3.1), cell viability and CAR expression of the cells 2 days post EP, respectively. Comparison of the DAPI staining results revealed a slight decrease in percentage of viable cells, from 94.1% to 92.3%, when genomic DNA contaminated prep was used. On the other hand, genomic DNA contamination caused a significant reduction in CAR expression. The percentage of CAR expressing cells dropped from 99.1% to 71.8%. I decided to continue with upscaling experiments after solving the contaminating genomic DNA problem present in the maxi preps.

New maxi preps were inoculated as there might have been a mistake during the first maxi prep isolation attempt with the DH5α strain. The first gel picture in Figure 4.3.2.1 C shows the result of the second batch of maxi prep isolations. Although there was less genomic DNA contamination compared to the first attempt, it was observed in the agarose gel highlighted in red box. To degrade these contaminating genomic DNA, I treated the isolated DNA with Plasmid-Safe ATP-Dependent DNase™ according to manufacturer's instructions (LGC, UK). The unique feature of this enzyme is it spares closed, circular DNA like plasmids, but specifically degrades linear double or single stranded DNA. After overnight incubation with Plasmid-Safe DNase™, to remove the reaction buffer and the DNase, maxi preps were cleaned up with PCR purification column (QIAGEN). The plasmid DNA was eluted from the columns with EF H_2O and a restriction digestion reaction was started. The second gel picture in Figure 4.3.2.1 C displays the result of the purification attempt. Purified preps were as clean as the 1 kb DNA ladder. The genomic DNA that was highlighted in the red box were completely removed. I electroporated 1.0E+07 J7i cells with the cleaned-up product, and again analyzed the viability and CAR expression of the cells.

Viability was 93.2%, consistent with the previous GTx™ electroporation experiments performed. CAR expression, on the other hand, higher compared to Figure 4.3.2.1 A. 94.5% of the cells expressed the CAR. Moreover, cells achieved a single peak shift in CAR expression as observed in Figure 4.3.2.1 B. Therefore, I decided to implement the Plasmid-Safe DNase™ treatment for maxi prep isolations that contained genomic DNA contamination.

However, PCR column purification had several disadvantages. Firstly, the plasmid recovery after purification was low. 1/3rd of the starting DNA amount was purified after treatment with Plasmid-Safe DNase™. Moreover, a maxi prep with DH5α strain yields around 400 to 500 ng DNA and each PCR purification column can bind up to 10 µg of DNA. This means 40 to 50 PCR purification columns had to be processed to clean up a maxi prep. To decrease the number of clean up reactions and increase the yield after DNase™ treatment, I loaded the next the batch of DNase treated samples into a midi prep column from MN. By doing so, one midi prep clean-up was performed per Plasmid-Safe DNase™ treated maxi prep isolation. Although new procedure removed genomic DNA contamination to some extent, they were still visible (Figure 4.3.2.1 D). Moreover, the recovery after purification did not improve and it again was around 30%. However, unlike samples cleaned up with PCR purification columns, the recovered 30% included genomic DNA contamination.

I switched the EF maxi prep isolation kit that I used from MN to Qiagen (QIAGEN N.V, NL). New batch of plasmid #1468 was isolated with Qiagen kit by following the manufacturer's recommendations. Gel image in Figure 4.3.2.1 E depicts the gel electrophoresis result of the control restriction digestion of the isolated plasmids. Even without any purification, plasmids isolated with Qiagen maxi prep kit had little to no genomic DNA contamination (Figure 4.3.2.1 E). I shocked 5.0E+06 cells with plasmid #1468 isolated using Qiagen maxi prep kit and analyzed the viability and CAR expression as before. A slight reduction in the percentage of live cells was observed with 89.3%. On the contrary, the CAR expression was improved and 99.6% of the cells were expressing the CAR. Expression level of the CAR was as high as the parameter optimization experiment (Figure 4.3.2.1 B). Therefore, I implemented Qiagen EF maxi prep isolation protocol as the standard method. In the following experiments, plasmid #1468 or generated κ and λ plasmid libraries were isolated with Qiagen kit.

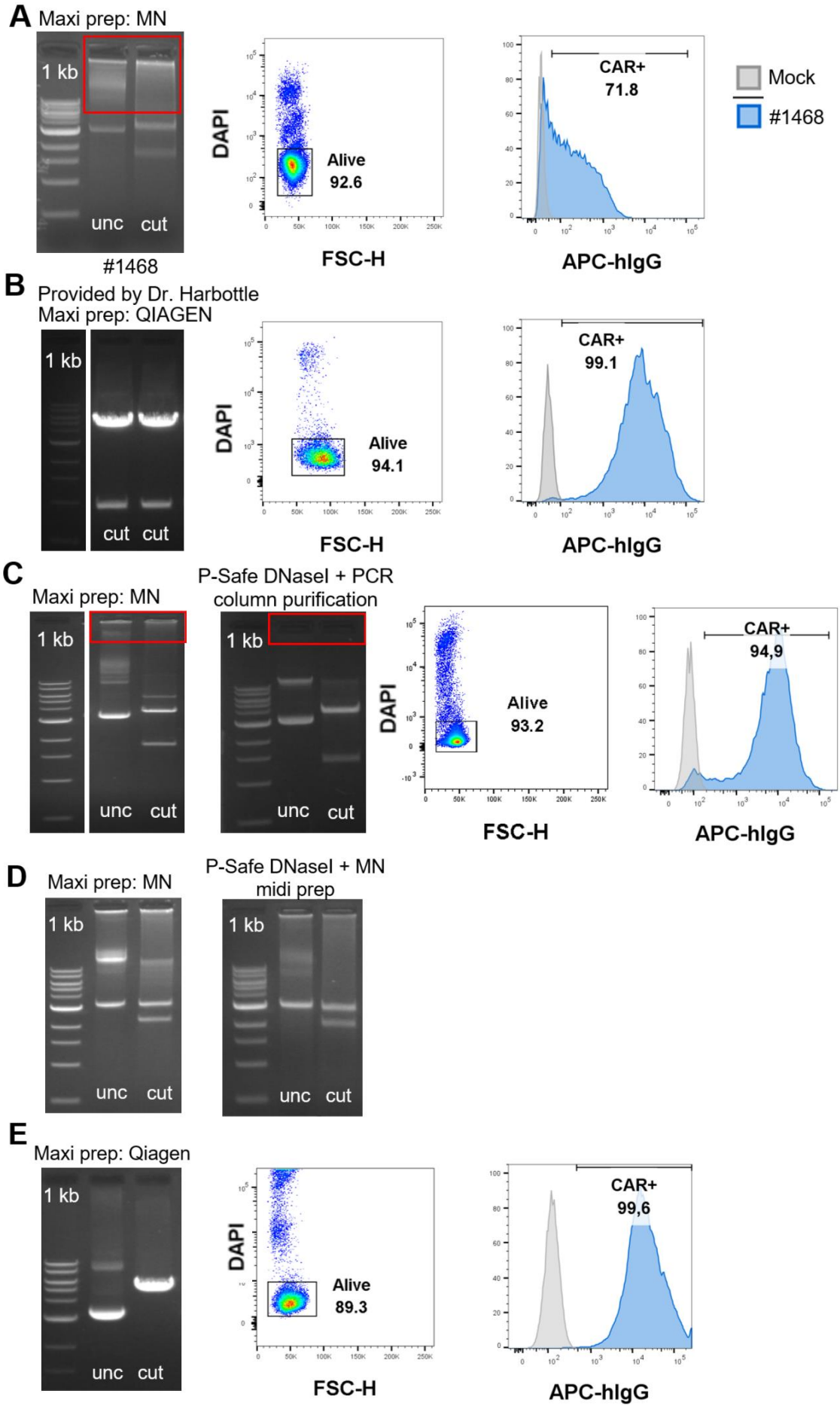
A
Maxi prep: MN
1 kb
unc
cut
#1468
DAPI
Alive
92.6
FSC-H
CAR+
71.8
APC-hIgG
Mock
#1468
B
Provided by Dr. Harbottle
Maxi prep: QIAGEN
1 kb
cut
cut
DAPI
Alive
94.1
FSC-H
CAR+
99.1
APC-hIgG
C
Maxi prep: MN
P-Safe DNaseI + PCR
column purification
1 kb
unc
cut
DAPI
Alive
93.2
FSC-H
CAR+
94,9
APC-hIgG
D
Maxi prep: MN
P-Safe DNaseI + MN
midi prep
1 kb
unc
cut
E
Maxi prep: Qiagen
1 kb
unc
cut
DAPI
Alive
89.3
FSC-H
CAR+
99,6
APC-hIgG

Figure 4.3.2.1: Optimization of maxi preps to achieve optimal CAR expression. Agarose gel images on the left panel show the purity of plasmid DNA used in the electroporation experiment. In all gel electrophoresis experiments, 2µg DNA was used for restriction digestions or loaded into agarose gel as uncut. All middle panel show the flow cytometry acquisition of J7i-1468 cells stained with DAPI 2 days post EP for viability analysis. All right panels depict the CAR expression of the respective alive J7i-1468 cells 2 days post EP. **A:** (Left) Genomic DNA contamination present in the plasmid #1468 after performing maxi prep isolation with Macherey Nagel EF Maxi kit is shown in the red rectangle. 1kb DNA ladder is labelled and provides a baseline for genomic DNA contamination in the preps. **B:** (Left) DNA aliquot was provided by Harbottle Group. Aliquot was either cut or left uncut before loading into an agarose gel. **C:** (Left) First gel image shows repeat of maxi prep isolation of #1468 with MN kit. Second image was taken after treating isolated plasmid DNA with Plasmid-Safe DNase (Biosearch Technologies) overnight and purifying the reaction with PCR clean-up columns (Qiagen). **D:** (Left) Plasmid prep that was isolated with MN kit is shown in the left image. Maxi prep was treated with Plasmid-Safe DNase overnight and cleaned-up by loading the reaction into a midi prep column of MN. Second image depicts the restriction digestion of the midi prep column cleaned-up prep. **E:** (Left) Maxi prep that was isolated with Qiagen Endo-Free Plasmid kit loaded into an agarose gel as cut and uncut.

4.3.3 Up scaling and optimization of library DNA electroporation

After setting up the shock parameters and solving the genomic DNA contamination problem observed in the maxi preps, I challenged the GTx™ capacity for upscaling in my next experiments. At first, 2.0E+07 and 2.0E+08 cells were electroporated as medium and large-scale reactions, respectively, with the parameters established on section 4.3.1. 1 day post EP, CAR expression and viability of the cells were analyzed. CAR expression profiles of both scales were nearly identical when they were overlaid. Moreover, viability of the cells was above 90% in both scales according to their DAPI staining (Figure 4.3.3.1 A, left column). During the next electroporation, 5.0E+06 cells were shocked in small-scale together with 2.0E+07 medium and 2.0E+08 large-scale. Cells were checked for the CAR expression 2 days post EP. Consistent with my previous experiment, CAR expression profiles in all 3 scales were nearly identical. Viability of the cells ranged between 75 to 80%. Thus, data obtained from the two experiments indicated that GTx™ upscaling did not significantly change the CAR expression and cell viability as long as the concentration of cells and plasmid DNA were kept constant.

In these two experiments, dead cell clumps were observed starting from 1 day post electroporation. The number and size of these clumps were increasing with the increasing EP scale. Resuspension with pipette or vortexing failed to resolve these clumps. When I was analyzing the data I obtained so far, I reported the DAPI negative cell population in flow cytometry measurements for cell viability. This viability measurement was misrepresentative as the dead cell clumps were not included in flow cytometry analysis. The same dead cell clumps were observed during the initial shock parameter establishment experiment when MEB was used during EP. However, in the same experiment, no dead cell clumps were visible in the cells shocked in the presence of OM. Therefore, I performed a medium-scale experiment where I shocked 2.0E+07 cells resuspended in either OM or MEB to determine the viability of the cells with manual hemacytometer counting. 1 day post EP, I visually observed both conditions and again confirmed the dead cell clumps in the cells electroporated in MEB. Consistent with previous results, cells shocked with OM were completely devoid of these clumps. To compare both conditions, I checked the CAR expression and viability of the cells. In both conditions, cells expressed similar levels

of CAR (Figure 4.3.3.1 B, left). Again, consistent with my previous data, there were more activated cells when OM was used during EP (Figure 4.3.3.1 B, middle). Moreover, the FITC MFI FC was around 2 for the cells shocked in the presence MEB compared to 6.5 of OM. The viability of the cells was quantified with both DAPI staining followed by flow cytometry analysis and trypan blue staining followed by manual cell counting. Flow cytometry analysis revealed both conditions had around 90% relative viability compared to mock (Figure 4.3.3.1 B, right). On the other hand, when a trypan blue dead/alive cell staining was performed and alive cells were counted 1 day post EP, there were 1.6E+07 cells present in OM culture. That meant the viability of this condition was around 80%. For the cells shocked in MEB, 1.0E+7 cells were counted after trypan blue staining, which meant that half of the cells were dead 1 day post EP. Due to high number of dead cells and dead cell clumps present in shocks performed with MEB, J7i cells were electroporated with OM during cellular CAR library generation to minimize the cell loss.

Before generation of the cellular CAR libraries, EP of isolated plasmid CAR libraries were tested in a small-scale experiment. In this experiment, cells were either electroporated with OM or OM and MEB mixture. In both conditions, cells were treated with DNaseI (Sigma, Germany) immediately after shock for 20 minutes. In the last conditions, cells were shocked in the presence of OM without any DNaseI treatment to reveal if the other two conditions result in any improvement in terms of viability, CAR expression or activated cell percentage. The cells were analyzed 2, 3 and 5 days post electroporation. When visually inspected, the absence of dead cell clumps was confirmed in all conditions. CAR expressions were similar in all three conditions when measurements taken at the same time point were compared to each other (Figure 4.3.3.1 C, left). On the other hand, comparison of the percentage of activated cells revealed that DNaseI treatment caused a lower level of cell activation. For example, 2 days post EP, 35.2% of the cells electroporated with OM was activated cells. On the other hand, the percentage of activated cells shocked with OM and treated with DNaseI was 19.3%. The activated cell percentage decreased to 13.3% when cells were shocked with OM and MEB mixture and treated with DNaseI. For all the 3 days the cells were analyzed, the observed activation was the lowest in the cells that were electroporated with MEB and OM mixture and treated with DNaseI (Figure 4.3.3.1 C, middle). Finally, the viability of the cells according to DAPI staining was found to be around 90% for all conditions (Figure 4.3.3.1 C, right). By looking at obtained results, I decided to use OM and MEB mixture in combination with DNaseI treatment for generation of the cellular CAR libraries. As it was concluded from the previous experiments that GTx™ EP conditions are upscalable when the cell and plasmid concentration was kept constant, I decided to use the same settings during large-scale EP experiment without performing any further shocks with intermediate scales.

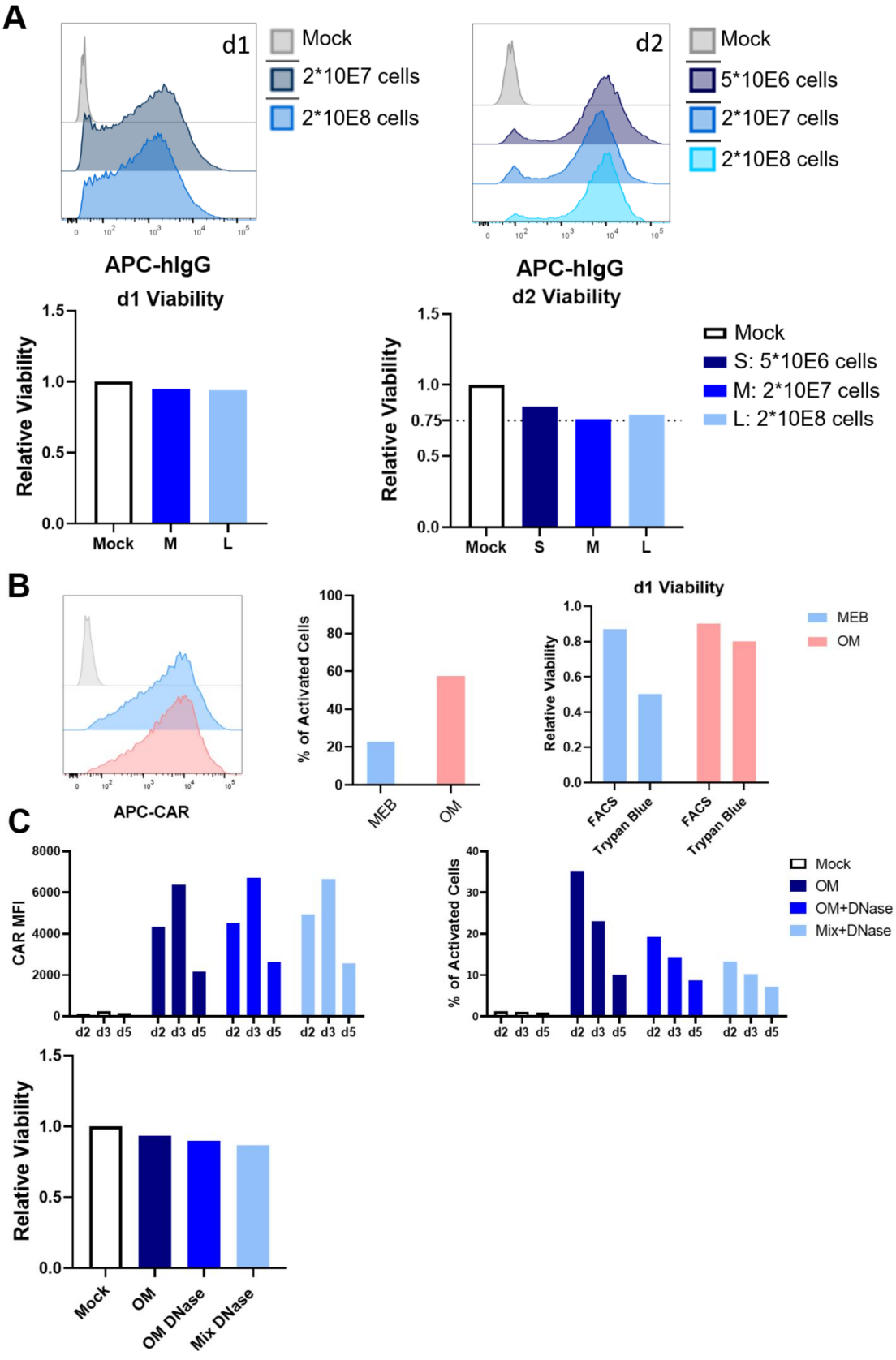
A
d1
Mock
2*10E7 cells
2*10E8 cells
APC-hIgG
d1 Viability
Relative Viability
1.5
1.0
0.5
0.0
Mock
M
L
d2
Mock
5*10E6 cells
2*10E7 cells
2*10E8 cells
APC-hIgG
d2 Viability
Relative Viability
1.5
1.0
0.75
0.5
0.0
Mock
S
M
L
Mock
S: 5*10E6 cells
M: 2*10E7 cells
L: 2*10E8 cells
B
APC-CAR
% of Activated Cells
100
80
60
40
20
0
MEB
OM
d1 Viability
Relative Viability
1.0
0.8
0.6
0.4
0.2
0.0
FACS
Trypan Blue
FACS
Trypan Blue
MEB
OM
C
CAR MFI
8000
6000
4000
2000
0
d2 d3 d5 d2 d3 d5 d2 d3 d5 d2 d3 d5
% of Activated Cells
40
30
20
10
0
d2 d3 d5 d2 d3 d5 d2 d3 d5 d2 d3 d5
Mock
OM
OM+DNase
Mix+DNase
Relative Viability
1.5
1.0
0.5
0.0
Mock
OM
OM DNase
Mix DNase

Figure 4.3.3.1: Testing scalability of electroporation and optimization of shock parameters. A: Different scales of J7i cells were shocked with #1468 according to the parameters decided in 4.3.1. On top row, CAR expression of the shocked cells in two different experiment is depicted after 1 and 2 days post EP, respectively. The bar plots on the bottom row illustrates the relative viability of the shocked cells compared to mock, corresponding to the samples shown in top row. **B:** J7i cells were shocked with #1468 either with MEB or OM. CAR expression, percentage of activated cells and the cell viability are depicted from left to right, respectively. For viability experiment, cells were manually counted with Trypan Blue solution besides flow cytometry analysis with DAPI staining. **C:** J7i cells were electroporated with pooled κ and λ CAR plasmid libraries with only OM (dark blue), with OM in combination with DNaseI treatment (blue) or with a mixture of OM and MEB in combination with DNaseI treatment (light blue) and followed up to 5 days for CAR expression and percentage of activated cells. Mock electroporated cells are shown in white bars as NC. The viability of the cells was analyzed 1 day post EP by flow cytometry acquisition.

4.4 Screening of the cellular CAR library

4.4.1 Summary of the pipeline

So far, I have successfully generated a reporter cell line and plasmid CAR libraries. I optimized the electroporation of J7i cells with the plasmid library DNA. In the next step, I performed the first proof-of-concept screening against CEACAM5 antigen by using cellular CAR libraries. Figure 4.4.1 depicts the established pipeline for the screening platform. Cellular CAR library screening pipeline starts with electroporation of the isolated plasmid CAR library into J7i cells. 3 days post EP, cellular CAR library is pre-enriched against CEACAM5 by FACS. Sorted cells are rested overnight and loaded into an OptoSelect™ chip together with antigen-coupled beads. Cells expressing a CEACAM5 specific receptor are identified through the induction reporter gene expression. These “hits” are then exported from the Lightning™ device to have their CARs sequenced by Oxford Nanopore Sequencing. Sequencing data of the hits are obtained in as little as 12 days after start of the experiment. Finally, identified *de novo* CAR sequences are functionally validated *in vitro*.

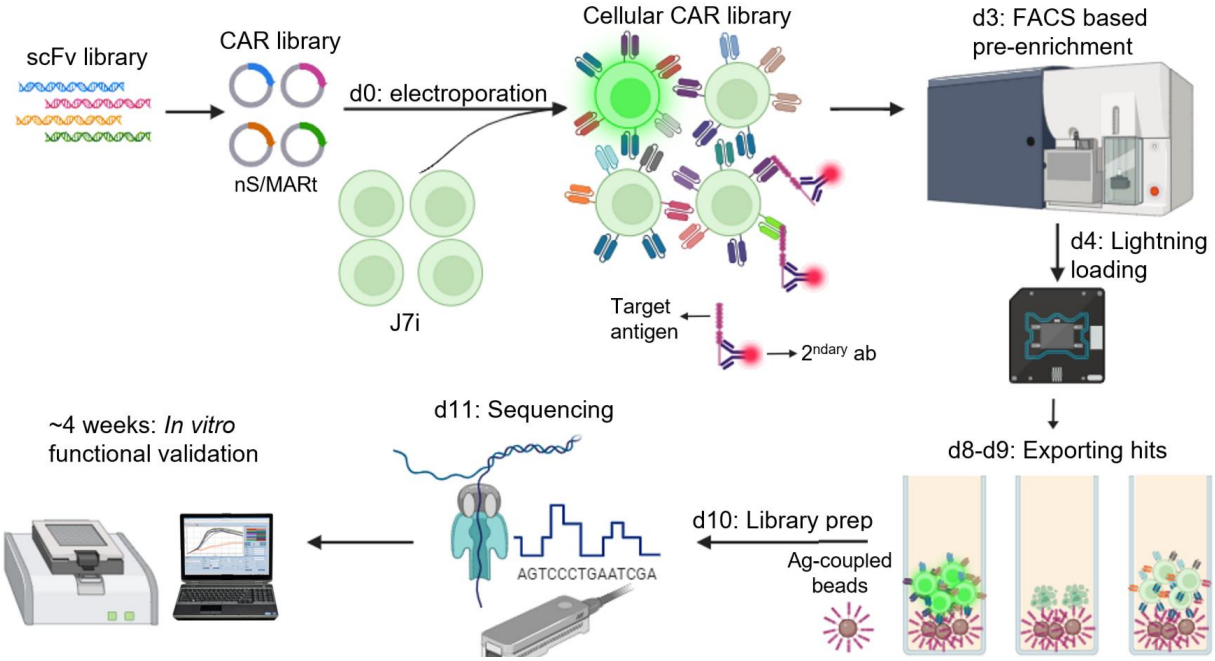

Figure 4.4.1.1: Pipeline for screening cellular CAR libraries for identification of antigen-specific CARs. Generated scFv library is cloned into a nS/MARt vector directly into a functional CAR backbone. Milligrams of CAR plasmid library are obtained from maxi prep isolations. Cellular CAR library is generated by electroporating J7i cells with plasmid library. 3 days post EP, cellular library is stained against an antigen of interest and stained, non-tonic signaling cells were pre-enriched via FACS. Sorted cells were rested overnight to be loaded into an OptoSelect™ chip together with antigen-coupled beads. Cells were grown inside the chip for several days while being imaged for every hour in FITC filter cube. Cells expressing an antigen-reactive CAR were expected to upregulate their reporter expression. These cells were then exported from the chip directly into lysis buffer for library sequencing preparation. Each amplified CAR sequence derived from a colony would be barcoded individually and pooled together into one sample for Oxford Nanopore sequencing. Potential de novo antigen-specific scFv sequences were then identified and functionally validated with functional assays like Xcelligence.

4.4.2 The first proof-of-principle run of the pipeline

Cellular CAR library screening pipeline starts with large-scale electroporation of 1.5E+09 cells with the plasmid Library DNA. As established in Section 4.3.3, J7i cells were electroporated with MEB and OP mixture. Immediately after electroporation, the cells were treated with DNaseI. Besides large-scale electroporation, small-scale electroporations were performed with 5.0E+06 cells the compare efficacy of the large-scale electroporation. In the small-scale experiment, the cells were shocked with the #1468 as the positive control and with the generated plasmid library. 2 days post EP, I analyzed CAR expression, activation and viability of the cells. The PC cells that were shocked with #1468 in small-scale achieved the highest CAR expression. Interestingly in shocks done with plasmid library DNA, the CAR MFI of J7i cells electroporated in large-scale was 3 fold higher than the cells electroporated in small-scale (Fig. 4.4.2.1 A, left). Nevertheless, all conditions had around 5% activated cell regardless their CAR expression levels (Figure 4.4.2.1 A, middle). The viability of the cells 2 days post EP were similar to mock in the small-scale samples. However, cell viability was reduced to 75% in the large-scale EP.

At day 3, cells were incubated with recombinant CEACAM-5. As incubated recombinant CEACAM-5 contains a His Tag at its C terminus, I stained the CEACAM5 bound J7i-Library cells by using a secondary anti His Tag APC antibody. The stained cells were pre-enriched via FACS. Figure 4.4.2.1 B shows the staining and sorting gate for mock and CAR Library expressing cells. 0.033% of the mock cells were positive for CEACAM-5 staining. As these cells did not express any CAR, this was the unspecific background staining (Fig. 4.4.2.1 B). 33 cells fell under the FACS gate. On the other hand, 0.052% of the J7i-Library cells were stained with CEACAM5 and there were 70 cells present in the same FACS gate. This meant that when J7i-Library cells were sorted, around 50% of the cells were false positive.

Sorted cells were rested overnight to avoid building up stress by performing FACS sort and OptoSelect™ chip loading on the same day. At day 4, I loaded the CEACAM-5 coupled beads to a chip by gravity penning to the bottom of each pen. Later, I penned single pre-enriched J7i-Library cells and started brightfield and FITC fluorescent imaging by taking a picture every hour. 24 hours post incubation, there were 30 cells that upregulated reporter expression only after interacting with the antigen-coupled beads. Since Jurkat cells proliferated inside the chip, I opted for single-colony sequencing rather than single-cell sequencing. Single-colony sequencing would increase the overall recovery rate of CAR sequences.

However, single cells had to be exported from the chip on day 2 of the experiment, as 17 of the hits committed apoptosis (Fig. 4.4.2.1 C, left). Thus, the remaining 13 cells were exported from the Lightning^{TM} device directly into the lysis buffer. Only 2 single cells showed cell division by the time of the export. I also exported a cell from PC population that is uniformly expressing plasmid #1468. For most of the hits, 3 hours of bead interaction was enough to see upregulation of Venus expression. In Figure 4.4.2.1 C, 3 representative J7i-Library cells getting activated upon interacting with the CEACAM5 coupled beads were illustrated. After the exports, nested PCRs were performed to amplify CAR cDNA. The PCR products were run in Fragment Analyzer (Agilent, US) to check if the amplified sequences have the correct length. All 14 samples had a single peak around 2.1 kb which is the average length of a CAR cDNA. The negative control did not show any bands, indicating my materials for PCR were not contaminated with any carry over vector (Supplementary Figure 3). These amplified CAR sequences from each colony were barcoded individually to be pooled together into one sample for sequencing. 1 sample was lost during the CAR recovery process. Overall, 13 barcoded sequences including the PC were submitted to Oxford Nanopore sequencing.

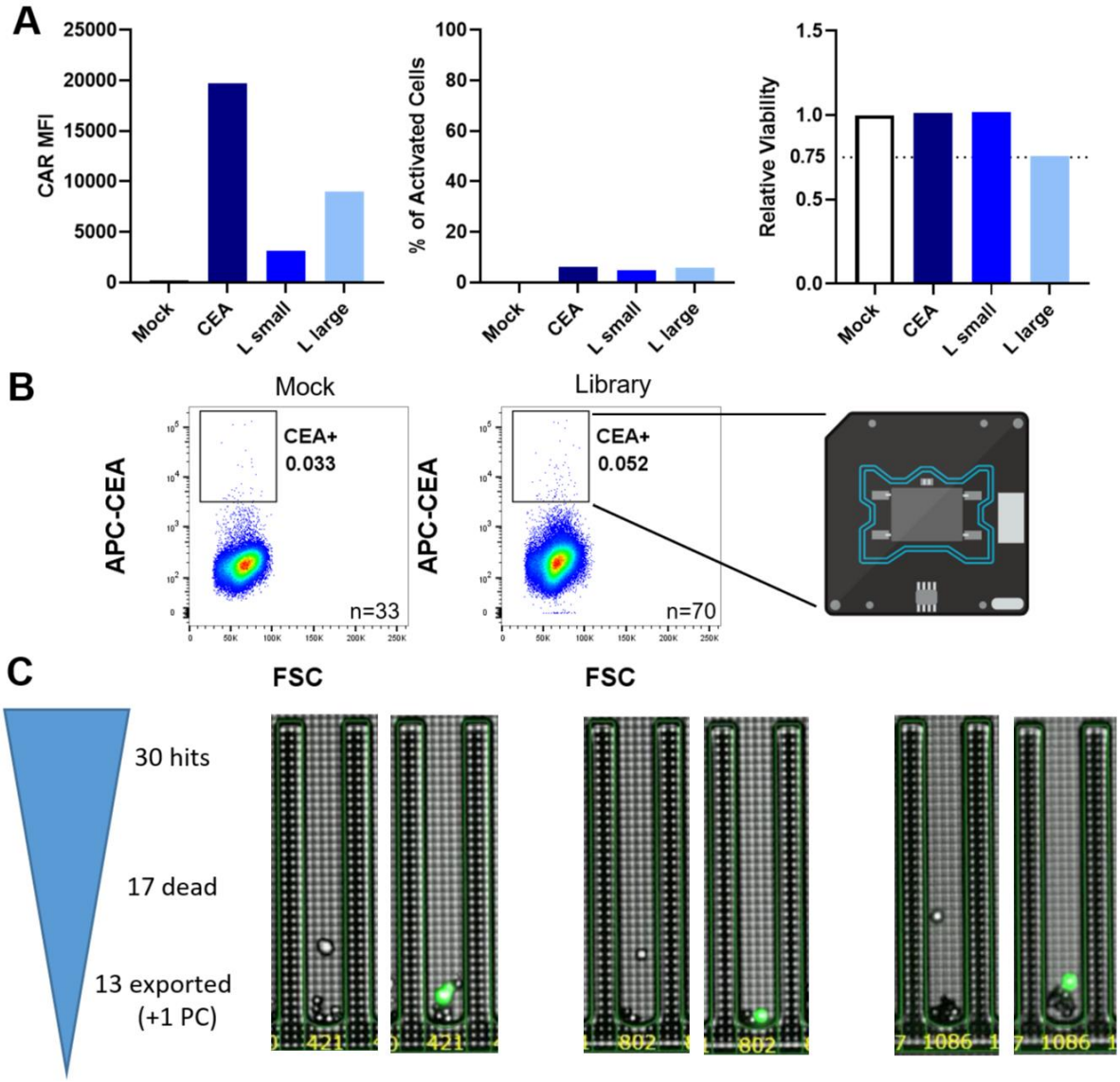

Figure 4.4.2.1: The first proof-of-principle experiment of the pipeline. A: 1.5E+09 cells were electroporated with MaxCyte GTx^{TM} in large scale (L large) together with 5E+06 cells in a small-scale electroporation to serve as positive control. In small scale, cells were shocked with plasmid #1468 (CEA), or with CAR plasmid library (L small). From left to right, CAR expression, percentage of activated cells and cell viability are depicted for each condition 2 days post electroporation, respectively. **B:** 3 days post electroporation, cells shocked with CAR library were stained against CEACAM-5 full length protein. Staining of mock, and CAR library electroporated cells are depicted. "n" represents the number of cells contained in the sorting gate. Cells sorted from CAR library EP were rested overnight and loaded into an Optoselect^{TM} chip. **C:** 2 days after the start of Lightning experiment, cells that upregulated their reporter expression were identified. Out of 30 hits, 13 of them were alive after 2 days. These 13 hits were exported from Lightning together with a PC cell expressing #1468 for sequencing of their CARs. Images display the activation of 3 antigen-reactive cells after 12h of incubation with antigen-coupled beads.

4.4.3 Sequencing analysis of the hits

Oxford nanopore sequencing yields in long reads up to Mbs. Prepared CAR cDNA libraries were expected to be around 2.2kb after ligation of barcodes and adapters for sequencing. Therefore, all amplified CAR sequences can be sequenced in a single read. When a sequencing run is finished, Oxford Nanopore Technologies (ONT) software prepares a run report. Through this run report, the success of the experiment is assessed. When the total amount of reads sequenced over time was analyzed, there were equal ratio of "Passed" and "Failed" reads (Supp. Fig. 4 A). Nevertheless, more than 2.0E+06 reads had quality score above the threshold set by the ONT. As Figure 4.4.3.1 A illustrates, most of the reads sized around 2.1 – 2.2kb that indicates actual size of a CAR sequence. The run report also contains information about how many reads were sequenced per barcode. According to the run report, barcode number 8 was overrepresented with nearly a million reads. The read numbers of rest of the barcodes were between 50,000 and 250,000 (Supplementary Figure 4 B).

Before starting the sequencing analysis, reads longer or shorter than 2.2kb were filtered out. I first analyzed the barcode 13 which is the PC sample that expressed plasmid #1468 uniformly. Even though in PC a unique CAR was expressed, I was unable to align the sequences to each other due to intrinsic 1% error rate of Oxford Nanopore Sequencing. These errors can happen in the form of false base calling or single nucleotide insertion/deletions (in/dels), especially during sequencing of repetitive regions. Nevertheless, I applied different multiple alignment algorithms, however I failed to get an alignment (Supplementary Figure 4 C). To solve this problem, I made use of IMGT software's V-QUEST function. This function accepts the FASTA files containing the BCR or TCR sequences and performs their alignment and annotation to the most probable V_H or V_L allele. V-QUEST is also able to analyze scFv sequences. As mentioned before, I filtered the sequencing reads according to their size and run the remaining sequences in V-QUEST algorithm. After *in silico* analysis of the sequences contained in barcode13, the percentage of similarity to annotated V genes for heavy and light chains were between 50-80%. The reason for low similarity was because the scFv in plasmid #1468, SCA431, was derived from *Mus musculus* and the algorithm was run against human sequences. Correcting the mistake resulted in above 85% similarity for every read. Algorithm annotated *Mus musculus* IGHV3-1*02 for heavy chain and *Mus musculus* IGKV4-80*01 for the light chain for almost all the reads. It also reported the correct CDR3 sequences, "CAREDYDYHWYFDVW" and "CHQWSSYP" for heavy and light chains, respectively. As *Mus musculus* derived SCA431 achieved as high as 80% sequence similarity with

certain human variable gene sequences, I set up a filter for sequence similarity of 90% for all annotated alleles when analyzing the hits against human database. This filter prevented any plasmid #1468 present in the other barcodes from being aligned against human alleles. V-QUEST output file also contained information about the functionality of the annotated heavy and light chains as being productive or unproductive. Functionality was determined by the presence of premature stop codon in the sequences. I investigated the functionality of the reads only when they had equal or above 90% sequence similarity to their respective annotated V_H and V_L alleles. I counted a read as productive only when both V_H and V_L chains resulted in productive sequences. The percentage of productive reads were calculated by dividing the number of productive reads to total number of reads passed the 90% sequence similarity filter. For example, barcode13 showed the highest percentage of productive reads with 10% (Figure 4.4.3.1 B).

When I analyzed the rest of barcodes, I only considered the reads that fulfilled following criteria:

1. Annotated V gene similarity of 90% and above for both heavy and light alleles to reported human sequences.
2. Reads with productive heavy and light chains.
3. Reads with an assigned CDR3 sequence for both heavy and light chains.

After applying the above filters, I ended up with total read numbers between 6 and 151 for 12 hits that were analyzed. I calculated the percentage of productive reads for each barcode as explained above. Most of the barcodes had around 5% productive reads, except for barcode03 which contained slightly less with 3% (Figure 4.4.3.1 B). As I filtered out the reads with less than 90% sequence similarity, SCA431 scFv sequence was absent in the remaining scFv reads. Its presence was manually checked across all the reads by searching for its CDR3 sequence in all heavy chain CDR3 sequences regardless of their functionality. I found out that in 8 out of 12 barcodes SCA431 sequences was present, therefore plasmid #1468. At least 1 productive SCA431 sequence was found in each of these barcodes. The remaining 4 barcodes did not have any sequence similar to SCA431, namely barcodes 6,8,11 and 12. This meant that activation of these cells was caused by a *de novo* CEACAM-5 specific scFv (Fig. 4.4.3.1 C). To find out the number of unique productive scFvs present in a barcode, I counted how many times an scFv occurs with the same annotated V_H and V_L alleles and subtracted these numbers from the total productive read number. I found out that there were 5 to 32 unique productive scFvs with a median of 14.5 per cell (Fig. 4.4.3.1 D). Furthermore, I analyzed the expressed V_H and V_L alleles and counted how many reads they were annotated for each barcode individually. I generated pie charts by illustrating each unique allele in a slice and distributing the size of the slices with respect to number of reads those alleles were annotated. As Supplementary Figure 5 D illustrates, barcodes with #1468 sequence did not show any enrichment of a certain allele. However, apart from Barcode08, barcodes that did not contain #1468 sequence showed enrichment of a certain V_H and V_L. In barcode 8, IGHV3-30-3*01 and IGHV4-59*08 were found to be represented equally in V_H alleles, but IGKV2-30*01 allele was enriched for V_L. On the other hand, for Barcode06 IGHV2-5*01 and IGKV3-20*1, for Barcode11 IGHV5-51*01 and IGKV3-11*01, for Barcode12 IGHV3-48*01 and IGLV6-57*03 alleles were enriched. Due to the enrichment of these alleles, I was able to deduce the CDR3 sequences for these 3 barcodes (Figure

4.4.3.1 E). V-QUEST also annotated all their V, D and J alleles, thus I generated the whole scFv sequence and ordered them to be cloned into a functional CAR backbone for *in vitro* validation assays. As enrichment of certain alleles was observed in the barcodes that lacked #1468, I re-analyzed the barcodes with #1468 a second time to assess whether *Mus musculus* derived SCA431 V_H and V_L alleles were enriched over annotated human alleles. To do so, I run the FASTA files of these barcodes in V-QUEST again, but this time against the *Mus musculus* database. I applied the same three filter criteria mentioned above to the obtained reads. In all the barcodes re-analyzed, only alleles IGHV3-1*02 for heavy chain and IGKV4-80*01 for the light chain were annotated as expected. The read number after filtering varied between the barcodes. Nevertheless, I generated another series of pie charts by including the reads that correspond to *Mus musculus* alleles. The pie charts for barcodes 6, 8, 11 and 12 were not changed as they do not contain any SCA431 sequence. For each pie chart, only the overrepresented allele was written in the legend and this particular allele was sliced out from the rest of the alleles. In all the barcodes that contained #1468, *Mus musculus* IGHV3-1*02 and IGKV4-80*01 alleles were enriched (Fig. 4.4.3.1 F). CDR3 amino acid sequences for all V_H and V_L alleles were constructed by taking the weight of amino acids for each position into consideration (Supp. Figure 5 E).

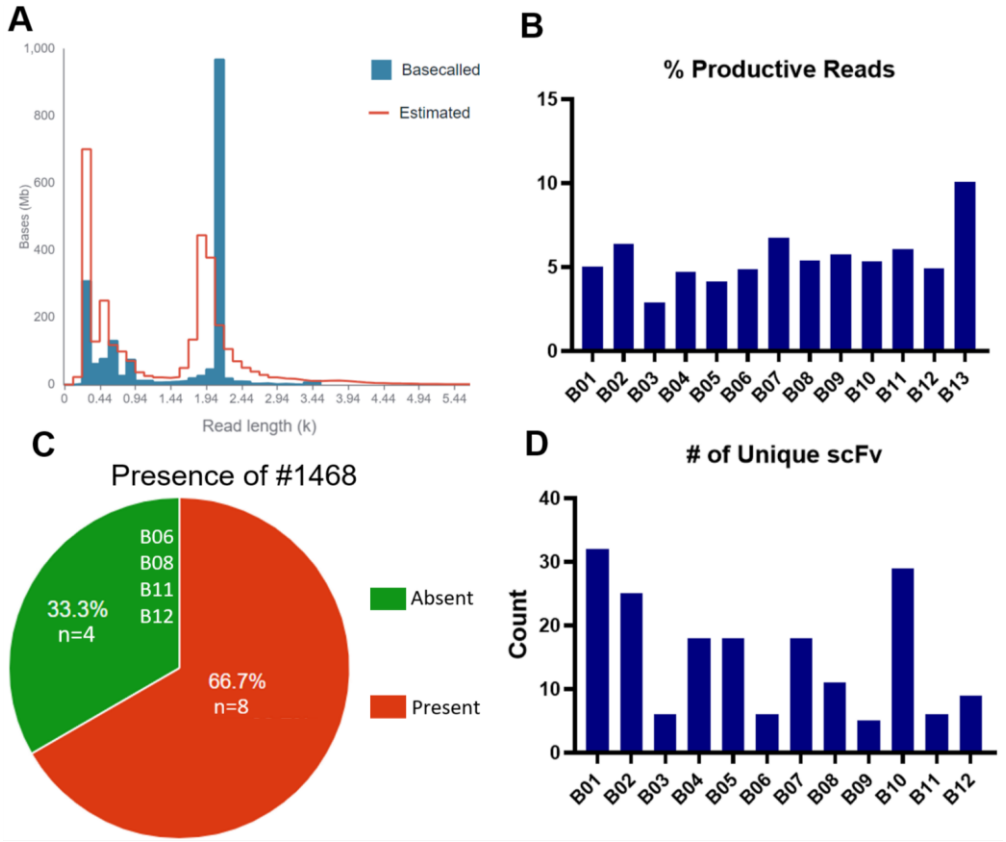

E

Barcodes	V_H CDR3	V_L CDR3
B06	CAHMRDYSKSYYYGMDVW	CQQYGSSPPSTF
B11	CASHNIRGDRRETYYYGMDVW	CQQRSNWPPTIF
B12	CARRGSLPTPGNYWYFFGLW	CMQGTHWRPT

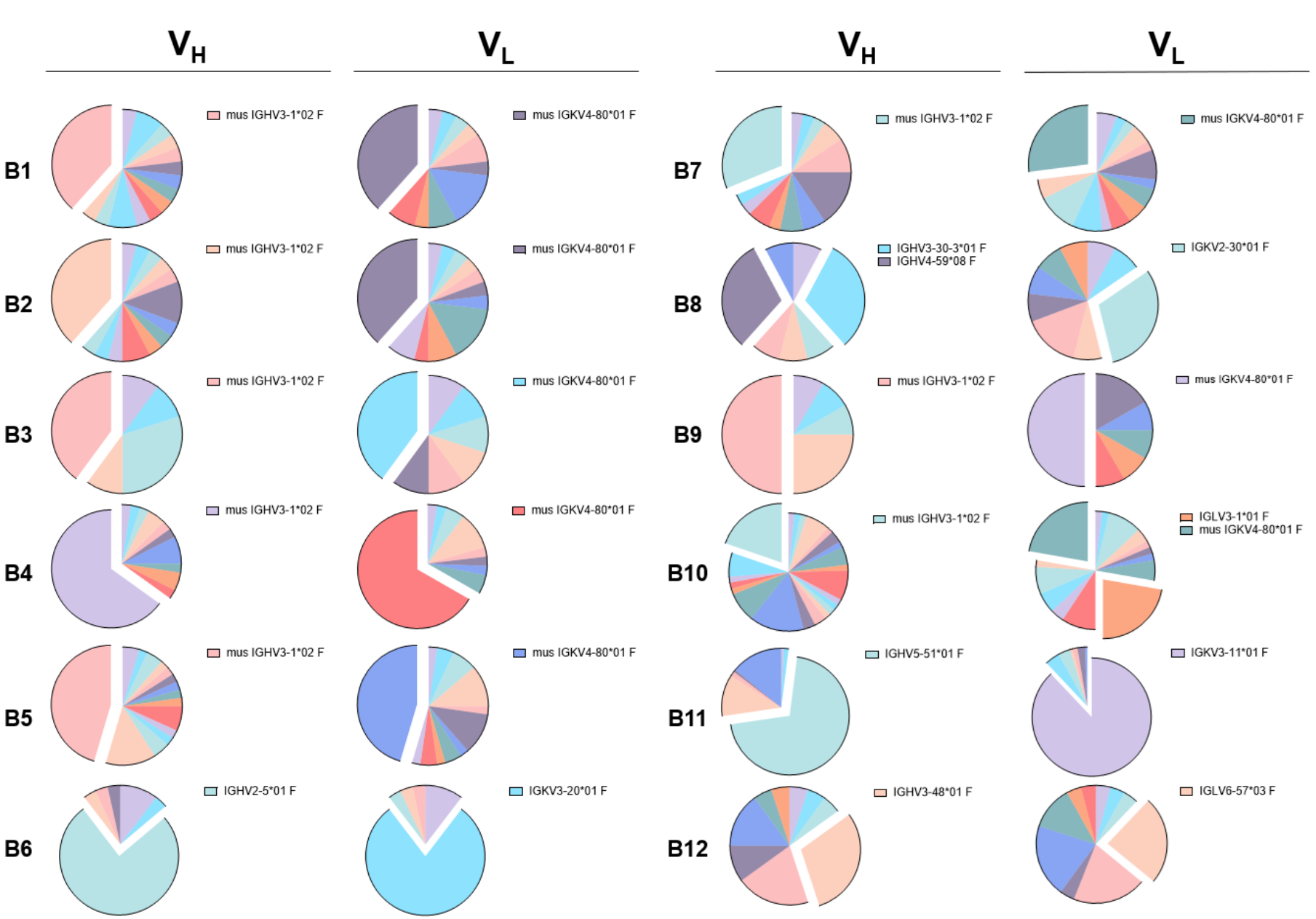
V_H
V_L
V_H
V_L
B1
mus IGHV3-1*02 F
mus IGKV4-80*01 F
B2
mus IGHV3-1*02 F
mus IGKV4-80*01 F
B3
mus IGHV3-1*02 F
mus IGKV4-80*01 F
B4
mus IGHV3-1*02 F
mus IGKV4-80*01 F
B5
mus IGHV3-1*02 F
mus IGKV4-80*01 F
B6
IGHV2-5*01 F
IGKV3-20*01 F
B7
mus IGHV3-1*02 F
mus IGKV4-80*01 F
B8
IGHV3-30-3*01 F
IGHV4-59*08 F
IGKV2-30*01 F
B9
mus IGHV3-1*02 F
mus IGKV4-80*01 F
B10
mus IGHV3-1*02 F
IGLV3-1*01 F
mus IGKV4-80*01 F
B11
IGHV5-51*01 F
IGKV3-11*01 F
B12
IGHV3-48*01 F
IGLV6-57*03 F

Figure 4.4.3.1: Analysis of the hits for identification of CEACAM5 specific de novo scFvs. A: The size of each sequenced read and the amount of data gathered for each length in megabase are plotted in x and y axes, respectively. **B:** Number of productive reads were obtained from IMGT V-QUEST. Number of productive reads were calculated after filtering the reads for having sequence similarity of 90% or above to their annotated V genes. The percentage of productive reads was calculated by dividing the number of productive reads by total reads. **C:** Pie chart shows the presence of #1468 in 12 barcodes as #1468. Barcodes that express #1468 was shown in red, and barcodes free of #1468 were shown in green. **D:** The number of productive unique scFvs were calculated for each barcode and depicted in bar plot. Median number of productive unique reads was found to be 14.5. **E:** For all 12 barcodes, total number of productive read found in a barcode, shown in dark blue, was compared to productive unique read number, shown in light blue. "*" indicates the barcodes in which the #1468 was absent. **F:** The CDR3 amino acid sequences of heavy and light chains from the barcodes that lacked #1468 and had enrichment for certain sequences were aligned. Amino acids highlighted in red indicates the enrichment of that particular amino acid in that particular position of the CDR3. The first sequence series shows the CDR3 of heavy chain and second series shows the CDR3 of the light chain.

4.4.4 *In vitro* analysis of the hits

Heavy and light chains in Barcode 6 and 11 achieved prominent enrichment of certain alleles, IGHV2-5 IGK3-20 and IGHV5-51 IGKV3-11, respectively (Figure 4.4.3.1 F). Moreover, constructed CDR3 amino acid sequences of their heavy and light chains resulted in sequences with high consensus. Therefore, both of the scFv sequences were assembled and flanked with NheI and NotI restisction enzyme recognition sites. These restriction sites enabled cloning these sequences into pS/MARt, nanoS/MARt or lentiviral backbones #272, #1468 and #53, respectively. Assembled full-length scFv sequences were ordered and scFv sequence obtained from barcode 6 was cloned into pS/MARt backbone #272 (performed by Alexandra Tuch), thus generating the plasmid #1475. The specificity of the newly generated CAR was checked by generation of J7i-1475 cells. J7i were also electroporated with plasmid #272 to be used as positive control in antigen-specific stimulation experiments. 2 days post electroporation, the J7i-272 and J7i-1475 cells were analyzed for their CAR expression level. Around 50% of the cells were positive for CAR expression in J7i-272 cells. However, only around 20% of J7i-1475 expressed the CAR (Figure 4.4.4.1 B left). Moreover, the level of CAR expression was decreased in J7i-1475 cells compared to J7i-272 (Figure 4.4.4.1 A, left). At day 2, the cells were incubated with CEACAM5 coupled PP beads in 2:1 beads to cell ratio. J7i-272 cells showed a mild stimulation as activated cell percentage was doubled compared to unstimulated cells. On the other hand, J7i-1475 cells did not react to antigen-specific stimulation as the percentage of activated cells stayed firmly around 3% regardless of the stimulation (Figure 4.4.4.1 B, right).

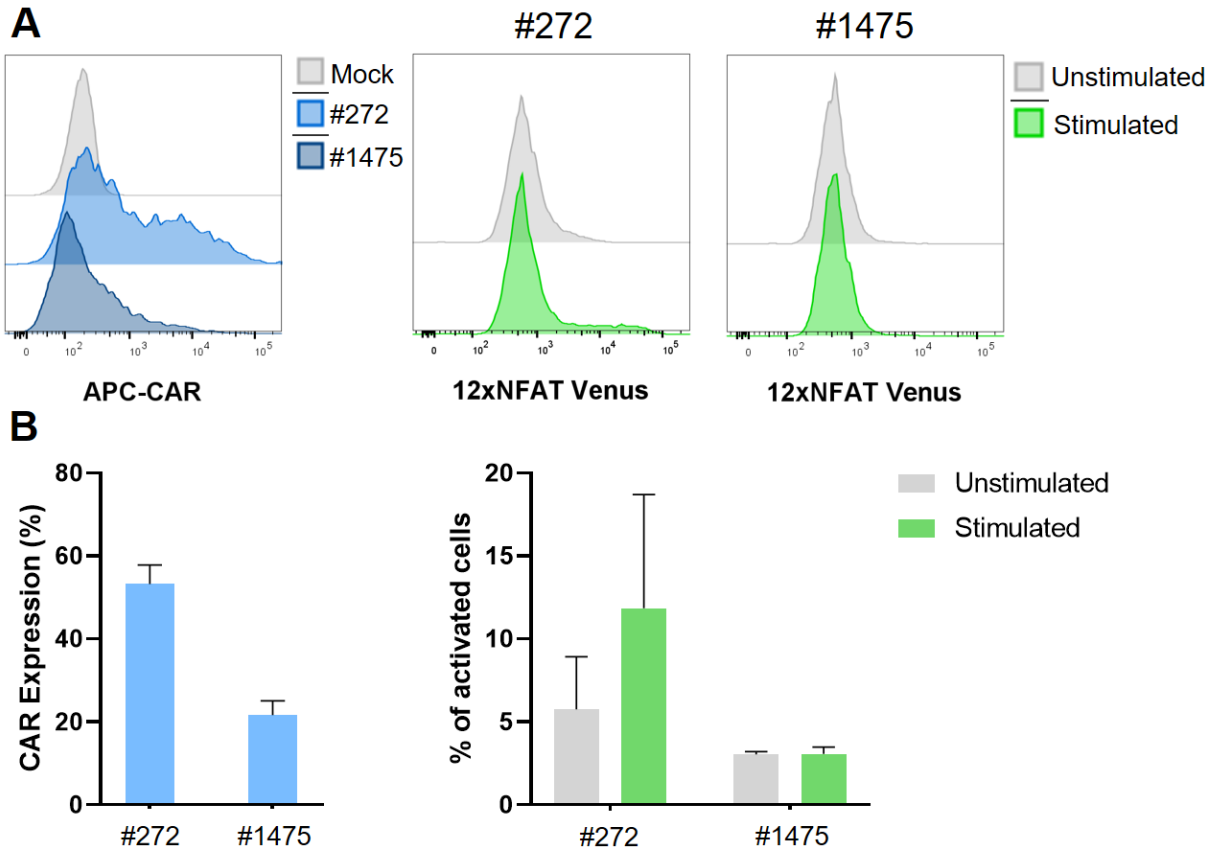

Figure 4.4.4.1: In vitro validation of overrepresented scFv in barcode 6. A: (Left) 5E+06 J7i cells were electroporated with either plasmid #272 or plasmid #1475 that encodes for the most represented scFv found in the barcode 6. CAR expression was determined via flow cytometry acquisition 2 days post EP. FACS plot is representative of 3 biological replicates. (Middle, Right) 2 days post EP, J7i-272 and J7i-1475 cells were stimulated with CEACAM5 coupled PP beads in 2:1 beads to cell ratio. Venus expression of stimulated cells (in green) are overlaid with unstimulated cells (in grey). FACS plots are representative of 3 biological replicates. **B:** CAR expression and percentage of activated cells depicted in A are quantified and depicted in bar plots. (Left) Percentage of CAR expressing cells 2 days post EP is shown for the J7i-272 and J7i-1475 cells. Error bars depict the standard deviation. (Right) Percentage of activated unstimulated (grey) and stimulated (cells) are depicted for J7i-272 and J7i-1475 from left to right. Error bars depict the standard deviation.

5 Discussion

Although phage display libraries can give rise to highly specific functional CAR molecules, reaching the final product may take several months. Therefore, CAR identification by phage display for development of personalized CAR T cell therapies is a challenging task. This project aimed to develop an alternative CAR isolation pipeline to scFv phage display libraries. In this pipeline, cellular libraries of CARs were generated and screened against an antigen of interest. From generation of the libraries to *in vitro* validation of the isolated CARs, pipeline can be finalized in as little as 6 weeks. Thus, this project provides a reliable platform for accelerated isolation of tumor antigen specific CARs that are suitable for ACT.

5.1 Development and characterization of a Jurkat reporter cell line

5.1.1 Cultivation and maintenance of highly responsive Jurkat reporter cells

In order to generate a cellular CAR library, I cultivated an antigen-specific stimulation sensitive Jurkat reporter cell line that will be used to engraft cloned plasmid CAR libraries. Jurkat cells are immortalized CD4 T cells isolated from an acute T cell leukemia patient [156]. They were chosen for generation of cellular library as they are extensively used for characterization of TCR signal transduction pathways that means they possess functional T cell activation pathways [157] [158]. As mentioned earlier, TCR signal transduction is mediated by the nuclear translocation of transcription factors AP-1, NF-κB and NFAT upon antigen-specific stimulation of TCRs. As early as in 2000, researchers took advantage of this nuclear NFAT influx to express a transgene of interest, mostly bright fluorescent proteins (FPs), by integrating artificial NFAT responsive elements to the genome of T cells [159]. By being one of the earliest pathways to be induced upon antigen recognition, NFAT-FP reporter constructs can produce quantifiable results as early as 12 hours after stimulation. Activated cells can then be visualized under a fluorescent microscope or can be acquired in FACS/flow cytometry without performing any antibody staining. Due to their intact TCR signaling pathways, Jurkat NFAT reporter cell lines were generated to be used in high-throughput screening platforms in combination with single cell microfluidic systems for antigen-specific immunoreceptor identification [146] [160, 161]. In order to induce the expression of the reporter genes upon stimulation, the regulatory elements consisting of 3 [159], 4 [162], 6 [159], [163, 164] or 9 [165] repetitive NFAT responsive element (RE) were constructed. Besides NFAT, reporter gene cassettes with NF-κB responsive element has been successfully generated [166, 167] [168]. Moreover, Jurkat cells with triple parameter reporter were generated to be used in TCR validation platforms. These cells were modified with reporter gene cassettes regulated by each of the AP-1, NF-κB and NFAT responsive elements. Upon activation, each gene cassette results in expression of different reporter FP without a spectral overlap [169, 170].

Use of dual or triple reporter systems would complicate the FACS staining and cloning each construct with a FP compatible with the fluorescent filter cubes of the Lightning™ device would have taken significant amount of time. Thus, in this project, I generated a Jurkat reporter cell line with $(NFAT)_{12}$-hIL2p-Venus construct by lentiviral transduction of wild type Jurkat cells. It was reported that, more NFAT RE repetition present in the expression cassette leads to higher levels of reporter expression [159]. Therefore, the construct with 12xNFAT RE repetition is expected to induce a robust reporter expression.

Nevertheless, when transduced cells were treated with PHA, their activation was observed to be heterogeneous as majority of the cells did not upregulate the reporter expression (Fig 4.1.1.1 B, top). This could be explained by the random copy number integrated into the genome of Jurkat cells. It is possible that integration of fewer copy number led to diminished recruitment of TFs to the reporter cassette, resulting in a dim fluorescent signal emission by the cells. With the observed heterogeneity in the activation profile, cells could not be used as a reporter cell line. I hypothesized that single-cell derived clones would have a uniform activation pattern. To obtain a single-cell derived clone with high a sensitivity, I performed 3 consecutive experiments. Firstly, the bulk Jurkat reporter cell population was stimulated with PHA overnight. The next day, cells that are able to react against PHA stimulation were sorted (Figure 4.1.1.1 B, bottom). These cells were then used for cultivation of single-cell derived clones by using the Lightning™ device.

During the single-cell stimulation experiment, I focused on the single-cell derived clones that started with a relatively low FITC MFI and induced a robust reporter expression upon stimulation. Since, during a screening campaign, the degree of reporter expression induction by antigen-reactive cells can give a preliminary information about the functionality of the CARs they express. However, it was observed that cells with high reactivity against PHA stimulation later committed apoptosis including the illustrated cell in Figure 4.1.1.1 F, possibly due to activation induced cell death (AICD) [171]. Therefore, single-cell stimulation experiments with Lightning™ device provided not only the elimination of unreactive cells, but also cells with tendency towards AICD. The clone exported from the pen 215 achieved the highest percentage of activated cells and FITC MFI FC upon overnight PHA stimulation (Supp. Fig. 1 A). However, further analysis of the images taken while export of clone 215 showed that cells from neighboring pens were spilled over (Supp. Fig. 1 B). This was caused by the extended culture period in the chip that allowed some pens to overgrow. For the following experiments, this phenomenon was taken into consideration as having contaminating cells during an export undermines the idea of cultivating single-cell derived clones.

As the 3rd step, I performed a limiting dilution assay to generate a second round of single-cell derived clones. As Figure 4.1.1.1 I depicts, clone number 7 outperformed other emerging clones in terms of activation capacity and I have established clone 7 as my reporter cell line, J7. However, I observed loss in sensitivity of the J7 and J7-53 clones with prolonged cultivation in the cell culture, possibly due to silencing of the transgene by epigenetic mechanisms [172]. To restore their sensitivity, the brightest 40% of the cells were sorted with respect to their reporter expression upon a PHA stimulation. This approach proved to be effective as the FITC MFI FC increased from 30 to 45 and from 20 to 33 for J7 and J7-53, respectively (Figure 4.1.3.1 B). If the sensitivity of the cell line to decline in the future, bulk sorting the activated population has potential to reverse the process.

5.1.2 Effect of antigen density on antigen-specific stimulation

So far, J7 cells were tested for their activation capacity by unspecific, antigen-independent stimulation with PHA. However, during the screening of cellular CAR libraries, antigen-specific CAR constructs are identified by their ability to induce reporter expression upon antigen-specific stimulation. Therefore, J7-53 cells were stimulated with Dynabeads that were coupled with CEACAM5. Beads coupled with 2.5x excess amount of protein resulted in a higher degree of activation in the cells, evident from both

percentage of activated cells and FITC MFI FC. (Figure 4.1.2.1 C, middle and right). However, compared to FITC MFI FC obtained after PHA treatment, the antigen-specific stimulation failed to result in similar level of activation.

As recent evidence suggests, upon antigen recognition, CARs on the cell surface are downmodulated by rapid ubiquitination and subsequent lysosomal degradation [173]. In one study, the CAR downmodulation was found to directly correlate with tumor burden in the tumor bearing mice [174]. Complete CAR removal from the cell surface was reported when CD19 CAR T cells were co-incubated with CD19 expressing target cells *in vitro* [175]. In light of these findings, I analyzed the CAR expression of the cells incubated with antigen-coupled Dynabeads. I realized that CAR expression on the cell surface was decreased to some extent in both 1x and 2.5x conditions. Higher degree of CAR downmodulation was observed with beads coupled with increased CEACAM5 concentration present during coupling (Figure 4.1.2.1 C, left). However, according to CAR MFI, 2/3 of the CARs were still on the cell surface after antigen-specific stimulation. This suggests that, majority of the CAR molecules did not interact with an antigen. This also explains why the activation of the cells was not robust as measured after PHA stimulation. Coupling Dynabeads in the presence of higher protein concentrations resulted in a modest improvement in the activation of the J7 cells (Figure 4.1.2.1 D). This suggests that Dynabeads were already saturated with target protein and presence of high protein concentration during coupling did not improve the coupling efficieny.

I stimulated J7-53 cells in single-cell level in an OptoSelect™ chip to check if they would achieve a higher degree of activation compared to bulk stimulation. However, after penning the Dynabeads, I realized pens had to be filtered before analysis of the paired measurements for FITC MFI FC calculation. The Lightning device is capable of evenly distributing imported cells across the channels and this in turn ensures an efficient penning of the cells. However, upon importing magnetic beads, an uneven bead distribution was observed across the channels. This led to uneven distribution of Dynabead mass in the pens, and consequently the stimulation of the cells would not expected to be uniform. Dynabeads exhibit autofluorescence in PE filter cube, so I performed an imaging of all pens with PE filter cube. This imaging allowed me to analyze the pens according to the size of their Dynabead clusters. I put an arbitrary cut off for the Dynabead surface area measured in PE channel by comparing measurements obtained by image analysis with actual raw images. Therefore, I excluded pens with insufficient beads from further analysis. Amongst the pens that satisfied all filtering criteria, a minority of the cells achieved FITC MFI FC of 4 and above (Figure 4.1.2.1 F). According to these results, most of the reporter cells failed to react against antigen-specific stimulation.

Although TCR T cells can react to a single pMHC molecule presented by the target cells, for CAR T cells it was found that this number can go up to hundreds or in some cases hundreds of thousands of molecules [176, 177]. Therefore, I coupled CEACAM5 protein to PureProteome (PP) beads with a surface area 16x more than Dynabeads. According to manufacturer's instruction, 1 µg of PP beads is able to couple 10 times more protein on their surface compared to Dynabeads. Moreover, a single PP bead is able to present up to 100-fold more antigen than a single Dynabead. Presentation of more antigen would lead to clustering of more CARs on the cell surface and cause enhanced cell stimulation. When J7i-53 were incubated with antigen-coupled PP beads, even the beads that were coupled with 0.25x

recommended protein amount manage to downmodulate CAR expression to 1/3 of the cells incubated with uncoupled beads. Moreover, around 90% of the cells got activated with FITC MFI FC comparable to positive control PHA stimulation (Figure 4.1.3.1 B, F).

The total amount of responsive cells did not increase drastically during single-cell stimulation experiment, only from 57% to 62%. However, PP beads resulted in higher degree of stimulation with 45% of the cells achieved FITC MFI FC equal to or greater than 4. As PP beads outperformed Dynabeads in both bulk and single-cell level antigen-specific stimulation, I decided to use these beads during the cellular CAR library screening platform.

5.1.3 Antigen-specific stimulation and CAR mRNA expression

During the J7i-53 single-cell stimulation experiment performed using the Lightning™ device, I exported several single-cell derived clones and further grew them off the chip. With the emerging subclones of J7i-53, I investigated the influence of antigen-specific stimulation on CAR mRNA expression level. This effect, whether upregulation or downregulation, has not been described yet. The reasoning behind this experiment was that during cellular CAR library screening, I electroporate a random plasmid CAR library into the J7i cells. Therefore, it is most probable that a single cell would receive multiple plasmids encoding for different CAR constructs. Upon identification of a hit during a screening campaign, the CAR sequence or sequences, that are specific against the screened antigen and causing the activation of the cell, are not known. I hypothesized that there might be a positive feedback mechanism that pushes the cells to express more of the CAR that is responsible for activation upon antigen-specific stimulation. In other words, if this positive feedback mechanism exists, the CAR activating the cells should be abundant in mRNA expression level. Therefore, if a scFv sequence is overrepresented in one of my hits after sequencing their cDNAs, it is highly likely that this sequence is the one that encodes for the antigen-specific CAR.

To test this hypothesis, I set up several qPCR experiments where I stimulated the single-cell derived colonies exported from the Lightning™ device with CEACAM5 coupled beads. Housekeeping gene β-actin was used as the reference in the qPCRs. After 24 hours of bead stimulation, I documented the activation of the clones with fluorescent microscopy. Results of the qPCR experiment performed against Venus mRNA expression directly correlated with the fluorescent images of the activated clones. This correlation indicated that the results of the qPCR experiments were reliable. However, results of the qPCRs performed to quantify CAR expression did not reveal any upregulation. Upon antigen-specific stimulation, cells either kept the CAR expression the same or downregulated it to certain extent (Figure 4.1.4.1 A, B).

All the colonies used in the previous experiment were virally transduced to express anti-CEA CAR. However, during a cellular CAR library screening, cells are engrafted with nanoS/MAR plasmid CAR library by electroporation. As nanoS/MAR vectors anchor to nuclear matrix proteins by their S/MAR sequences [178], their transcriptional regulation happens distinctively from randomly integrated transgenic CAR sequences. S/MAR sequences facilitate the accessibility of enhancers and TFs to regulatory sequences present in the vectors, increasing the transgene expression [179]. Therefore, I included J7i-320 cells in the next qPCR experiments to check the presence of the hypothesized positive feedback mechanism in CAR encoding nanoS/MARt vectors. Moreover, in addition to analysis of the cells 24

hours post antigen-specific stimulation, I analyzed the CAR and Venus expression of the cells after 2, 4, 8, 12 hours after the start of the incubation. I decided to check the earlier time points due to the fast kinetics of activation through CAR stimulation as CD69, an early T activation cell surface marker, starts to get expressed as early as 2 hours of T cell stimulation [180]. Analysis of Venus mRNA expression showed upregulation patterns in all the samples across each time point. Again, it served as an internal positive control. Consistent with previous result, CAR expression of the virally transduced cells either stayed in the same level or downregulated throughout the stimulation period. Interestingly, downregulation of CAR mRNA in electroporated cells persisted throughout the 24 hours of stimulation (Figure 4.1.4.1 C). When the same experiment was repeated with electroporated cells, downregulation of the CAR mRNA in stimulated cells was further confirmed (Supplementary Figure 3 C). Considering these experiments, I rejected the initial hypothesis that antigen-specific stimulation causes induction in CAR expression. On the contrary, this data suggests that it either stays the same or gets downregulated.

5.1.4 Effect of electroporation on viability, CAR expression and activation

5.1.4.1 Electroporation using the Neon™ device

As the first step of the cellular CAR library screening platform is electroporation of J7i cells, shock parameters for CAR expression and subsequent antigen-specific stimulation of the cells had to be optimized. I first investigated the effect of electroporation on the activation capacity of the cells when stimulated with their cognate antigen. When electroporated and transduced cells expressing anti-CEA CAR were incubated with antigen-coupled beads or MCF7 cells, in both conditions, activated cells gave rise to a distinct peak, similar to the PHA treated PC cells, with respect to reporter expression regardless of the engraftment method (Figure 4.1.5.1 A). When unstimulated J7i-53 and J7i-320 cells are compared with each other, electroporation induced antigen independent activation of unstimulated cells. This phenomenon was absent in mock electroporated cells. This rules out EP as a potential cause for the observed activation. It was reported that high levels of CAR expression could cause antigen independent activation of the cells [181] [121]. Consistent with these reports, the activation was indeed observed in the cells with high CAR expression (data not shown).

Besides bulk antigen-specific stimulation, J7i-320 cells were tested for their activation capacity on single-cell level. 2 days post electroporation, single J7i-320 cells were stimulated with CEACAM5-coupled PP beads in an OptoSelect™ chip. Even though every cell analyzed in this experiment was derived from a single-cell derived clone, has been transfected with the same CAR construct and stimulated with the same batch of CEACAM5 coupled beads, the observed response of J7i-320 cells to antigen-specific stimulation in single-cell level was heterogeneous (Figure 4.1.5.1 C). The heat map generated by the ln(FITC MFI) of each single cell during 30 hours of stimulation showed different clusters of cells with distinct activation patterns. There were “early responder” cells that induced reporter expression only after several hours of bead stimulation. On the other hand, “late responder” cells responded to stimulation after 20 hours. Moreover, a considerable amount of cells was already activated in the beginning of the experiment. These cells failed to respond to antigen-specific stimulation. I clustered the cells according to their CAR expression and analyzed the activation pattern of each cluster over the 30 hours of stimulation. I realized that cells expressing high levels of CAR were the ones already activated and failed to react against bead stimulation.

This points towards that the cells were already exhausted at the start of the experiment due to antigen-independent tonic signaling as it is an established cause for early exhaustion of CAR T cells. In several studies, tonic signaling is linked to insufficient expansion, inhibitory receptor expression induction and diminished effector activity [182, 183]. Several reasons have been detailed in the literature to explain this phenomenon. It was found that the CD28 TM followed by CD28, CD3 ζ chain causes tonic signaling in certain CAR constructs such as anti-c-Met, anti-mesothelin and anti GD2 scFvs, but not when an anti-CD19 scFv was used.[121] [184]. Moreover, high CAR expression is found to be directly associated with tonic signaling and change the regulatory element that drives the CAR expression have reversed the observed phenotype [121, 181]. Indeed, the CAR construct used in this experiment contains CD28 transmembrane domain followed by CD28 and CD3ζ. Overexpression of this CAR caused exhaustion of the Jurkat cells due to tonic signaling, as backed up by the scientific evidence. Thus, this data suggests that aiming for high CAR expression in ACT products can hinder their effectiveness due to possible tonic signaling mediated early exhaustion of CAR T cells. Several strategies could be employed to the decrease the tonic signaling mediated exhaustion observed in the single-cells stimulation experiment. As antigen-independent activation happens due to elevated expression of CARs, the regulatory element used to drive the CAR expression could be switched to a weaker promoter [181] [185]. Moreover, introduction of 4-1BB costimulatory domain instead of CD28 potentially decrease the exhaustion caused by tonic signaling [182]. Nevertheless, J7i-320 cells proved their ability to react against antigen-specific stimulation upon electroporation. Moreover, they managed to get exhausted due to tonic signaling demonstrating their ability to be used as a reliable model T cell line for primary T cell research.

I observed that use of Neon™ electroporator with S/MAR vectors causes a heterogeneous CAR expression amongst the cells. As depicted in Figure 4.1.1.1 D top middle plot, the CAR expression that is measured by the fluorescent intensity in APC channel spans several logs. This discrepancy results in different activation profiles of the cells upon antigen-specific stimulation (Figure 4.1.5.1 C). The reason for reduced transfection efficiency for a portion of cells could depend on several factors such as the parameters of the applied shock, the composition and conductivity of the buffer cells resuspended during the shock, cell density and plasmid concentration. There have been several attempts to optimize the Jurkat electroporations using different solutions and cell concentrations with Lonza Nucleofector™ [186, 187], Celetrix [188], GenePulser™ [189]. For example, except for study with GenePulser™, all other studies recommended square-wave voltage pulse over exponential wave for Jurkat electroporation. Neon™ electroporator is also designed to deliver pulses square-wave voltage [190]. Although some electroporators allow customers to define their own parameters for further optimization (Gene Pulser™, Neon™, CliniMACS™), some arrive with pre-defined pulse codes that cannot be customized (Lonza and MaxCyte devices). In the case of EP with Neon™ device, even though manufacturer's recommended settings were used for Jurkat electroporation [191], further optimizations are needed to improve the efficiency of Neon™ device.

During the cellular CAR library screening, ideally cells should express similar levels of CAR. This would at least eliminate a potential variable during CAR mediated activation process. Moreover, only 5E+06 cells can be electroporated at once with Neon™ electroporator. This makes large-scale electroporation

of 1.5E+09 cells with Neon device practically impossible. A flow electroporator that is able to perform automated shocks greatly improves the throughput of the EP. Therefore, I decided to switch to GTx™ electroporator from MaxCyte that offers processing up to 2E+11 cells with automated flow EP [155].

5.1.4.2 Electroporation using the GTx™ device

I compared small-scale electroporation results obtained with GTx™ electroporator with the results obtained from Neon™ electroporator to find the superior system. To decrease variability during the optimization experiments, I used vector #1468 as it was the vector I used for CAR library generation. J7i cells were electroporated with GTx™ electroporator in varying plasmid concentrations resuspended in either MaxCyte Electorporation Buffer (MEB) or Opti-MEM (OM) and compared to cells shocked with Neon™ device. The lowest cell viability was observed when the cells were shocked with Neon™ electroporator. I observed use of MEB or OM in EP with GTx™ did not affect the level of CAR expression and viability of the cells. The reason for the observed similarity between MEB and OM could be due to the similar conductivity of the buffers (Figure 4.3.1.1). According to the literature, the effect of increased or decreased EP buffer conductivity on cell viability and EP efficiency is still unclear [192-194]. Nevertheless, obtained overlapping results from MEB and OM conditions could stem from the comparable conductivity of the buffers. Composition of all three buffers used for the electroporation are proprietary. Thus, they cannot be compared to each other to investigate the effect of their composition on the observed outcome. Overall, EP with GTx™ outperformed Neon™ device by resulting in improved cell viability and causing lesser activation. Moreover, evident from Figure 4.3.2.1 B, C and E; EP with GTx™ achievedd a uniform CAR expression compared to what was observed in Neon™ EP (Figure 4.1.1.1 D, top middle).

OM and MEB may have similar conductivity, thus viability and CAR expression, but EP with OM resulted in higher activation levels compared to MEB (Figure 4.3.1.1 B). Higher activation level cannot be explained by the possible tonic signaling due to CAR overexpression as in both conditions, cells express the same level of CAR. Therefore, composition of the buffers could be responsible for higher activation. Indeed, OM is derived from Basal Medium Eagle (BME) that has 1.8 mM $CaCl_2$ concentration [195], around the concentration found in extracellular space [196]. However, in a resting cell, cytoplasmic concentration of Ca^{2+} is around 50 to 100nM, more than 10^3 fold lower than BME. Assuming OM has similar $CaCl_2$ concentration with BME, through the pores opened during EP, a Ca^{2+} influx could happen towards the cell cytoplasm. This sudden spike in Ca^{2+} concentration could activate calcineurin, that results in translocation of NFAT to nucleus, driving reporter gene expression. As MEB resulted in less cellular activation upon EP, I decided to continue electroporating with MEB.

Besides the effect of electroporator and shock parameters used for transfection, the quality of isolated plasmid DNA has been found to be detrimental for the optimal CAR expression (Figure 4.3.2.1). Interestingly, when the Macherey-Nagel (MN) kit was used for DNA preparations inoculated with lab grown XL-1 strain, the isolated plasmids were free of genomic DNA contamination (Data not shown). It was only present when the DH5α strain, that is able to host the nanoS/MARt vectors, were inoculated for DNA preparation. However, mentioned genomic DNA contamination present in the maxi prep isolations did not decrease the cell viability, but dramatically affected the CAR expression. This is because a large proportion of the electroporated DNA consisted of contaminating genomic DNA, diluting

the concentration of CAR plasmid DNA. When these contaminants were cleaned up optimal, uniform CAR expression was detected upon EP with GTx™ devices. Unlike MN maxi prep kit, the Qiagen kit resulted in pure plasmid isolation without the need of any further clean-up steps.

When GTx™ electroporator was tested for its capability for upscaling the reaction, it provided consistent, reliable results (Figure 4.3.3.1 A). However, I observed cell clumps that could not be resuspended appearing 24 hours after the shock when MEB was used for EP. I once again compared the OM with MEB by performing an EP with cells resuspended either in MEB or OM to calculate the number of live cells before and 1 day after GTx shock. For the cells shocked with MEB, the flow cytometry drastically overestimated the viability of the cells 1 day post EP as manual cell counting resulted in half the viability calculated from flow cytometry (Figure 4.3.3.1 B, right). As discussed before, CAR expression was not affected by the buffer that the cells were resuspended during EP and shock with OM caused higher percentage of activated cells, possibly due to Ca^{2+} influx (Figure 4.3.3.1 B, middle). Due to improved cell viability after EP, I chose to continue with OM for the subsequent EP experiments. As the buffer in which the cells were resuspended is the only difference between the two shock conditions, the low viability can be attributed to the non-optimal composition of MEB.

During the last shock optimization experiment, I decided to include a DNaseI treatment after the shocks. Potentially, the excess plasmid remaining in the solution after the electrical pulse could be phagocytosed by the cells over time. In the endosomes, the unmethylated CpG DNA is then available for recognition by the innate immunity receptors, specifically toll like receptor 9 (TLR9) [197]. Moreover, plasmids ending up in the cytoplasm can activate the cGAS-STING pathway that recognizes dsDNA [198]. Both pathways lead to activation of J7i cells by initiating different signaling pathways. Even though nanoS/MAR vectors have minimal CpG islands, the remaining islands cannot be methylated as the DH5a strain that host these vectors has been genetically modified to abrogate methylase enzymes. The unmethylated CpGs and presence of free plasmid DNA in cytoplasm possibly induces activation of the Jurkat cells as a byproduct of electroporation. To test possible TLR9 and STING initiated unspecific cellular activation hypothesis, I treated the cells with DNaseI immediately after the electroporation to degrade any excess plasmid. Supporting my hypothesis, DNaseI treatment resulted in decreased activation of the cells. Moreover, mixing OM and MEB on top of DNaseI digestion had a cumulative effect, causing a further reduction in the percentage of activated cells. (Figure 4.3.3.1 C). The reason for the observed phenomenon could be due to dilution of Ca^{2+} concentration by the MEB, or presence of calcium chelators in MEB that prevents the Ca^{2+} influx. Therefore, for the large scale shock with 1.5E+09 cells, I decided to resuspend the cells in OM and MEB mixture and treat them with DNaseI immediately after EP.

5.2 CAR library generation and possible improvements

In the first attempt of generation of a naïve scFv library, I adopted primers for amplification of V_H and V_L sequences from Pansri et al. [151] which they modified from previously published work [124, 199]. In total, 75 PCRs were performed to amplify theoretically all V_H and V_L alleles. However, as illustrated in Figure 4.2.1.1 B, especially primers used for V_L λ chains did not result in optimal amplification. During *in silico* tests, V_L λ primers failed to give amplification products meaning that they were poorly designed. Nevertheless, I performed small-scale V_H-V_L κ and V_H-V_L λ CAR plasmid library productions to determine

the CAR expression in Jurkat cells. A scFv sequence with correct ORF obtained from small-scale library production was cloned into pS/MARt backbone #272 and upon electroporation into J7i cells, no CAR expression on the cell surface was observed (Figure 4.2.1.1 E). The reason for the lack of cell surface CAR expression was that the primers designed by Pansri et al. did not amplify the leader sequences that are present in the beginning of V genes of heavy and light chains. These sequences are required to translocate the heavy and light chains into the ER lumen for correct folding, assembly and post-translational modifications [200]. Due to poor design of oligos and their inability to amplify leader sequences, I decided to formulate my own primer pairs that would amplify theoretically every possible V_H and V_L chains reported in IMGT database [154].

In total 47 desalted primers were ordered to perform 177 PCRs to increase the diversity of the generated library. However, 2 VL5' (HVL3 4, HVL11) and 1 VL3' (HJL4) primers did not give rise to a product in any of the reactions they were used. The alleles that these 3 primers amplify are listed as "ORF" in IMGT database instead of "F", meaning functional. "ORF" signifies that the reported allele has changes in conserved sequences that may lead to misfolded proteins [201]. The remaining primers functioned as expected and in 144 PCRs a product around 400 bp was observed. Addition of a synthetic V_L κ leader sequence to the generated libraries resulted in the expression of the CARs on the cell surface (Figure 4.2.2.1).

However, when plasmids isolated from emerging V_H-V_L κ and V_H-V_L λ libraries were sequenced, majority of the scFvs were found to be out of frame (Figure 4.2.2.1 E). Further analysis showed that the single nucleotide deletions were observed exclusively in primer binding sites. This suggested that primer synthesis might be faulty. Due to the restriction site and Glysine-Serine linker sequence extensions that the primers contained, their sizes varied between 40 to 60 bp. Even with the 99.5% coupling efficiency during oligo production, only 77.8% of the 50bp primers would have the correct nucleotide sequence [202]. The primers that were used to generate the scFv libraries were desalted after synthesis. They were not subjected to any size exclusion purification protocol, as desalting removes only small impurities like carry over salts, but do not remove any shortmers [203]. To assemble a scFv, heavy and light chains have to be amplified by using in total 4 primers. Thus, for each primer binding site, there is a 22.2% chance that an incomplete primer will be used to prime the PCR. This cumulative effect further decreases the probability of obtaining a scFv fragment without any frameshift mutation. Therefore, I used primers purified with HPLC and PAGE after synthesis to test if the ratio of in frame scFvs could be improved. The ratio of scFv fragments in correct ORF increased with purification quality of the ordered oligos (Supp. Table 2). Due to achieved comparable in-frame ratios, I decided to order the working primers with HPLC purification.

When the heavy-κ and heavy-λ libraries were generated with HPLC purified primers, the sequencing of the emerging colonies showed that majority of the scFv sequences were again out of frame due to faulty primer synthesis. The HPLC purification can effectively purify oligos up to 50 bp by typically achieving purity of ~85% full-length sequence [203, 204]. Therefore, it is possible that this method failed to eliminate all shortmers occurred during the synthesis. Moreover, a substantial proportion of the ordered oligos contained secondary structures, and these structures complicates the HPLC purification process [205]. PAGE purification, on the other hand, achieves purity of >95% full-length sequence [203]. Therefore,

despite the high cost and low yield associated with PAGE purification, oligos purified with PAGE can improve the percentage of scFv fragments in the correct ORF.

In the last decade, naïve scFv libraries with estimated sizes from 1.5E+10 to 3.6E+11 were reported by academic institutes or industrial companies [206-210]. However, in most of these libraries the quality of the libraries with respect to percentage of in frame scFvs is not mentioned. As a quality control, authors analyzed the libraries by restriction digestion or PCR to observe the obtained sequence sizes in agarose gel electrophoresis. However, these quality control methods cannot distinguish single nucleotide in/dels that can cause frameshift mutations. In this project, I reported a modest library with approximately 1.7E+7 colony forming units (cfus) with 43% in frame scFvs. Earlier, possible strategies to increase the ratio of scFvs with correct ORF has been discussed. On the other hand, in order to increase the diversity of the library, couple of improvements can be implemented. Firstly, the amount of ligation product electroporated into the DH5α strain can be optimized. I performed the optimization experiment for electroporated plasmid amount with another *E.coli* strain DH10B (Supp. Table 1). Thus, obtained results may not be representative for DH5α strain that is used to transform nanoS/MARt vectors. So far, the efficiency of the strain has not been reported by Nature Technology Corporation (NTC). Moreover, the genotype and phenotype of this strain is different from what is used to generate scFv libraries with greater than 1.5E+10 cfus. These libraries were generated with commercially available, highly efficient electrocompetent bacteria. It is possible that DH5α strain might have intrinsic constrains that lowers the transformation efficiency. Besides improvement of bacteria transformation, generation of sublibraries is a common strategy to increase the size and diversity of the scFv libraries [207, 210]. In this approach, subfamilies of amplified heavy chains are kept separate and each heavy chain subfamily is assembled with a pooled V_L κ and λ chains separately. This leads to generation of 2 scFv sublibraries for each heavy chain subfamily. According to IMGT, there are 8 heavy chain subfamilies. Thus, it is possible to generate 16 different scFv sublibraries to be pooled later, each consisting of theoretically unique set of scFv sequences.

5.3 CAR identification by cellular library screening

Although GTx™ device achieved excellent upscalability (Figure 4.3.3.1 A), the cells shocked in large-scale exhibited 3 fold more CAR MFI in flow cytometry analysis compared to cells shocked in small-scale during the first proof-of-principle run of the pipeline. However, large-scale electroporation resulted in decreased viability (Figure 4.4.2.1 A). As mentioned before, GTx™ devices operates with predefined electroporation protocols and the parameters used during an EP experiment are hidden from the operator. Thus, different shock parameters might be applied during automated flow EP for the large-scale shock compared to small-scale shock without the knowledge of the operator, leading to observed outcome. Nevertheless, 5% of the cells were activated for both small-scale and large-scale shocks 2 days post EP. For tonic signaling to occur, it was reported that the CAR multimerization on the cell surface through interaction between positively charged patches (PCP) found in the framework regions of the scFvs is crucial [122]. Therefore, samples from this activated population can be sorted to have their CARs sequenced. Obtained sequences can then be screened for presence of PCP in the framework regions.

3 days post EP, J7i-Library cells were pre-enriched with a FACS sort against CEACAM-5 antigen. In the FACS gating for antigen staining, mock cells exhibited unspecific staining to some degree. Around half of the sorted cells were expected to be false positives according to the applied gating strategy. Nevertheless, this would mean that there might be theoretically as much as 750 pens with a true CEACAM5 specific CAR expressing cell during single-cell stimulation experiment performed with Lightning™ device. From a technical point of view, analysis of 750 cells for CAR identification would still be a challenging task.

During single-cell stimulation experiment, I observed 30 hits that upregulated reporter expression upon interaction with CEACAM-5 beads. However, I realized that majority of the cells committed apoptosis during the first 12 hours of the stimulation, apparent from the loss of basal reporter expression (data not shown). The ratio of dead cells steadily increased with the extended incubation time. 36 hours post penning, I realized 17 out of 30 hits also committed apoptosis. Therefore, I exported the remaining cells for sequencing library preparation. Loss of 17 hits after 36 hours of antigen-specific stimulation could be due to AICD as observed during initial the subcloning of “GFP+” population, discussed in Section 5.1.1. Furthermore, the reason for general low viability during the single-cell antigen-specific stimulation experiment could derive from the FACS experiment performed a day earlier. Depending on the nozzle diameter used during a FACS experiment, it is possible to apply shear stress on the cells leading to lower viability [211-213]. Then, loading the pre-enriched cells into an OptoSelect™ chip can cause further stress as Optoelectro-Positioning™ (OEP™) during cell penning creates reactive oxygen species within the cells. Thus, application of FACS and OEP™ consecutively might have a detrimental effect on cell viability. One possible solution to improve the viability may be the use of magnetic-activated cell sorting (MACS) for isolation of antigen-reactive J7i-Library cells. MACS takes considerably less time to perform and gravity-driven isolation process do not apply any shear force to the cells [213]. In the literature, it was reported that the MACS outperforms FACS in terms of viability of the isolated cells with a cost of reduced purity [212-214]. However, in this pipeline implementation of MACS could be beneficial as cells could be sorted faster while being exposed to less stress. MACS and Lightning™ loading could be done at the same day, thus shortening the overall processing time of the pipeline. Reduced purity would not affect the outcome of the single-cell stimulation experiment, as there might be significantly more viable cells inside the OptoSelect™ chip with slightly more ratio of false positive cells. Besides high false positive cell ratio, one additional drawback of MACS pre-enrichment could be the activation of cells expressing CARs recognizing the antigen of interest before the initiation of single-cell antigen-specific stimulation experiment. Since, the magnetic beads used during the MACS pre-enrichment could potentially cause clustering of CARs during the enrichment process. Keeping the cells at 4 °C to minimize their metabolic activitiy during MACS pre-enrichment and subsequent Lightning™ loading may be taken as a precaution to hinder this effect.

Analysis of the time-lapse images of single-cell stimulation experiment revealed, that only two hits underwent cell division, again pointing towards the cellular stress caused by consecutive FACS and Lightning™ loading. Interestingly, one of the hits started reacting to the antigen-specific stimulation only after completing a cell division (data not shown). Only one of the daughter cell was observed to be reactive. This points towards that there might a competition between nanoS/MARt vectors for

establishment to nuclear matrix proteins. Only after the division, the nanoS/MARt vector with antigen-specific CAR received a chance to be established in the presumably newly formed matrix. It is possible that available sites for nanoS/MARt establishment on nuclear matrix proteins limits how many copies could be expressed by a single cell. For example, the cell may have hundreds of copies present inside the nucleus, but only a fraction of them could be expressed and subsequently sequenced as they are the ones that got established successfully. Indeed, number of unique productive scFv sequences identified in each barcode varied from 5 to 32 unique productive scFvs with a median of 14.5 per cell. With nearly a million reads, only 11 unique scFv sequences were identified in barcode 8. On the other hand, for barcode 5 around 50.000 reads were sequenced and 18 unique scFv sequences were identified. This data suggests that a read number as little as 50.000 is enough to identify unique scFv sequences. Thus, analysis of a million reads for the same barcode results in substantial sequencing depth that the identified 11 unique scFv sequences is highly likely to be the actual number. These results provides evidence for episomal establishment of nanoS/MARt vectors in low copy number, in line with what was observed with S/MAR containing Plasmid Episomal (pEPI) establishment in late 1990s [142].

During the sequencing analysis of the hits, I failed to align the sequences due to Oxford Nanopore's intrinsic 1% error rate. The errors manifest themselves as wrong base calling, or single nucleotide insertion/deletions, especially during sequencing of repetitive regions. False base calls can be compensated if they do not cause a premature stop codon. However, an in/del mutation shifts the whole ORF resulting in a completely different protein. The IMGT V-QUEST software offers couple of features that overcomes technical restriction posed by Nanopore technology. Firstly, it provides direct analysis of scFv sequences. The software is able to recognize and report the V_H, linker and V_L sequences from beginning to the end together with their most probable gene annotations for each scFv read. Secondly, it can recognize and correct the in/del mutations introduced by Oxford Nanopore sequencing. Introduction of V-QUEST into the pipeline with the mentioned features considerably accelerated the analysis and identification of possible hit scFv sequences.

In the barcodes that contained plasmid #1468, heavy and light chains of SCA431 were exclusively enriched in productive scFv sequences (Figure 4.4.3.1 F). The reason for presence of plasmid #1468 could be that it was the backbone used during library cloning and it is possible that the intact vector may spillover during library generation. Nevertheless, in 3 out of 4 barcodes without the plasmid #1468, I observed enrichment of certain scFv sequences and these scFv sequences were ordered for validation against CEACAM5 (Figure 4.4.3.1 E).

So far, scFv that was enriched in barcode 6 was cloned into the #272 pS/MARt backbone to be electroporated into J7i cells. Incubation of shocked cells with antigen-coupled beads did not result in reporter induction. However, CAR expression was detected only 20% of the electroporated cells. This could be the reason why the J7i-1475 cells did not react against the antigen. Even in the positive control sample #272, around 50% of the cells expressed the CAR and achieved a poor activation (4.4.4). The presence unmethylated CpG islands in 1.5kb long antibiotics resistance and bacterial origin of replication sequences in pS/MARt vectors might inhibit the episomal establishment of these sequences. Currently, all ordered scFv sequences are being cloned into lentiviral vectors to achieve higher CAR expression levels in J7i cells (performed by Alexandra Tuch). If these constructs induces CEACAM5-

specific stimulation of J7i cells, then the first proof-of-principle run of the pipeline could be concluded successfully. Challenging the cellular CAR library screening approach to identify scFvs against another antigen that has not been targeted with a CAR construct yet would be the logical next step.

5.4 Outlook

This project developed an alternative, novel screening platform for CAR isolation that accelerates identification of functional, antigen-specific CARs suitable for ACT. From start to the beginning, the pipeline enables *de novo* CAR isolation and subsequent validation within 6 weeks. I have performed the first proof-of-principle experiment and isolated candidate CARs that are in the process of functional validation. As a next step, frozen aliquots of the cellular CAR library could be challenged to identify *de novo* scFv sequences against an antigen of interest. By screening thawed aliquots, isolation process of functional CARs is shortened even further as there is no need for cloning a CAR library and subsequent generation of cellular CAR libraries.

If the generated cellular CAR library fails to result in functional CARs when screened against certain antigens, failure most possibly stems from the size and diversity of the generated CAR library. As mentioned before, it is possible to generate libraries with a larger sizes, thus diversities by optimization of scFv library generation and DH5α strain electroporation. Moreover, generation of scFv sublibraries facilitates further increment of the CAR library size. These improvements have potential the increase the size of the library by 10^2 to 10^3 fold. A library with such a size could be confidently used to screen for any antigen of interest.

Sequencing of 12 hits provided evidence for establishment of nanoS/MAR vectors in low copy numbers. In contrast to our hypothesis, if the enriched scFv sequences found in each barcode do not result in antigen recognition, the remaining scFvs can be cloned and screened in a high-throughput platform that encompasses use of automated, robotic systems. As mentioned before, 8 out of 12 hits contained the plasmid backbone #1468 that is used to clone plasmid CAR libraries. Observed spillover of *Mus musculus* derived SCA431 sequences into the library would not have an effect, if the cellular library is screened against any antigen but CEACAM5.

I have generated a naïve cellular CAR library with B cells isolated from 11 healthy donors. Besides naïve libraries, it is possible to personalize the cellular library screening approach by generation of plasmid CAR libraries with B cells isolated from cancer patients. Then, autologous cellular CAR T cell libraries could be constructed to be screened against patients' own tumor antigens. Presence of humoral responses against tumor associated antigens like, CEA and HER-2 has been reported in cancer patients [215-217]. Therefore, personalized cellular CAR libraries are expected to give rise to libraries with smaller sizes, but they may encompass a higher ratio of relevant, tumor antigen-specific scFvs.

6 References

1. World Health Organization. *Cancer*. 2022 [cited 2023 17.09.2023]; Available from: https://www.who.int/news-room/fact-sheets/detail/cancer.
2. Cancer, I.A.f.R.o. *Cancer Today*. 2023 [cited 2023 17.09.2023]; Available from: https://gco.iarc.fr/today/online-analysis-table?v=2020&mode=cancer&mode_population=continents&population=900&populations=900&key=asr&sex=0&cancer=39&type=0&statistic=5&prevalence=0&population_group=0&ages_group%5B%5D=0&ages_group%5B%5D=17&group_cancer=1&include_nmsc=0&include_nmsc_other=1#collapse-group-1-5.
3. Pavlova, N.N. and C.B. Thompson, *The Emerging Hallmarks of Cancer Metabolism.* Cell Metab, 2016. **23**(1): p. 27-47.
4. Hanahan, D. and R.A. Weinberg, *Hallmarks of cancer: the next generation.* Cell, 2011. **144**(5): p. 646-74.
5. Garcia-Fernandez, C., et al., *Cancer immunotherapies revisited: state of the art of conventional treatments and next-generation nanomedicines.* Cancer Gene Ther, 2021. **28**(9): p. 935-946.
6. Morrissey, K.M., et al., *Immunotherapy and Novel Combinations in Oncology: Current Landscape, Challenges, and Opportunities.* Clin Transl Sci, 2016. **9**(2): p. 89-104.
7. Kim, R., M. Emi, and K. Tanabe, *Cancer immunoediting from immune surveillance to immune escape.* Immunology, 2007. **121**(1): p. 1-14.
8. McCarthy, E.F., *The toxins of William B. Coley and the treatment of bone and soft-tissue sarcomas.* Iowa Orthop J, 2006. **26**: p. 154-8.
9. Galluzzi, L., et al., *Classification of current anticancer immunotherapies.* Oncotarget, 2014. **5**(24): p. 12472-508.
10. Huang, P.W. and J.W. Chang, *Immune checkpoint inhibitors win the 2018 Nobel Prize.* Biomed J, 2019. **42**(5): p. 299-306.
11. Pardoll, D.M., *The blockade of immune checkpoints in cancer immunotherapy.* Nat Rev Cancer, 2012. **12**(4): p. 252-64.
12. Sharma, P., et al., *Primary, Adaptive, and Acquired Resistance to Cancer Immunotherapy.* Cell, 2017. **168**(4): p. 707-723.
13. Okazaki, T., et al., *A rheostat for immune responses: the unique properties of PD-1 and their advantages for clinical application.* Nat Immunol, 2013. **14**(12): p. 1212-8.
14. Zou, W., J.D. Wolchok, and L. Chen, *PD-L1 (B7-H1) and PD-1 pathway blockade for cancer therapy: Mechanisms, response biomarkers, and combinations.* Sci Transl Med, 2016. **8**(328): p. 328rv4.
15. Wang, D., J. Bauersachs, and D. Berliner, *Immune Checkpoint Inhibitor Associated Myocarditis and Cardiomyopathy: A Translational Review.* Biology (Basel), 2023. **12**(3).
16. Garon, E.B., et al., *Pembrolizumab for the treatment of non-small-cell lung cancer.* N Engl J Med, 2015. **372**(21): p. 2018-28.
17. Hodi, F.S., et al., *Improved survival with ipilimumab in patients with metastatic melanoma.* N Engl J Med, 2010. **363**(8): p. 711-23.
18. Kalbasi, A. and A. Ribas, *Tumour-intrinsic resistance to immune checkpoint blockade.* Nat Rev Immunol, 2020. **20**(1): p. 25-39.
19. Palucka, K. and J. Banchereau, *Cancer immunotherapy via dendritic cells.* Nat Rev Cancer, 2012. **12**(4): p. 265-77.
20. Anassi, E. and U.A. Ndefo, *Sipuleucel-T (provenge) injection: the first immunotherapy agent (vaccine) for hormone-refractory prostate cancer.* P T, 2011. **36**(4): p. 197-202.
21. Higano, C.S., et al., *Integrated data from 2 randomized, double-blind, placebo-controlled, phase 3 trials of active cellular immunotherapy with sipuleucel-T in advanced prostate cancer.* Cancer, 2009. **115**(16): p. 3670-9.
22. Kreiter, S., et al., *Intranodal vaccination with naked antigen-encoding RNA elicits potent prophylactic and therapeutic antitumoral immunity.* Cancer Res, 2010. **70**(22): p. 9031-40.
23. Kreiter, S., et al., *Mutant MHC class II epitopes drive therapeutic immune responses to cancer.* Nature, 2015. **520**(7549): p. 692-6.
24. Phua, K.K., et al., *Intranasal mRNA nanoparticle vaccination induces prophylactic and therapeutic anti-tumor immunity.* Sci Rep, 2014. **4**: p. 5128.
25. He, Q., et al., *mRNA cancer vaccines: Advances, trends and challenges.* Acta Pharm Sin B, 2022. **12**(7): p. 2969-2989.

26. Abd-Aziz, N. and C.L. Poh, *Development of Peptide-Based Vaccines for Cancer.* J Oncol, 2022. **2022**: p. 9749363.
27. Tay, R.E., E.K. Richardson, and H.C. Toh, *Revisiting the role of CD4(+) T cells in cancer immunotherapy-new insights into old paradigms.* Cancer Gene Ther, 2021. **28**(1-2): p. 5-17.
28. Raval, R.R., et al., *Tumor immunology and cancer immunotherapy: summary of the 2013 SITC primer.* J Immunother Cancer, 2014. **2**: p. 14.
29. Houot, R., H. Kohrt, and R. Levy, *Boosting antibody-dependant cellular cytotoxicity against tumor cells with a CD137 stimulatory antibody.* Oncoimmunology, 2012. **1**(6): p. 957-958.
30. Lefebvre, M.L., et al., *Ex vivo-activated human macrophages kill chronic lymphocytic leukemia cells in the presence of rituximab: mechanism of antibody-dependent cellular cytotoxicity and impact of human serum.* J Immunother, 2006. **29**(4): p. 388-97.
31. Strohl, W.R., *Optimization of Fc-mediated effector functions of monoclonal antibodies.* Curr Opin Biotechnol, 2009. **20**(6): p. 685-91.
32. Grillo-Lopez, A.J., *Zevalin: the first radioimmunotherapy approved for the treatment of lymphoma.* Expert Rev Anticancer Ther, 2002. **2**(5): p. 485-93.
33. Macklis, R.M., *Iodine-131 tositumomab (Bexxar) in a radiation oncology environment.* Int J Radiat Oncol Biol Phys, 2006. **66**(2 Suppl): p. S30-4.
34. Gogia, P., et al., *Antibody-Drug Conjugates: A Review of Approved Drugs and Their Clinical Level of Evidence.* Cancers (Basel), 2023. **15**(15).
35. Fan, G., et al., *Bispecific antibodies and their applications.* J Hematol Oncol, 2015. **8**: p. 130.
36. Einsele, H., et al., *The BiTE (bispecific T-cell engager) platform: Development and future potential of a targeted immuno-oncology therapy across tumor types.* Cancer, 2020. **126**(14): p. 3192-3201.
37. Krishnamurthy, A. and A. Jimeno, *Bispecific antibodies for cancer therapy: A review.* Pharmacol Ther, 2018. **185**: p. 122-134.
38. d'Argouges, S., et al., *Combination of rituximab with blinatumomab (MT103/MEDI-538), a T cell-engaging CD19-/CD3-bispecific antibody, for highly efficient lysis of human B lymphoma cells.* Leuk Res, 2009. **33**(3): p. 465-73.
39. Gokbuget, N., et al., *Blinatumomab for minimal residual disease in adults with B-cell precursor acute lymphoblastic leukemia.* Blood, 2018. **131**(14): p. 1522-1531.
40. Rohaan, M.W., S. Wilgenhof, and J. Haanen, *Adoptive cellular therapies: the current landscape.* Virchows Arch, 2019. **474**(4): p. 449-461.
41. Rosenberg, S.A., et al., *Durable complete responses in heavily pretreated patients with metastatic melanoma using T-cell transfer immunotherapy.* Clin Cancer Res, 2011. **17**(13): p. 4550-7.
42. Besser, M.J., et al., *Adoptive transfer of tumor-infiltrating lymphocytes in patients with metastatic melanoma: intent-to-treat analysis and efficacy after failure to prior immunotherapies.* Clin Cancer Res, 2013. **19**(17): p. 4792-800.
43. Hiltensperger, M. and A.M. Krackhardt, *Current and future concepts for the generation and application of genetically engineered CAR-T and TCR-T cells.* Front Immunol, 2023. **14**: p. 1121030.
44. Maude, S.L., et al., *Chimeric antigen receptor T cells for sustained remissions in leukemia.* N Engl J Med, 2014. **371**(16): p. 1507-17.
45. Xin Yu, J., V.M. Hubbard-Lucey, and J. Tang, *The global pipeline of cell therapies for cancer.* Nat Rev Drug Discov, 2019. **18**(11): p. 821-822.
46. Rosenberg, S.A., et al., *Treatment of patients with metastatic melanoma with autologous tumor-infiltrating lymphocytes and interleukin 2.* J Natl Cancer Inst, 1994. **86**(15): p. 1159-66.
47. Andersen, R., et al., *Long-Lasting Complete Responses in Patients with Metastatic Melanoma after Adoptive Cell Therapy with Tumor-Infiltrating Lymphocytes and an Attenuated IL2 Regimen.* Clin Cancer Res, 2016. **22**(15): p. 3734-45.
48. Lee, H.J., et al., *Expansion of tumor-infiltrating lymphocytes and their potential for application as adoptive cell transfer therapy in human breast cancer.* Oncotarget, 2017. **8**(69): p. 113345-113359.
49. Andersen, R., et al., *T-cell Responses in the Microenvironment of Primary Renal Cell Carcinoma-Implications for Adoptive Cell Therapy.* Cancer Immunol Res, 2018. **6**(2): p. 222-235.
50. Stevanovic, S., et al., *Complete regression of metastatic cervical cancer after treatment with human papillomavirus-targeted tumor-infiltrating T cells.* J Clin Oncol, 2015. **33**(14): p. 1543-50.
51. Geukes Foppen, M.H., et al., *Tumor-infiltrating lymphocytes for the treatment of metastatic cancer.* Mol Oncol, 2015. **9**(10): p. 1918-35.
52. Rosenberg, S.A. and N.P. Restifo, *Adoptive cell transfer as personalized immunotherapy for human cancer.* Science, 2015. **348**(6230): p. 62-8.

53. Kessels, H.W., et al., *Immunotherapy through TCR gene transfer.* Nat Immunol, 2001. **2**(10): p. 957-61.
54. Morgan, R.A., et al., *Cancer regression in patients after transfer of genetically engineered lymphocytes.* Science, 2006. **314**(5796): p. 126-9.
55. Barrow, C., et al., *Tumor antigen expression in melanoma varies according to antigen and stage.* Clin Cancer Res, 2006. **12**(3 Pt 1): p. 764-71.
56. Chapuis, A.G., et al., *T cell receptor gene therapy targeting WT1 prevents acute myeloid leukemia relapse post-transplant.* Nat Med, 2019. **25**(7): p. 1064-1072.
57. Palmer, D.C., et al., *Effective tumor treatment targeting a melanoma/melanocyte-associated antigen triggers severe ocular autoimmunity.* Proc Natl Acad Sci U S A, 2008. **105**(23): p. 8061-6.
58. Morgan, R.A., et al., *Cancer regression and neurological toxicity following anti-MAGE-A3 TCR gene therapy.* J Immunother, 2013. **36**(2): p. 133-51.
59. Maher, J., *Immunotherapy of malignant disease using chimeric antigen receptor engrafted T cells.* ISRN Oncol, 2012. **2012**: p. 278093.
60. Eshhar, Z., et al., *Specific activation and targeting of cytotoxic lymphocytes through chimeric single chains consisting of antibody-binding domains and the gamma or zeta subunits of the immunoglobulin and T-cell receptors.* Proc Natl Acad Sci U S A, 1993. **90**(2): p. 720-4.
61. Lee, D.W., et al., *T cells expressing CD19 chimeric antigen receptors for acute lymphoblastic leukaemia in children and young adults: a phase 1 dose-escalation trial.* Lancet, 2015. **385**(9967): p. 517-528.
62. Porter, D.L., et al., *Chimeric antigen receptor T cells persist and induce sustained remissions in relapsed refractory chronic lymphocytic leukemia.* Sci Transl Med, 2015. **7**(303): p. 303ra139.
63. Chen, Y.J., B. Abila, and Y. Mostafa Kamel, *CAR-T: What Is Next?* Cancers (Basel), 2023. **15**(3).
64. Brentjens, R.J., et al., *CD19-targeted T cells rapidly induce molecular remissions in adults with chemotherapy-refractory acute lymphoblastic leukemia.* Sci Transl Med, 2013. **5**(177): p. 177ra38.
65. Lee, D.W., et al., *Current concepts in the diagnosis and management of cytokine release syndrome.* Blood, 2014. **124**(2): p. 188-95.
66. Le, R.Q., et al., *FDA Approval Summary: Tocilizumab for Treatment of Chimeric Antigen Receptor T Cell-Induced Severe or Life-Threatening Cytokine Release Syndrome.* Oncologist, 2018. **23**(8): p. 943-947.
67. Turtle, C.J., et al., *Immunotherapy of non-Hodgkin's lymphoma with a defined ratio of CD8+ and CD4+ CD19-specific chimeric antigen receptor-modified T cells.* Sci Transl Med, 2016. **8**(355): p. 355ra116.
68. Gross, G., T. Waks, and Z. Eshhar, *Expression of immunoglobulin-T-cell receptor chimeric molecules as functional receptors with antibody-type specificity.* Proc Natl Acad Sci U S A, 1989. **86**(24): p. 10024-8.
69. Hege, K.M., et al., *Safety, tumor trafficking and immunogenicity of chimeric antigen receptor (CAR)-T cells specific for TAG-72 in colorectal cancer.* J Immunother Cancer, 2017. **5**: p. 22.
70. Till, B.G., et al., *Adoptive immunotherapy for indolent non-Hodgkin lymphoma and mantle cell lymphoma using genetically modified autologous CD20-specific T cells.* Blood, 2008. **112**(6): p. 2261-71.
71. Hombach, A., et al., *Tumor-specific T cell activation by recombinant immunoreceptors: CD3 zeta signaling and CD28 costimulation are simultaneously required for efficient IL-2 secretion and can be integrated into one combined CD28/CD3 zeta signaling receptor molecule.* J Immunol, 2001. **167**(11): p. 6123-31.
72. Kowolik, C.M., et al., *CD28 costimulation provided through a CD19-specific chimeric antigen receptor enhances in vivo persistence and antitumor efficacy of adoptively transferred T cells.* Cancer Res, 2006. **66**(22): p. 10995-1004.
73. Melenhorst, J.J., et al., *Decade-long leukaemia remissions with persistence of CD4(+) CAR T cells.* Nature, 2022. **602**(7897): p. 503-509.
74. Park, J.H., et al., *Long-Term Follow-up of CD19 CAR Therapy in Acute Lymphoblastic Leukemia.* N Engl J Med, 2018. **378**(5): p. 449-459.
75. Kawalekar, O.U., et al., *Distinct Signaling of Coreceptors Regulates Specific Metabolism Pathways and Impacts Memory Development in CAR T Cells.* Immunity, 2016. **44**(2): p. 380-90.
76. Maude, S.L., et al., *Tisagenlecleucel in Children and Young Adults with B-Cell Lymphoblastic Leukemia.* N Engl J Med, 2018. **378**(5): p. 439-448.
77. Song, D.G., et al., *CD27 costimulation augments the survival and antitumor activity of redirected human T cells in vivo.* Blood, 2012. **119**(3): p. 696-706.
78. Guedan, S., et al., *ICOS-based chimeric antigen receptors program bipolar TH17/TH1 cells.* Blood, 2014. **124**(7): p. 1070-80.
79. Tan, J., et al., *Chimeric antigen receptors containing the OX40 signalling domain enhance the persistence of T cells even under repeated stimulation with multiple myeloma target cells.* J Hematol Oncol, 2022. **15**(1): p. 39.

80. Drent, E., et al., *Combined CD28 and 4-1BB Costimulation Potentiates Affinity-tuned Chimeric Antigen Receptor-engineered T Cells.* Clin Cancer Res, 2019. **25**(13): p. 4014-4025.
81. Zhong, X.S., et al., *Chimeric antigen receptors combining 4-1BB and CD28 signaling domains augment PI3kinase/AKT/Bcl-XL activation and CD8+ T cell-mediated tumor eradication.* Mol Ther, 2010. **18**(2): p. 413-20.
82. Ramos, C.A., et al., *In Vivo Fate and Activity of Second- versus Third-Generation CD19-Specific CAR-T Cells in B Cell Non-Hodgkin's Lymphomas.* Mol Ther, 2018. **26**(12): p. 2727-2737.
83. George, P., et al., *Third-generation anti-CD19 chimeric antigen receptor T-cells incorporating a TLR2 domain for relapsed or refractory B-cell lymphoma: a phase I clinical trial protocol (ENABLE).* BMJ Open, 2020. **10**(2): p. e034629.
84. Schubert, M.L., et al., *Treatment of patients with relapsed or refractory CD19+ lymphoid disease with T lymphocytes transduced by RV-SFG.CD19.CD28.4-1BBzeta retroviral vector: a unicentre phase I/II clinical trial protocol.* BMJ Open, 2019. **9**(5): p. e026644.
85. Hombach, A.A., et al., *Adoptive immunotherapy with redirected T cells produces CCR7- cells that are trapped in the periphery and benefit from combined CD28-OX40 costimulation.* Hum Gene Ther, 2013. **24**(3): p. 259-69.
86. Guercio, M., et al., *CD28.OX40 co-stimulatory combination is associated with long in vivo persistence and high activity of CAR.CD30 T-cells.* Haematologica, 2021. **106**(4): p. 987-999.
87. Chmielewski, M. and H. Abken, *TRUCKs: the fourth generation of CARs.* Expert Opin Biol Ther, 2015. **15**(8): p. 1145-54.
88. Kunert, A., et al., *Intra-tumoral production of IL18, but not IL12, by TCR-engineered T cells is non-toxic and counteracts immune evasion of solid tumors.* Oncoimmunology, 2017. **7**(1): p. e1378842.
89. Chmielewski, M. and H. Abken, *CAR T Cells Releasing IL-18 Convert to T-Bet(high) FoxO1(low) Effectors that Exhibit Augmented Activity against Advanced Solid Tumors.* Cell Rep, 2017. **21**(11): p. 3205-3219.
90. Chmielewski, M., et al., *IL-12 release by engineered T cells expressing chimeric antigen receptors can effectively Muster an antigen-independent macrophage response on tumor cells that have shut down tumor antigen expression.* Cancer Res, 2011. **71**(17): p. 5697-706.
91. June, C.H., et al., *Inhibition of tyrosine phosphorylation prevents T-cell receptor-mediated signal transduction.* Proc Natl Acad Sci U S A, 1990. **87**(19): p. 7722-6.
92. Love, P.E. and S.M. Hayes, *ITAM-mediated signaling by the T-cell antigen receptor.* Cold Spring Harb Perspect Biol, 2010. **2**(6): p. a002485.
93. Samelson, L.E., et al., *Antigen activation of murine T cells induces tyrosine phosphorylation of a polypeptide associated with the T cell antigen receptor.* Cell, 1986. **46**(7): p. 1083-90.
94. Janeway CA Jr, T.P., Walport M, et al., *Janeway's Immunobiology*. 2001, Garland Science: New York.
95. Boomer, J.S. and J.M. Green, *An enigmatic tail of CD28 signaling.* Cold Spring Harb Perspect Biol, 2010. **2**(8): p. a002436.
96. Esensten, J.H., et al., *CD28 Costimulation: From Mechanism to Therapy.* Immunity, 2016. **44**(5): p. 973-88.
97. Gramaglia, I., et al., *The OX40 costimulatory receptor determines the development of CD4 memory by regulating primary clonal expansion.* J Immunol, 2000. **165**(6): p. 3043-50.
98. So, T., et al., *Signals from OX40 regulate nuclear factor of activated T cells c1 and T cell helper 2 lineage commitment.* Proc Natl Acad Sci U S A, 2006. **103**(10): p. 3740-5.
99. Kawamata, S., et al., *Activation of OX40 signal transduction pathways leads to tumor necrosis factor receptor-associated factor (TRAF) 2- and TRAF5-mediated NF-kappaB activation.* J Biol Chem, 1998. **273**(10): p. 5808-14.
100. Jhunjhunwala, S., C. Hammer, and L. Delamarre, *Antigen presentation in cancer: insights into tumour immunogenicity and immune evasion.* Nat Rev Cancer, 2021. **21**(5): p. 298-312.
101. Simpson, A.J., et al., *Cancer/testis antigens, gametogenesis and cancer.* Nat Rev Cancer, 2005. **5**(8): p. 615-25.
102. Kingwell, K., *T cell receptor therapeutics hit the immuno-oncology stage.* Nat Rev Drug Discov, 2022. **21**(5): p. 321-323.
103. Parkhurst, M.R., et al., *T cells targeting carcinoembryonic antigen can mediate regression of metastatic colorectal cancer but induce severe transient colitis.* Mol Ther, 2011. **19**(3): p. 620-6.
104. Swain, S.M., M. Shastry, and E. Hamilton, *Targeting HER2-positive breast cancer: advances and future directions.* Nat Rev Drug Discov, 2023. **22**(2): p. 101-126.
105. Feng, K., et al., *Phase I study of chimeric antigen receptor modified T cells in treating HER2-positive advanced biliary tract cancers and pancreatic cancers.* Protein Cell, 2018. **9**(10): p. 838-847.

106. Zhang, C., et al., *Phase I Escalating-Dose Trial of CAR-T Therapy Targeting CEA(+) Metastatic Colorectal Cancers.* Mol Ther, 2017. **25**(5): p. 1248-1258.
107. Hu, Z., P.A. Ott, and C.J. Wu, *Towards personalized, tumour-specific, therapeutic vaccines for cancer.* Nat Rev Immunol, 2018. **18**(3): p. 168-182.
108. Xie, N., et al., *Neoantigens: promising targets for cancer therapy.* Signal Transduct Target Ther, 2023. **8**(1): p. 9.
109. Majzner, R.G. and C.L. Mackall, *Tumor Antigen Escape from CAR T-cell Therapy.* Cancer Discov, 2018. **8**(10): p. 1219-1226.
110. Cohen, A.D., et al., *B cell maturation antigen-specific CAR T cells are clinically active in multiple myeloma.* J Clin Invest, 2019. **129**(6): p. 2210-2221.
111. Furqan, F. and N.N. Shah, *Bispecific CAR T-cells for B-cell Malignancies.* Expert Opin Biol Ther, 2022. **22**(8): p. 1005-1015.
112. Hossain, N., et al., *Phase I Experience with a Bi-Specific CAR Targeting CD19 and CD22 in Adults with B-Cell Malignancies.* Blood, 2018. **132**(Supplement 1): p. 490-490.
113. Dai, H., et al., *Bispecific CAR-T cells targeting both CD19 and CD22 for therapy of adults with relapsed or refractory B cell acute lymphoblastic leukemia.* J Hematol Oncol, 2020. **13**(1): p. 30.
114. Whilding, L.M., et al., *CAR T-Cells Targeting the Integrin alphavbeta6 and Co-Expressing the Chemokine Receptor CXCR2 Demonstrate Enhanced Homing and Efficacy against Several Solid Malignancies.* Cancers (Basel), 2019. **11**(5).
115. Caruana, I., et al., *Heparanase promotes tumor infiltration and antitumor activity of CAR-redirected T lymphocytes.* Nat Med, 2015. **21**(5): p. 524-9.
116. Sterner, R.C. and R.M. Sterner, *CAR-T cell therapy: current limitations and potential strategies.* Blood Cancer J, 2021. **11**(4): p. 69.
117. Grosser, R., et al., *Combination Immunotherapy with CAR T Cells and Checkpoint Blockade for the Treatment of Solid Tumors.* Cancer Cell, 2019. **36**(5): p. 471-482.
118. Adusumilli, P.S., et al., *A Phase I Trial of Regional Mesothelin-Targeted CAR T-cell Therapy in Patients with Malignant Pleural Disease, in Combination with the Anti-PD-1 Agent Pembrolizumab.* Cancer Discov, 2021. **11**(11): p. 2748-2763.
119. Yan, T., L. Zhu, and J. Chen, *Current advances and challenges in CAR T-Cell therapy for solid tumors: tumor-associated antigens and the tumor microenvironment.* Exp Hematol Oncol, 2023. **12**(1): p. 14.
120. Ajina, A. and J. Maher, *Strategies to Address Chimeric Antigen Receptor Tonic Signaling.* Mol Cancer Ther, 2018. **17**(9): p. 1795-1815.
121. Frigault, M.J., et al., *Identification of chimeric antigen receptors that mediate constitutive or inducible proliferation of T cells.* Cancer Immunol Res, 2015. **3**(4): p. 356-67.
122. Chen, J., et al., *Tuning charge density of chimeric antigen receptor optimizes tonic signaling and CAR-T cell fitness.* Cell Res, 2023. **33**(5): p. 341-354.
123. Wang, V., et al., *Systematic Review on CAR-T Cell Clinical Trials Up to 2022: Academic Center Input.* Cancers (Basel), 2023. **15**(4).
124. McCafferty, J., et al., *Phage antibodies: filamentous phage displaying antibody variable domains.* Nature, 1990. **348**(6301): p. 552-4.
125. Lonberg, N., *Human antibodies from transgenic animals.* Nat Biotechnol, 2005. **23**(9): p. 1117-25.
126. Lonberg, N., et al., *Antigen-specific human antibodies from mice comprising four distinct genetic modifications.* Nature, 1994. **368**(6474): p. 856-9.
127. Kohler, G. and C. Milstein, *Continuous cultures of fused cells secreting antibody of predefined specificity.* Nature, 1975. **256**(5517): p. 495-7.
128. Smith, G.P., *Filamentous fusion phage: novel expression vectors that display cloned antigens on the virion surface.* Science, 1985. **228**(4705): p. 1315-7.
129. Shan, D., et al., *Characterization of scFv-Ig constructs generated from the anti-CD20 mAb 1F5 using linker peptides of varying lengths.* J Immunol, 1999. **162**(11): p. 6589-95.
130. Marks, J.D., et al., *By-passing immunization. Human antibodies from V-gene libraries displayed on phage.* J Mol Biol, 1991. **222**(3): p. 581-97.
131. Schirrmann, T. and M. Hust, *Construction of human antibody gene libraries and selection of antibodies by phage display.* Methods Mol Biol, 2010. **651**: p. 177-209.
132. Smith, E.L., et al., *Development and Evaluation of an Optimal Human Single-Chain Variable Fragment-Derived BCMA-Targeted CAR T Cell Vector.* Mol Ther, 2018. **26**(6): p. 1447-1456.
133. Smith, E.L., et al., *GPRC5D is a target for the immunotherapy of multiple myeloma with rationally designed CAR T cells.* Sci Transl Med, 2019. **11**(485).

134. Mailankody, S., et al., *GPRC5D-Targeted CAR T Cells for Myeloma.* N Engl J Med, 2022. **387**(13): p. 1196-1206.
135. Mailankody, S., et al., *JCARH125, Anti-BCMA CAR T-cell Therapy for Relapsed/Refractory Multiple Myeloma: Initial Proof of Concept Results from a Phase 1/2 Multicenter Study (EVOLVE).* Blood, 2018. **132**(Supplement 1): p. 957-957.
136. Ran, T., et al., *Cost of decentralized CAR T-cell production in an academic nonprofit setting.* Int J Cancer, 2020. **147**(12): p. 3438-3445.
137. Kebriaei, P., et al., *Phase I trials using Sleeping Beauty to generate CD19-specific CAR T cells.* J Clin Invest, 2016. **126**(9): p. 3363-76.
138. Bishop, D.C., et al., *Development of CAR T-cell lymphoma in 2 of 10 patients effectively treated with piggyBac-modified CD19 CAR T cells.* Blood, 2021. **138**(16): p. 1504-1509.
139. Beatty, G.L., et al., *Mesothelin-specific chimeric antigen receptor mRNA-engineered T cells induce anti-tumor activity in solid malignancies.* Cancer Immunol Res, 2014. **2**(2): p. 112-20.
140. Bozza, M., et al., *Novel Non-integrating DNA Nano-S/MAR Vectors Restore Gene Function in Isogenic Patient-Derived Pancreatic Tumor Models.* Mol Ther Methods Clin Dev, 2020. **17**: p. 957-968.
141. Bozza, M., et al., *A nonviral, nonintegrating DNA nanovector platform for the safe, rapid, and persistent manufacture of recombinant T cells.* Sci Adv, 2021. **7**(16).
142. Piechaczek, C., et al., *A vector based on the SV40 origin of replication and chromosomal S/MARs replicates episomally in CHO cells.* Nucleic Acids Res, 1999. **27**(2): p. 426-8.
143. Luke, J., et al., *Improved antibiotic-free DNA vaccine vectors utilizing a novel RNA based plasmid selection system.* Vaccine, 2009. **27**(46): p. 6454-9.
144. Zhou, W.M., et al., *Microfluidics applications for high-throughput single cell sequencing.* J Nanobiotechnology, 2021. **19**(1): p. 312.
145. Gerard, A., et al., *High-throughput single-cell activity-based screening and sequencing of antibodies using droplet microfluidics.* Nat Biotechnol, 2020. **38**(6): p. 715-721.
146. Ng, A.H.C., et al., *MATE-Seq: microfluidic antigen-TCR engagement sequencing.* Lab Chip, 2019. **19**(18): p. 3011-3021.
147. Segaliny, A.I., et al., *Functional TCR T cell screening using single-cell droplet microfluidics.* Lab Chip, 2018. **18**(24): p. 3733-3749.
148. Lights, B., *LIGHTNING™ PLATFORM Training Manual*. 2019.
149. Mullen, T.E., et al., *Accelerated antibody discovery targeting the SARS-CoV-2 spike protein for COVID-19 therapeutic potential.* Antib Ther, 2021. **4**(3): p. 185-196.
150. Zost, S.J., et al., *Rapid isolation and profiling of a diverse panel of human monoclonal antibodies targeting the SARS-CoV-2 spike protein.* Nat Med, 2020. **26**(9): p. 1422-1427.
151. Pansri, P., et al., *A compact phage display human scFv library for selection of antibodies to a wide variety of antigens.* BMC Biotechnol, 2009. **9**: p. 6.
152. Hemadou, A., et al., *Pacific Biosciences Sequencing and IMGT/HighV-QUEST Analysis of Full-Length Single Chain Fragment Variable from an In Vivo Selected Phage-Display Combinatorial Library.* Front Immunol, 2017. **8**: p. 1796.
153. Chmielewski, M. and H. Abken, *CAR T cells transform to trucks: chimeric antigen receptor-redirected T cells engineered to deliver inducible IL-12 modulate the tumour stroma to combat cancer.* Cancer Immunol Immunother, 2012. **61**(8): p. 1269-77.
154. IMGT. *IMGT Repertoire (IG and TR)*. Proteins and alleles 2023 [cited 2023 08.10.23]; Available from: https://www.imgt.org/IMGTrepertoire/Proteins/.
155. MaxCyte. *Processing Assemblies*. Scalability with a Range of Processing Assemblies 2023 [cited 2023 07.10.23]; Available from: https://maxcyte.com/processing-assemblies/.
156. Abraham, R.T. and A. Weiss, *Jurkat T cells and development of the T-cell receptor signalling paradigm.* Nat Rev Immunol, 2004. **4**(4): p. 301-8.
157. Crabtree, G.R. and N.A. Clipstone, *Signal transmission between the plasma membrane and nucleus of T lymphocytes.* Annu Rev Biochem, 1994. **63**: p. 1045-83.
158. Northrop, J.P., K.S. Ullman, and G.R. Crabtree, *Characterization of the nuclear and cytoplasmic components of the lymphoid-specific nuclear factor of activated T cells (NF-AT) complex.* J Biol Chem, 1993. **268**(4): p. 2917-23.
159. Hooijberg, E., et al., *NFAT-controlled expression of GFP permits visualization and isolation of antigen-stimulated primary human T cells.* Blood, 2000. **96**(2): p. 459-66.

160. Li, Y., et al., *High-Throughput Screening of Functional Neo-Antigens and Their Specific T-Cell Receptors via the Jurkat Reporter System Combined with Droplet Microfluidics.* Anal Chem, 2023. **95**(25): p. 9697-9705.
161. Wang, S., et al., *High-Throughput Functional Screening of Antigen-Specific T Cells Based on Droplet Microfluidics at a Single-Cell Level.* Anal Chem, 2022. **94**(2): p. 918-926.
162. Ponomarev, V., et al., *Imaging TCR-dependent NFAT-mediated T-cell activation with positron emission tomography in vivo.* Neoplasia, 2001. **3**(6): p. 480-8.
163. Altvater, B., et al., *CAR T cells as microphar macies against solid cancers: Combining effector T-cell mediated cell death with vascular targeting in a one-step engineering process.* Cancer Gene Ther, 2023.
164. Reichenbach, P., et al., *A lentiviral vector for the production of T cells with an inducible transgene and a constitutively expressed tumour-targeting receptor.* Nat Biomed Eng, 2023. **7**(9): p. 1063-1080.
165. Zhang, W., et al., *Cellular Ca(2+)-Responding Nanoluciferase Reporter Gene System Directed by Tandemly Repeated Pseudo-palindromic NFAT-Response Elements.* Methods Mol Biol, 2019. **1929**: p. 95-109.
166. Jutz, S., et al., *A cellular platform for the evaluation of immune checkpoint molecules.* Oncotarget, 2017. **8**(39): p. 64892-64906.
167. Kuri, P., et al., *A high-sensitivity bi-directional reporter to monitor NF-kappaB activity in cell culture and zebrafish in real time.* J Cell Sci, 2017. **130**(3): p. 648-657.
168. Humeniuk, P., et al., *Generation of a Jurkat-based fluorescent reporter cell line to evaluate lipid antigen interaction with the human iNKT cell receptor.* Sci Rep, 2019. **9**(1): p. 7426.
169. Jutz, S., et al., *Assessment of costimulation and coinhibition in a triple parameter T cell reporter line: Simultaneous measurement of NF-kappaB, NFAT and AP-1.* J Immunol Methods, 2016. **430**: p. 10-20.
170. Rosskopf, S., et al., *A Jurkat 76 based triple parameter reporter system to evaluate TCR functions and adoptive T cell strategies.* Oncotarget, 2018. **9**(25): p. 17608-17619.
171. Lawrence, C.P. and S.C. Chow, *FADD deficiency sensitises Jurkat T cells to TNF-alpha-dependent necrosis during activation-induced cell death.* FEBS Lett, 2005. **579**(28): p. 6465-72.
172. Cabrera, A., et al., *The sound of silence: Transgene silencing in mammalian cell engineering.* Cell Syst, 2022. **13**(12): p. 950-973.
173. Li, W., et al., *Chimeric Antigen Receptor Designed to Prevent Ubiquitination and Downregulation Showed Durable Antitumor Efficacy.* Immunity, 2020. **53**(2): p. 456-470 e6.
174. Eyquem, J., et al., *Targeting a CAR to the TRAC locus with CRISPR/Cas9 enhances tumour rejection.* Nature, 2017. **543**(7643): p. 113-117.
175. Walker, A.J., et al., *Tumor Antigen and Receptor Densities Regulate Efficacy of a Chimeric Antigen Receptor Targeting Anaplastic Lymphoma Kinase.* Mol Ther, 2017. **25**(9): p. 2189-2201.
176. Caruso, H.G., et al., *Tuning Sensitivity of CAR to EGFR Density Limits Recognition of Normal Tissue While Maintaining Potent Antitumor Activity.* Cancer Res, 2015. **75**(17): p. 3505-18.
177. Harris, D.T., et al., *Comparison of T Cell Activities Mediated by Human TCRs and CARs That Use the Same Recognition Domains.* J Immunol, 2018. **200**(3): p. 1088-1100.
178. Mirkovitch, J., M.E. Mirault, and U.K. Laemmli, *Organization of the higher-order chromatin loop: specific DNA attachment sites on nuclear scaffold.* Cell, 1984. **39**(1): p. 223-32.
179. Jenke, A.C., et al., *Nuclear scaffold/matrix attached region modules linked to a transcription unit are sufficient for replication and maintenance of a mammalian episome.* Proc Natl Acad Sci U S A, 2004. **101**(31): p. 11322-7.
180. Testi, R., J.H. Phillips, and L.L. Lanier, *Leu 23 induction as an early marker of functional CD3/T cell antigen receptor triggering. Requirement for receptor cross-linking, prolonged elevation of intracellular [Ca++] and stimulation of protein kinase C.* J Immunol, 1989. **142**(6): p. 1854-60.
181. Gomes-Silva, D., et al., *Tonic 4-1BB Costimulation in Chimeric Antigen Receptors Impedes T Cell Survival and Is Vector-Dependent.* Cell Rep, 2017. **21**(1): p. 17-26.
182. Long, A.H., et al., *4-1BB costimulation ameliorates T cell exhaustion induced by tonic signaling of chimeric antigen receptors.* Nat Med, 2015. **21**(6): p. 581-90.
183. Guedan, S., et al., *Enhancing CAR T cell persistence through ICOS and 4-1BB costimulation.* JCI Insight, 2018. **3**(1).
184. Lynn, R.C., et al., *c-Jun overexpression in CAR T cells induces exhaustion resistance.* Nature, 2019. **576**(7786): p. 293-300.
185. Rad, S.M.A., et al., *Promoter choice: Who should drive the CAR in T cells?* PLoS One, 2020. **15**(7): p. e0232915.

186. Chicaybam, L., et al., *An Efficient Electroporation Protocol for the Genetic Modification of Mammalian Cells.* Front Bioeng Biotechnol, 2016. **4**: p. 99.
187. Chicaybam, L., et al., *An efficient low cost method for gene transfer to T lymphocytes.* PLoS One, 2013. **8**(3): p. e60298.
188. Zhang, Z., et al., *Optimized DNA electroporation for primary human T cell engineering.* BMC Biotechnol, 2018. **18**(1): p. 4.
189. Jordan, E.T., et al., *Optimizing electroporation conditions in primary and other difficult-to-transfect cells.* J Biomol Tech, 2008. **19**(5): p. 328-34.
190. Fisher, T. *Electroporation Support—Getting Started*. System and Kit Components 2023 [cited 2023 07.10.23]; Available from: https://www.thermofisher.com/de/en/home/technical-resources/technical-reference-library/transfection-support-center/electroporation-support/electroporation-support-getting-started.html#:~:text=The%20Neon%C2%AE%20device%20uses%20a%20square%20pulse%20wave%3B,ms%20and%20the%20pulse%20number%20ranges%20from%201%E2%80%9310.
191. Fisher, T., *Jurkat microporation*, in *Electroporation parameters*. 2023.
192. Djuzenova, C.S., et al., *Effect of medium conductivity and composition on the uptake of propidium iodide into electropermeabilized myeloma cells.* Biochim Biophys Acta, 1996. **1284**(2): p. 143-52.
193. Pucihar, G., et al., *The influence of medium conductivity on electropermeabilization and survival of cells in vitro.* Bioelectrochemistry, 2001. **54**(2): p. 107-15.
194. Ruzgys, P., et al., *Effect of electroporation medium conductivity on exogenous molecule transfer to cells in vitro.* Sci Rep, 2019. **9**(1): p. 1436.
195. Eagle, H., *The minimum vitamin requirements of the L and HeLa cells in tissue culture, the production of specific vitamin deficiencies, and their cure.* J Exp Med, 1955. **102**(5): p. 595-600.
196. Wang, Y., et al., *Calcium regulation of T cell metabolism.* Curr Opin Physiol, 2020. **17**: p. 207-223.
197. Hemmi, H., et al., *A Toll-like receptor recognizes bacterial DNA.* Nature, 2000. **408**(6813): p. 740-5.
198. Decout, A., et al., *The cGAS-STING pathway as a therapeutic target in inflammatory diseases.* Nat Rev Immunol, 2021. **21**(9): p. 548-569.
199. Okamoto, T., et al., *Optimal construction of non-immune scFv phage display libraries from mouse bone marrow and spleen established to select specific scFvs efficiently binding to antigen.* Biochem Biophys Res Commun, 2004. **323**(2): p. 583-91.
200. Haryadi, R., et al., *Optimization of heavy chain and light chain signal peptides for high level expression of therapeutic antibodies in CHO cells.* PLoS One, 2015. **10**(2): p. e0116878.
201. IMGT. *IMGT Scientific chart*. IMGT functionality 2023 [cited 2023 08.1023]; Available from: https://www.imgt.org/IMGTScientificChart/SequenceDescription/IMGTfunctionality.html#orf.
202. Merck. *DNA Oligonucleotide Synthesis*. YIELD 2023 [cited 2023 08.10.2023]; Available from: https://www.sigmaaldrich.com/DE/en/technical-documents/technical-article/genomics/pcr/dna-oligonucleotide-synthesis.
203. Merck. *Oligonucleotide Purification*. METHODS 2023 [cited 2023 08.10.23]; Available from: https://www.sigmaaldrich.com/DE/en/technical-documents/technical-article/genomics/dna-and-rna-purification/best-purification.
204. Fisher, T. *Standard DNA oligonucleotides*. Choosing the right DNA oligos for your application 2023 [cited 2023 08.10.2023]; Available from: https://www.thermofisher.com/de/de/home/life-science/oligonucleotides-primers-probes-genes/custom-dna-oligos/standard-oligos.html#:~:text=The%20table%20is%20designed%20to%20help%20you%20choose,but%20gives%20excellent%20purity%20up%20to%2055%20bases.
205. Fisher, T. *How to Choose the Best Oligonucleotide Purification Method for Your Research*. High-performance liquid chromatography (HPLC) purification 2023 [cited 2023 10.08.23]; Available from: https://www.thermofisher.com/de/de/home/brands/thermo-scientific/molecular-biology/molecular-biology-learning-center/molecular-biology-resource-library/spotlight-articles/oligonucleotide-purification-methods.html#ref.
206. Kim, S., et al., *Generation, Diversity Determination, and Application to Antibody Selection of a Human Naive Fab Library.* Mol Cells, 2017. **40**(9): p. 655-666.
207. Kugler, J., et al., *Generation and analysis of the improved human HAL9/10 antibody phage display libraries.* BMC Biotechnol, 2015. **15**: p. 10.
208. Schwimmer, L.J., et al., *Discovery of diverse and functional antibodies from large human repertoire antibody libraries.* J Immunol Methods, 2013. **391**(1-2): p. 60-71.

209. Valadon, P., et al., *ALTHEA Gold Libraries: antibody libraries for therapeutic antibody discovery.* MAbs, 2019. **11**(3): p. 516-531.
210. Schofield, D.J., et al., *Application of phage display to high throughput antibody generation and characterization.* Genome Biol, 2007. **8**(11): p. R254.
211. Durack, G., in *Emerging Tools for Single-Cell Analysis: Advances in Optical Measurement Technologies*, J.P.R. Gary Durack, Editor. 8 May 2000, 8 May 2000.
212. Pan, J. and J. Wan, *Methodological comparison of FACS and MACS isolation of enriched microglia and astrocytes from mouse brain.* J Immunol Methods, 2020. **486**: p. 112834.
213. Sutermaster, B.A. and E.M. Darling, *Considerations for high-yield, high-throughput cell enrichment: fluorescence versus magnetic sorting.* Sci Rep, 2019. **9**(1): p. 227.
214. Li, Q., et al., *Comparison of the sorting efficiency and influence on cell function between the sterile flow cytometry and immunomagnetic bead purification methods.* Prep Biochem Biotechnol, 2013. **43**(2): p. 197-206.
215. Disis, M.L., et al., *Immunity to the HER-2/neu oncogenic protein.* Ciba Found Symp, 1994. **187**: p. 198-207; discussion 207-11.
216. Haidopoulos, D., et al., *Circulating anti-CEA antibodies in the sera of patients with breast cancer.* Eur J Surg Oncol, 2000. **26**(8): p. 742-6.
217. Pupa, S.M., et al., *Antibody response against the c-erbB-2 oncoprotein in breast carcinoma patients.* Cancer Res, 1993. **53**(24): p. 5864-6.

7 Appendix

7.1 Supplementary data

7.1.1 Supplementary Figure 1: FACS/Flow Cytometry gating strategy

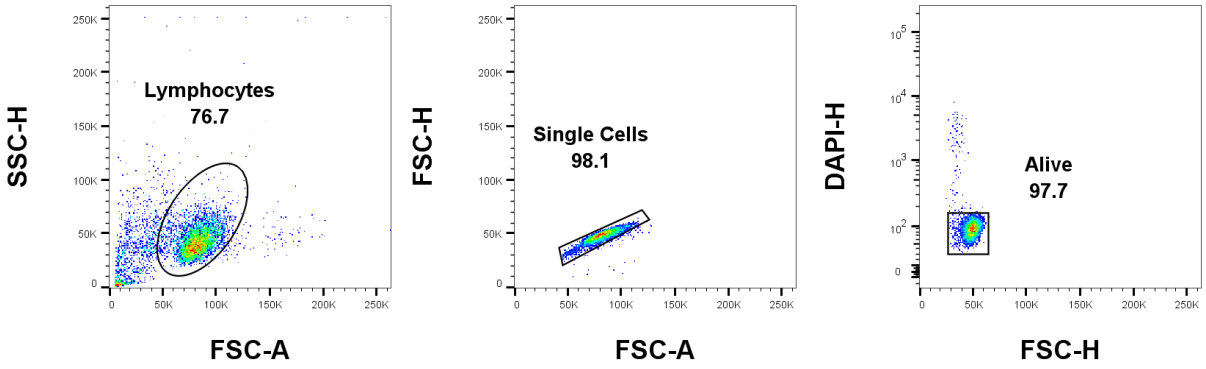

Supplementary Figure 1: FACS/Flow Cytometry gating strategy for alive cells. Jurkat cells are selected and annotated as “Lymphocytes”. Only the single cells were considered for further analysis. Cells were stained with DAPI for dead cell exclusion. In the final plot, DAPI- alive population was gated.

7.1.2 Supplementary Figure 2: Characteristics of reporter GFP+ LightningTM exports

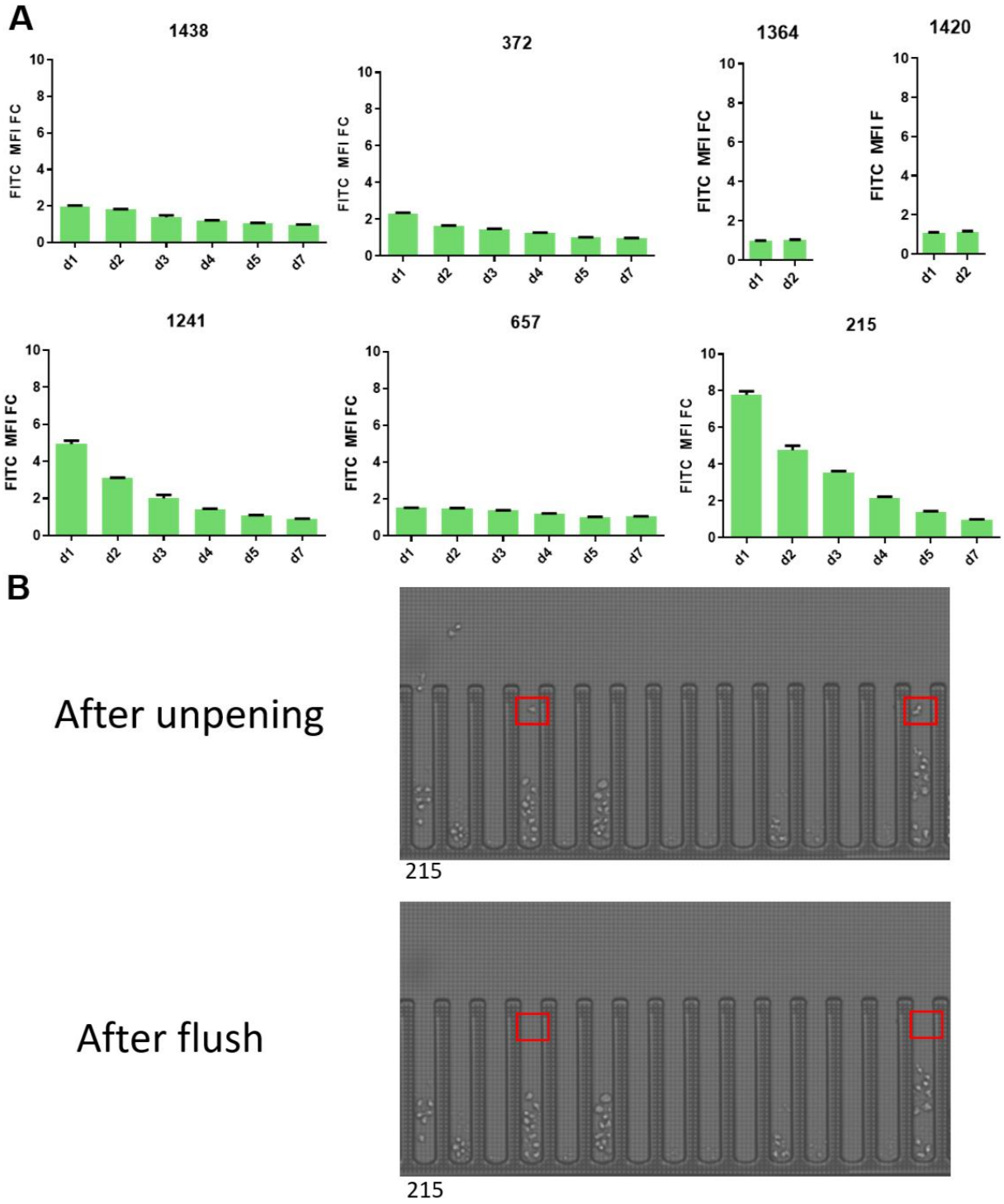

Supplementary Figure 2: Characterization of clone 215. A: Exports from respective Optoselect™ pens were stimulated with 5 µg/ml PHA overnight. After 1 day of stimulation, PHA was washed and cells were allowed to cool down. FITC MFI FC of each clone is shown for 7 days. **B:** During the export of 215, the single-cell derived colony was contaminated cells from 212 and 201. These two contaminant clones did show no activation during PHA treatment.

7.1.3 Supplementary Figure 3: qPCR experiments

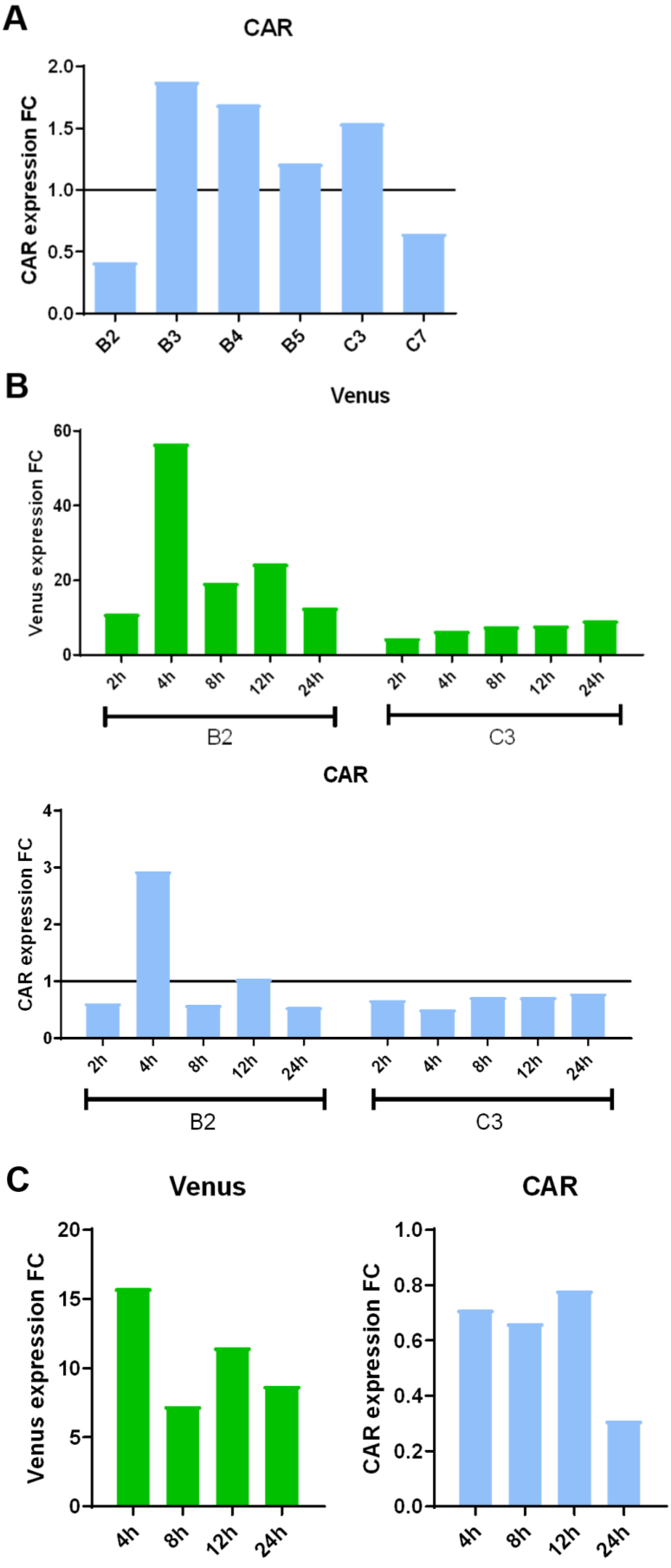

Supplementary Figure 3: qPCRs and their analysis were done as explained in section 4.3.1 and 3.3.6. **A:** Initial results of qPCR experiment for CAR expression for Lightning J7i-53 exports 24 hours after antigen-coupled bead stimulation. Venus expression was not analyzed. **B:** qPCR results of 2 Lightning exports B2 and C3 are depicted. The expression of CAR and Venus was quantified for earlier time points 2,4,8,12 and 24 hours after bead stimulation. **C:** qPCR for CAR and Venus expression was repeated for antigen-coupled bead stimulated 7i-320 cells. CAR and Venus expression were quantified 4,8,12 and 24 hours after the start of antigen-specific stimulation.

7.1.4 Supplementary Figure 4: Example amplicon sizes of recovered CARs from Lightning exports

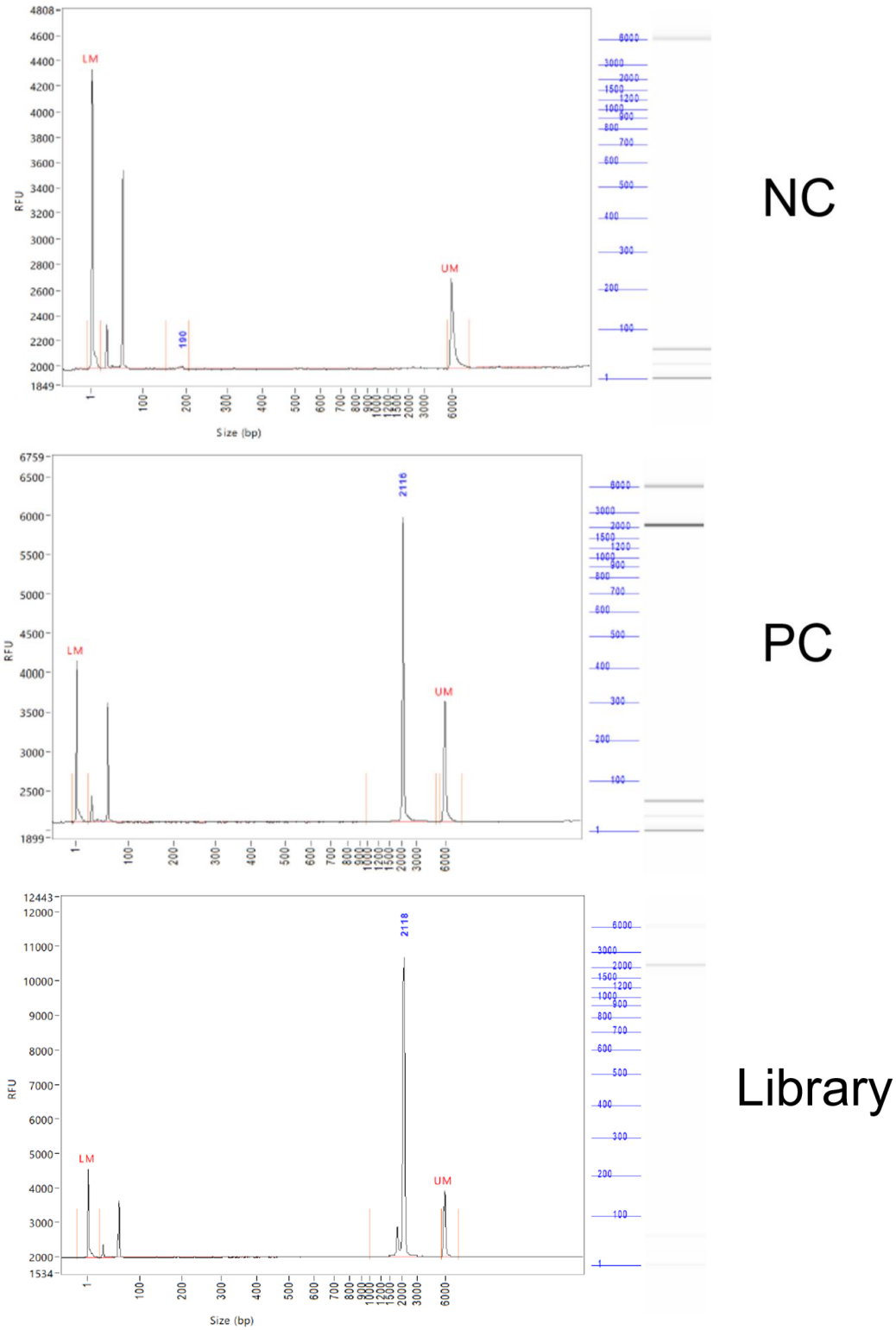

Supplementary Figure 4: Fragment Analyzer results of amplified CARs during single cell CAR recovery experiment. Hits obtained from the Lightning™ were exported into the lysis buffer and first and second strand cDNA synthesis were performed. Products from second strand synthesis was fed

into PCR for CAR sequences. After the first 30 cycles of amplification, PCR products were cleaned-up and run in a Fragment Analyzer to check the size of the amplicons.

7.1.5 Supplementary Figure 5: Sequencing quality, alignment and V gene annotations

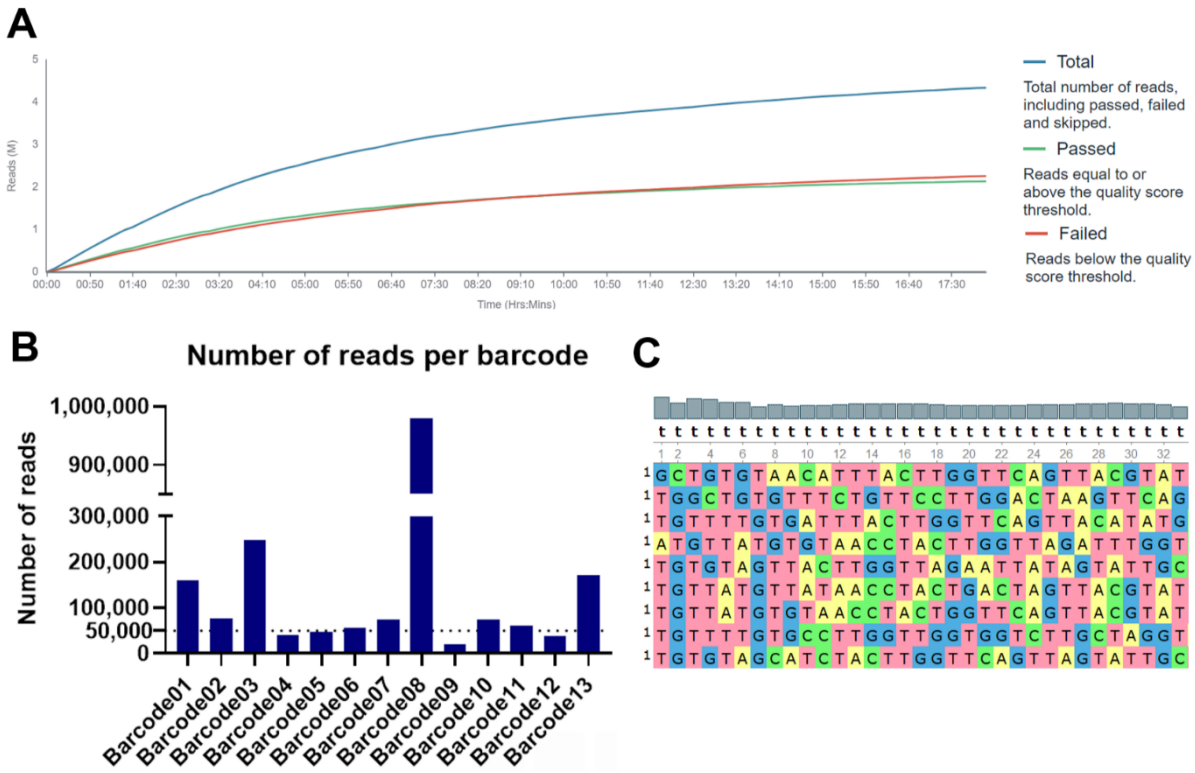

D

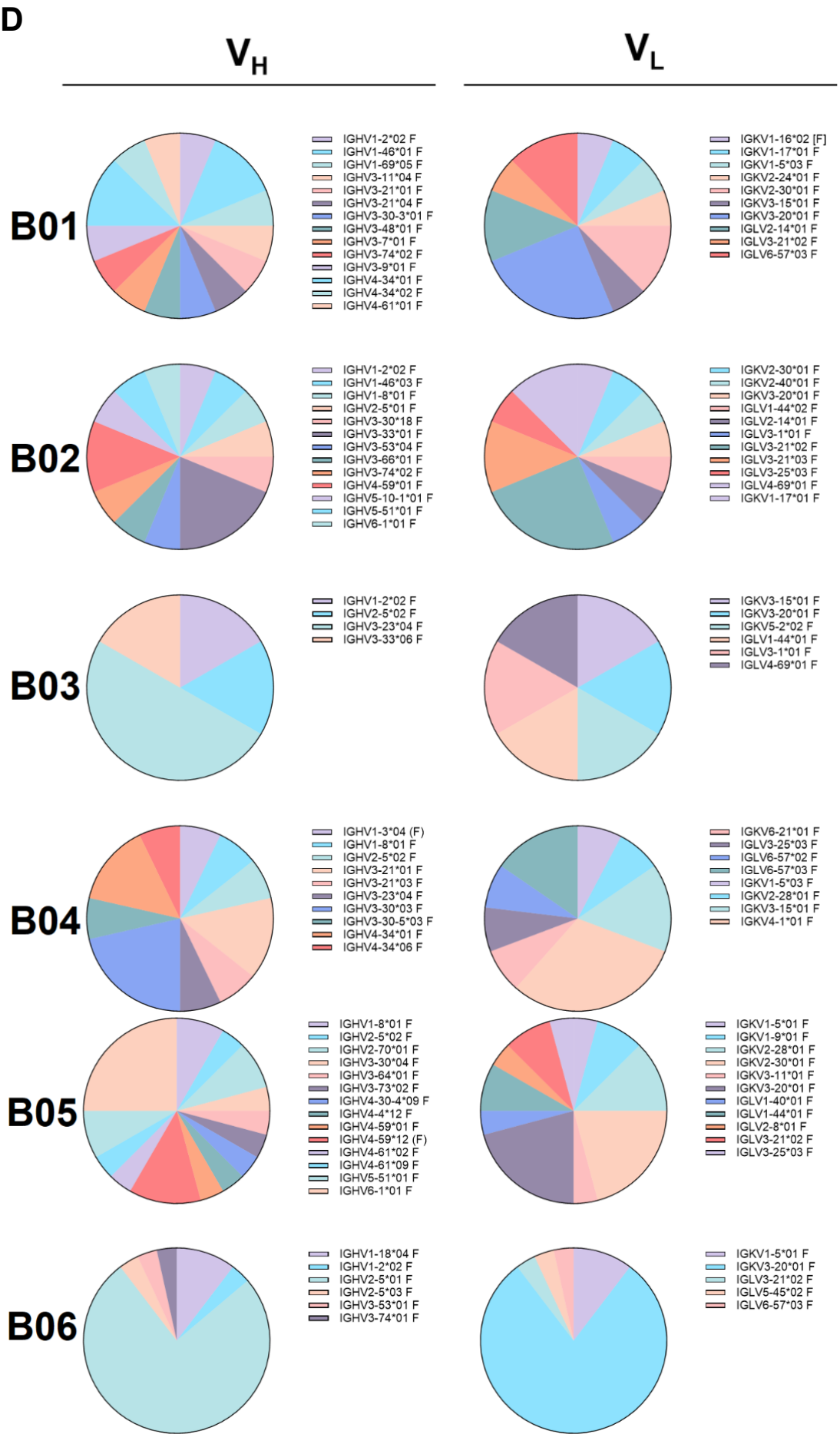
V_H
V_L
B01
IGHV1-2*02 F
IGHV1-46*01 F
IGHV1-69*05 F
IGHV3-11*04 F
IGHV3-21*01 F
IGHV3-21*04 F
IGHV3-30-3*01 F
IGHV3-48*01 F
IGHV3-7*01 F
IGHV3-74*02 F
IGHV3-9*01 F
IGHV4-34*01 F
IGHV4-34*02 F
IGHV4-61*01 F
IGKV1-16*02 [F]
IGKV1-17*01 F
IGKV1-5*03 F
IGKV2-24*01 F
IGKV2-30*01 F
IGKV3-15*01 F
IGKV3-20*01 F
IGLV2-14*01 F
IGLV3-21*02 F
IGLV6-57*03 F
B02
IGHV1-2*02 F
IGHV1-46*03 F
IGHV1-8*01 F
IGHV2-5*01 F
IGHV3-30*18 F
IGHV3-33*01 F
IGHV3-53*04 F
IGHV3-66*01 F
IGHV3-74*02 F
IGHV4-59*01 F
IGHV5-10-1*01 F
IGHV5-51*01 F
IGHV6-1*01 F
IGKV2-30*01 F
IGKV2-40*01 F
IGKV3-20*01 F
IGLV1-44*02 F
IGLV2-14*01 F
IGLV3-1*01 F
IGLV3-21*02 F
IGLV3-21*03 F
IGLV3-25*03 F
IGLV4-69*01 F
IGKV1-17*01 F
B03
IGHV1-2*02 F
IGHV2-5*02 F
IGHV3-23*04 F
IGHV3-33*06 F
IGKV3-15*01 F
IGKV3-20*01 F
IGKV5-2*02 F
IGLV1-44*01 F
IGLV3-1*01 F
IGLV4-69*01 F
B04
IGHV1-3*04 (F)
IGHV1-8*01 F
IGHV2-5*02 F
IGHV3-21*01 F
IGHV3-21*03 F
IGHV3-23*04 F
IGHV3-30*03 F
IGHV3-30-5*03 F
IGHV4-34*01 F
IGHV4-34*06 F
IGKV6-21*01 F
IGLV3-25*03 F
IGLV6-57*02 F
IGLV6-57*03 F
IGKV1-5*03 F
IGKV2-28*01 F
IGKV3-15*01 F
IGKV4-1*01 F
B05
IGHV1-8*01 F
IGHV2-5*02 F
IGHV2-70*01 F
IGHV3-30*04 F
IGHV3-64*01 F
IGHV3-73*02 F
IGHV4-30-4*09 F
IGHV4-4*12 F
IGHV4-59*01 F
IGHV4-59*12 (F)
IGHV4-61*02 F
IGHV4-61*09 F
IGHV5-51*01 F
IGHV6-1*01 F
IGKV1-5*01 F
IGKV1-9*01 F
IGKV2-28*01 F
IGKV2-30*01 F
IGKV3-11*01 F
IGKV3-20*01 F
IGLV1-40*01 F
IGLV1-44*01 F
IGLV2-8*01 F
IGLV3-21*02 F
IGLV3-25*03 F
B06
IGHV1-18*04 F
IGHV1-2*02 F
IGHV2-5*01 F
IGHV2-5*03 F
IGHV3-53*01 F
IGHV3-74*01 F
IGKV1-5*01 F
IGKV3-20*01 F
IGLV3-21*02 F
IGLV5-45*02 F
IGLV6-57*03 F

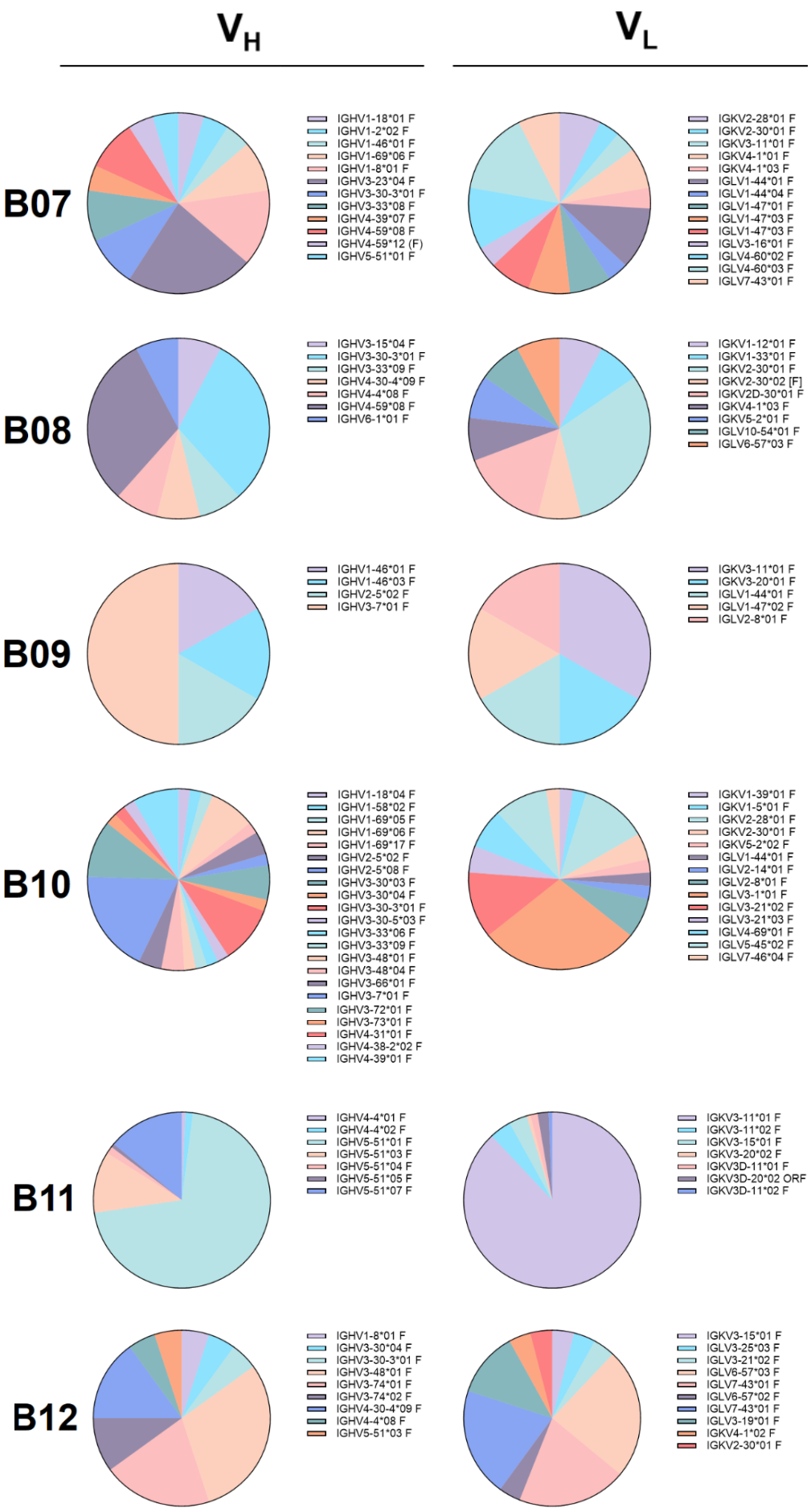
V_H
V_L
B07
IGHV1-18*01 F
IGHV1-2*02 F
IGHV1-46*01 F
IGHV1-69*06 F
IGHV1-8*01 F
IGHV3-23*04 F
IGHV3-30-3*01 F
IGHV3-33*08 F
IGHV4-39*07 F
IGHV4-59*08 F
IGHV4-59*12 (F)
IGHV5-51*01 F
IGKV2-28*01 F
IGKV2-30*01 F
IGKV3-11*01 F
IGKV4-1*01 F
IGKV4-1*03 F
IGLV1-44*01 F
IGLV1-44*04 F
IGLV1-47*01 F
IGLV1-47*03 F
IGLV1-47*03 F
IGLV3-16*01 F
IGLV4-60*02 F
IGLV4-60*03 F
IGLV7-43*01 F
B08
IGHV3-15*04 F
IGHV3-30-3*01 F
IGHV3-33*09 F
IGHV4-30-4*09 F
IGHV4-4*08 F
IGHV4-59*08 F
IGHV6-1*01 F
IGKV1-12*01 F
IGKV1-33*01 F
IGKV2-30*01 F
IGKV2-30*02 [F]
IGKV2D-30*01 F
IGKV4-1*03 F
IGKV5-2*01 F
IGLV10-54*01 F
IGLV6-57*03 F
B09
IGHV1-46*01 F
IGHV1-46*03 F
IGHV2-5*02 F
IGHV3-7*01 F
IGKV3-11*01 F
IGKV3-20*01 F
IGLV1-44*01 F
IGLV1-47*02 F
IGLV2-8*01 F
B10
IGHV1-18*04 F
IGHV1-58*02 F
IGHV1-69*05 F
IGHV1-69*06 F
IGHV1-69*17 F
IGHV2-5*02 F
IGHV2-5*08 F
IGHV3-30*03 F
IGHV3-30*04 F
IGHV3-30-3*01 F
IGHV3-30-5*03 F
IGHV3-33*06 F
IGHV3-33*09 F
IGHV3-48*01 F
IGHV3-48*04 F
IGHV3-66*01 F
IGHV3-7*01 F
IGHV3-72*01 F
IGHV3-73*01 F
IGHV4-31*01 F
IGHV4-38-2*02 F
IGHV4-39*01 F
IGKV1-39*01 F
IGKV1-5*01 F
IGKV2-28*01 F
IGKV2-30*01 F
IGKV5-2*02 F
IGLV1-44*01 F
IGLV2-14*01 F
IGLV2-8*01 F
IGLV3-1*01 F
IGLV3-21*02 F
IGLV3-21*03 F
IGLV4-69*01 F
IGLV5-45*02 F
IGLV7-46*04 F
B11
IGHV4-4*01 F
IGHV4-4*02 F
IGHV5-51*01 F
IGHV5-51*03 F
IGHV5-51*04 F
IGHV5-51*05 F
IGHV5-51*07 F
IGKV3-11*01 F
IGKV3-11*02 F
IGKV3-15*01 F
IGKV3-20*02 F
IGKV3D-11*01 F
IGKV3D-20*02 ORF
IGKV3D-11*02 F
B12
IGHV1-8*01 F
IGHV3-30*04 F
IGHV3-30-3*01 F
IGHV3-48*01 F
IGHV3-74*01 F
IGHV3-74*02 F
IGHV4-30-4*09 F
IGHV4-4*08 F
IGHV5-51*03 F
IGKV3-15*01 F
IGLV3-25*03 F
IGLV3-21*02 F
IGLV6-57*03 F
IGLV7-43*01 F
IGLV6-57*02 F
IGLV7-43*01 F
IGLV3-19*01 F
IGKV4-1*02 F
IGKV2-30*01 F

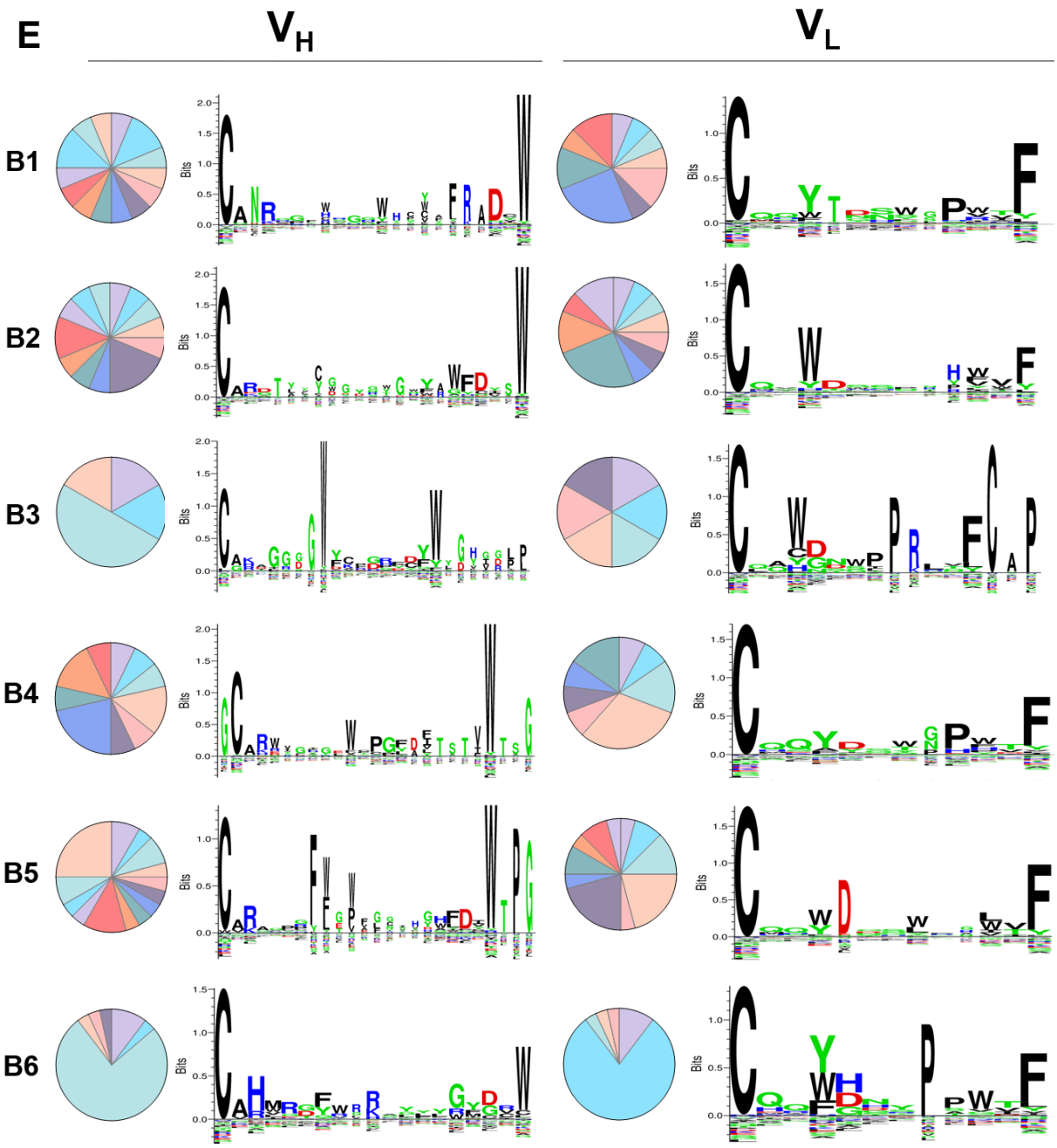
E
V_H
V_L
B1
B2
B3
B4
B5
B6
Bits

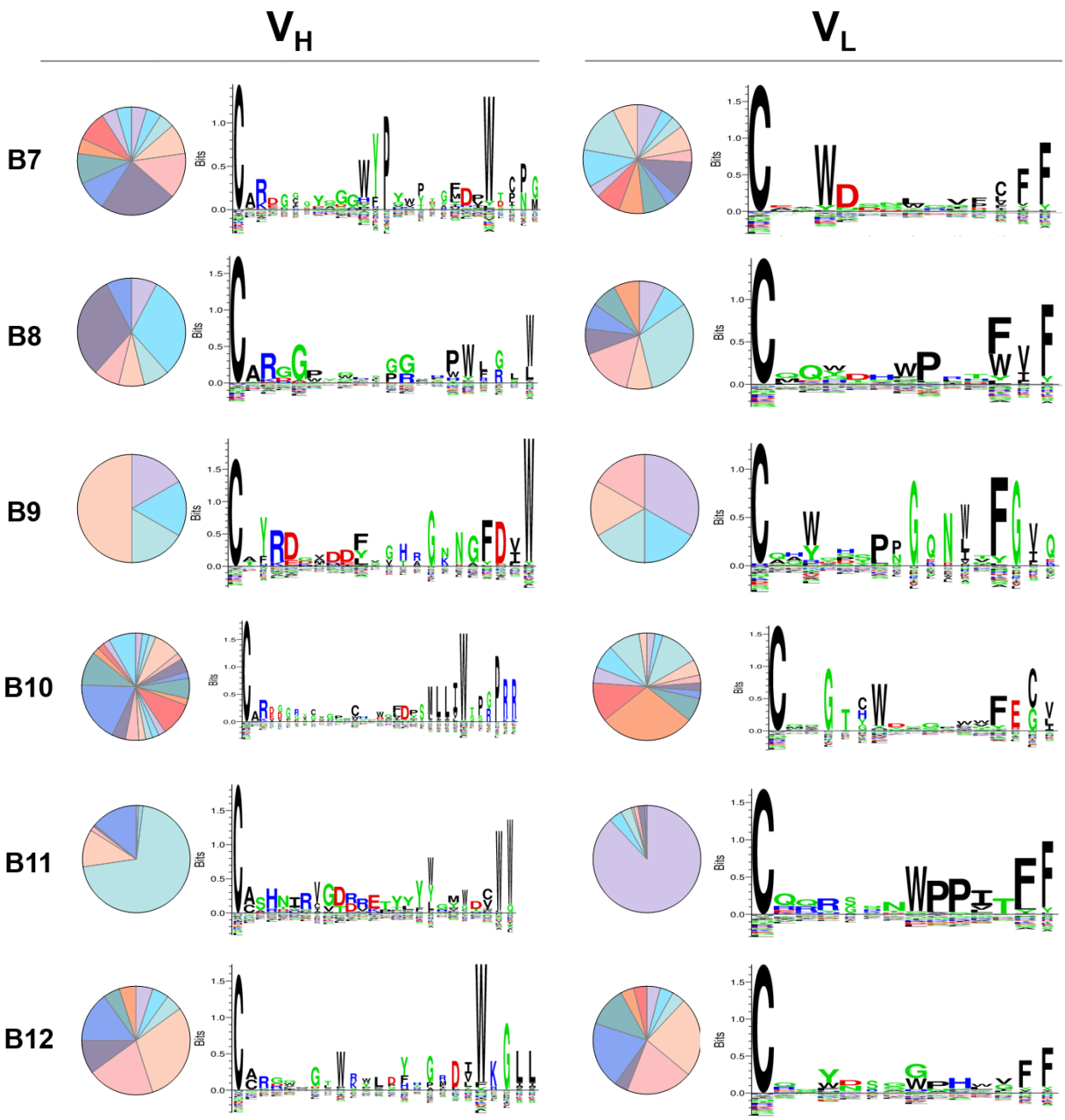

Supplementary Figure 5: Quality of sequencing, alignment and V gene annotations: A: The amount of reads that exceeded or failed to exceed the quality treshold are shown in green and red, respectively with regard to run time of the experiment. Total number of reads is shown in blue. **B:** Bar plot depicts the number of reads corresponding to each barcode used during the sequencing library preparation. **C:** Failed alignment of the barcode 13 in which only the #1468 was expressed is shown. Ugene software was used for alignment (Ugene, RU). **D:** Reads with the correct length were run in V-QUEST algorithm against the human database. Obtained scFv sequences were filtered with the criteria as mentioned. All annotated V_H and V_L sequences in a unique productive read is depicted in the generated pie charts for each individual barcode. The size of the slices were determined by the number of productive reads corresponding to a unique scFv sequence. **E:** The consesnsus CDR3 sequences for V_H and V_L chains were constructed for the scFv sequences that were run against the human database in V-QUEST.

7.1.6 Supplementary Table 1: Testing the effect of electroporated ligation product amount

	Colonies Counted	Estimated transformants
0.5µg κ 10^{-4} dilution	340	3.4x10E7
0.5µg κ 10^{-5} dilution	44	4.4x10E7
0.5µg λ 10^{-4} dilution	>1000	>1x10E8
0.5µg λ 10^{-5} dilution	118	1.18x10E8
1µg κ 10^{-4} dilution	150	1.5x10E7
1µg κ 10^{-5} dilution	16	1.6x10E7
1µg λ 10^{-4} dilution	61	6.1x10E7
1µg λ 10^{-5} dilution	450	4.5x10E7

Supplementary Table 1: Resulting estimated transformants upon using 0.5 or 1 µg vector for ligation. Ligations were set up with either 0.5 or 1 µg cut and gel purified vectors. They were ligated with 3:1 insert to vector ratio. Ligation products were then precipitated and resuspended in ddH_2O. 25µ bacteria was mixed with respective ligation products and electroporated. Dilutions from the transformations were spread over LB AMP agar plates for selection. Emerging colonies were counted and total CFU was calculated for each condition. Total number of colonies were calculated as follows:

	λ	κ	Total
0.5µg library:	1.18x10E8 +	0.44x10E8	= 1.62x10E8
1µg library:	6.1x10E7 +	1.6x10E7	= 7.7x10E7

7.1.7 Supplementary Table 2: The effect of primer purification on in frame sequences

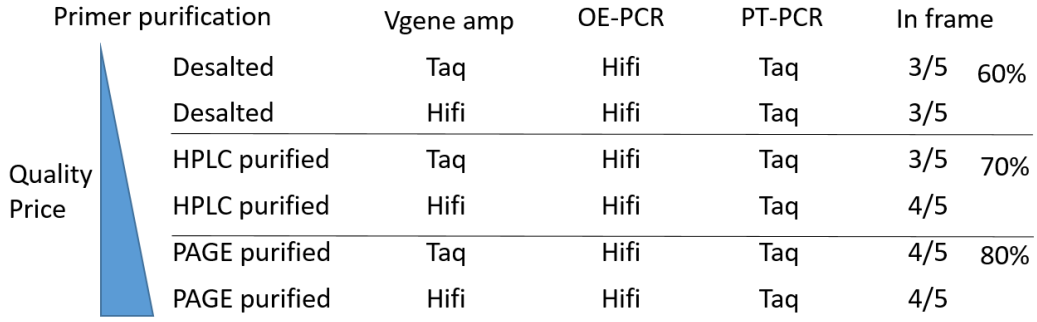

Supplementary Table 2: Primer purification methods eliminate malfunctional oligos and increase the frequency of in frame sequences. To see the effect of primer purification quality, primers purified with different methods were ordered. The quality and the price of oligos with respect to their purification method was increasing from top to bottom of the table. During V gene amplification, the DNA polymerase was alternated between a Taq polymerase and a high-fidelity polymerase to determine if the observed frameshift mutations occur due to polymerase.

7.2 Sequences and maps of the used plasmid DNA

#53:

agcttaatgtagtcttatgcaatactcttgtagtcttgcaacatggtaacgatgagttagcaacatgccttacaaggagagaaaaagcaccgtgc
atgccgattggtggaagtaaggtggtacgatcgtgccttattaggaaggcaacagacgggtctgacatggattggacgaaccactgaattgcc
gcattgcagagatattgtatttaagtgcctagctcgatacaataaacgggtctctctggttagaccagatctgagcctgggagctctctggctaact
agggaacccactgcttaagcctcaataaagcttgccttgagtgcttcaagtagtgtgtgcccgtctgttgtgtgactctggtaactagagatccctc
agacccttttagtcagtgtggaaaatctctagcagtggcgcccgaacagggacctgaaagcgaaagggaaaccagagctctctcgacgcag
gactcggcttgctgaagcgcgcacggcaagaggcgaggggcggcgactggtgagtacgccaaaaattttgactagcggaggctagaagg
agagagatgggtgcgagagcgtcagtattaagcgggggagaattagatcgcgatgggaaaaaattcggttaaggccaggggaaagaaa
aaatataaattaaaacatatagtatgggcaagcagggagctagaacgattcgcagttaatcctggcctgttagaaacatcagaaggctgtaga
caaatactgggacagctacaaccatcccttcagacaggatcagaagaacttagatcattatataatacagtagcaaccctctattgtgtgcatca
aaggatagagataaaagacaccaaggaagctttagacaagatagaggaagagcaaaacaaaagtaagaccaccgcacagcaagcgg
ccgctgatcttcagacctggaggaggagatatgagggacaattggagaagtgaattatataaatataaagtagtaaaaattgaaccattagga
gtagcacccaccaaggcaaagagaagagtggtgcagagagaaaaaagagcagtgggaataggagctttgttccttgggttcttgggagca
gcaggaagcactatgggcgcagcctcaatgacgctgacggtacaggccagacaattattgtctggtatagtgcagcagcagaacaatttgctg
agggctattgaggcgcaacagcatctgttgcaactcacagtctggggcatcaagcagctccaggcaagaatcctggctgtggaaagatacct
aaaggatcaacagctcctggggatttggggttgctctggaaaactcatttgcaccactgctgtgccttggaatgctagttggagtaataaatctctg
gaacagatttggaatcacacgacctggatggagtgggacagagaaattaacaattacacaagcttaatacactccttaattgaagaatcgcaa
aaccagcaagaaaagaatgaacaagaattattggaattagataaatgggcaagtttgtggaattggtttaacataacaaattggctgtggtatat
aaaattattcataatgatagtaggaggcttggtaggtttaagaatagtttttgctgtactttctatagtgaatagagttaggcagggatattcaccatta
tcgtttcagacccacctcccaaccccgaggggacccgacaggcccgaaggaatagaagaagaaggtggagagagagacagagacaga
tccattcgattagtgaacggatctcgacggtatcggttaacttttaaaagaaaaggggggattgggggtacagtgcaggggaaagaatagta
gacataatagcaacagacatacaaactaaagaattacaaaaacaaattacaaaaattcaaaattttatcgatcacgagactagcctcgagaa
gcttgatatcgaattcccacgggttggggttgcgccttttccaaggcagccctgggtttgcgcagggacgcggctgctctgggcgtggttccggg
aaacgcagcggcgccgaccctgggtctcgcacattcttcacgtccgttcgcagcgtcacccggatcttcgccgctacccttgtgggccccccgg
cgacgcttcctgctccgcccctaagtcgggaaggttccttgcggttcgcggcgtgccggacgtgacaaacggaagccgcacgtctcactagta
ccctcgcagacggacagcgccagggagcaatggcagcgcgccgaccgcgatgggctgtggccaatagcggctgctcagcggggcgcgc
cgagagcagcggccgggaaggggcggtgcgggaggcggggtgtggggcggtagtgtgggccctgttcctgcccgcgcggtgttccgcattc
tgcaagcctccggagcgcacgtcggcagtcggctccctcgttgaccgaatcaccgacctctctccccaggggatccggatcacaagtttgtac
aaaaaagcaggctttggccgctctagcgtttaaacttaagcttgccgccaccatggattttcaggtgcagattttcagcttcctgctaatcagtgcct
cagtcataatgtctagaggtgtacactccgactacaaagacgagcaggtccaactgcaggagtcaggacctgacctggtgaaaccttctcagt
cactttcactgacttgcactgtcactggctactccatcaccagtggttatagctggcactggattcggcagtttccaggaaacaaactggaatggat
gggctacatacaatacagtggtatcactaactacaacccctctctcaaaagtcgaatctctatcacccgagacacatccaagaaccagttcttcc
tgcagttgaattctgtgactactgaggacacagccacatattactgtgcaagagaagactatgattaccactggtacttcgatgtctggggccaag
ggaccacggtcaccgtctcctcaggaggtggtggatcgggcggtggcgggtcgggtggcggcggatctgacatccagctgacccagtctcca
gcaatcatgtctgcatctctaggggaggagatcaccctaacctgcagtgccagctcgagtgtaagttacatgcactggtaccagcagaagtca
ggcacttctcccaaactcttgatttatagcacatccaacctggcttctggagtcccttctcgcttcagtggcagtgggtctgggacctttttattctctcac
aatcagcagtgtggaggctgaagatgctgccgattattactgccatcagtggagtagttatcccacgttcggaggtggtactaagctggaaatca
aacgggcggccgctgagcccaaatctcctgacaaaactcacacatgcccaccgtgcccagcacctgaactcctgggggggaccgtcagtcttc
ctcttccccccaaaacccaaggacaccctcatgatctcccggacccctgaggtcacatgcgtggtggtggacgtgagccacgaagaccctga

ggtcaagttcaactggtacgtggacggcgtggaggtgcataatgccaagacaaagccgcgggaggagcagtacaacagcacgtaccgtgt
ggtcagcgtcctcaccgtcctgcaccaggactggctgaatggcaaggagtacaagtgcaaggtctccaacaaagccctcccagcccccatc
gagaaaaccatctccaaagccaaagggcagccccgagaaccacaggtgtacaccctgcccccaagccgggatgagctgaccaagaacc
aggtcagcctgacctgcctggtcaaaggcttctatcccagcgacatcgccgtggagtgggagagcaatgggcagccggagaacaactacaa
gaccacgcctcccgtgttggactccgacggctccttcttcctctacagcaagctcaccgtggacaagagcaggtggcagcaggggaacgtctt
ctcatgctccgtgatgcatgaggctctgcacaaccactacacgcagaagagcctctccctgtctcccgggaaattttgggtgctggtggtggttgg
tggagtcctggcttgctatagcttgctagtaacagtggcctttattattttctgggtgaggagtaagaggagcaggctcctgcacagtgactacatg
aacatgactcccagacgccctggccccacccgcaagcattaccagccctatgccccccacgcgacttcgcagcctatagatctctgagagtg
aagttcagcaggagcgcagacgccccgcgtaccagcagggccagaaccagctctataacgaactcaatctaggacgaagagaggagta
cgatgttttggacaagagacgtggccgggaccctgagatgggggggaaagccgagaaggaagaaccctcaggagggcctgtataatgaact
ccagaaagataagatggcggaggcttacagtgagattgggatgaaaggcgagcgccggaggggcaaggggcacgatggcctttaccagg
gtctcagtacagccaccaaggacacctacgacgcccttcacatgcaggctctgcctcctaggcgggaccagaggctgcctcccgatgctcac
aagccccctggaggaggcagtttcaggacccccatccaagaggagcaggccgacgcccactccaccctggctaaaatctagacccagcttt
cttgtacaaagtggtgatcgcgtgtcgacaatcaacctctggattacaaaatttgtgaaagattgactggtattcttaactatgttgctccttttacgct
atgtggatacgctgctttaatgcctttgtatcatgctattgcttcccgtatggctttcattttctcctccttgtataaatcctggttgctgtctctttatgaggag
ttgtggcccgttgtcaggcaacgtggcgtggtgtgcactgtgtttgctgacgcaacccccactggttggggcattgccaccacctgtcagctcctttc
cgggactttcgctttccccctccctattgccacggcggaactcatcgccgcctgccttgcccgctgctggacaggggctcggctgttgggcactga
caattccgtggtgttgtcggggaagctgacgtcctttccatggctgctcgcctgtgttgccacctggattctgcgcgggacgtccttctgctacgtccc
ttcggccctcaatccagcggaccttccttcccgcggcctgctgccggctctgcggcctcttccgcgtcttcgccttcgccctcagacgagtcggatc
tccctttgggccgcctccccgcctggaattcgagctcggtacctttaagaccaatgacttacaaggcagctgtagatcttagccacttttaaaaga
aaaggggggactggaagggctaattcactcccaacgaagacaagatctgctttttgcttgtactgggtctctctggttagaccagatctgagcctg
ggagctctctggctaactagggaacccactgcttaagcctcaataaagcttgccttgagtgcttcaagtagtgtgtgcccgtctgttgtgtgactctg
gtaactagagatccctcagacccttttagtcagtgtggaaaatctctagcagtagtagttcatgtcatcttattattcagtatttataacttgcaaagaa
atgaatatcagagagtgagaggaacttgtttattgcagcttataatggttacaaataaagcaatagcatcacaaatttcacaaataaagcatttttttt
cactgcattctagttgtggtttgtccaaactcatcaatgtatcttatcatgtctggctctagctatcccgcccctaactccgcccagttccgcccattctc
cgccccatggctgactaatttttttttatttatgcagaggccgaggccgcctcggcctctgagctattccagaagtagtgaggaggctttttggaggc
ctaggcttttgcgtcgagacgtacccaattcgccctatagtgagtcgtattacgcgcgctcactggccgtcgttttacaacgtcgtgactgggaaaa
ccctggcgttacccaacttaatcgccttgcagcacatccccctttcgccagctggcgtaatagcgaagaggcccgcaccgatcgcccttcccaa
cagttgcgcagcctgaatggcgaatggcgcgacgcgccctgtagcggcgcattaagcgcggcgggtgtggtggttacgcgcagcgtgaccg
ctacacttgccagcgccctagcgcccgctcctttcgctttcttcccttcctttctcgccacgttcgccggctttccccgtcaagctctaaatcgggggct
cccttagggttccgatttagtgctttacggcacctcgaccccaaaaaacttgattagggtgatggttcacgtagtgggccatcgccctgatagacg
gtttttcgcccttgacgttggagtccacgttctttaatagtggactcttgttccaaactggaacaacactcaaccctatctcggtctattcttttgatttata
agggattttgccgatttcggcctattggttaaaaaatgagctgatttaacaaaaatttaacgcgaattttaacaaaatattaacgtttacaatttccca
ggtggcacttttcggggaaatgtgcgcggaacccctatttgtttatttttctaaatacattcaaatatgtatccgctcatgagacaataaccctgataa
atgcttcaataatattgaaaaaggaagagtatgagtattcaacatttccgtgtcgcccttattcccttttttgcggcattttgccttcctgtttttgctcaccc
agaaacgctggtgaaagtaaaagatgctgaagatcagttgggtgcacgagtgggttacatcgaactggatctcaacagcggtaagatccttga
gagttttcgccccgaagaacgttttccaatgatgagcacttttaaagttctgctatgtggcgcggtattatcccgtattgacgccgggcaagagcaa
ctcggtcgccgcatacactattctcagaatgacttggttgagtactcaccagtcacagaaaagcatcttacggatggcatgacagtaagagaatt
atgcagtgctgccataaccatgagtgataacactgcggccaacttacttctgacaacgatcggaggaccgaaggagctaaccgcttttttgcac
aacatgggggatcatgtaactcgccttgatcgttgggaaccggagctgaatgaagccataccaaacgacgagcgtgacaccacgatgcctgt

agcaatggcaacaacgttgcgcaaactattaactggcgaactacttactctagcttcccggcaacaattaatagactggatggaggcggataa
agttgcaggaccacttctgcgctcggcccttccggctggctggtttattgctgataaatctggagccggtgagcgtgggtctcgcggtatcattgca
gcactggggccagatggtaagccctcccgtatcgtagttatctacacgacggggagtcaggcaactatggatgaacgaaatagacagatcgc
tgagataggtgcctcactgattaagcattggtaactgtcagaccaagtttactcatatatactttagattgatttaaaacttcatttttaatttaaaaggga
tctaggtgaagatccttttttgataatctcatgaccaaaatcccttaacgtgagttttcgttccactgagcgtcagaccccgtagaaaagatcaaagg
atcttcttgagatcctttttttctgcgcgtaatctgctgcttgcaaacaaaaaaaccaccgctaccagcggtggtttgtttgccggatcaagagctacc
aactctttttccgaaggtaactggcttcagcagagcgcagataccaaatactgtccttctagtgtagccgtagttaggccaccacttcaagaactct
gtagcaccgcctacatacctcgctctgctaatcctgttaccagtggctgctgccagtggcgataagtcgtgtcttaccgggttggactcaagacga
tagttaccggataaggcgcagcggtcgggctgaacgggggttcgtgcacacagcccagcttggagcgaacgacctacaccgaactgaga
tacctacagcgtgagctatgagaaagcgccacgcttcccgaagggagaaaggcggacaggtatccggtaagcggcagggtcggaacagg
agagcgcacgagggagcttccagggggaaacgcctggtatctttatagtcctgtcgggtttcgccacctctgacttgagcgtcgatttttgtgatgc
tcgtcaggggggcggagcctatggaaaaacgccagcaacgcggccttttacggttcctggccttttgctggccttttgctcacatgttctttcctgc
gttatcccctgattctgtggataaccgtattaccgcctttgagtgagctgataccgctcgccgcagccgaacgaccgagcgcagcgagtcagtg
agcgaggaagcggaagagcgcccaatacgcaaaccgcctctccccgcgcgttggccgattcattaatgcagctggcacgacaggtttcccg
actggaaagcgggcagtgagcgcaacgcaattaatgtgagttagctcactcattaggcaccccagggtttaaactttatgcttccggctcgtatgt
tgtgtggaattgtgagcggataacaatttcacacaggaaacagctatgaccatgattacgccaagcgcgcaattaaccctcactaaagggaac
aaaagctggagctgca

#272:

ggcattgattattgactagtccacggggttggggttgcgccttttccaaggcagccctgggtttgcgcagggacgcggctgctctgggcgtggttc
cgggaaacgcagcggcgccgaccctgggtctcgcacattcttcacgtccgttcgcagcgtcacccggatcttcgccgctacccttgtgggcccc
ccggcgacgcttcctgctccgcccctaagtcgggaaggttccttgcggttcgcggcgtgccggacgtgacaaacggaagccgcacgtctcact
agtaccctcgcagacggacagcgccagggagcaatggcagcgcgccgaccgcgatgggctgtggccaatagcggctgctcagcggggc
gcgccgagagcagcggccgggaaggggcggtgcgggaggcggggtgtggggcggtagtgtgggccctgttcctgcccgcgcggtgttccg
cattctgcaagcctccggagcgcacgtcggcagtcggctccctcgttgaccgaatcaccgacctctctccccaggactagtagctttattgcggta
gtttatcacagttaaattgctaacgcagtcagtgctcgactgatcacaggtaagtatcaaggttacaagacaggtttaaggaggccaatagaaa
ctgggcttgtcgagacagagaagattcttgcgtttctgataggcacctattggtcttactgacatccactttgcctttctctccacaggggtaccgaag
ccgctagcatggattttcaggtgcagattttcagcttcctgctaatcagtgcctcagtcataatgtctagaggtgtacactccgactacaaagacga
gcaggtccaactgcaggagtcaggacctgacctggtgaaaccttctcagtcactttcactgacttgcactgtcactggctactccatcaccagtgg
ttatagctggcactggattcggcagtttccaggaaacaaactggaatggatgggctacatacaatacagtggtatcactaactacaaccccctctc
tcaaaagtcgaatctctatcacccgagacacatccaagaaccagttcttcctgcagttgaattctgtgactactgaggacacagccacatattact
gtgcaagagaagactatgattaccactggtacttcgatgtctggggccaagggaccacggtcaccgtctcctcaggaggtggtggatcgggcg
gtggcgggtcgggtggcggcggatctgacatccagctgacccagtctccagcaatcatgtctgcatctctaggggaggagatcaccctaacct
gcagtgccagctcgagtgtaagttacatgcactggtaccagcagaagtcaggcacttctcccaaactcttgatttatagcacatccaacctggctt
ctggagtcccttctcgcttcagtggcagtgggtctgggacctttattctctcacaatcagcagtgtggaggctgaagatgctgccgattattactgcc
atcagtggagtagttatcccacgttcggaggtggtactaagctggaaatcaaacgggcggccgctgagcccaaatctcctgacaaaactcac
acatgcccaccgtgcccagcacctgaactcctgggggggaccgtcagtcttcctcttccccccaaaacccaaggacaccctcatgatctcccgg
acccctgaggtcacatgcgtggtggtggacgtgagccacgaagaccctgaggtcaagttcaactggtacgtggacggcgtggaggtgcataa
tgccaagacaaagccgcgggaggagcagtacaacagcacgtaccgtgtggtcagcgtcctcaccgtcctgcaccaggactggctgaatgg
caaggagtacaagtgcaaggtctccaacaaagccctcccagcccccatcgagaaaaccatctccaaagccaaagggcagccccgagaa
ccacaggtgtacaccctgcccccaagccgggatgagctgaccaagaaccaggtcagcctgacctgcctggtcaaaggcttctatcccagcg
acatcgccgtggagtgggagagcaatgggcagccggagaacaactacaagaccacgcctcccgtgttggactccgacggctccttcttcctct
acagcaagctcaccgtggacaagagcaggtggcagcaggggaacgtcttctcatgctccgtgatgcatgaggctctgcacaaccactacac
gcagaagagcctctccctgtctcccgggaaattttgggtgctggtggtggttggtggagtcctggcttgctatagcttgctagtaacagtggcctttat
tattttctgggtgaggagtaagaggagcaggctcctgcacagtgactacatgaacatgactcccagacgccctggccccacccgcaagcatta
ccagccctatgccccccacgcgacttcgcagcctatagatctctgagagtgaagttcagcaggagcgcagacgcccccgcgtaccagcag
ggccagaaccagctctataacgaactcaatctaggacgaagagaggagtacgatgttttggacaagagacgtggccgggaccctgagatg
gggggaaagccgagaaggaagaaccctcaggagggcctgtataatgaactccagaaagataagatggcggaggcttacagtgagattgg
gatgaaaggcgagcgccggaggggcaaggggcacgatggcctttaccagggtctcagtacagccaccaaggacacctacgacgcccttc
acatgcaggctctgcctcctaggcgggaccagaggctgcctcccgatgctcacaagccccctggaggaggcagtttcaggacccccatcca
agaggagcaggccgacgcccactccaccctggctaaaatctagctcgaggcctaccggagagccttgccttgcaaaggcagacagtcagt
gaggaagactatgtggcacatgaagacaccagaggtgttcctcaggatcaaagtatgtacaagcctttgtgaatatttttttccttctcacttggcaa
atacaattcctgagatcaataacctcgtctttttaatttttcctcgtcttttttaactatttataaaatattgaattataaaatatgtaattataaatactttaatt
ataaaatatgtaattataaatactttaattataaaatatttaattataaaaacacaattacctcatctttttaaatatttttgcaaaatatttccctccataat
ttctccgtttccatttttattctgttacttaaataattctgcagtcgacggtaccgcgggcccgggatccaccggatctagataactgatcataatcagc
cataccacatttgtagaggttttacttgctttaaaaaacctcccacacctccccctgaacctgaaacataaaatgaatgcaattgttgttgttaacttg
tttattgcagcttataatggttacaaataaagcaatagcatcacaaatttcacaaataaagcatttttttcactgcattctagttgtggtttgtccaaact
catcaatgtatcttacatgtgagcaaaaggccagcaaaaggccaggaaccgtaaaaaggccgcgttgctggcgtttttccataggctccgccc

ccctgacgagcatcacaaaaatcgacgctcaagtcagaggtggcgaaacccgacaggactataaagataccaggcgtttccccctggaag
ctccctcgtgcgctctcctgttccgaccctgccgcttacgggatacctgtccgcctttctcccttcgggaagcgtggcgctttctcatagctcacgctgt
aggtatctcagttcggtgtaggtcgttcgctccaagctgggctgtgtgcacgaacccccgttcagcccgaccgctgcgccttatccggtaactat
cgtcttgagtccaacccggtaagacacgacttatcgccactggcagcagccactggtaacaggattagcagagcgaggtatgtaggcggtgc
tacagagttcttgaagtggtggcctaactacggctacactagaagaacagtatttggtatctgcgctctgctgaagccagttaccttcggaaaaag
agttggtagctcttgatccggcaaacaaaccaccgctggtagcggtggttttttgtttgcaagcagcagattacgcgcagaaaaaaaggatctc
aagaagatcctttgatcttttctacggggtctgacgctcagtggaacgaaaactcacgttaagggattttggtcatgccgtctcagaagaactcgtc
aagaaggcgatagaaggcgatgcgctgcgaatcgggagcggcgataccgtaaagcacgaggaagcggtcagcccattcgccgccaagc
tcttcagcaatatcacgggtagccaacgctatgtcctgatagcggtccgccacacccagccggccacagtcgatgaatccagaaaagcggcc
attttccaccatgatattcggcaagcaggcatcgccatgggtcacgacgagatcctcgccgtcgggcatgctcgccttgagcctggcgaacagt
tcggctggcgcgagcccctgatgctcttcgtccagatcatcctgatcgacaagaccggcttccatccgagtacgtgctctctcgatgcgatgtttcg
cttggtggtcgaatgggcaggtagccggatcaagcgtatgcagccgccgcattgcatcagccatgatggatactttctcggcaggagcaaggt
gagatgacaggagatcctgccccggcacttcgcccaatagcagccagtcccttcccgcttcagtgacaacgtcgagtacagctgcgcaagga
acgcccgtcgtggccagccacgatagccgcgctgcctcgtcttgcagttcattcagggcaccggacaggtcggtcttgacaaaaagaaccgg
gcgcccctgcgctgacagccggaacacggcggcatcagagcagccgattgtctgttgtgcccagtcatagccgaatagcctctccacccaag
cggccggagaacctgcgtgcaatccatcttgttcaatcataatattattgaagcatttatcagggttcgtctcgtcccggtctcctcccatgcatgtca
atattggccattagccatattattcattggttatatagcataaatcaatattggctattggccattgcatacgttgtatctatatcataatatgtacaaagc
ttgatcaagaaagcactccgggctccagaaggagccttccaggccagctttgagcataagctgctgatgagcagtgagtgtcttgagtagtgttc
agggcagcatgttaccattcatgcttgacttctagccagtgtgacgagaggctggagtcaggtctctagagagttgagcagctccagccttagat
ctcccagtcttatgcggtgtgcccattcgctttgtgtctgcagtcccctggccacacccagtaacagttctgggatctatgggagtagcttccttagtg
agctttcccttcaaatactttgcaaccaggtagagaagtttggagtgaaggttttgttcttcgtttcttcacaatatggatatgcatcttcttttgaaaatgt
taaagtaaattacctctcttttcagatactgtcttcatgcgaacttggtatcctgtttccatcccagccttctataacccagtaacatctttttgaaacca
gtgggtgagaaagacacctggtcaggaacgcggaccacaggacaactcaggctcacccacggcatcagactaaaggcaaacaaggact
ctgtataaagtaccggtggcatgtgtattagtggagatgcagcctgtgctctgcagacagggagtcacacagacacttttctataatttcttaagtg
ctttgaatgttcaagtagaaagtctaacattaaatttgattgaacaattgtatattcatggaatattttggaacggaataccaaaaaatggcaatagt
ggttctttctggatggaagacaaacttttcttctttaaaataaattttatttttatatatttgaggttgaccacatgaccttaaggatacatatagacagtaa
actggttactacagtgaagcaaattaacatatctaccatcgtacatagttacatttttttgtgtgacaggaacagctaaaatctacgtatttaacaaa
actcctaaagacaatacatttttattaactatagccctcatgatgtacattagatctgtacatttatattggctcatgtccaatatgaccgccatgtt

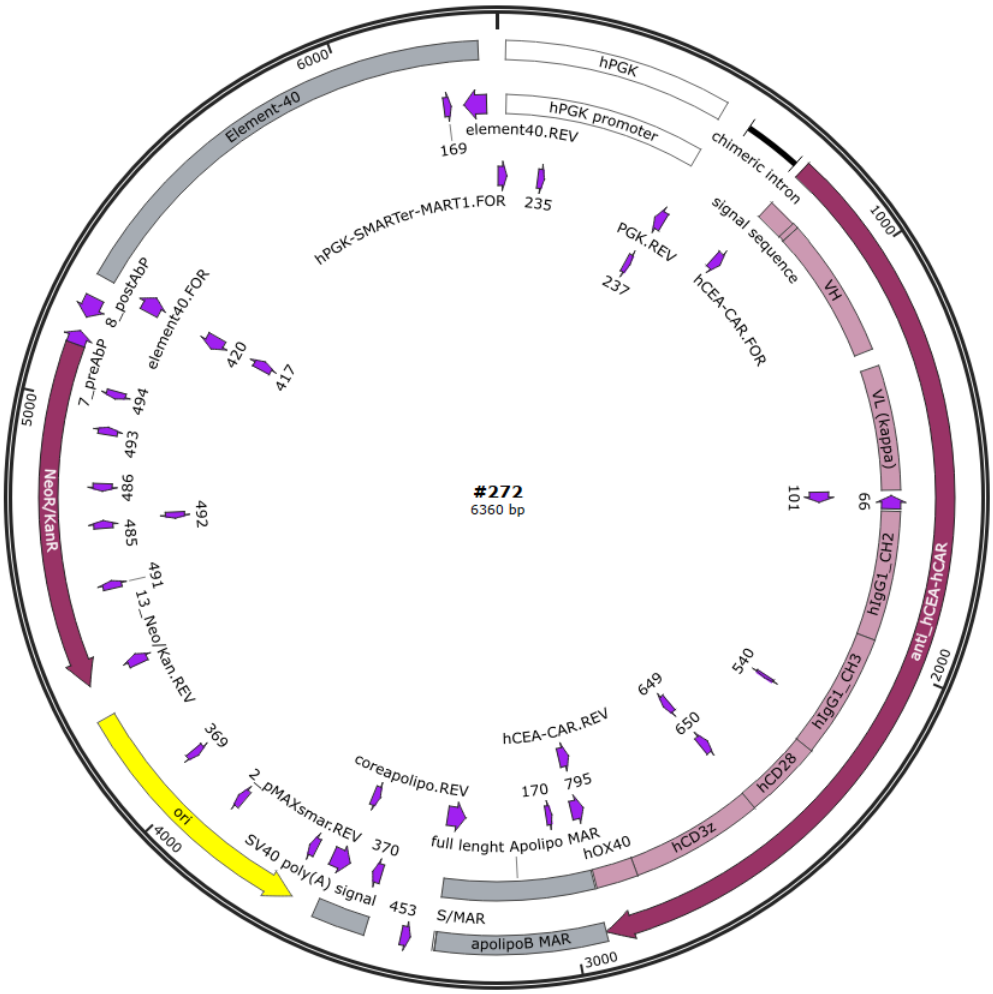

#320:

ggcattgattattgactagtccacggggttggggttgcgccttttccaaggcagccctgggtttgcgcagggacgcggctgctctgggcgtggttc
cgggaaacgcagcggcgccgaccctgggtctcgcacattcttcacgtccgttcgcagcgtcacccggatcttcgccgctacccttgtgggcccc
ccggcgacgcttcctgctccgcccctaagtcgggaaggttccttgcggttcgcggcgtgccggacgtgacaaacggaagccgcacgtctcact
agtaccctcgcagacggacagcgccagggagcaatggcagcgcgccgaccgcgatgggctgtggccaatagcggctgctcagcggggc
gcgccgagagcagcggccgggaaggggcggtgcgggaggcggggtgtggggcggtagtgtgggccctgttcctgcccgcgcggtgttccg
cattctgcaagcctccggagcgcacgtcggcagtcggctccctcgttgaccgaatcaccgacctctctccccaggactagtagctttattgcggta
gtttatcacagttaaattgctaacgcagtcagtgctcgactgatcacaggtaagtatcaaggttacaagacaggtttaaggaggccaatagaaa
ctgggcttgtcgagacagagaagattcttgcgtttctgataggcacctattggtcttactgacatccactttgcctttctctccacaggggtaccgaag
ccgctagcatggattttcaggtgcagattttcagcttcctgctaatcagtgcctcagtcataatgtctagaggtgtacactccgactacaaagacga
gcaggtccaactgcaggagtcaggacctgacctggtgaaaccttctcagtcactttcactgacttgcactgtcactggctactccatcaccagtgg
ttatagctggcactggattcggcagtttccaggaaacaaactggaatggatgggctacatacaatacagtggtatcactaactacaaccctctc
tcaaaagtcgaatctctatcacccgagacacatccaagaaccagttcttcctgcagttgaattctgtgactactgaggacacagccacatattact
gtgcaagagaagactatgattaccactggtacttcgatgtctggggccaagggaccacggtcaccgtctcctcaggaggtggtggatcgggcg
gtggcgggtcgggtggcggcggatctgacatccagctgacccagtctccagcaatcatgtctgcatctctaggggaggagatcaccctaacct
gcagtgccagctcgagtgtaagttacatgcactggtaccagcagaagtcaggcacttctcccaaactcttgatttatagcacatccaacctggctt
ctggagtcccttctcgcttcagtggcagtgggtctgggacctttttattctctcacaatcagcagtgtggaggctgaagatgctgccgattattactgcc
atcagtggagtagttatcccacgttcggaggtggtactaagctggaaatcaaacgggcggccgctgagcccaaatctcctgacaaaactcac
acatgcccaccgtgcccagcacctgaactcctgggggggaccgtcagtcttcctcttccccccaaaacccaaggacaccctcatgatctcccgg

acccctgaggtcacatgcgtggtggtggacgtgagccacgaagaccctgaggtcaagttcaactggtacgtggacggcgtggaggtgcataa
tgccaagacaaagccgcgggaggagcagtacaacagcacgtaccgtgtggtcagcgtcctcaccgtcctgcaccaggactggctgaatgg
caaggagtacaagtgcaaggtctccaacaaagccctcccagcccccatcgagaaaaccatctccaaagccaaagggcagccccgagaa
ccacaggtgtacaccctgcccccaagccgggatgagctgaccaagaaccaggtcagcctgacctgcctggtcaaaggcttctatcccagcg
acatcgccgtggagtgggagagcaatgggcagccggagaacaactacaagaccacgcctcccgtgttggactccgacggctccttcttcctct
acagcaagctcaccgtggacaagagcaggtggcagcaggggaacgtcttctcatgctccgtgatgcatgaggctctgcacaaccactacac
gcagaagagcctctccctgtctcccgggaaattttgggtgctggtggtggttggtggagtcctggcttgctatagcttgctagtaacagtggcctttat
tattttctgggtgaggagtaagaggagcaggctcctgcacagtgactacatgaacatgactcccagacgccctggccccacccgcaagcatta
ccagccctatgccccccacgcgacttcgcagcctatagatctctgagagtgaagttcagcaggagcgcagacgcccccgcgtaccagcag
ggccagaaccagctctataacgaactcaatctaggacgaagagaggagtacgatgttttggacaagagacgtggccgggaccctgagatg
gggggaaagccgagaaggaagaaccctcaggagggcctgtataatgaactccagaaagataagatggcggaggcttacagtgagattgg
gatgaaaggcgagcgccggaggggcaaggggcacgatggcctttaccagggtctcagtacagccaccaaggacacctacgacgcccttc
acatgcaggctctgcctcctaggcgggaccagaggctgcctcccgatgctcacaagccccctggaggaggcagtttcaggacccccatcca
agaggagcaggccgacgcccactccaccctggctaaaatctagctcgagatctatgcatgcagaagttggtcgtgaggcactgggcaggta
agtatcaaggttacaagacaggtctcgaggcctaccggagagccttgccttgcaaaggcagacagtcagtgaggaagactatgtggcacatg
aagacaccagaggtgttcctcaggatcaaagtatgtacaagcctttgtgaatatttttccttctcacttggcaaatacaattcctgagatcaataac
ctcgtctttttaatttttcctcgtctttttaactatttataaaatattgaattataaaatatgtaattataaatactttaattataaaatatgtaattataaatactt
taattataaaatatgtaattataaatactttataaaatatgtaattataaaatatgtaattataaacattttaattataaaatatgtaattataaacatttta
attataaaatatgtaattataaacattttaattataaaatatgtaattataaacattttaattataaaatatgtaattataaacattttaattataaaatattt
aattataaacattttaattataaaatatttaattataaatattttaattataaaatatttaattataaatattttaattataaaatatttaattataaatattttaat
tataaaatatttaattataaatactttaattataaaatatttaattataaatattttaattataaaatatttaattataaatattttaattataaatattttaattat
aaaatatttaattataaaaacacaattacctcatctttttaaatatttttgcaaaatatttccctccataatttctccgtttccatttttattctgttacttaaatg
aattcttactgacatccactttgcctttctctccacaggtgtccactcggatccaccggatctagataactgatcataatcagccataccacatttgta
gaggttttacttgctttaaaaaacctcccacacctccccctgaacctgaaacataaaatgaatgcaattgttgttgttaacttgtttattgcagcttata
atggttacaaataaagcaatagcatcacaaatttcacaaataaagcatttttttcactgcattctagttgtggtttgtccaaactcatcaatgtatctta
catgtagcccgcctaatgagcgggctttttttttggcttgttgtccacaaccgttaaaccttaaaagctttaaaagccttatatattcttttttttcttataaaa
cttaaaaccttagaggctatttaagttgctgatttatattaattttattgttcaaacatgagagcttagtacgtgaaacatgagagcttagtacgttagc
catgagagcttagtacgttagccatgagggtttagttcgttaaacatgagagcttagtacgttaaacatgagagcttagtaagtactatcaacagg
ttgaactgctgatccacgttgtggtagaattggtaaagagagtcgtgtaaaatatcgagttcgcacatcttgttgtctgattattgatttttggcgaaac
catttgatcatatgacaagatgtgtatctaccttaacttaatgattttgataaaaatcattaggtaccacatgtcctgcagaggcctgcatgcaagctt
gatcaagaaagcactccgggctccagaaggagccttccaggccagctttgagcataagctgctgatgagcagtgagtgtcttgagtagtgttca
gggcagcatgttaccattcatgcttgacttctagccagtgtgacgagaggctggagtcaggtctctagagagttgagcagctccagccttagatct
cccagtcttatgcggtgtgcccattcgctttgtgtctgcagtcccctggccacacccagtaacagttctgggatctatgggagtagcttccttagtga
gctttcccttcaaatactttgcaaccaggtagagaagtttggagtgaaggttttgttcttcgtttcttcacaatatggatatgcatcttcttttgaaaatgtt
aaagtaaattacctctcttttcagatactgtcttcatgcgaacttggtatcctgtttccatcccagccttctataacccagtaacatctttttgaaaccag
tgggtgagaaagacacctggtcaggaacgcggaccacaggacaactcaggctcacccacggcatcagactaaaggcaaacaaggactct
gtataaagtaccggtggcatgtgtattagtggagatgcagcctgtgctctgcagacagggagtcacacagacacttttctataatttcttaagtgctt
tgaatgttcaagtagaaagtctaacattaaatttgattgaacaattgtatattcatggaatattttggaacggaataccaaaaaatggcaatagtgg
ttctttctggatggaagacaaacttttcttctttaaaataaattttattttatatatttgaggttgaccacatgaccttaaggatacatatagacagtaaac

tggttactacagtgaagcaaattaacatatctaccatcgtacatagttacatttttttgtgtgacaggaacagctaaaatctacgtatttaacaaaact
cctaaagacaatacatttttattaactatagccctcatgatgtacattagatctgtacatttatattggctcatgtccaatatgaccgccatgtt

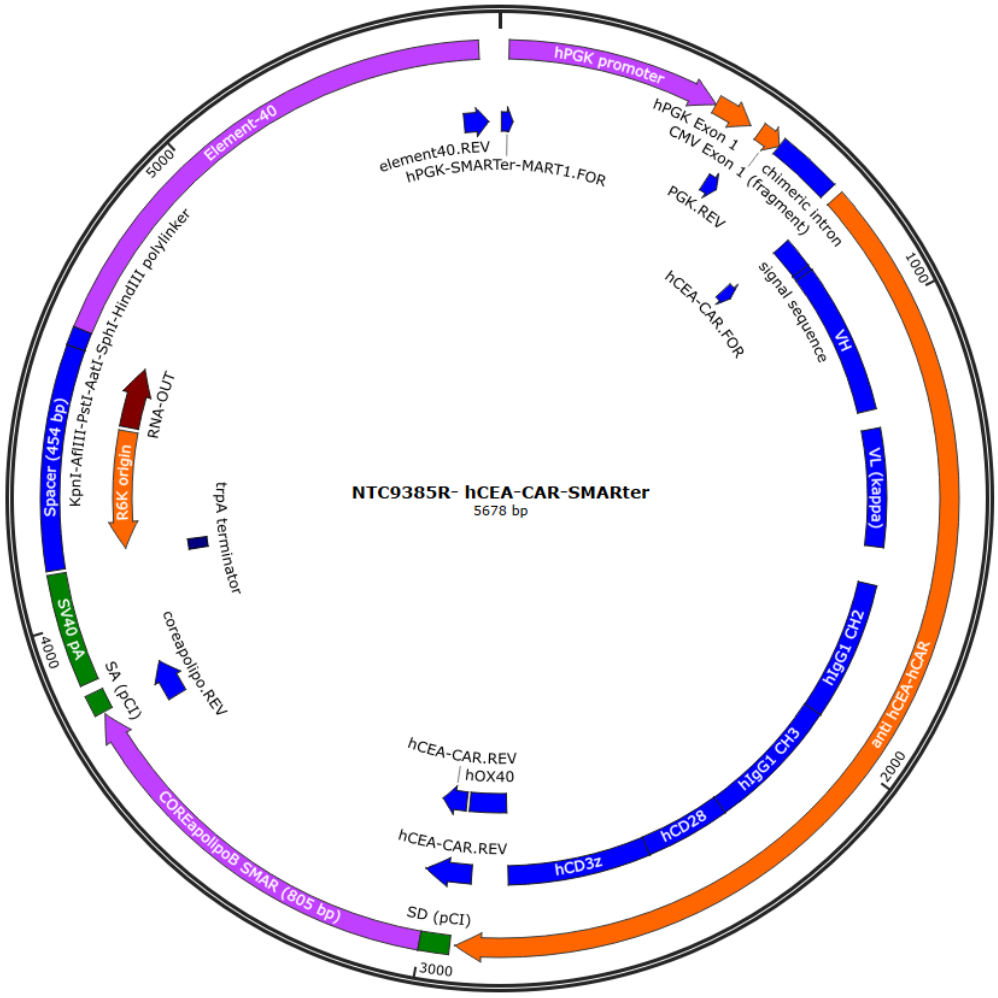

#1468:

tccacggggttggggttgcgccttttccaaggcagccctgggtttgcgcagggacgcggctgctctgggcgtggttccgggaaacgcagcggc
gccgaccctgggtctcgcacattcttcacgtccgttcgcagcgtcacccggatcttcgccgctacccttgtgggccccccggcgacgcttcctgct
ccgcccctaagtcgggaaggttccttgcggttcgcggcgtgccggacgtgacaaacggaagccgcacgtctcactagtaccctcgcagacgg
acagcgccagggagcaatggcagcgcgccgaccgcgatgggctgtggccaatagcggctgctcagcggggcgcgccgagagcagcgg
ccgggaaggggcggtgcgggaggcggggtgtggggcggtagtgtgggccctgttcctgcccgcgcggtgttccgcattctgcaagcctccgg
agcgcacgtcggcagtcggctccctcgttgaccgaatcaccgacctctctccccaggactagtagctttattgcggtagtttatcacagttaaattg
ctaacgcagtcagtgctcgactgatcacaggtaagtatcaaggttacaagacaggtttaaggaggccaatagaaactgggcttgtcgagaca
gagaagattcttgcgtttctgataggcacctattggtcttactgacatccactttgcctttctctccacaggggtaccgaagccgctagcatggattttc
aggtgcagattttcagcttcctgctaatcagtgcctcagtcataatgtctagaggtgtacactccgactacaaagacgagcaggtccaactgcag
gagtcaggacctgacctggtgaaaccttctcagtcactttcactgacttgcactgtcactggctactccatcaccagtggttatagctggcactgga
ttcggcagtttccaggaaacaaactggaatggatgggctacatacaatacagtggtatcactaactacaacccctctctcaaaagtcgaatctct
atcacccgagacacatccaagaaccagttcttcctgcagttgaattctgtgactactgaggacacagccacatattactgtgcaagagaagact
atgattaccactggtacttcgatgtctggggccaagggaccacggtcaccgtctcctcaggaggtggtggatcgggcggtggcgggtcgggtg
gcggcggatctgacatccagctgacccagtctccagcaatcatgtctgcatctctaggggaggagatcaccctaacctgcagtgccagctcga
gtgtaagttacatgcactggtaccagcagaagtcaggcacttctcccaaactcttgatttatagcacatccaacctggcttctggagtcccttctcgc

ttcagtggcagtgggtctgggacctttattctctcacaatcagcagtgtggaggctgaagatgctgccgattattactgccatcagtggagtagtta
tcccacgttcggaggtggtactaagctggaaatcaaacgggcggccgctgagcccaaatctcctgacaaaactcacacatgcccaccgtgcc
cagcacctgaactcctgggggggaccgtcagtcttcctcttccccccaaaacccaaggacaccctcatgatctcccggacccctgaggtcacat
gcgtggtggtggacgtgagccacgaagaccctgaggtcaagttcaactggtacgtggacggcgtggaggtgcataatgccaagacaaagcc
gcgggaggagcagtacaacagcacgtaccgtgtggtcagcgtcctcaccgtcctgcaccaggactggctgaatggcaaggagtacaagtgc
aaggtctccaacaaagccctcccagcccccatcgagaaaaccatctccaaagccaaagggcagccccgagaaccacaggtgtacaccct
gcccccaagccgggatgagctgaccaagaaccaggtcagcctgacctgcctggtcaaaggcttctatcccagcgacatcgccgtggagtgg
gagagcaatgggcagccggagaacaactacaagaccacgcctcccgtgttggactccgacggctccttcttcctctacagcaagctcaccgt
ggacaagagcaggtggcagcaggggaacgtcttctcatgctccgtgatgcatgaggctctgcacaaccactacacgcagaagagcctctcc
ctgtctcccgggaaattttgggtgctggtggtggttggtggagtcctggcttgctatagcttgctagtaacagtggcctttattattttctgggtgaggag
taagaggagcaggctcctgcacagtgactacatgaacatgactcccagacgccctggccccacccgcaagcattaccagccctatgccccc
ccacgcgacttcgcagcctatagatctctgagagtgaagttcagcaggagcgcagacgcccccgcgtaccagcagggccagaaccagctct
ataacgaactcaatctaggacgaagagaggagtacgatgttttggacaagagacgtggccgggaccctgagatgggggggaaagccgaga
aggaagaaccctcaggagggcctgtataatgaactccagaaagataagatggcggaggcttacagtgagattgggatgaaaggcgagcgc
cggaggggcaaggggcacgatggcctttaccagggtctcagtacagccaccaaggacacctacgacgcccttcacatgcaggctctgcctc
ctaggcgggaccagaggctgcctcccgatgctcacaagccccctggaggaggcagtttcaggacccccatccaagaggagcaggccgac
gcccactccaccctggctaaaatctagctcgagatctgtcgacatgcatgcagaagttggtcgtgaggcactgggcaggtaagtatcaaggtta
caagacaggtctcgagatttataaaatattgaattataaaatatgtaattataaatactttaattataaaatatgtaattataaatactttaattataaaa
tatgtaattataaatactttataaaatatgtaattataaaatatgtaattataaacattttaattataaaatatgtaattataaacattttaattataaaatat
gtaattataaacattttaattataaaatatgtaattataaacattttaattataaaatatgtaattataaacattttaattataaaatatttaattataaacat
tttaattataaaatatttaattataaatattttaattataaaatatttaattataaatattttaattataaaatatttaattataaatattttaattataaaatattta
attataaatactttaattataaaatatttaattataaatattttaattataaaatatttaattataaatattttaattataaaatatttaatt
ataaaaacacaattagaattcttactgacatccactttgcctttctctccacaggtgtccactcggatccaccggatctagataactgatcataatca
gccataccacatttgtagaggttttacttgctttaaaaaacctcccacacctccccctgaacctgaaacataaaatgaatgcaattgttgttgttaact
tgtttattgcagcttataatggttacaaataaagcaatagcatcacaaatttcacaaataaagcatttttttcactgcattctagttgtggtttgtccaaa
ctcatcaatgtatcttacatgtagcccgcctaatgagcgggctttttttggcttgttgtccacaaccgttaaaccttaaaagctttaaaagccttatata
ttctttttttcttataaaacttaaaaccttagaggctatttaagttgctgatttatattaattttattgttcaaacatgagagcttagtacgtgaaacatgag
agcttagtacgttagccatgagagcttagtacgttagccatgagggtttagttcgttaaacatgagagcttagtacgttaaacatgagagcttagta
agtactatcaacaggttgaactgctgatccacgttgtggtagaattggtaaagagagtcgtgtaaaatatcgagttcgcacatcttgttgtctgattat
tgatttttggcgaaaccatttgatcatatgacaagatgtgtatctaccttaacttaatgattttgataaaaatcattaggactagtaagcttgatcaaga
aagcactccgggctccagaaggagccttccaggccagctttgagcataagctgctgatgagcagtgagtgtcttgagtagtgttcagggcagc
atgttaccattcatgcttgacttctagccagtgtgatgagaggctggagtcaggtctctagagagttgagcagctccagccttagatctcccagtctt
atgcggtgtgcccattcgctttgtgtctgcagtcccctggccacacccagtaacagttctgggatctatgggagtagcttccttagtgagctttcccttc
aaatactttgcaaccaggtagagaagtttggagtgaaggttttgttctttgtttcttcacaatatggatatgcatcttcttttgaaaatgttaaagtaaatt
acctctcttttcagatactgtcttcatgcgaacttggtatcctgtttccatcccagccttctataacccagtaacatctttttttgaaaccagtgggtgaga
aagacacctggtcaggaacgcggaccacaggacaactcaggctcacccacggcatcagactaaaggcaaacaaggactctgtataaagt
accggtggcatgtgtattagtggagatgcagcctgtgctctgcagacagggagtcacacagacacttttctataatttcttaagtgctttgaatgttc
aagtagaaagtctaacattaaatttgattgaacaattgtatattcatggaatattttggaacggaataccaaaaaatggcaatagtggttctttctgg
atggaagacaaacttttcttttttaaattttatcttatatatttgaggttgaccacatgaccttaaggatacatatagacagtaaactggttactacagtg

aagcaaattaacatatctaccatcttacatagttacatttttttgtgtgacaggaacagctaaaatctacgtatttaacaaaaatcctaaagacaata
cattttattaactatagccctcatgatgtacgactag

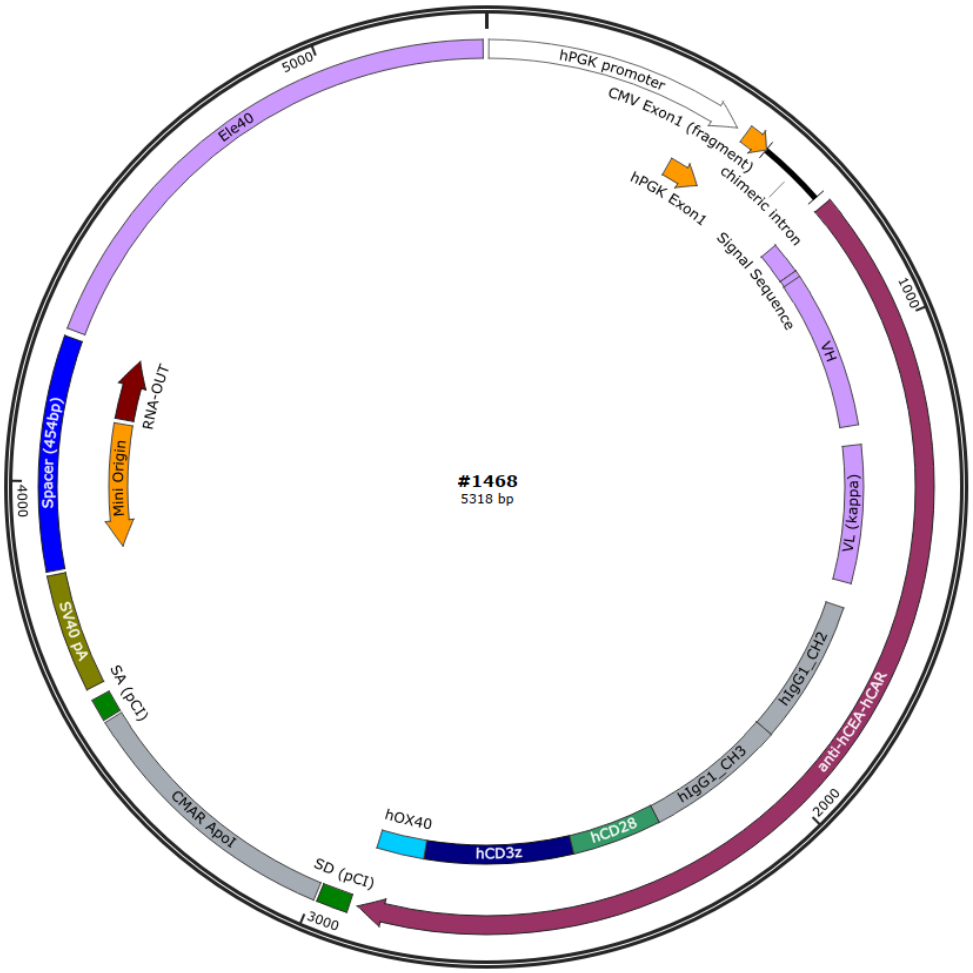

#1475:

ggcattgattattgactagtccacggggttggggttgcgccttttccaaggcagccctgggtttgcgcagggacgcggctgctctgggcgtggttc
cgggaaacgcagcggcgccgaccctgggtctcgcacattcttcacgtccgttcgcagcgtcacccggatcttcgccgctacccttgtgggcccc
ccggcgacgcttcctgctccgcccctaagtcgggaaggttccttgcggttcgcggcgtgccggacgtgacaaacggaagccgcacgtctcact
agtaccctcgcagacggacagcgccagggagcaatggcagcgcgccgaccgcgatgggctgtggccaatagcggctgctcagcggggc
gcgccgagagcagcggccgggaaggggcggtgcgggaggcggggtgtggggcggtagtgtgggccctgttcctgcccgcgcggtgttccg
cattctgcaagcctccggagcgcacgtcggcagtcggctccctcgttgaccgaatcaccgacctctctccccaggactagtagctttattgcggta
gtttatcacagttaaattgctaacgcagtcagtgctcgactgatcacaggtaagtatcaaggttacaagacaggtttaaggaggccaatagaaa
ctgggcttgtcgagacagagaagattcttgcgtttctgataggcacctattggtcttactgacatccactttgcctttctctccacaggggtaccgaag
ccgctagcgccaccatggattttcaggtgcagattttcagcttcctgctaatcagtgcctcagtcataatgtctagaggtgtacactcccaggtcacc
ttgaaggagtctggtcctacgctggtgaaacccacacagaccctcacgctgacctgcaccttctctgggttctcactcagcactagtggagtggg
tgtgggctggatccgtcagcccccaggaaaggccctggagtgtcttgcactcatttattggaatgatgataagcgctacagcccatctctgaaga
gcaggctcaccatcaccaaggacacctccaaaaaccaggtggtccttacaatgaccaacatggaccctgtggacacagccacatcttactgt
gcacacatgagggactacagtaagagctactactacggtatggacgtctggggccaagggaccacggtcaccgtctcctcaggtggtggtgg
tagcggcggcggcggctctggtggtggtggatccgaaacgacactcacgcagtctccaggcaccctgtctttgtctccacgggaaagagcca
ccctctcctgcagggccagtcagagtgttaggagcagctacttagcctggtaccagcagaaacttggccaggctcccaggctcctcatctatggt
gcatccagcagggccactggcatcccagacaggttcagtggcagtgggtctgggacagacttcactctcaccatcagcagactggagcctga

ggattttgcagtgtattactgtcagcagtatggtagctcacctccgtcgacgttcggccaagggaccaaagtggatatcaaacgtgcggccgctg
agcccaaatctcctgacaaaactcacacatgcccaccgtgcccagcacctgaactcctgggggggaccgtcagtcttcctcttccccccaaaac
ccaaggacaccctcatgatctcccggacccctgaggtcacatgcgtggtggtggacgtgagccacgaagaccctgaggtcaagttcaactgg
tacgtggacggcgtggaggtgcataatgccaagacaaagccgcgggaggagcagtacaacagcacgtaccgtgtggtcagcgtcctcacc
gtcctgcaccaggactggctgaatggcaaggagtacaagtgcaaggtctccaacaaagccctcccagcccccatcgagaaaaccatctcca
aagccaaagggcagccccgagaaccacaggtgtacaccctgccccccaagccgggatgagctgaccaagaaccaggtcagcctgacctg
cctggtcaaaggcttctatcccagcgacatcgccgtggagtgggagagcaatgggcagccggagaacaactacaagaccacgcctcccgt
gttggactccgacggctccttcttcctctacagcaagctcaccgtggacaagagcaggtggcagcaggggaacgtcttctcatgctccgtgatg
catgaggctctgcacaaccactacacgcagaagagcctctccctgtctcccgggaaattttgggtgctggtggtggttggtggagtcctggcttgc
tatagcttgctagtaacagtggcctttattattttctgggtgaggagtaagaggagcaggctcctgcacagtgactacatgaacatgactcccaga
cgccctggccccacccgcaagcattaccagccctatgccccccacgcgacttcgcagcctatagatctctgagagtgaagttcagcaggag
cgcagacgcccccgcgtaccagcagggccagaaccagctctataacgaactcaatctaggacgaagagaggagtacgatgttttggacaa
gagacgtggccgggaccctgagatgggggaaagccgagaaggaagaaccctcaggagggcctgtataatgaactccagaaagataag
atggcggaggcttacagtgagattgggatgaaaggcgagcgccggaggggcaaggggcacgatggcctttaccagggtctcagtacagcc
accaaggacacctacgacgcccttcacatgcaggctctgcctcctaggcgggaccagaggctgcctcccgatgctcacaagccccctggag
gaggcagtttcaggacccccatccaagaggagcaggccgacgcccactccaccctggctaaaatctagctcgaggcctaccggagagcctt
gccttgcaaaggcagacagtcagtgaggaagactatgtggcacatgaagacaccagaggtgttcctcaggatcaaagtatgtacaagccttt
gtgaatatttttccttctcacttggcaaatacaattcctgagatcaataacctcgtctttttaatttttcctcgtctttttaactatttataaaatattgaattat
aaaatatgtaattataaatactttaattataaaatatgtaattataaatactttaattataaaatatttaattataaaaacacaattacctcatctttttaaa
tatttttgcaaaatatttccctccataatttctccgtttccatttttattctgttacttaaataattctgcagtcgacggtaccgcgggcccgggatccaccg
gatctagataactgatcataatcagccataccacatttgtagaggttttacttgctttaaaaaacctcccacacctccccctgaacctgaaacataa
aatgaatgcaattgttgttgttaacttgtttattgcagcttataatggttacaaataaagcaatagcatcacaaatttcacaaataaagcatttttttcac
tgcattctagttgtggtttgtccaaactcatcaatgtatcttacatgtgagcaaaaggccagcaaaaggccaggaaccgtaaaaaggccgcgttg
ctggcgtttttccataggctccgccccctgacgagcatcacaaaaatcgacgctcaagtcagaggtggcgaaacccgacaggactataaag
ataccaggcgtttcccccctggaagctccctcgtgcgctctcctgttccgaccctgccgcttacgggatacctgtccgcctttctcccttcgggaagcg
tggcgctttctcatagctcacgctgtaggtatctcagttcggtgtaggtcgttcgctccaagctgggctgtgtgcacgaacccccccgttcagcccga
ccgctgcgccttatccggtaactatcgtcttgagtccaacccggtaagacacgacttatcgccactggcagcagccactggtaacaggattagc
agagcgaggtatgtaggcggtgctacagagttcttgaagtggtggcctaactacggctacactagaagaacagtatttggtatctgcgctctgct
gaagccagttaccttcggaaaaagagttggtagctcttgatccggcaaacaaaccaccgctggtagcggtggttttttgtttgcaagcagcagat
tacgcgcagaaaaaaaggatctcaagaagatcctttgatcttttctacggggtctgacgctcagtggaacgaaaactcacgttaagggattttgg
tcatgccgtctcagaagaactcgtcaagaaggcgatagaaggcgatgcgctgcgaatcgggagcggcgataccgtaaagcacgaggaag
cggtcagcccattcgccgccaagctcttcagcaatatcacgggtagccaacgctatgtcctgatagcggtccgccacacccagccggccaca
gtcgatgaatccagaaaagcggccattttccaccatgatattcggcaagcaggcatcgccatgggtcacgacgagatcctcgccgtcgggcat
gctcgccttgagcctggcgaacagttcggctggcgcgagcccctgatgctcttcgtccagatcatcctgatcgacaagaccggcttccatccga
gtacgtgctctctcgatgcgatgtttcgcttggtggtcgaatgggcaggtagccggatcaagcgtatgcagccgccgcattgcatcagccatgat
ggatactttctcggcaggagcaaggtgagatgacaggagatcctgccccggcacttcgcccaatagcagccagtcccttcccgcttcagtgac
aacgtcgagtacagctgcgcaaggaacgcccgtcgtggccagccacgatagccgcgctgcctcgtcttgcagttcattcagggcaccggaca
ggtcggtcttgacaaaaagaaccgggcgcccctgcgctgacagccggaacacggcggcatcagagcagccgattgtctgttgtgcccagtc
atagccgaatagcctctccacccaagcggccggagaacctgcgtgcaatccatcttgttcaatcataatattattgaagcatttatcagggttcgtc
tcgtcccggtctcctcccatgcatgtcaatattggccattagccatattattcattggttatatagcataaatcaatattggctattggccattgcatacg

ttgtatctatatcataatatgtacaaagcttgatcaagaaagcactccgggctccagaaggagccttccaggccagctttgagcataagctgctg
atgagcagtgagtgtcttgagtagtgttcagggcagcatgttaccattcatgcttgacttctagccagtgtgacgagaggctggagtcaggtctcta
gagagttgagcagctccagccttagatctcccagtcttatgcggtgtgcccattcgctttgtgtctgcagtcccctggccacacccagtaacagttct
gggatctatgggagtagcttccttagtgagctttcccttcaaatactttgcaaccaggtagagaagtttggagtgaaggttttgttcttcgtttcttcaca
atatggatatgcatcttcttttgaaaatgttaaagtaaattacctctcttttcagatactgtcttcatgcgaacttggtatcctgtttccatcccagccttcta
taacccagtaacatctttttgaaaccagtgggtgagaaagacacctggtcaggaacgcggaccacaggacaactcaggctcacccacggc
atcagactaaaggcaaacaaggactctgtataaagtaccggtggcatgtgtattagtggagatgcagcctgtgctctgcagacagggagtcac
acagacacttttctataatttcttaagtgctttgaatgttcaagtagaaagtctaacattaaatttgattgaacaattgtatattcatggaatattttggaa
cggaataccaaaaaatggcaatagtggttctttctggatggaagacaaacttttcttctttaaaataaattttatttttatatatttgaggttgaccacatg
accttaaggatacatatagacagtaaactggttactacagtgaagcaaattaacatatctaccatcgtacatagttacatttttttgtgtgacaggaa
cagctaaaatctacgtatttaacaaaactcctaaagacaatacatttttattaactatagccctcatgatgtacattagatctgtacatttatattggctc
atgtccaatatgaccgccatgtt

7.3 List of figures

Figure 1.1.2.1: Current landscape in adoptive T cell therapy. 10
Figure 1.2.1.1: Generations of CAR constructs. 13
Figure 1.5.2: scFv phage display screening platform. 18
Figure 1.7.2: Single-cell assays by using Bruker's Lightning™ device. 21
Figure 4.1.1.1: Establishment of Jurkat reporter cell line J7 by single cell cloning. 61
Figure 4.1.2.1: Testing antigen-specific stimulation capacity of J7. 64
Figure 4.1.3.1: Improving antigen-specific stimulation of J7i. 67
Figure 4.1.4.1: Protein and mRNA CAR expression upon antigen-specific stimulation. 70
Figure 4.1.5.1: Challenging J7i in bulk and single-cell level stimulation. 72
Figure 4.2.1.1: First attempt to generate the plasmid CAR library. 76
Figure 4.2.2.1: Cloning scFv library with revised primers. 79
Figure 4.2.3.1: Generation of the plasmid CAR libraries with HPLC purified primers. 81
Figure 4.3.1.1: Initial setup of the electroporation parameters. 84
Figure 4.3.2.1: Optimization of maxi preps to achieve optimal CAR expression. 87
Figure 4.3.3.1: Testing scalability of electroporation and optimization of shock parameters. 90
Figure 4.4.1.1: Pipeline for screening cellular CAR libraries for identification of antigen-specific CARs. 91
Figure 4.4.2.1: The first proof-of-principle experiment of the pipeline. 93
Figure 4.4.3.1: Analysis of the hits for identification of CEACAM5 specific de novo scFvs. 97
Figure 4.4.4.1: In vitro validation of overrepresented scFv in barcode 6. 98

7.4 List of tables

Table 3.1.2.1 Preparation of the transfection medium 39
Table 3.2.1.1 Preparation of TAE buffer 40
Table 3.2.2.1 Preparation of Lysogeny broth (LB) medium 40
Table 3.2.2.2: Preparation of Selection medium 41
Table 3.2.2.3: Preparation of Terrific broth (LB) medium 41
Table 3.2.6.1: An example restriction digestion reaction 43
Table 3.2.8.1: PCR conditions for amplification of heavy and light chain variable regions 45
Table 3.2.8.2: PCR conditions for OE-PCR 45
Table 3.2.8.3: PCR conditions for PT-PCR 46
Table 3.2.9.1: RT Mix 1 46
Table 3.2.9.2: RT Mix 2 46
Table 3.2.9.3: First strand cDNA synthesis 47
Table 3.2.9.4: RT Mix 3 47
Table 3.2.9.5: Second strand cDNA synthesis 47
Table 3.2.9.6: First CAR cDNA PCR mix 48
Table 3.2.9.7: First CAR cDNA PCR conditions 48
Table 3.2.9.8: Second CAR cDNA PCR mix 48
Table 3.2.9.9: Second CAR cDNA PCR conditions 48
Table 3.7.1.1: Parameters used during import of “GFP+” cells into the channels of the OptoSelect™ chip 54
Table 3.7.1.2: Parameters used during export of “GFP+” cells into a U-bottom 96 well plate 54
Table 3.7.2.1: Parameters used during import of magnetic beads 56
Table 3.7.2.2: Parameters used during import of J7i-53 and J7i-Library cells 56
Table 3.7.2.3: Parameters used during export of J7i-Library hits 56

7.5 Abbreviations

°C	Degree Celsius
$(G_4S)_3$	Glycine-Serine flexible linker
aa	amino acid
ACT	adoptive T cell therapy
ADCs	antibody-drug conjugates
ADCC	antibody-dependent cellular cytotoxicity
AICD	activation induced cell death
AML	acute myeloid leukemia
AP-1	Activator protein 1
APC	allophycocyanin
APCs	antigen presenting cells
B-ALL	B-cell precursor acute lymphoblastic leukemia
BCMA	B-cell maturation antigen
BCR	B cell receptor
BiTEs	bispecific T cell engagers
bp	base pair
BsAbs	bispecific antibodies
CAR	chimeric antigen receptor
CDC	complement-dependent cytotoxicity
CLL	chronic lymphocytic leukemia
CRS	Cytokine release syndrome
CTA	Cancer testis antigens
CTLA4	cytotoxic T-lymphocyte-associated protein 4
DAG	diacylglycerol
DAPI	4′,6-diamidino-2-phenylindole
DC	Dendritic cell
dNTP	deoxyribonucleotide triphosphate
DMEM	Dulbecco's Modified Eagle's Medium
DMSO	dimethyl sulfoxide
DNA	deoxyribonucleic acid
dsDNA	double-stranded DNA
E. coli	Escherichia coli
EF	endotoxin free
EP	electroporation
ER	endoplasmic reticulum
E:T	effector to target
Fab	fragment antigen-binding
FACS	fluorescence-activated cell sorting
FC	fold change
Fc	constant domain
FcγR	Fc gamma receptors
FCS	fetal calf serum

FDA	U.S. Food and Drug Administration
FITC	fluorescein
FOV	Field of view
FP	fluorescent protein
g	gravitational force
GFP	Green fluorescent protein
GMP	good manufacturing practice
HCT	hematopoietic cell transplantation
HEK	human embryonic kidney
hPGK	human phosphoglycerate kinase
HPLC	high pressure liquid chromatography
HSPG	heparin sulfate proteoglycan
ICIs	immune checkpoint inhibitors
IFNγ	Interferon gamma
IgG	immunoglobulin G
IL	interleukin
in/del	insertions and deletions
IMGT	International Immunogenetics Information System
IP_3	inositol trisphosphate
ITAMs	immunoreceptor tyrosine-based activation motifs
kb	kilobase
LAT	linker of activation in T cells
LB medium	lysogeny broth medium
Lck	lymphocyte-specific protein tyrosine kinase
mAb	Monoclonal antibody
MACS	magnetic-activated cell sorting
MART-1	melanoma-melanocyte differentiation antigen 1
MDSC	myeloid-derived suppressor cells
MEB	MaxCyte Electroporation Buffer
MFI	mean fluorescence intensity
MHC	major histocompatibility complex
mL	milliliter
MM	multiple myeloma
MN	Macherey-Nagel
mRNA	Messenger RNA
ms	milisecond
NFAT	nuclear factor of activated T-cells
NF-κB	nuclear factor 'kappa-light-chain-enhancer' of activated B-cells
NK	Natural Killer cells
NSCLC	non-small cell lung cancer
NTC	Nature Technology Corporation
OD	optical density
OEP™	optoelectro-positioning
OE-PCR	Overlap Extension PCR
OM	Opti-MEM
ONT	Oxford Nanopore Techonologies
ORF	Open reading frame

pIII	phage coat protein III
PAGE	denaturing polyacrylamide gel electrophoresis
PAP	prostatic acid phosphatase
PBMCs	Peripheral blood mononuclear cells
PBS	phosphate-buffered saline
PCP	positively charged patches
PCR	polymerase chain reaction
PD1	programmed cell death protein 1
PD-L1	programmed death-ligand 1
PE	phycoerythrin
PEI	polyethylenimine
pEPI	Plasmid Episomal
Pen/Strep	penicillin + streptavidin
PHA	phytohemagglutinin
PIP_2	phosphatidylinositol bisphosphate
PKC	protein kinase C
PLC-γ	phospholipase Cγ
PP	PureProteome
PT-PCR	Pull-through PCR
RE	response element
RPMI	Gibco Roswell Park Memorial Institute 1640 Medium
RPM	rounds per minute
r/r	relapsed or refractory
RT	room temperature
RT	revese transcription
S/MAR	scaffold/matrix attachment region
SB	Sleeping Beauty
scFv	single chain variable fragment
SEM	standard error of mean
SNV	single-nucleotide variants
ssDNA	single stranded DNA
TAA	tumor-associated antigens
TAE	Tris-acetate EDTA
TAM	tumor-associated macrophages
TB	Terrific Broth
TCL	T cell lysis buffer
TCR	T cell receptor
TF	transcription factor
TIL	tumor-infiltrating lymphocytes
TLR9	toll like receptor 9
TM	transmembrane
TME	tumor microenvironment
TPS	Target pen selection
Tregs	regulatory T cells
TRUCK	T cells redirected for antigen-unrestricted cytokine-initiated killing
TSA	tumor-specific antigens
U	enzyme unit

V	volt
V_H	human variable heavy chain
V_H3’	heavy chain reverse primer
V_H5’	heavy chain forward primer
V_L	human variable light chain
V_L3‘	light chain reverse primer
V_L5‘	light chain forward primer
WT1	Wilms’ Tumor Antigen 1
µg	microgram
µL	microliter
µM	micromolar
µm	micrometer

8 Acknowledgements

To start with, I would like to thank Prof. Dr. Dirk Jäger for giving me the opportunity to work on this cutting-edge project and all the scientific advice I received. I would like to also thank my academic supervisors Prof. Dr. Ilse Hofmann and Prof. Dr. Hinrich Abken for all the fruitful discussions and advice during my TAC meetings. I am grateful to Prof. Dr Dirk Jäger, Prof. Dr. Michael Boutros, Prof. Dr. Ilse Hofmann, Prof. Dr. Hinrich Abken and Dr. Richard Harbottle for reviewing this work and accepting to be a part of my disputation.

I am grateful to my project supervisor Dr. Patrick Schmidt for all the discussions and guidance throughout my PhD journey. I am grateful for all the scientific input that I have received over the years.

Special thanks go to AG Jäger not only for assisting me in the laboratory, but also for sharing my achievements and frustrations. Alex, Sarah, Kathi, Deva, Jasmin, Meli, Ebi and Max and everybody else in the corridor, I very much appreciated your company and working with you was a privilege. Thank you all for all the great memories we accumulated.

A big thank you goes to Prof. Dr. Stefan Eichmüller, Dr. Richard Harbottle and Dr. Edward Green not only for their valuable scientific advice, but also helping me with hands-on practice.

I am grateful to Toros, Alice, Luisa, Gordon and Tim for their company during all the long hours they had to suffer with me.

Endless gratitude to my family for their support all these years and believing in me more than I did. Fenia, Nives, Erdem, Gökberk, Simay, Felix I am glad to get to know you during my journey and sharing all the ups and downs of life with you was a pleasure.